# PROJECT ADVISORY COMMITTEE

## Subcommittee on

## Engineering

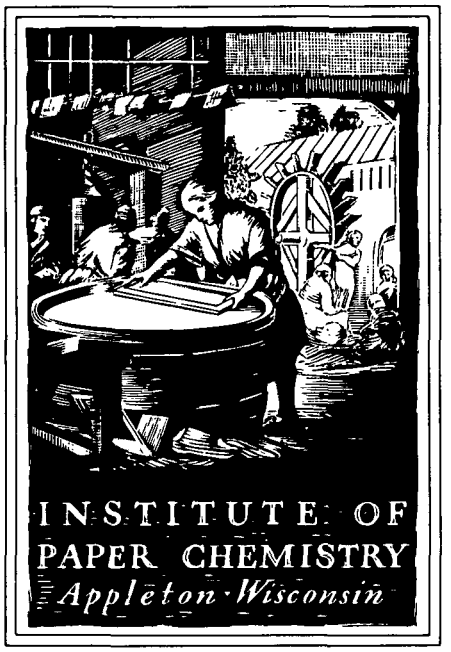


# IPC STAFF STATUS REPORTS

This information represents a review of on-going research for use by the Project Advisory Subcommittees. The information is not intended to be a definitive progress report on any of the projects and should not be cited or referenced in any paper or correspondence external to your company.

Your advice and suggestions on any of the projects will be most welcome.

**FOR MEMBER COMPANIES ONLY**

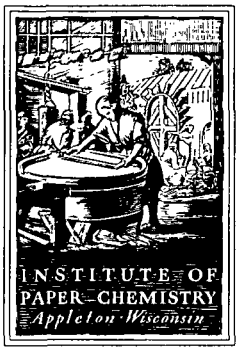


THE INSTITUTE OF PAPER CHEMISTRY
Post Office Box 1039
Appleton, Wisconsin 54912
Phone: 414/734-9251
Telex: 469289

October 1, 1984

TO: Members of the Engineering Project Advisory Committee

Enclosed is advance reading material for the October 24-25 meeting of the Engineering Project Advisory Committee. Included are status reports for active projects, a revised agenda, and a current membership list.

Rooms have been reserved in the Continuing Education Center, and meals will be provided as stated on the agenda. If you haven't already indicated your attendance, please do so at your earliest convenience.

We look forward to meeting with you on October 24-25.

Sincerely,

Clyde H. Sprague

Clyde H. Sprague, Director
Engineering Division

CHS/el
Enclosures

# TABLE OF CONTENTS


| | Page |
|---|---|
| TABLE OF CONTENTS | i |
| AGENDA | ii |
| COMMITTEE LIST | iii |
| Project 3384: Refining of Chemical Pulps for Improved Properties | 1 |
| Project 3480: Wet Pressing Fundamentals | 35 |
| Project 3470: Fundamentals of Drying | 65 |
| Project 3479: Higher Consistency Processing | 84 |
| Project 3556: Fundamentals of Kraft Liquor Corrosivity | 94 |
| Project 3309: Fundamentals of Corrosion Control in Paper Mills | 114 |

* * * REVISED AGENDA * * *

ENGINEERING
PROJECT ADVISORY COMMITTEE

October 24-25, 1984

Continuing Education Center (CEC)
The Institute of Paper Chemistry
Appleton, Wisconsin

* * * * * * * * * * * * * * * * *

## Wednesday, October 24, 1984

| | | |
|---|---|---|
| 10:00am -- | INTRODUCTION | Sprague/White |
| | PROJECT REVIEWS | |
| | - Refining of Chemical Pulps for Improved Properties | Sinkey |
| | - Wet Pressing Fundamentals | Ahrens |
| 12:00pm -- | LUNCH | |
| 1:00pm -- | PROJECT REVIEWS - continued | |
| | - Fundamentals of Drying | Ahrens |
| | - Higher-Consistency Processing | Sinkey |
| 3:00pm -- | BREAK | |
| 3:15pm -- | PROJECT REVIEWS - continued | |
| | - Fundamentals of Kraft Liquor Corrosivity | Yeske |
| | - Fundamentals of Corrosion Control in Paper Mills | Yeske |
| 5:30pm -- | COCKTAILS | |
| 6:00pm -- | DINNER - CEC Dining Room | |
| 7:15pm -- | Selected Topic | |

## Thursday, October 25, 1984

| | | |
|---|---|---|
| 7:15am -- | BREAKFAST -- CEC Dining Room | |
| 8:00am -- | Discussion of Projects | Committee & Research Staff |
| 9:30am -- | BREAK | |
| 9:45am -- | Continued Discussion of Projects | |
| 10:30am -- | Report Preparation | Committee |
| 11:30am -- | Adjourn | |
| -- | LUNCH - CEC Dining Room | |

# ENGINEERING PROJECT ADVISORY COMMITTEE

Mr. David E. White -- (Chairman) 6/87*
Group Leader
Research & Development
Union Camp Corporation
P.O. Box 412
Princeton, NJ 08543
(609) 896-1200

Professor John C. Berg -- 6/85
Department of Chemical Engineering
University of Washington
Seattle, WA 98195
(206) 543-2029

Mr. Jan Bergstrom -- 6/87
Vice President - Reseach
Beloit Corporation
Beloit, WI 53511
(608) 365-3311

Mr. Dennis Betz -- 6/85
Assistant Research Director
P. H. Glatfelter Company
228 S. Main Street
Spring Grove, PA 17362
(717) 225-4711

Dr. Alan F. Button -- 6/85
Section Leader
Fiber & Materials Science Group
Champion Papers
Champion International Corporation
Knightsbridge
Hamilton, OH 45020
(513) 868-5319

Dr. Sam Lin -- 6/86
Senior Process Engineer
Owens-Illinois, Inc.
LDP - Building No. 25
25875, U.S. Route No. 25
Perrysburg, OH 43551
(419) 247-5000

Mr. Robert Murphy -- 6/87
Vice President, Pulp & Paper Technology
James River Corporation
P.O. Box 6000
800 Connecticut Ave. - Riverpark
Norwalk, CT 06856
(203) 854-2374

Mr. Herbert C. Nelson -- 6/85
Senior Research Scientist
Consumer & Service Tissue R & D
Kimberly-Clark Corporation
2100 Winchester Road
Neenah, WI 54956
(414) 721-5329

Mr. Amar Neogi -- 6/87
Section Manager
Weyerhaeuser Technical Center
Tacoma, WA 98477
(206) 924-6722

Mr. David South -- 6/86
Technical Director
Chesapeake Corporation
P. O. Box 311
West Point, VA 23181
(804) 843-5252

Dr. Donald Wensley -- 6/86
Corrosion Group Leader
MacMillan Bloedel
3350 East Broadway
Vancouver, British Columbia V5M 4E6
CANADA
(604) 254-5151

Mr. Raymond Whorton -- 6/85
Manager, Research
International Paper Company
P.O. Box 2787
Mobile, AL 36652
(205) 457-8911

*date of retirement
7/23/84

THE INSTITUTE OF PAPER CHEMISTRY

Appleton, Wisconsin

Status Report

to the

ENGINEERING PROJECT ADVISORY COMMITTEE

Project 3384

# REFINING OF CHEMICAL PULPS FOR IMPROVED PROPERTIES

October 1, 1984

PROJECT SUMMARY FORM

DATE: August 31, 1984

PROJECT NO. & TITLE: 3384 - Refining of Chemical Pulps for Improved Properties

PROJECT LEADER: J. D. Sinkey

IPC GOAL: Develop ways to measure and control manufacturing processes.

OBJECTIVE: To identify or develop ways of measuring and controlling refining intensity, so that the operation can be carried out at the appropriate level of severity without detrimental fiber shortening and fines generation, as a function of fiber type (hardwood vs. softwood, e.g.), pulp end-use requirements, and refiner design and operation

CURRENT FISCAL BUDGET: $105,000

SUMMARY OF RESULTS SINCE LAST REPORT: (February, 1984 - August, 1984)

Work has progressed on the program to test the validity of the refining severity model developed, and to obtain actual measurements of the magnitude and variability of $P_N$, the normal pressure on a bar segment in a refining machine. Specifically, we have:

- Equipped a Valley beater with torque-measuring capability.
- Devised a technique for measuring normal and transverse forces on a segment of a bedplate bar, put that apparatus in place, and obtained preliminary data.
- Quantified the response of a bleached softwood sulfite pulp to various beating load conditions, so that "high-intensity" beating and its effects can be studied. Also established a technique using brightness measurements to determine the fate of dyed fibers in refined pulp mixtures.
- Established the capability of measuring coefficient of friction and specific energy in a Valley beater. Results with the bleached softwood sulfite pulp indicate that its response to low-intensity refining is similar to that of hardwood pulp, but unlike that of softwood kraft: low-intensity refining affords significant property improvements, and significant savings in net specific energy.

# REFINING OF CHEMICAL PULPS FOR IMPROVED PROPERTIES

## INTRODUCTION

It has long been recognized that various pulps respond differently to refining under conditions of high severity, as expressed by specific edge load (SEL). Levlin (1) reported that pine kraft requires much less energy to attain a given tensile strength when refined at high SEL, with only minor loss of tear strength. Birch kraft, on the other hand, exhibited the opposite effects at high SEL: higher energy and much lower tear at a given tensile. A similar comparison with spruce sulfite (2) revealed only small effects on energy efficiency over the same SEL range, but a substantial deficiency in tear-tensile relationships resulted from the more severe refining. Canon and DeFoe (3) have recently substantiated significant advantages in very low-intensity refining (SEL below 1 Ws/m) of bleached hardwood kraft pulps. They report both the energy savings and property improvement trends noted previously with Scandinavian birch at low SEL.

The objective of this work is to develop ways to measure and control refining intensity, so that the pulp property potential of such species as hardwoods can be more fully realized, with minimal energy usage. Indeed, Canon and DeFoe (3) reported that low-intensity refining of bleached hardwood kraft produced a pulp with 33% higher burst, 22% higher tensile, and equivalent or higher tear with 25% savings in net energy. The commercial realization of such results would open the way for much greater use of hardwoods with substantial cost benefits.

From the previously reported analysis of stress on a single fiber segment (4), the following model expressions can be derived for the average normal

stress, shear stress, and tensile stress experienced by a fiber in a disk refiner:

$$\text{Normal stress } \bar{P}_N = \frac{T}{Z^2 L \bar{\ell}} = \frac{P}{\pi \mu \Omega Z^2 L \bar{\ell}(D - \frac{1}{2}L\cos\theta)} \quad (1)$$

$$\text{Shear stress } \bar{\tau}_f = \mu_f \bar{P}_N = \frac{\mu_f T}{Z^2 L \bar{\ell}} = \frac{(\mu_f/\mu)P}{\pi \Omega Z^2 L \bar{\ell}(D - \frac{1}{2}L\cos\theta)} \quad (2)$$

$$\text{Tensile stress } \bar{\sigma}_f = \frac{\mu_f \bar{P}_N \ell_f}{t_f} = \frac{\mu_f T \ell_f}{Z^2 L \bar{\ell} t_f} = \frac{(\mu_f/\mu)P\ell_f}{\pi \Omega Z^2 L \bar{\ell}(D - \frac{1}{2}L\cos\theta)t_f} \quad (3)$$

where $T$ = thrust or load on the plates

$Z$ = number of bars on a ring (rotor and stator the same)

$L$ = effective bar length

$P$ = net power being consumed (not including "no-load")

$\Omega$ = relative disk rotational speed (revolutions per unit time)

$D$ = outside diameter of disks

$\theta$ = angle between rotor and stator bars

$\mu$ = overall coefficient of friction between disks

$\mu_f$ = local interfiber coefficient of friction

$\ell_f$ = length of a given fiber under tensile stress $\bar{\sigma}_f$

$t_f$ = collapsed thickness of a given fiber

$\bar{\ell}$ = average fiber length of pulp being refined

It was suggested that, since the expression for $\overline{P}_N$, Eq. 1, contains all the SEL terms plus additional parameters not included in specific edge load theory, it may be a better indicator of refining severity. Moreover, the form of the shear and tensile stress expressions suggests that $\overline{P}_N$ and the individual fiber characteristics may be relatable to fiber shortening and fines generation. However, $\overline{P}_N$ and the other stress parameters are average values over the whole refiner. Undoubtedly, levels much higher than the average are encountered in real machinery, so that a fiber would see a distribution of stress levels during its journey through the refiner. Hence, the question of whether a fiber receives damaging levels of impacts may be more relatable to $P_{Nmax}$ than $\overline{P}_N$.

To test these theories, a program was proposed involving two parallel but independent efforts. The first entailed obtaining actual measurements of $\overline{P}_N$ in a refining machine. The second involved attempts to confirm or refute the predicted effects of certain fiber parameters ($\mu_f$, $\ell_f$, and $\overline{\ell}$) on fiber shortening and fines production, per Eq. 2 and 3, using dyed, well-characterized fibers in pulp mixtures.

This report contains a more detailed outline of the experimental plan, and a discussion of modifications and instrumentation work carried out on a Valley beater, as required to obtain the results. Base-line data are presented, which confirm the viability of the approach and point out some interesting responses of a sensitive pulp to various levels of beating severity.

## EXPERIMENTAL

### BACKGROUND AND APPROACH

The original proposal (4) involved a study of the cutting and fines generation from dyed fibers of known characteristics when processed in a Valley beater

with pulp of known $\bar{\ell}$. As a parallel, but independent effort, it was planned to develop the means of measuring $P_N$ in the Sprout-Waldron Twin-Flo refiner. However, subsequent consideration of ways in which such pressures could be determined led to the decision to develop the instrumentation for a Valley beater first. It was felt that the geometry and the less severe environment in the refining zone of the beater would make the task easier, and it seemed reasonable to begin with a small-scale machine prior to instrumenting the refiner. Moreover, if the capability of measuring $P_N$ could be developed for a beater, that data would be extremely useful in the work with dyed fibers. Hence, it became desirable to accelerate the effort to measure $P_N$, so that if possible, data could be obtained simultaneously with the work with dyed fibers.

The geometry of rotor and stator bars in a "TAPPI Standard" Valley beater (T200-os 70) is such that two rotor bars are in contact with the bedplate at all times. Given the 5° angle in the herringbone pattern of the seven stator bars, and other geometrical factors (Fig. 1), it can be shown that the area of stapled fiber which bears the load is $2[15.24 - 2(\frac{0.24}{\sin 5^\circ})]\bar{\ell} = 19.5\bar{\ell}$. This assumes that the width of stapled fibrage is indeed equal to $\ell$(cm), and that it is less than the stator bar width of 0.32 cm (1/8 in.). If the fibrage width is greater than or equal to 0.32 cm, then the area is $(19.5)(0.32) = 6.2$ cm$^2$.

Following the reasoning presented previously (4), the load or thrust $T = 19.5\ \bar{\ell}\ \bar{P}_N$. If $\Lambda$ equals the torque on the 19.38 cm diameter beater roll, then $T = \Lambda/9.69\mu$, and the expressions for fiber stress are:

$$\bar{P}_N = \frac{T}{19.5\bar{\ell}} = \frac{\Lambda}{189\mu\bar{\ell}} \qquad (4)$$

$$\bar{\tau}_f = \frac{\mu_f T}{19.5\bar{\ell}} = \frac{(\mu_f/\mu)\Lambda}{189\bar{\ell}} \qquad (5)$$

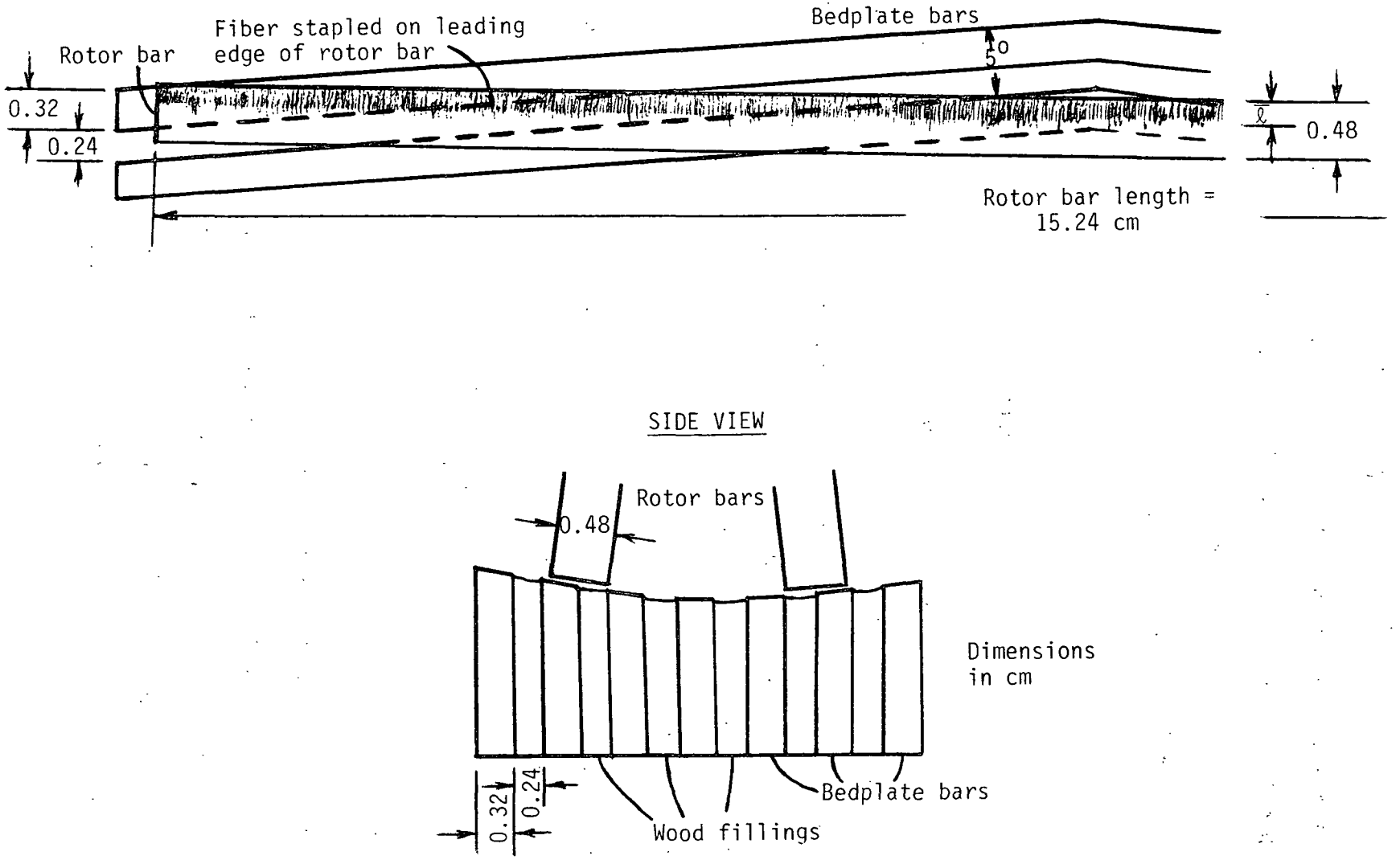


Figure 1. Valley beater bar geometry.

$$\bar{\sigma}_f = \frac{\mu_f T \ell_f}{19.5 \bar{\ell} t_f} = \frac{(\mu_f/\mu)\Lambda \ell_f}{189 \bar{\ell}\, t_f} \qquad (6)$$

With the standard 5500 g load on the lever arm and the 17.9:9.0 ratio, the load T on the bedplate is 10939 g. For a pulp with average fiber length $\bar{\ell}$ = 0.2 cm, Eq. 4 would predict a $\bar{P}_N$ value of 41 psi; this is in contrast to values near 500 psi reported for larger refiners (4,5). For a fiber in such a slurry with

$$\ell_f = 3 \text{ mm}$$

$$t_f = 4 \text{ m}$$

$$\mu_f = 0.15,$$

then the tensile stress $\bar{\sigma}_f$ would be 4500 psi. Estimating from zero-span tensile, the fiber strength of sulfite pulp is closer to 26000 psi. The level of $P_N$ would have to hit a value of several times $\bar{P}_N$ to break the 3 mm long fiber in tension. This ignores viscoelastic frequency effects and the effects of the wood fillings on the impact severity, and of course assumes the proposed model of cutting is correct.

An estimation of specific edge load further emphasizes the gentleness of Valley beater action:

$$\text{SEL} = \frac{P}{Z_r Z_S L \Omega} = \frac{2\pi\mu RT}{Z_r Z_S L} = \frac{(2\pi)(0.15)(9.69)(10939)(980)}{(32)(7)(15.3)} = 28600 \text{ dynes},$$

or 0.29 Ws/m.

Clearly, if the beater is to be used to study fiber cutting, its severity of action must be increased. This might be done by increasing the load T or by reducing the bedplate area by grinding off a portion of the stator bars. In addition, the pulp used should be a long-fibered pulp which is sensitive to cutting. A western softwood bleached sulfite was chosen.

RESEARCH PLAN

Figure 2 indicates the fibers and fractions to be procured and processed in "high-intensity" Valley beating. The compositions have been chosen so that values of $\overline{\mu}_f$, $\overline{\ell}$, $\ell_f$, and $t_f$ could be independently varied, and their effects on cutting and fines generation (and hopefully $P_N$ measurements) assessed. Independent control of these variables, of course, is not possible with pulp - smaller fiber length fractions will undoubtedly have different values of $\mu_f$ and $t_f$, for example. Hence, the use of rayon model fibers will hopefully supplement the fiber cutting results with pulp fibers. Rayon has a wet tensile strength similar to that of sulfite pulp.

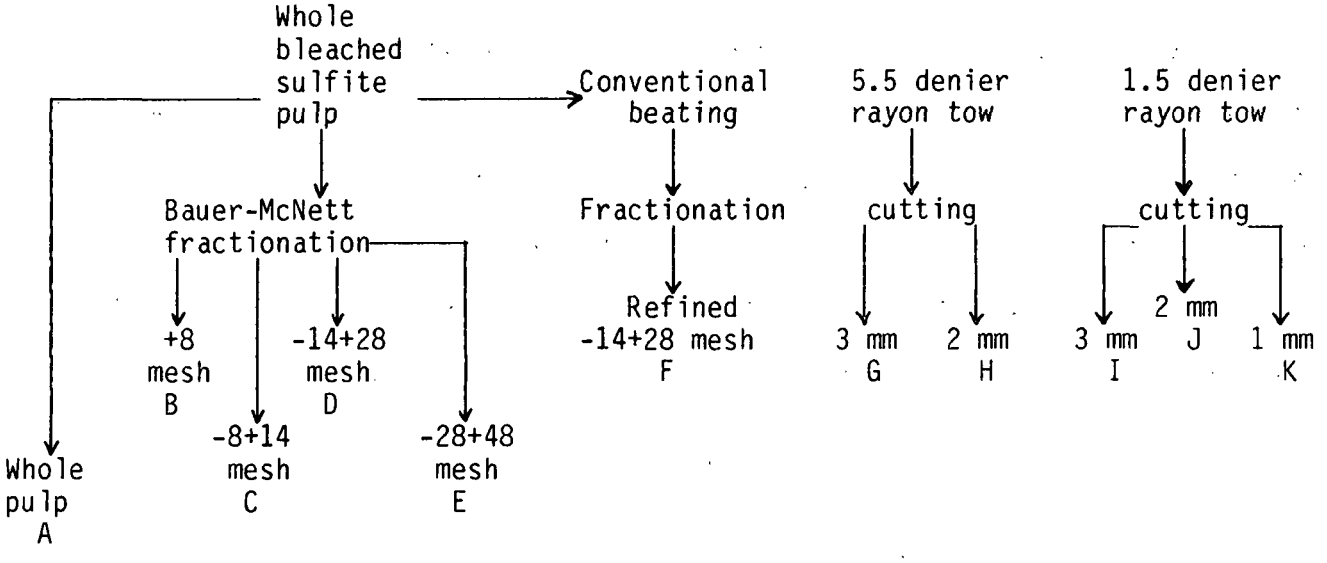


Mixtures to be processed:

| | Pulps | | | | | | | | | | | | Pulp + Rayon | | Rayon | | | |
|---|---|---|---|---|---|---|---|---|---|---|---|---|---|---|---|---|---|---|
| 95% undyed portion | A | A | A | A | B | C | D | D | E | A* | F | C | I | J | H | H | H | H |
| 5% dyed portion | A | C | D | E | B | C | D | C | C | C | C | E | C | C | G | I | H | K |

*Plus 5% locust bean gum.

Figure 2. Fiber to be processed in "high-intensity" beating.

The smaller (5%) component of the mixtures will be dyed and characterized as to zero-span tensile, fiber length, and fiber thickness. After beating of the mixtures, they will be fractionated on the Bauer-McNett classifier, and the distribution of dyed material in each fiber length class will be quantified by brightness measurements on the fractions. This will indicate the tendency of the dyed material to be cut or to be the source of fines, etc., in the case of wood fibers.

The measurement of torque $\Lambda$ during these runs permits the calculation of apparent coefficients of friction $\mu$, as well as net power P, hopefully to elucidate the influence of pulp properties such as $\bar{\ell}$ on their values.

Figure 3 lists 18 tasks designed to test the theoretical model relating refining severity to fiber cutting and fines generation. The lines between boxes indicate which tasks are prerequisites for others to be carried out. Double-lined boxes indicate tasks which have been substantially completed as of this writing. Appendix I gives some experimental detail of these tasks. The following section presents results obtained from tasks 9 and 4.

## RESULTS AND DISCUSSION

### EFFECTS OF LOAD ON BEATING RESPONSE

Table 1 lists beating parameter data obtained at the four levels of load studied with the bleached sulfite pulp. The apparent coefficient of friction of the pulp rapidly decreases initially, but eventually levels off with beating as the pulp develops a slimy character. The initial coefficient of friction is difficult to determine, but the final coefficient appears to be independent of load. Steenberg (6) reported values of 0.06 to 0.14 for the initial coefficient

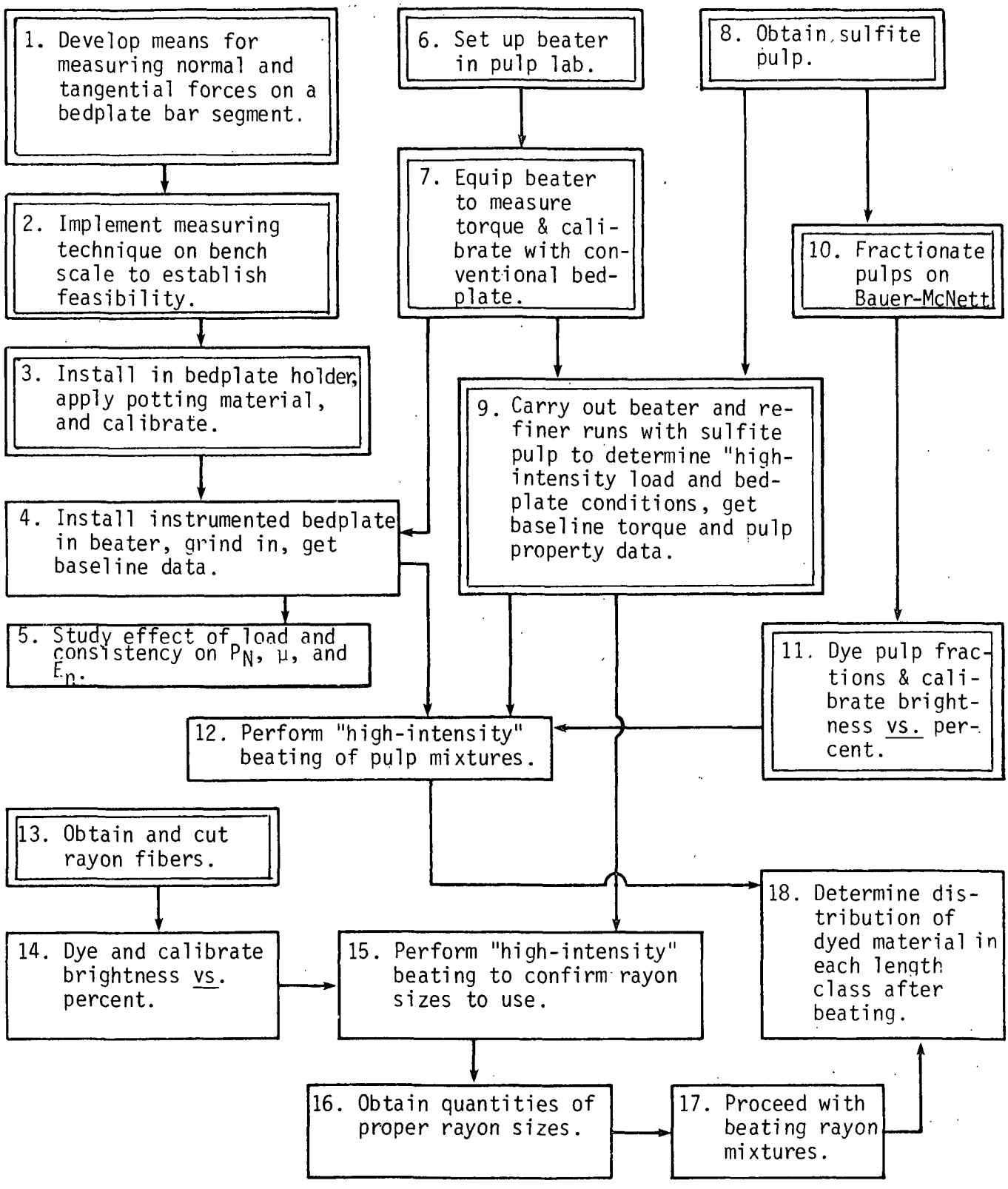


Figure 3. Experimental plan.

Table 1. Beating parameters as function of bedplate load[a].

| Load (g on lever arm) | Total beating time, min | Power, hp[b] No-load $P_o$ | Gross $P_t$ | Net $P_n$ | Net Specific Energy $E_n$ Sample | Cumulative | App. Coeff. of Friction, $\mu$ | Sp. Edge Load, Ws/m |
|---|---|---|---|---|---|---|---|---|
| 5500 | 5 | 0.22 | 0.33 | 0.11 | 0.99 | 0.99 | 0.15 | 0.30 |
| (standard) | 10 | 0.21 | 0.30 | 0.09 | 0.82 | 1.81 | 0.12 | 0.23 |
| | 15 | 0.20 | 0.28 | 0.08 | 0.73 | 2.54 | 0.11 | 0.20 |
| | 20 | 0.19 | 0.26 | 0.07 | 0.80 | 3.34 | 0.11 | 0.20 |
| | 30 | 0.18 | 0.25 | 0.07 | 1.56 | 4.89 | 0.10 | 0.18 |
| 8250 | 3 | 0.21 | 0.38 | 0.17 | 0.88 | 0.88 | 0.15 | 0.44 |
| (1.5 x std.) | 8 | 0.20 | 0.33 | 0.13 | 1.20 | 2.08 | 0.12 | 0.34 |
| | 13 | 0.19 | 0.31 | 0.12 | 1.17 | 3.25 | 0.11 | 0.31 |
| | 18 | 0.18 | 0.30 | 0.12 | 1.22 | 4.47 | 0.11 | 0.31 |
| | 23 | 0.18 | 0.30 | 0.12 | 1.32 | 5.79 | 0.10 | 0.31 |
| 16500 | 3 | 0.22 | 0.52 | 0.30 | 1.61 | 1.61 | 0.14 | 0.80 |
| (3.0 x std.) | 6 | 0.21 | 0.45 | 0.24 | 1.37 | 2.98 | 0.11 | 0.63 |
| | 9 | 0.20 | 0.42 | 0.22 | 1.29 | 4.27 | 0.10 | 0.57 |
| | 12 | 0.19 | 0.41 | 0.22 | 1.36 | 5.63 | 0.10 | 0.57 |
| | 15 | 0.19 | 0.42 | 0.23 | 1.52 | 7.15 | 0.10 | 0.60 |
| 24750 | 2 | 0.22 | 0.70 | 0.48 | 1.69 | 1.69 | 0.15 | 1.28 |
| (4.5 x std.) | 4 | 0.22 | 0.56 | 0.34 | 1.25 | 2.94 | 0.11 | 0.89 |
| | 6 | 0.21 | 0.51 | 0.30 | 1.19 | 4.13 | 0.10 | 0.80 |
| | 9 | 0.21 | 0.50 | 0.29 | 1.83 | 5.96 | 0.09 | 0.77 |
| | 12 | 0.19 | 0.50 | 0.31 | 2.04 | 8.00 | 0.09 | 0.80 |

[a]Average of duplicate runs at each load; calculation methods described in Section 9 of Appendix I.
[b]The rotor speed $\Omega$ was 500 $\pm$ 7 rpm.

of friction of dissolving pulp in a Valley beater, with higher values observed at lower loads and higher consistencies.

The changing frictional character of the pulp produced corresponding changes in both the no-load and the net power consumption, as well as the specific edge load. These values were high initially but dropped rapidly, then leveled off.

Figures 4-6 illustrate the effects of load on the energy efficiency of pulp property development. To achieve a given level of freeness, density, or tensile strength, significantly less net energy is required under gentler refining conditions. This is similar to the behavior of hardwood pulps, but is the opposite of that observed with softwood kraft (1,3). In addition, Fig. 5 depicts behavior which is quite different from that reported by Amero (7) with softwood kraft pulps. He noted that the slope of the net specific energy-density line, a measure of refining efficiency, was independent of refiner size, plate design, throughput, consistency, and type of kraft pulp. Apparently the sulfite pulp used in the present study possesses a sensitivity to refining severity which is totally different from softwood kraft pulps.

Figures 7-11 illustrate the pulp property relationships obtained at the various loads. As functions of density, the levels of tear strength and scattering coefficient are essentially unaffected by load, while freeness shows only minor influence. However, the benefits of gentler refining on tear-tensile and tear-density relationships are obvious. In addition, the initial rate of fiber cutting and fines generation is very sensitive to beating severity (Fig. 12).

The load levels of 3.0 and 4.5 times the standard produce sufficient fines and fiber shortening to constitute reasonable conditions for a "high-intensity" beating study. Since the highest level shows the beginnings of a tensile plateau (Fig. 11), the level of 3.0 times standard may be preferable. Fortunately, it does not appear necessary to reduce bedplate area or width to study "high-intensity" beating of this pulp.

## FORCES ON BAR SEGMENT

As of this writing, the only force data obtained was that observed on the oscilloscope during the grinding-in of the second instrumented bar segment.

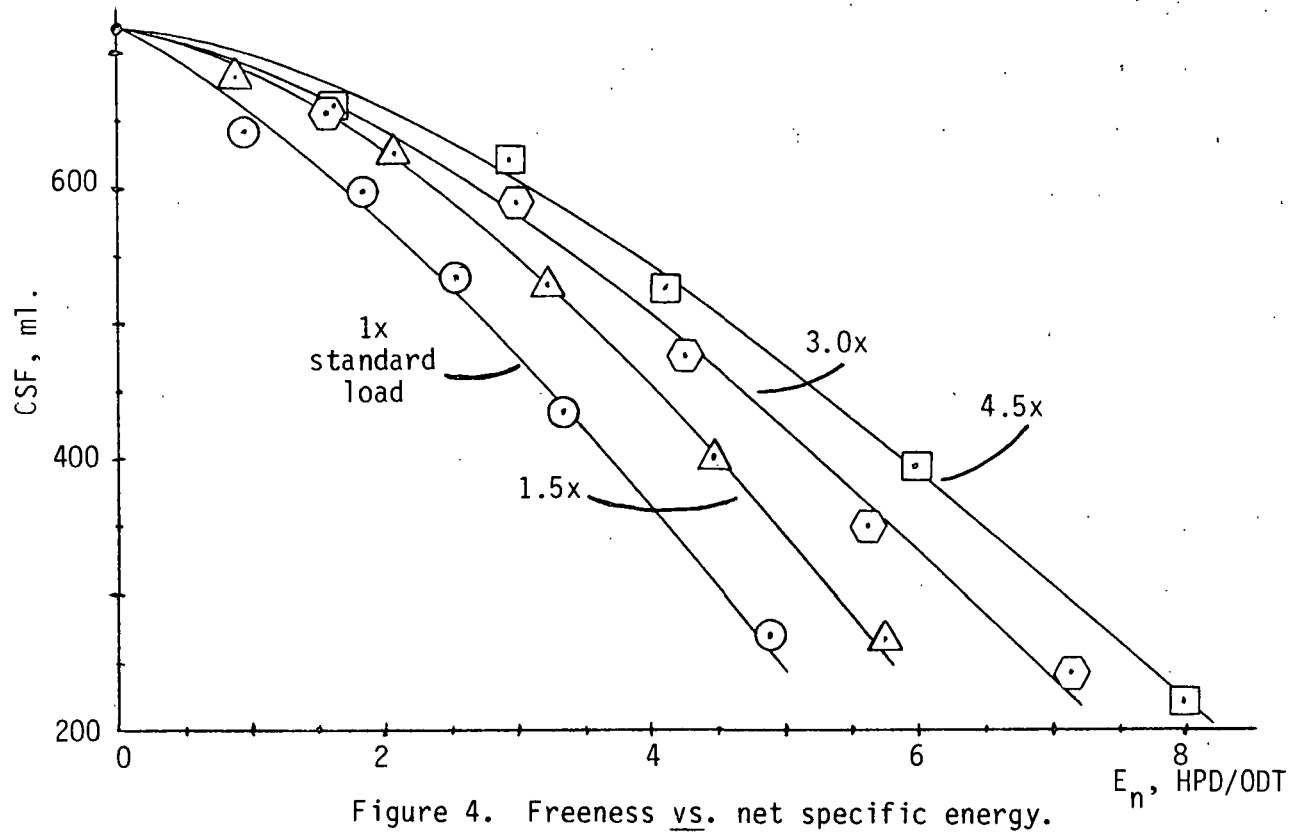


Figure 4. Freeness vs. net specific energy.

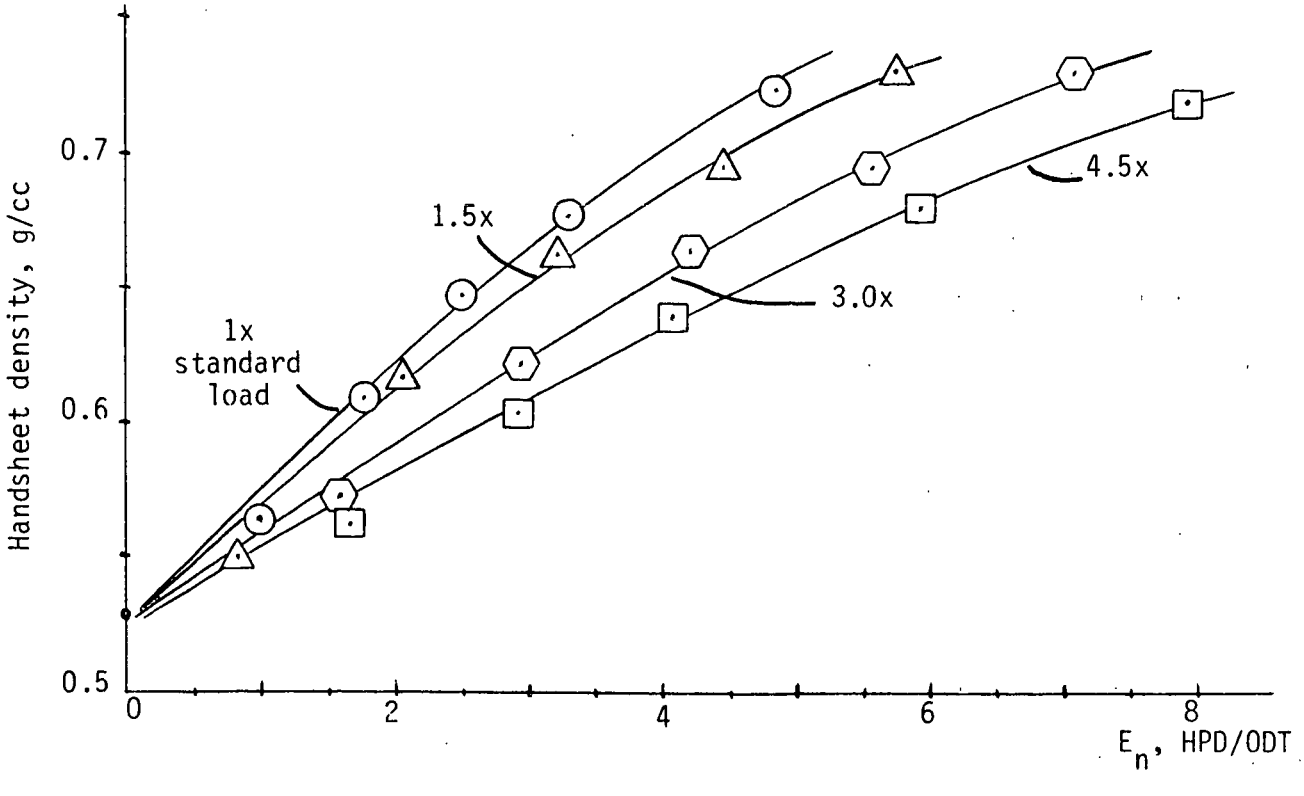


Figure 5. Density vs. net specific energy.

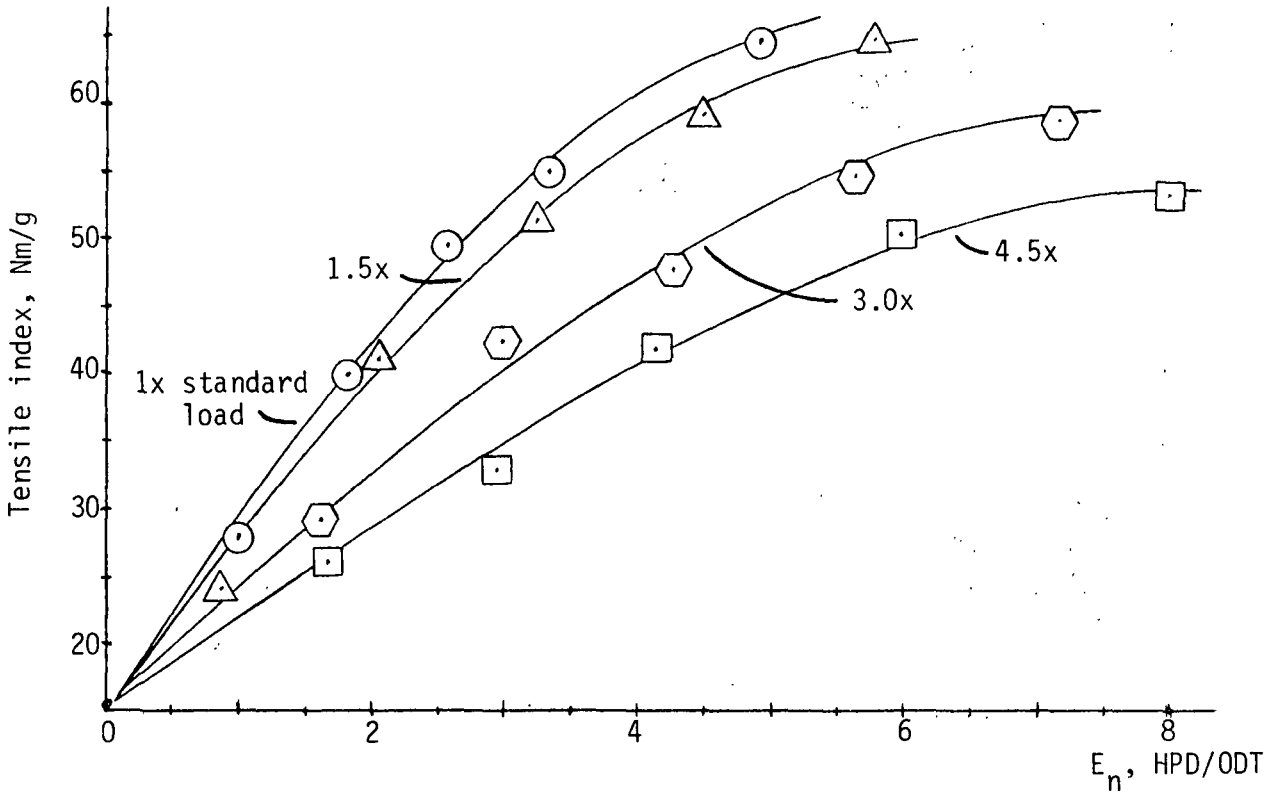


Figure 6. Tensile strength vs. net specific energy.

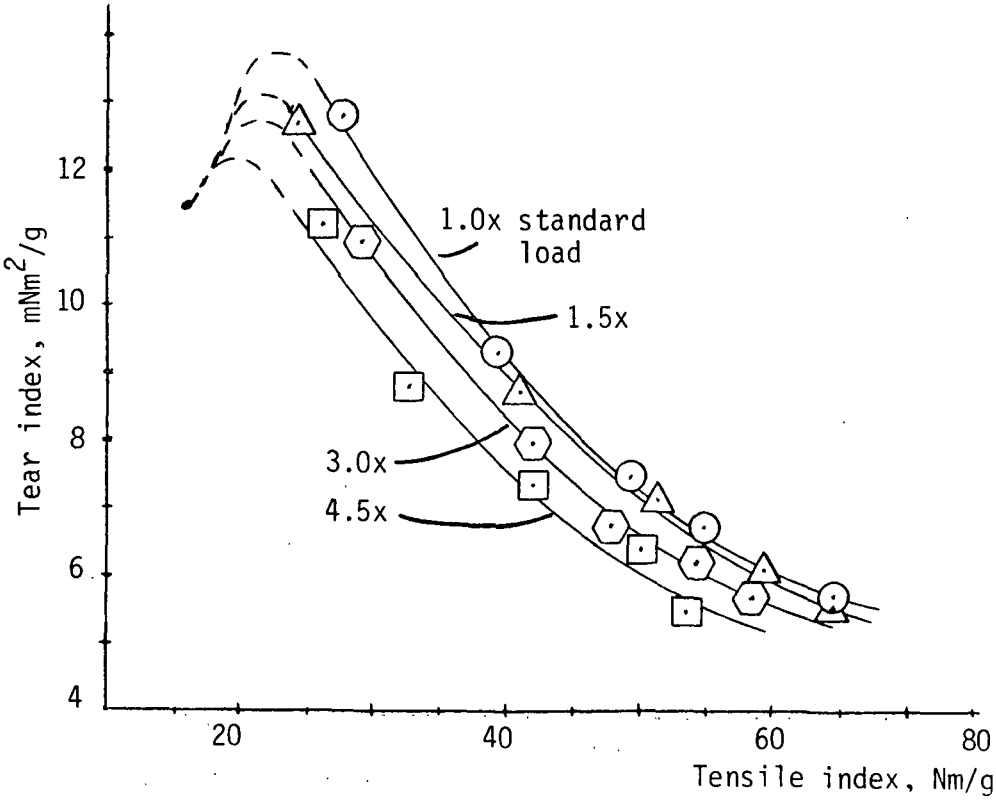


Figure 7. Tear vs. tensile strength.

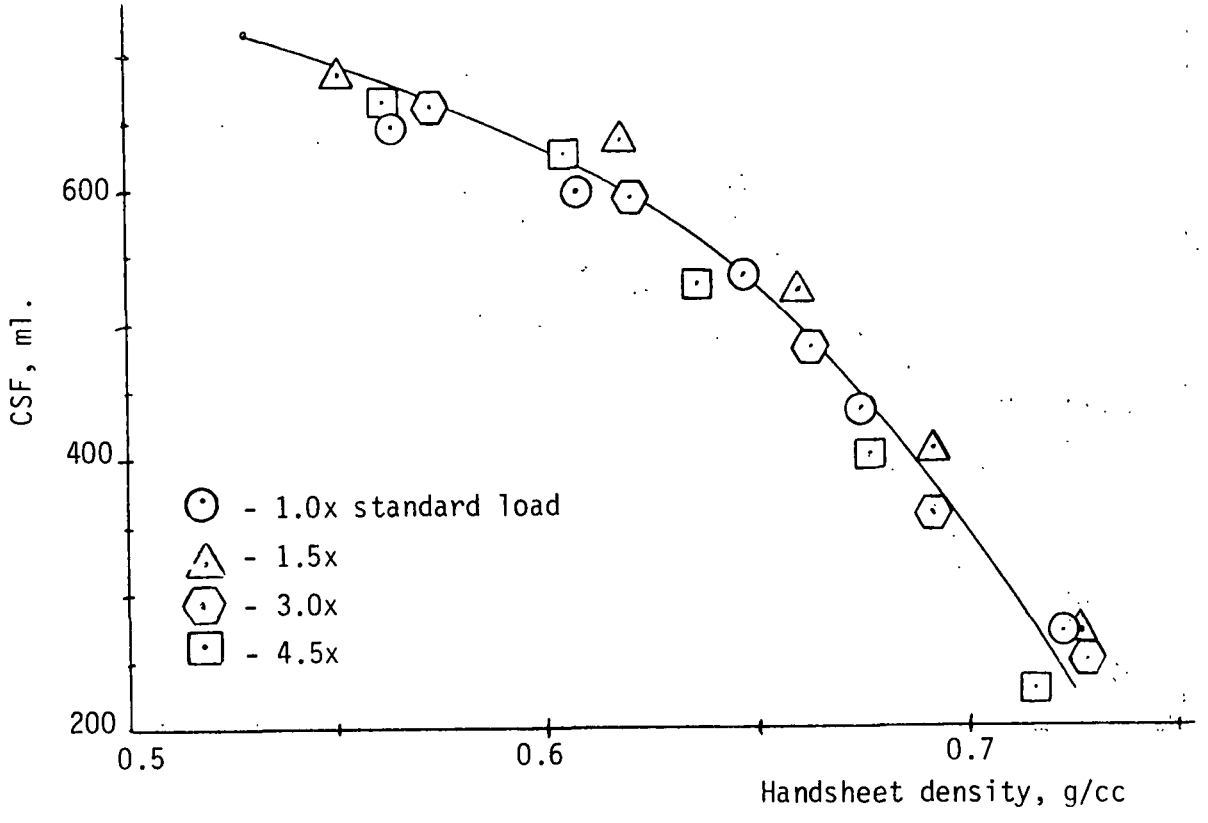


Figure 8. Freeness vs. density.

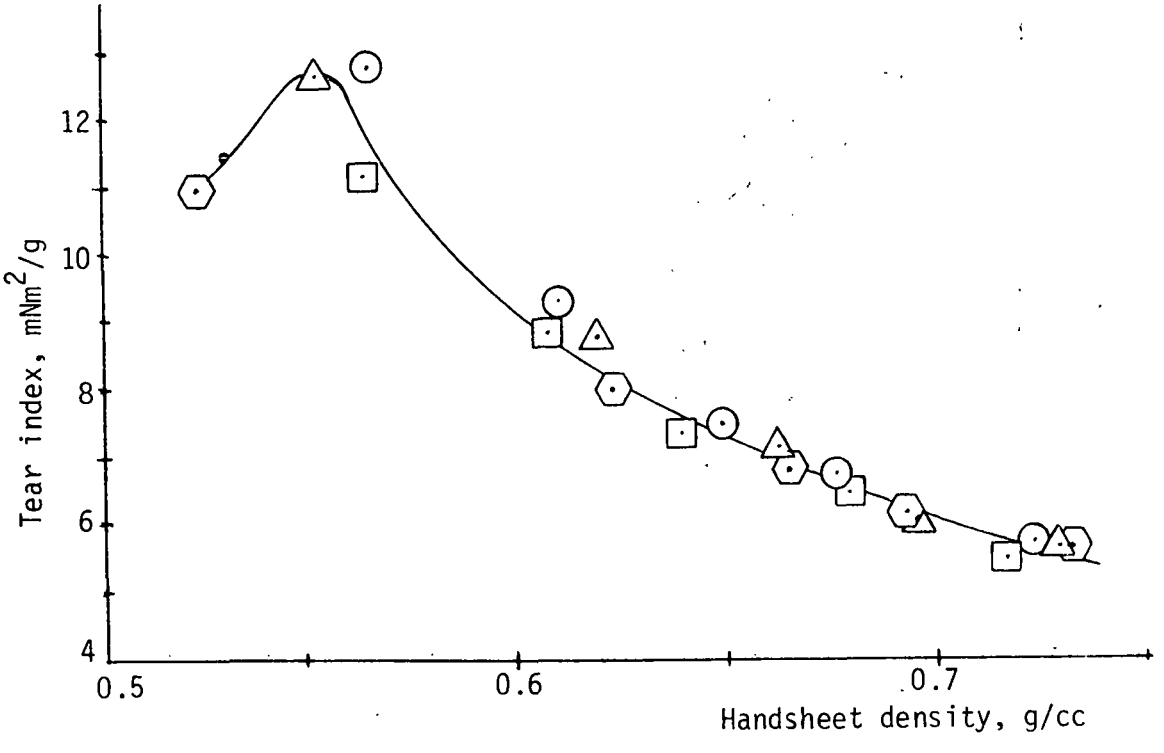


Figure 9. Tear strength vs. density.

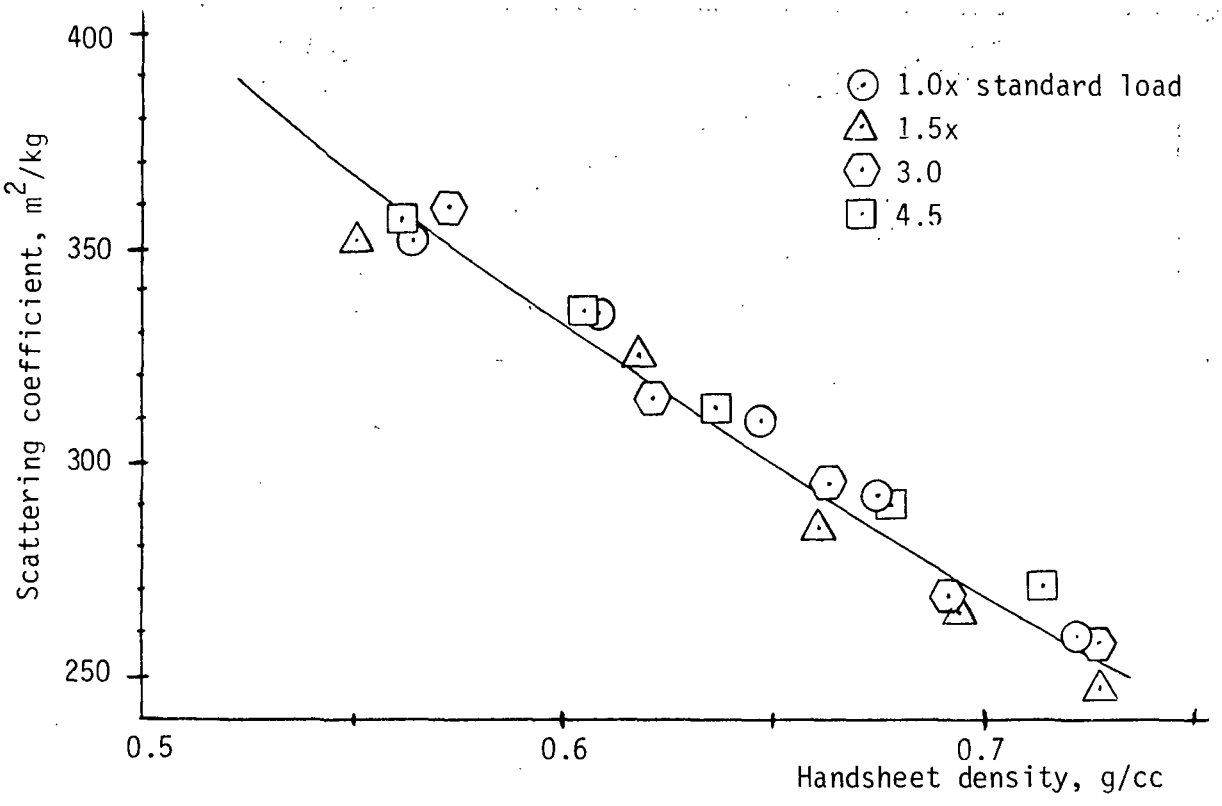


Figure 10. Scattering coefficient vs. density.

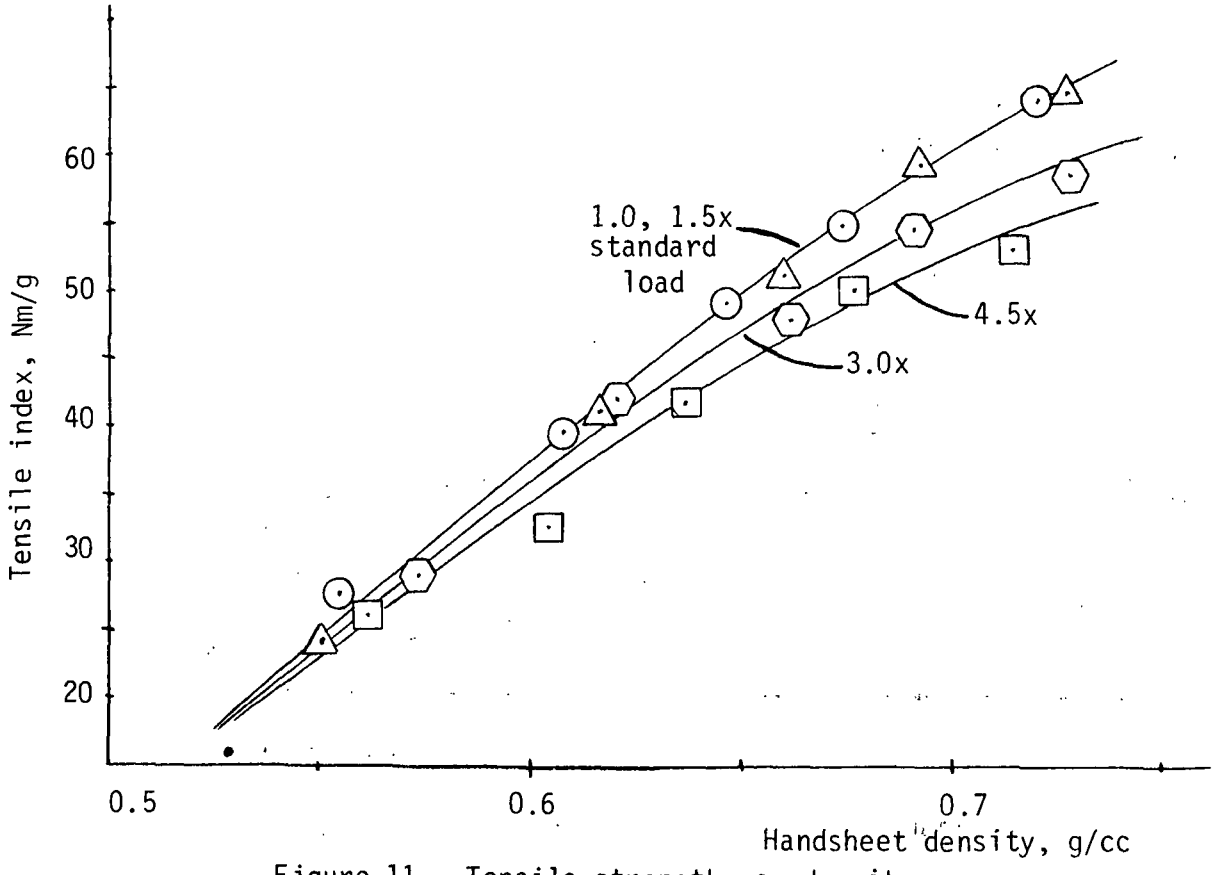


Figure 11. Tensile strength vs. density.

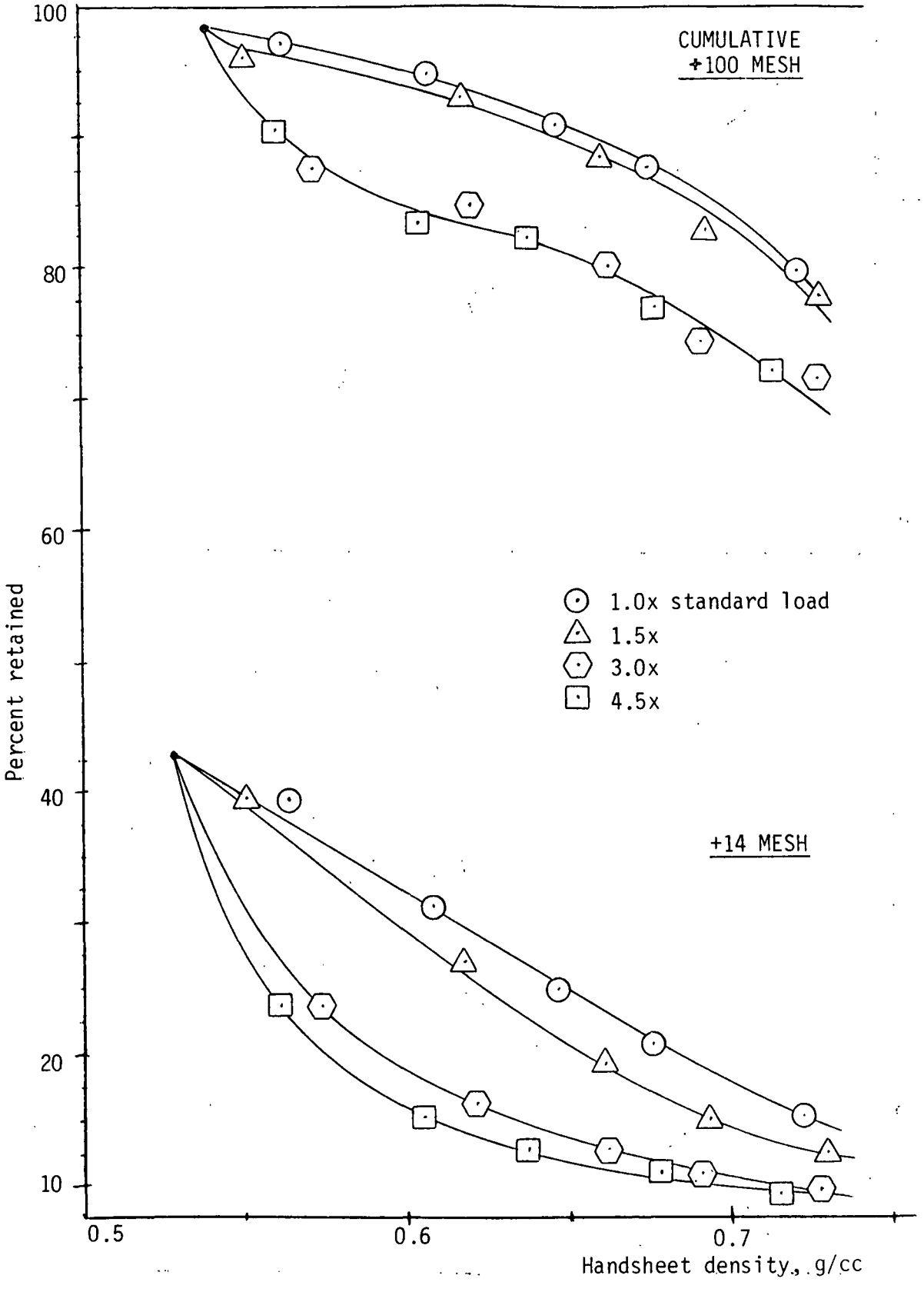


Figure 12. Fiber classification vs. density.

During this time, maximum average levels of ca. 0.3 lb were observed in both the normal and tangential outputs. In addition, the tangential output had a negative signal of ca. 0.2 lb, which followed the initial positive signal, for a total signal duration of ca. 1 ms. The time between impacts was 3.7 ms (as expected), and the duration of the normal signal was almost 1 ms, corresponding closely to the rotor bar width of 3/16 inch at a rotor speed of 0.20 in./ms. Sometimes the start of the tangential signal preceeded the start of the normal signal. Considerable variation in the signal shapes was observed during the course of the grinding-in. Near the end, occasional maxima of up to 1 lb were observed in the normal output.

The interpretation of these preliminary results must be very tentative, since the grinding-in conditions are quite unlike conventional beating: the changing nature of the bedplate, the presence of the abrasive, and the clamping of the lever arm in fixed position rather than the application of constant load. Several points are worthy of comment, however. The tangential reading was surprising, being nearly equal to that of the normal, rather than the 0.1-0.2 ratio expected as a coefficient of friction. Also, the shape of the tangential signal, with a negative response following a positive one, is puzzling. A possible explanation would be that most of the tangential signal is due to a pulse transmitted through the preceeding wood filling as the rotor bar approaches. This would cause a forward deflection of the bar segment (which would not correspond to a force experienced by the fiber), perhaps followed by a negative deflection in springing back beyond the neutral position. Further data is needed to clarify this point.

## CONCLUSIONS AND IMPLICATIONS

1. The measurement of torque on the Valley beater rotor shaft is a reasonable technique for determining specific energy and apparent coefficient of friction. The latter varies from above 0.15 to 0.09 with the sulfite pulp used, decreasing assymptotically to the lower figure with beating.
2. A Valley beater bedplate load of three times the standard or higher, produces significant fines and fiber cutting with the pulp used. This will be sufficient for a study of "high-intensity" beating, without the need to reduce bedplate area.
3. With the sulfite pulp used, gentler refining conditions showed:
   - superior energy efficiency in the development of pulp properties (density and tensile increase, and freeness reduction)
   - improved retention of fiber length (less cutting)
   - improved relationships between properties (tear-tensile and tensile-density).

   This is similar to the behavior of hardwood pulps, but contrasts with that of softwood kraft pulps, especially with respect to the (opposite) energy effect. This has practical implications in the consideration of very gentle (separate) refining of sensitive pulps such as this or hardwoods: a reduction in gross specific energy may be seen with gentler refining depending upon how the refining intensity is reduced and how it affects no-load power. Any credit in energy savings should be included with the benefit of possible increased usage of the cheaper pulps because of superior properties and weighed against any changes in refining capacity and the need for separate systems.

4. The fact that reasonable levels of normal force were measured on the expected time scale indicates that the strain gage setup has good potential for providing the needed $P_N$ data. The shapes and magnitudes of tangential signals may indicate an interference caused by the presence of the wood fillings; further work will clarify the meaning of this signal.

## FUTURE WORK AND ITS BENEFIT

- Complete the experimental plan of Fig. 3 with sulfite pulp

  This effort is expected to establish the significance of local normal pressure as a key parameter in the severity of action experienced by fibers during refining, as well as provide evidence to support or refute the theoretical model of severity previously derived.

- Repeat task 5 with hardwood pulps

  This is to establish the universality of conclusions drawn with the model sulfite pulp and to provide specific data with pulps of greater commercial significance.

- Instrument the Sprout-Waldron Twin-Flo refiner for similar data acquisition

  Assuming the attempts to measure $P_N$ in the Valley beater have been successful, it will be desirable to similarly instrument the 12-inch refiner to measure $P_N$, and thrust T (the machine is already equipped with torque sensor). Questions of particular interest relate to the breadth of distribution of $P_N$ at a given point on a stator as a function of time and as a function of radial and circumferential position in the refiner. Results from this may point the way to narrowing the distribution of $P_N$, and hence optimizing the intensity and energy consumption. This may be accomplished through control of refiner precision or changing taper or bar crossing frequency in

different zones of the refiner, for example. A successful implementation here would probably then lead to the step of instrumenting a commercial machine.

## REFERENCES

1. Levlin, J-E. Some differences in the beating behavior of softwood and hardwood pulps. Preprint, International Symposium on Fundamental Concepts of Refining, Appleton, WI, Sept., 1980, p. 51-60; Pulp Paper Can. 81(12):51-9 (1980).

2. Levlin, J-E. Characterization of the beating result. Ibid, p. 131-38.

3. Canon, J. G.; DeFoe, R. J. Benefits of low intensity refining. Proceedings, TAPPI Papermakers' Conf., Atlanta, GA, April, 1984, p. 41-5.

4. Sinkey, J. D. Refining of chemical pulps for improved properties. Status Report to the IPC Engineering Project Advisory Committee, Project 3384, February 10, 1984.

5. Goncharov, V. N. Force factors in a disk refiner and their effect on the beating process. Bumazh. Prom. no. 5:12-14(May, 1971).

6. Steenberg, B. In Symposium on Beating. Proc. Tech. Sect. Brit. Paper and Board Makers' Assoc. 32(2):388-95(1951).

7. Amero, B. A. Refining optimization: Single-pass disk refiners vs. multiple-pass laboratory beaters. Preprint, International Symposium on Fundamental Concepts of Refining, Appleton, WI, Sept., 1980, p. 179-89.

# APPENDIX I

## TECHNIQUES AND PROCEDURES

The following is a discussion of experimental methods used in carrying out the tasks depicted in Fig. 3.

1. Develop means for measuring normal and tangential forces on a bedplate bar segment

After consideration of a number of options, it was decided to approach this task by affixing strain gages to a beam to which the bar segment was attached. Accordingly, a bar segment and beam assembly was machined from a single piece of 440C stainless (Fig. 13). The bar is 1/8-inch square by 1/2-inch high in the center of a 1/4-inch wide 0.080-inch thick beam to be supported at two ends, one inch apart. Strain gages affixed along the beam, on both sides of the bar, are incorporated into Wheatstone bridge circuits to give readings proportional to normal and tangential loads on the bar. Static calibration was used to establish sensitivity and to quantify cross-talk between normal and tangential signals.

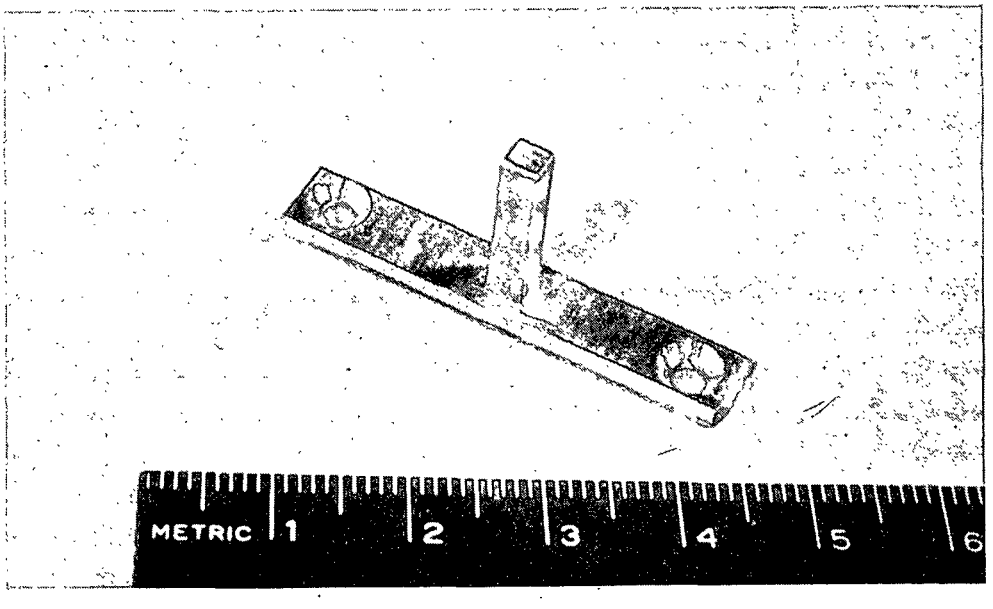


Figure 13. Bar segment and beam prior to strain gage attachment.

2. Implement measuring technique on bench scale to establish feasibility

For the first attempt at instrumenting a bar segment, a total of 20 strain gages (type EA-06-031ME-120* in strips of 10) were attached to the beam and connected as shown in Fig. 14. A preliminary calibration was carried out with the Instron tensile tester by mounting the beam in a small specially-made brass holder and applying known loads in the normal and tangential directions. The output from the "normal" bridge cell gave a linear response with normal load of 0.81 V/lb force in the range of 0-30 lb. There was a slight dependence on the position of application of the normal force (leading edge vs. trailing edge). The output from the "tangential" bridge with normal loading varied from -0.09 to 0.07 V/lb, dependent on position of loading. The application of tangential forces gave linear output from the "tagential" bridge of 0.95 V/lb with less than 0.01 V/lb "normal" bridge output. At the level of normal loading of 41 psi calculated above for standard beating conditions, the force on a 1/8-inch square bar segment would be 0.6 lb; the "high-intensity" beating conditions would probably be several times that, but certainly not exceeding the 30 lb level in this preliminary calibration. Hence, it appeared that $P_N$ could be measured with this technique with suitable electronic corrections for cross-talk with a calibration voltage.

3. Install in bedplate holder, apply potting material, and calibrate

The instrumented bar was removed from the small holder and installed in a specially-made brass bedplate holder (Fig. 15). The central bar of a seven-bar bedplate assembly was cut in two and shortened prior to heat-treating to provide an opening for the instrumented bar segment. The bars

*Micro-Measurements Div., Measurement Group, Inc., Raleigh, NC.

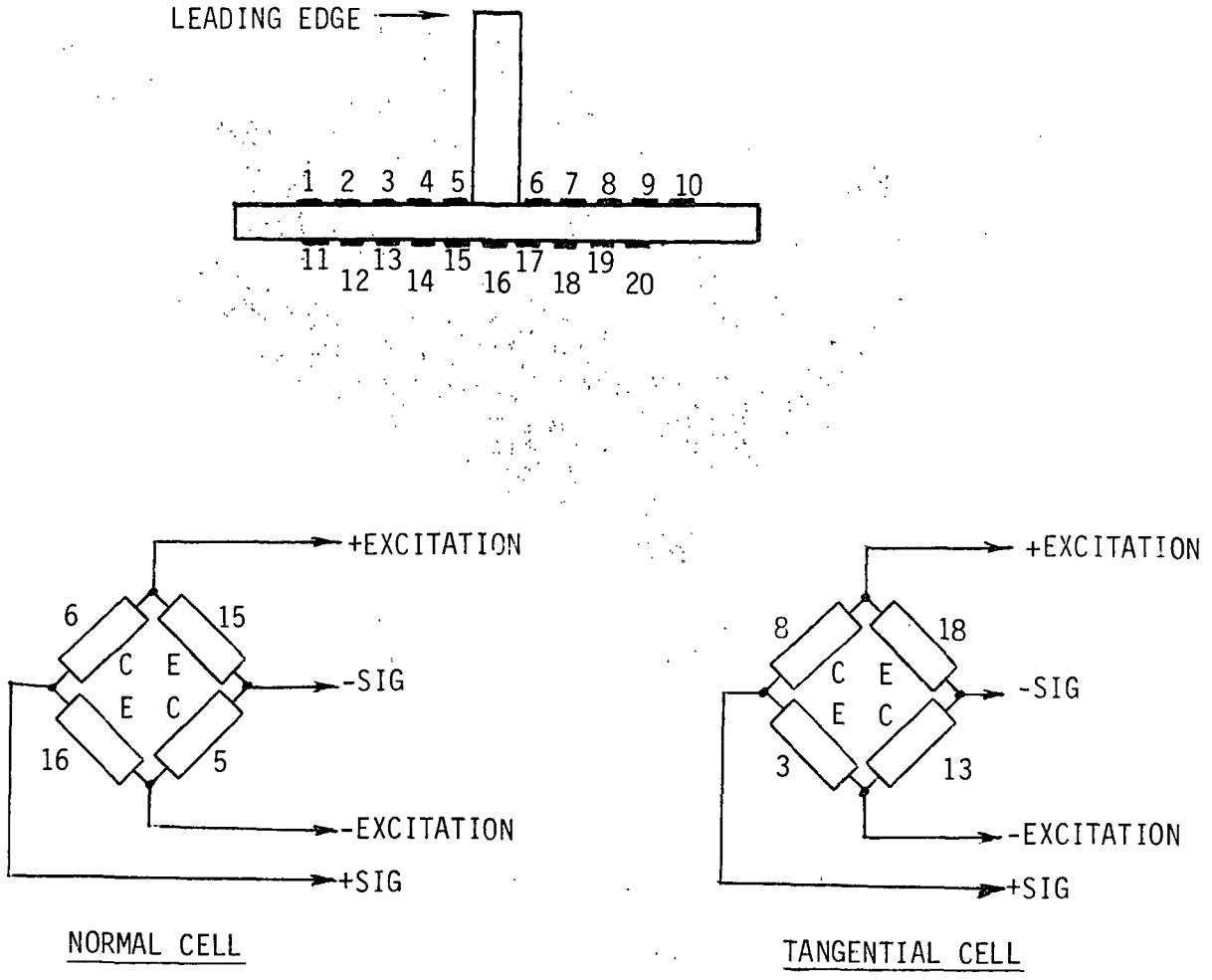


C - Strain gage under compression
E - Strain gage under extension
Excitation: +5V dc
Amplifier Gain: 5625

Figure 14. Strain gage placements on beam and in Wheatstone bridge circuits - initial experiment.

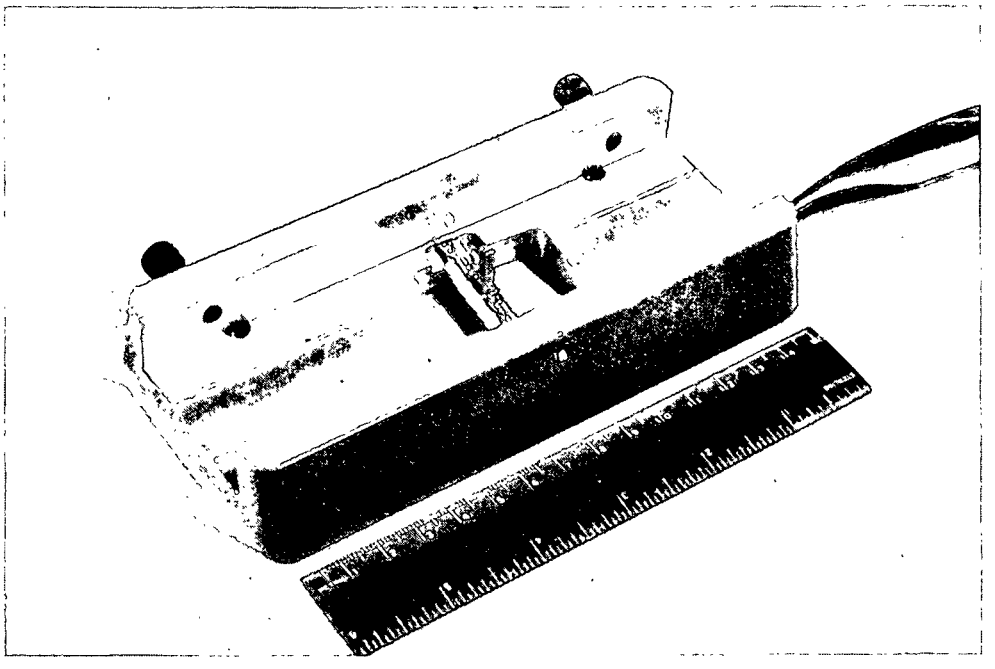

Figure 15. Strain gages attached to beam, bar segment installed in bedplate holder.

were then heat-treated, assembled with the oak fillings and riveted together, and placed in the brass holder over the bar segment (Fig. 16). Prior to being potted, a recalibration was carried out in the range of 0-11 lb force in the two directions. Normal output was 0.80 V/lb normal force; tangential output 0.95 V/lb tangential force; cross-talk was about one-tenth these responses and was electronically compensated.

The area around the instrumented bar segment and the beater bars and oak fillings was potted with a silicone sealant as were the openings around the ribbon cable leads. The bar assembly itself was potted with a steel putty (Devcon).

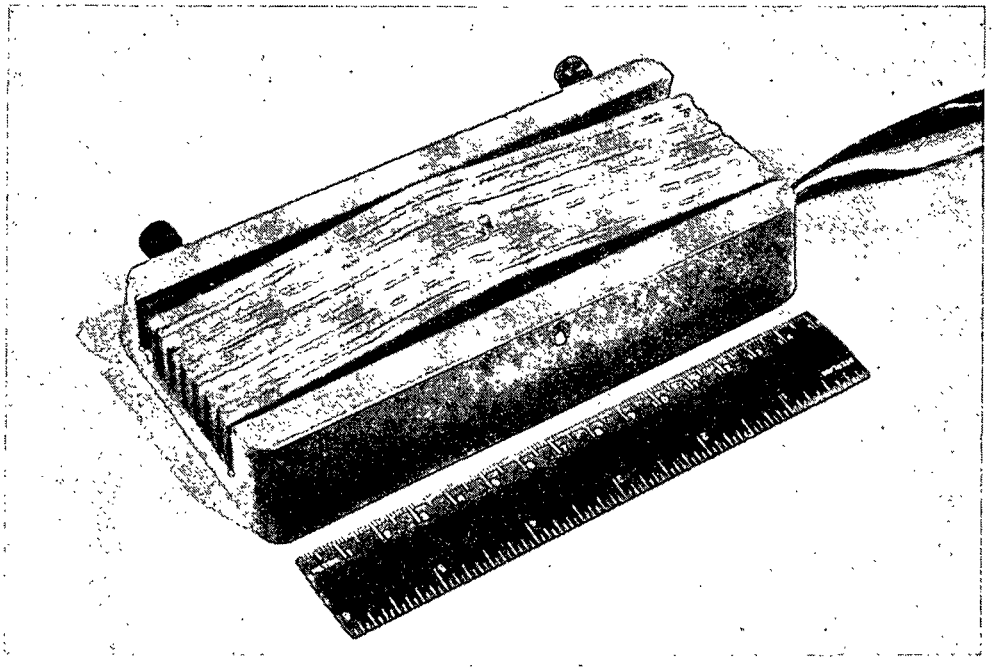

Figure 16. Beater bar assembly in place around instrumented bar segment, prior to potting.

4. Install instrumented bedplate in beater, grind in, get base-line data

After installing the assembly in the beater, about 1 mm of bar surface was ground off with a pulp-abrasive slurry to bring the tops of the beater bars flush with the top of the bar segment. Upon connecting the leads to an oscilloscope during the grinding, it was found that several of the strain gages on the top side of the beam were no longer functional. As the grinding continued, signals were lost from all the gages on the top side, while those on the bottom remained intact.

The assembly was removed from the beater, taken apart, and inspected. Microscopic examination revealed considerable corrosion of the strain gages on the top side of the beam. Those on the bottom side had been covered with an extra layer of epoxy and appeared to be intact. It was theorized that the corrosion was induced by acetic acid in the silicone sealant.

A second bar was fitted with strain gages, this time fewer in number, as illustrated in Fig. 17. All gages were coated with epoxy and the assembly dipped in melted beeswax prior to installing in the bedplate holder.

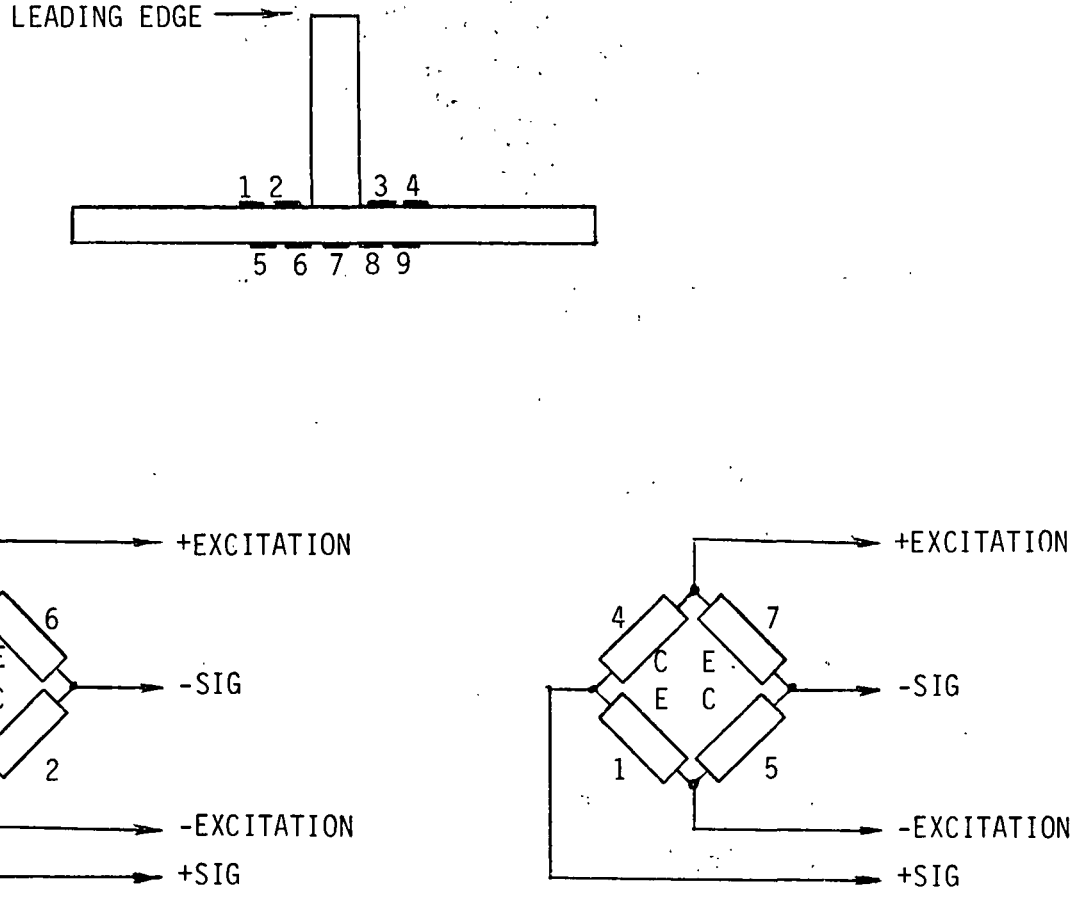


Figure 17. Strain gage placement - second beam.

After being potted as before, this assembly was installed in the beater and ground in, while observing normal and tangential signals on an oscilloscope. At the point when a carbon paper impression revealed uniform contact across the entire bedplate, including contact with the top of the bar segment, the assembly was removed for calibration. The strain gages were connected in the bridge circuits in several configurations and calibration responses determined. The normal and tangential configurations of Fig. 17 were found to be least sensitive to the position of normal loading (leading edge to trailing edge), with reasonable level of sensitivity and cross-talk, and so was deemed the preferred configuration.

The beater shaft was equipped with a two-pole magnetic rotor and Hall cell effect switch as a triggering mechanism for obtaining the Wheatstone bridge signals for one rotor bar crossing per revolution. For this preliminary work, the signals were observed on an oscilloscope system for recording and analyzing the force data in the two directions.

5. Study effect of load and consistency on $P_N$

This will be carried out by performing beater runs on whole pulp at loads of 1X and 3X standard and at consistencies of 1% and 2% in addition to the standard 1.5%. Torque and $P_N$ data will be supplemented by pulp testing results.

6. Set up beater in pulp lab

This task and the following one, of course, were completed prior to task 4 above. A stainless steel TAPPI Standard Valley beater was installed for this project on a specially constructed base to accommodate the torque sensing device and a 1 hp motor.

7. Equip beater to measure torque, calibrate with conventional bedplate

The shaft on the beater roll was pressed out and replaced with a longer one to accommodate the torque sensor between the roll and the drive pulley. The shaft was equipped with a G.S.E. Model 2104-100 torque sensor with a range of 0-100 in.-lb (Fig. 18). Calibration was carried out by suspending known weights from a 20-inch lever arm connected to the shaft. A Texmate voltmeter (0-2 V) is used to read out the torque.

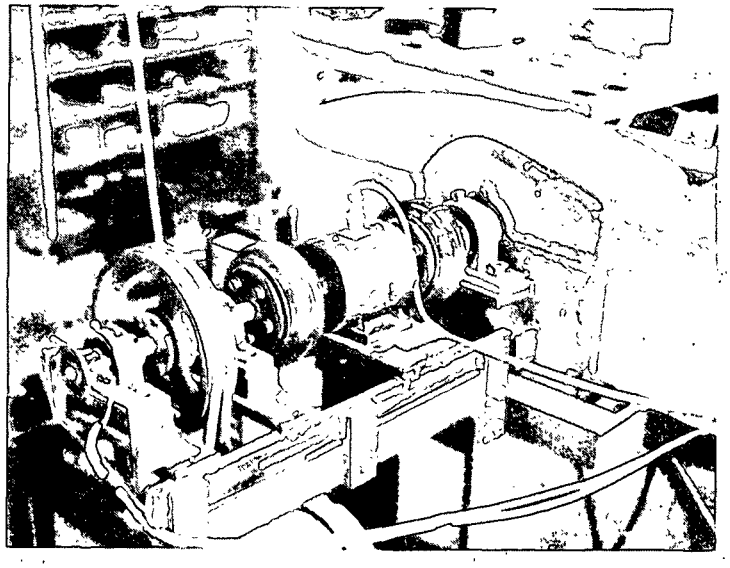

Figure 18. Valley beater with rotor shaft modification to accommodate torque sensor.

In addition, the end of the shaft was equipped with a magnetic rotor and Hall cell effect switch; signals from this are converted to voltage readouts proportional to rpm through Electro Corp. tachometers and 0-2 V Texmate voltmeters.

The beater was then calibrated according to TAPPI Standard T200-os 70, with a new, conventional bedplate.

8. Obtain sulfite pulp

The pulp chosen for this study was a Western softwood bleached sulfite ("Puget Prime"). It is a long-fibered pulp available in fairly uniform quality and sensitive to fiber cutting in refining.

9. Carry out beater and refiner runs to determine "high-intensity" conditions and get base-line torque and pulp property data

The beater runs were carried out by following TAPPI Standards, with the exception of the load on the bedplate. Runs were performed at bedplate lever arm loads of 1.0, 1.5, 3.0, and 4.5 times the standard 5500 g. In addition, Sprout-Waldron Twin-Flo refining of the pulp will be carried out in a similar range of SEL to provide comparative base-line data with beater results.

The following notation is used for the beater data obtained:

$\Lambda_i$ = torque in inch-pounds

$\Omega$ = rotor speed in rpm

$P_i$ = power in hp

$E_i$ = specific energy applied between sampling times, hp day/o.d. t.

$t$ = time since previous sampling, min

$W$ = weight of pulp remaining in the beater after the previous sampling in o.d. g (all samples were 18.6 g o.d.)

$T$ = load applied on the beater arm, in g

i subscript denotes the value for total gross value (i = t), no-load value (i = o), or net (i = n); i.e., $P_n$ is net power, $\Lambda_n$ net torque, etc.

The following formulas were used to calculate other parameters:

$$\text{Power } P_i = (\Lambda_i \text{ in.-lb})\left(2\pi\Omega\frac{\text{rad}}{\text{min}}\right)(\text{ft}/12 \text{ in.})(\text{hp}/33000 \text{ ft. lb/min}) = \frac{\Lambda_i\Omega}{63025} \text{ hp}$$

Specific energy applied between sampling times:

$$E_i = \frac{(P_i \text{ hp})(t \text{ min})(\text{hr}/60 \text{ min})(\text{day}/24 \text{ hr})}{(W \text{ g})(\text{lb}/454 \text{ g})(\text{t.}/2000 \text{ lb})} = 630.56\ P_i t \frac{\text{hp day}}{\text{ton}}$$

Apparent coefficient of friction:

$$\mu = \frac{(\Lambda_n \text{ in.-lb})(2.54 \text{ cm/in.})(454 \text{ g/lb})}{(9.69 \text{ cm})(T \text{ g})(\frac{17.9}{9} \text{ ratio})} = \frac{59.8\ \Lambda_n}{T}$$

Specific edge load:

$$SEL = \frac{(P_n \text{ hp})(745.7 \text{ W/hp})(60 \text{ s/min})}{(32 \frac{\text{rotor bars}}{\text{rev}})(\frac{7 \text{ stator impacts}}{\text{rotor bar}})(\frac{0.153 \text{ m}}{\text{stator bar}})(\Omega \frac{\text{rev}}{\text{min}})} = \frac{1305\ P_n}{\Omega} \frac{Ws}{m}$$

10. Fractionate pulps on Bauer-McNett

After considering the Sweco screen and Dynamic Drainage Jar as options for acquiring the needed quantities of pulp fractions B-E (Fig. 2), it was decided that the use of the Bauer-McNett Fiber Classifier would be more efficient. The procedure involved processing ca. 30 o.d. g samples of pulp in the apparatus for 30 min, using 8, 14, 28, and 48 mesh screens. The fractions caught on muslin cloths were put into separate plastic bags for subsequent fluffing and storage. Approximately 7000 g of pulp were processed.

11. Dye pulp fractions and calibrate brightness vs. percent

Aliquots of fractions C, D, and E were dyed with Chlorazol Black E and thoroughly washed on a fritted glass funnel. Mixtures of dyed portions of each fraction were made up and brightness R determined. Results are presented in Fig. 19.

12. Perform "high-intensity" beating of pulp mixtures

The objective of this task is to determine the initial rate of cutting and rate of fines generation from dyed, well-characterized fiber, when beaten with another pulp fraction under "high-intensity" conditions (mixtures of Fig. 2). The Bauer-McNett classifications and brightness of the screen fractions will be determined as functions of beating and related to the objective.

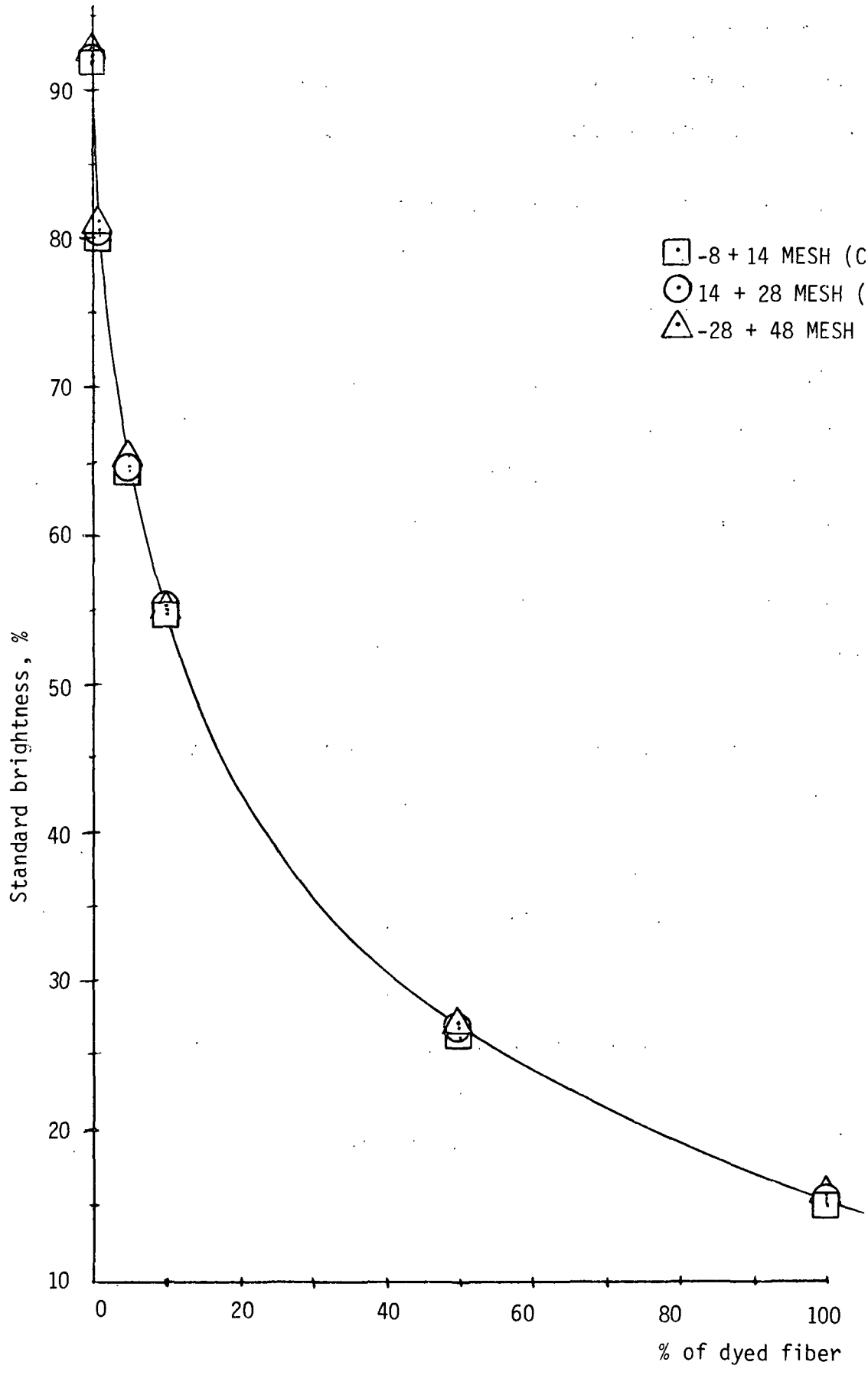


Figure 19. Brightness calibration of dyed/undyed pulp mixtures.

13. Obtain and cut rayon fibers

Rayon (1.5 and 5.5 denier) was obtained in the form of tow and cut into 3 mm lengths with a razor blade cutting arrangement.

14. Dye and calibrate rayon brightness vs. percent

The two rayon sizes will be dyed and mixed with pulp fraction C, D, and E and brightness vs. percent dyed rayon curves determined.

15. Perform "high-intensity" beating to confirm rayon sizes to use

Mixtures of each of the two rayon sizes with pulp A will be beaten (5% dyed rayon) and the rate of dyed fiber shortening assessed through brightness measurements on Bauer-McNett fractions.

16. Obtain quantities of proper rayon sizes

Based on the results of task 15, rayon fractions G through K, of the proper denier, will be obtained as cut fibers. Samples G and H should be resistant to cutting, but I, J, and K should be of a size which exhibits considerable cutting under the "high-intensity" beating conditions.

17. Proceed with beating rayon mixtures

The effects of rayon fiber length and denier will be assessed.

18. Determine distribution of dyed material in each length class after beating

The brightness measurements of Bauer-McNett fractions from tasks 12 and 17 will be converted to percent dyed fiber in each fraction, and the rate of shortening and fines generation from dyed fiber assessed.

THE INSTITUTE OF PAPER CHEMISTRY

Appleton, Wisconsin

Status Report

to the

ENGINEERING PROJECT ADVISORY COMMITTEE

Project 3480

# WET PRESSING FUNDAMENTALS

October 1, 1984

PROJECT SUMMARY FORM

DATE: September 10, 1984

PROJECT NO. & TITLE: 3480 - Wet Pressing Fundamentals

PROJECT LEADERS: F. Ahrens/N. Chang

IPC GOAL:

Fundamentally increase the potential capacity of processes.

OBJECTIVES:

1. To increase press effectiveness through improving the water receiving system.
2. To determine the feasibility and performance of displacement pressing in achieving high dryness, press effectiveness, and property control.

CURRENT FISCAL BUDGET: $140,000

SUMMARY OF RESULTS SINCE LAST REPORT: (February, 1984 - August, 1984)

Displacement pressing experiments have shown that, for lightweight sheets formed from high freeness pulps, attractive amounts of water removal and high dryness levels can be achieved under operating conditions that seem reasonable from an engineering (and cost) standpoint. A simplified mathematical model explains the trends observed.

Experiments to date on the effect of water receiver type on pressing effectiveness have shown that pressing with a felt gives greater water removal than pressing with porous plates.

# WET PRESSING FUNDAMENTALS

## INTRODUCTION

During the present reporting period, work has continued on both of the broad objectives established at the last meeting. These objectives are: pressing to higher dryness and increased pressing efficiency. The first objective is primarily related to increasing water removal (and gaining some other benefits as a by-product) with the assistance of an external gas pressure driving force; the technique has been termed displacement pressing. The second objective is related to promoting increased water removal for a given press impulse, through improvement of the water-receiving system. Recent work and future plans in both of these areas are reviewed in this report.

## DISPLACEMENT PRESSING

### INTRODUCTION

As used in the context of water removal at high dryness, displacement pressing refers to the combined process of mechanical compression to squeeze water from the fibers and application of a gas pressure difference across the web to drive water from it.

Recent work on this process has centered on improving our understanding of the displacement pressing mechanism and on evaluating the effects of potentially important variables on the performance of the process, under dynamic conditions close to those employed in available pressing equipment. This work and plans for future work on displacement pressing are reviewed here. A review of some related work done in Poland is first presented.

REVIEW OF POLISH WORK ON BLOWTHROUGH DEWATERING OF PAPER WEBS

Drainage or pressing of paper by passing (blowing) air through the wet web is not a new concept. Several devices for this purpose are described in a patent by Holden (1), filed for in March, 1963, and granted November 8, 1966. His work and that of Brundrett and Baines (2) were extended by Kawka and co-workers in Lodz, Poland. Several articles (3-10) have been published since.

Most of the work in Poland has been aimed at the use of the blow-through principle to raise the solids content of the sheet from values in the 10-30% range up to 40-45%. Two representative devices due to Holden (1), used by Kawka, are shown in Fig. 1. An additional device, developed in Poland and called an air press, is shown in Fig. 2. Several other similar devices have been proposed or used (3-10). All have the following characteristics:

a. low mechanical compression forces on the wet fiber network

b. long exposure times (0.1-several seconds)

c. a porous fabric or structure backing the wet web

d. modest pressure differentials through the wet web (1-30 psi)

e. low load levels (50-100 pli) on the pressing components, where they were used

f. low operating speeds (up to 300 m/min)

g. unheated blowthrough air, in most cases.

Blowthrough dewatering has been applied primarily to lightweight grades where bulk, absorbency, and porosity are important, such as tissue, toweling, and bag papers. There is mention of application to heavyweight board and pulp dewatering (9), but no data are given.

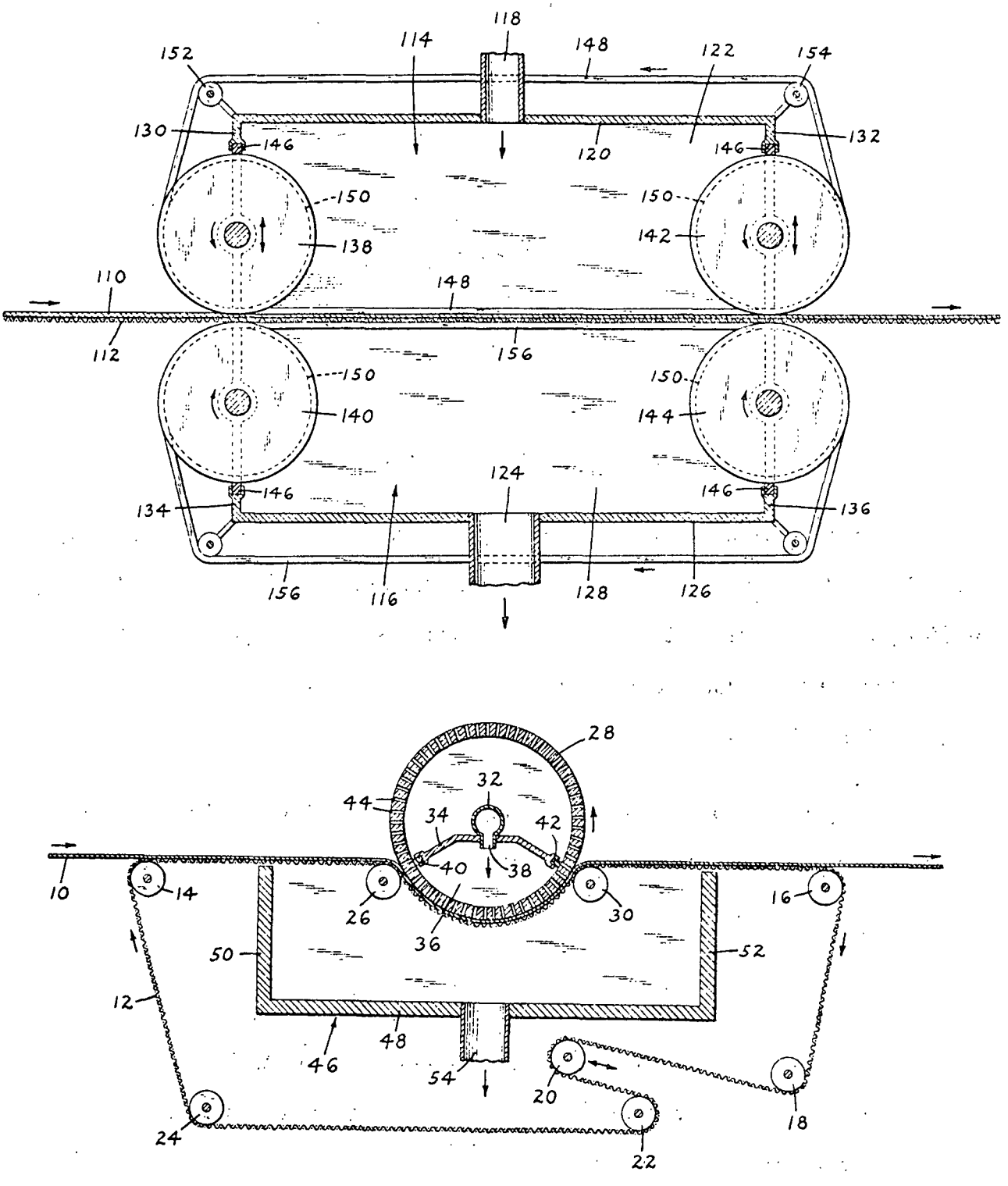


Figure 1. Two blowthrough configurations due to Holden (1).

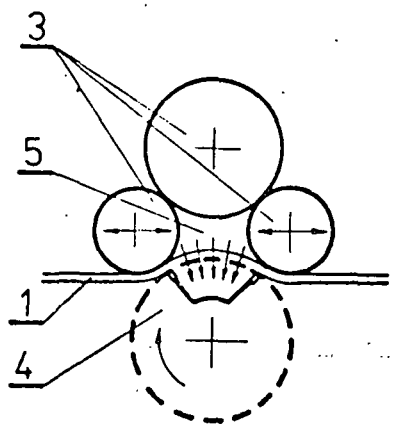


Figure 2. Polish "air press."

Some typical results for a 70 g/m$^2$ bag paper are presented in Fig. 3-5. These data were obtained by subjecting sheets with initial solids contents of 18.8, 25.3, and 31.4% to one, two, or three passes through an air press (Fig. 2). Corresponding exposure times were 0.2, 0.4, and 0.6 seconds. Press loads were about 50-100 pli.

Figure 3 shows final solids values as a function of the blowthrough air pressure differential. The following observations apply to these data:

a. This type of blowthrough water removal is most effective on wet sheets (10-20% solids).

b. Increased dryness from additional passes - more blowthrough time - seems mostly due to mechanical pressing and not to blowthrough.

c. For the web tested and the prevailing dewatering conditions, the maximum solids level is limited to about 42%.

d. More air pressure gives higher dryness levels, but the effect diminishes at a transition pressure (1.0-1.7 atm) which decreases with increasing initial dryness.

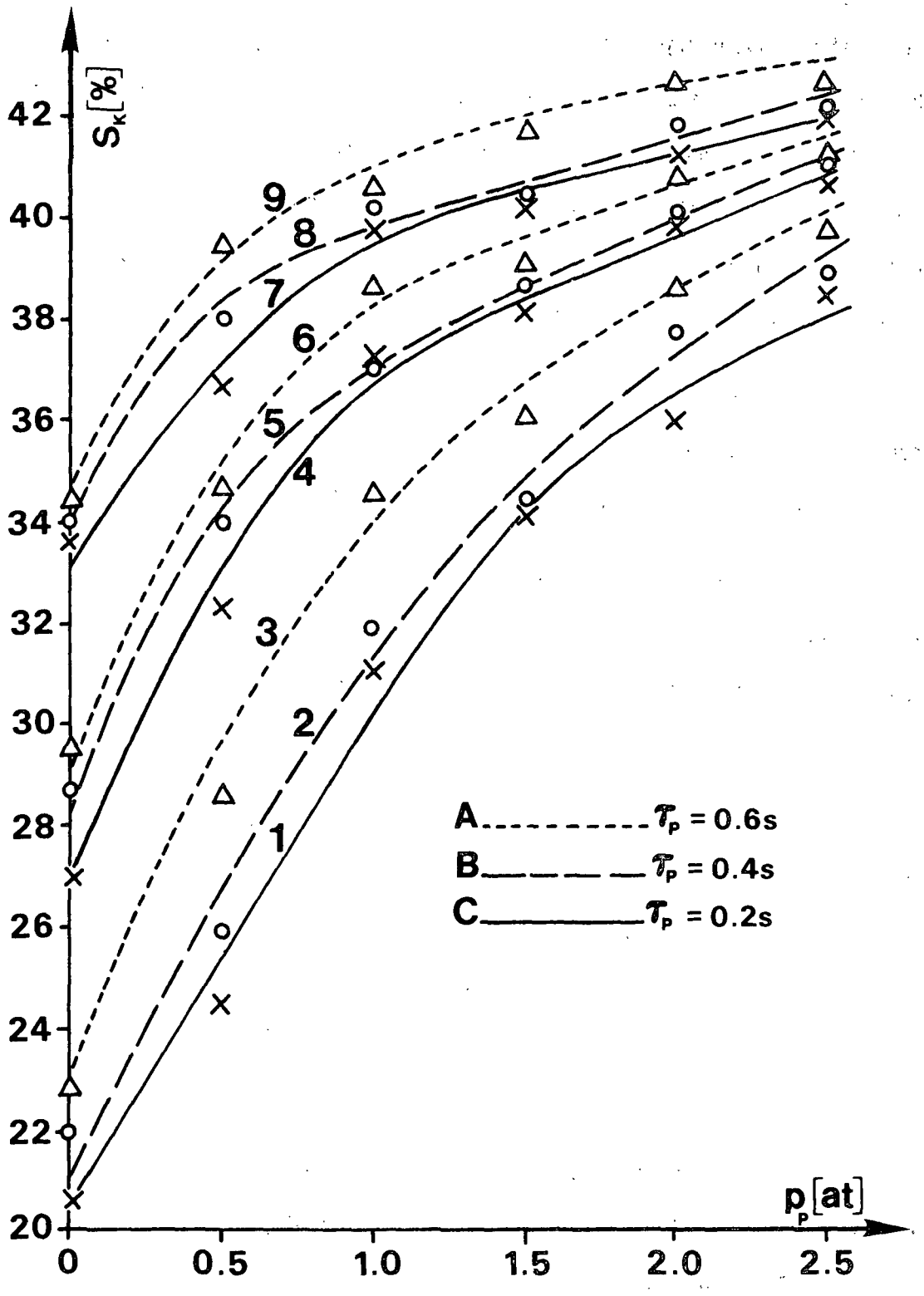


Figure 3. Final dryness ($S_k$) as a function of blowthrough air pressure difference ($p_p$) and blowthrough time ($\tau_p$), initial dryness as a parameter. Initial dryness: 18.8% for 1-3, 25.3% for 4-6, 31.4% for 7-9.

Figure 4 shows m.d. breaking length (a) and squareness ratio (b) as a function of the blowthrough pressure differential. Strength development appears to be due primarily to mechanical pressing ($p_p$ = o), whereas blowthrough tends to degrade tensile strength by a small amount. This is probably due to sheet disruption because of the low degree of mechanical constraint on the web. Both mechanical pressing and blowthrough tend to increase sheet squareness (Fig. 4b). Blowthrough time appears unimportant to either property.

Figure 5 shows elongation at failure and tear strength as functions of blowthrough pressure. Both show significant improvement with mechanical pressing ($p_p$ = o) and even more dramatic improvement with increased blowthrough.

Other properties, not shown in these figures, were also altered. Blowthrough dewatering tends to give much higher bulk (100% more), higher porosity, and higher absorbency than conventionally consolidated papers.

Air pressing is thus effective in dewatering wet webs ($\leq$ 40% solids) and in promoting bulk, absorbency, stretch, tear, and squareness. Tensile strengths tend to be degraded slightly. The efficiency (cost) of such pressing is hard to assess, but in one example cited (3) the direct air power delivered to the web was about 4 million Btu/ton which is substantial. The authors state that the primary advantage is in property control and not in energy cost reductions.

In some of the papers, experiments involving high temperature air and long exposures are cited. These constitute through drying experiments and are not germane to the IPC projects.

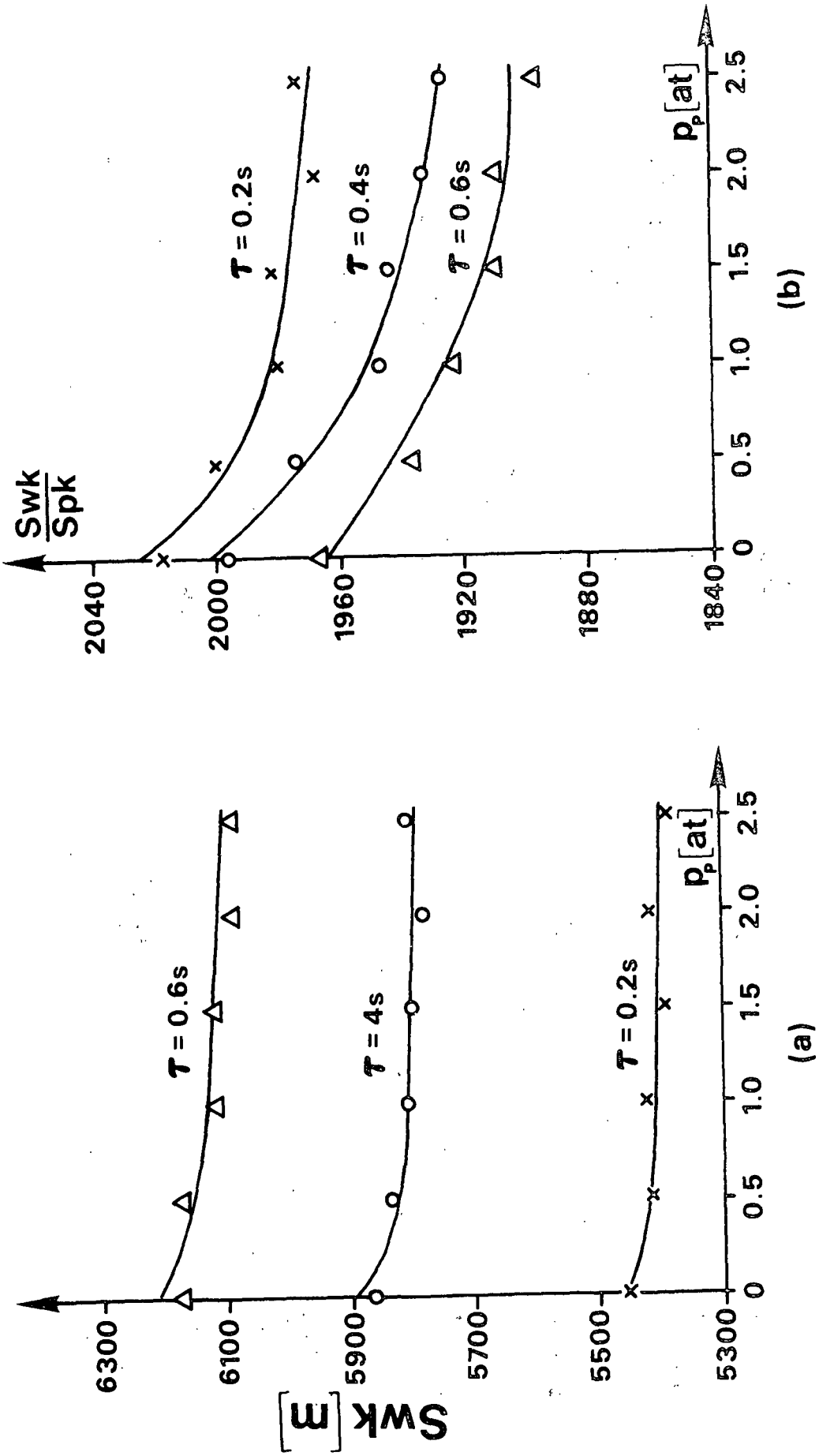


Figure 4. Breaking length and squareness as functions of blowthrough pressure differential.

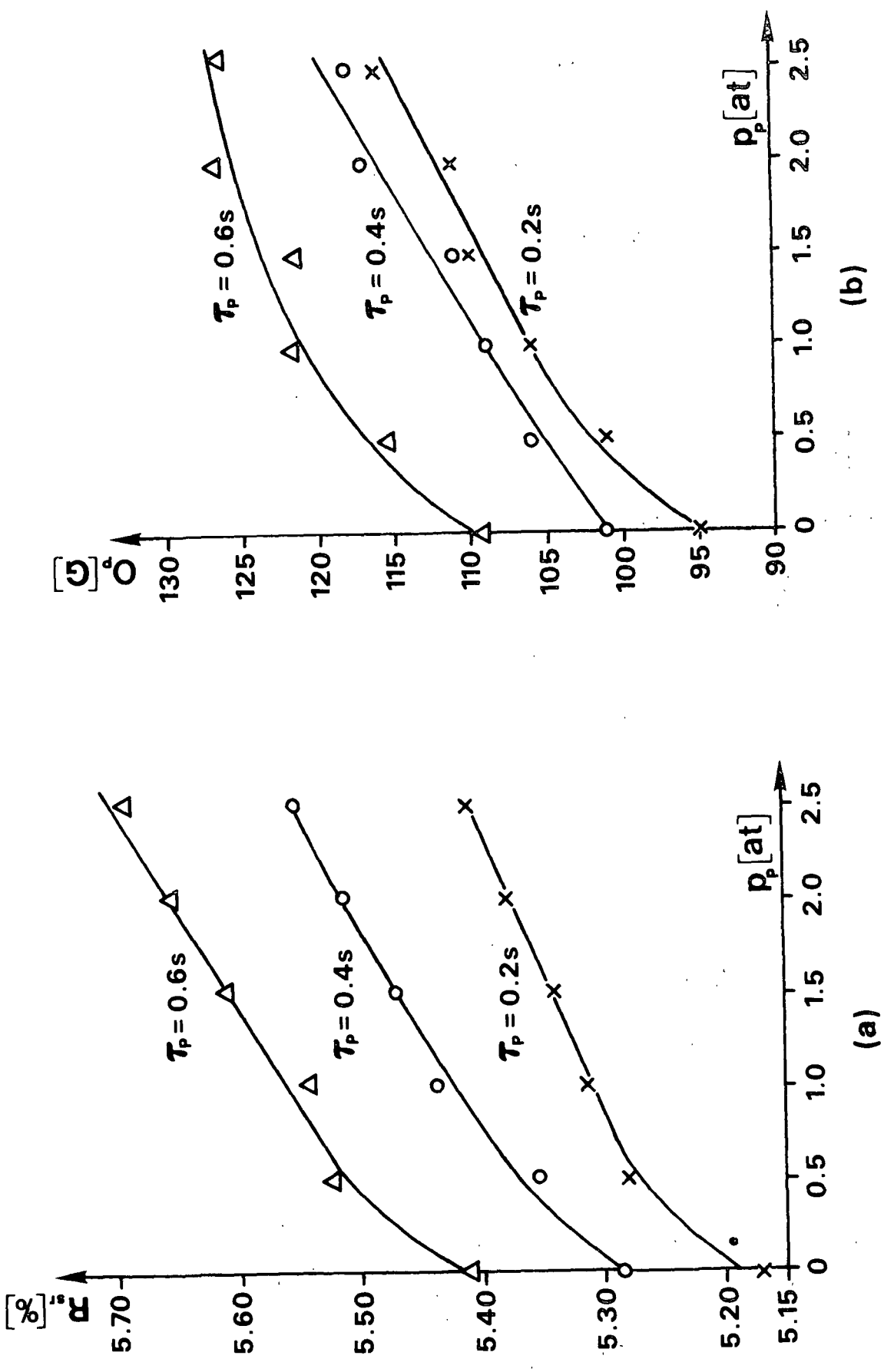


Figure 5. Elongation at failure and tear strength as functions of blowthrough pressure differential.

The work outlined above has been cited because it is relevant and complementary to the IPC work, and it supports the expectation that displacement pressing of low solids sheets will result in high bulk levels. Most of the IPC work, however, is aimed at quite different objectives and operating regimes. For example, the displacement pressing process is expected to:

a. extend pressing solids levels from 50 up to 65% thus augmenting conventional drainage and pressing elements and displacing dryers
b. work over a range of mechanical pressures up to high levels to permit improvement and control of properties, including strength or bulk, thus making it attractive for use on several grades
c. reduce drying energy levels substantially and reduce dryer size or increase productivity
d. work over the short time intervals characteristic of modern, high-speed machines.

All of these expectations fall well outside the range of the completed work and the capability of the various presses that have been developed. None has the potential for extension to the displacement pressing regime.

RECENT/CURRENT WORK

Simplified Analysis of Displacement Pressing

In order to gain understanding of the primary effects of web and operating parameters, a highly simplified analysis of displacement pressing has been performed. Because of the success of zonal models in describing high-intensity drying, a two-zone model has been adopted (see Fig. 6). In this model, the water available for displacement by an air pressure gradient is considered to be displaced from the web as a unit (wet zone), leaving behind (in

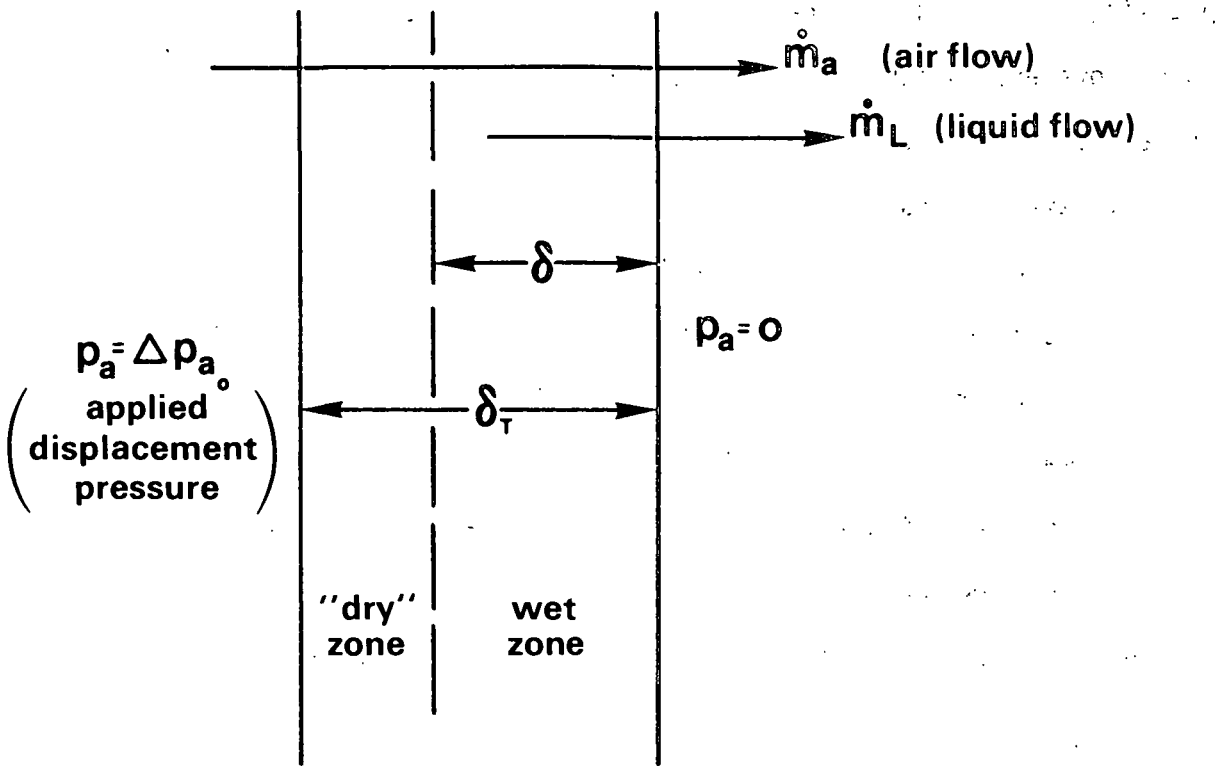


Figure 6. Two-zone model of displacement pressing.

the "dry" zone) that water which is unavailable for displacement. The analysis was performed for the general case in which air flows through the entire web removing water by viscous entrainment. However, the special case of a saturated wet zone, with water removal by a "push-through" mechanism, is readily handled in the model by setting the air permeability of the wet zone to zero.

A brief outline of the analysis is as follows. As a result of mechanical compression, the web has a thickness ($\delta_T$), an effective density of water available for displacement ($\bar{\rho}_L$), air permeabilities for the wet and "dry" zones

($k_{a_w}$, $k_{a_d}$), and a liquid permeability in the wet zone ($k_L$). The above quantities, as well as the applied air pressure difference ($\Delta p_{a_o}$), are considered constant. For simplicity, the compressibility of the air is neglected [i.e., the air density ($\rho_a$) is treated as constant].

It is assumed that Darcy's law adequately describes both the air and water flows. Although the wet zone thickness will decrease with time, a quasi-steady-state analysis is employed. Thus, the air flow rates ($\dot{m}_a$) through the "dry" and wet zones must be equal at every instant, yielding:

$$\dot{m}_a = \frac{\rho_a \, k_{a_d}}{\mu_a} \frac{\Delta p_{a_d}}{(\delta_T - \delta)} = \frac{\rho_a \, k_{a_w}}{\mu_a} \frac{\Delta p_{a_w}}{\delta}$$

where $\mu_a$ = air viscosity

$\Delta p_{a_d}$ = air pressure drop across "dry" zone

$\Delta p_{a_w}$ = air pressure drop across wet zone

Of course, the total pressure drop is fixed:

$$\Delta p_{a_d} + \Delta p_{a_w} = \Delta p_{a_o}$$

If capillary pressure effects are neglected, it is $\Delta p_{a_w}$ that drives the liquid flow. Thus, the liquid flow rate ($\dot{m}_L$) is given by:

$$\dot{m}_L = \frac{\rho_L \, k_L}{\mu_L} \frac{\Delta p_{a_w}}{\delta}$$

where $\rho_L$ = density of water

$\mu_L$ = viscosity of water

Finally, the rate of change of the wet zone thickness ($\delta$) can be obtained from a mass balance on the wet zone:

$$\overline{\rho}_L \frac{d\delta}{dt} = - \dot{m}_L$$

with $\delta(o) = \delta_T$.

The above equations have been solved, yielding the following expression for the wet zone thickness:

$$\frac{\delta}{\delta_T} = \frac{-\bar{k} + \sqrt{1 - (1-\bar{k}^2)\bar{t}}}{1 - \bar{k}}, \quad 0 \leq \bar{t} \leq 1$$

where $\bar{k} = k_{a_w}/k_{a_d}$

$\bar{t} = t/t_D$

$t_D$ = "drying time" = $\dfrac{(1+\bar{k})\mu_L \, m_L'' \, \delta_T}{2 \, \rho_L \, k_L \, \Delta p_{a_o}}$

$m_L'' = \rho_L \delta_T$ = mass of water available for displacement per unit area

Of course, for $\bar{t} > 1$, no further water removal occurs, since $\delta = 0$. The relative water removal (cumulative) is easily derived from the above result as:

$$\bar{M}_{out} = 1 - \delta/\delta_T.$$

Figure 7 shows the predicted behavior for the physically meaningful range, $0 \leq \bar{k} \leq 1$.

Perhaps the most important result of the analysis is the expression for "drying time" ($t_D$) listed above. It, in conjunction with the expression for $m_L''$, indicates that drying time is proportional to the square of the web thickness (basis weight) and inversely proportional to applied air pressure and web liquid permeability (a strong function of compression level, moisture ratio, and freeness for a given pulp).

According to the model, there is no incentive to perform displacement pressing for times longer than $t_D$. The real challenges, then, are to minimize $t_D$, while maximizing $m_L''$ (the water available for displacement). This will require understanding and use of optimal operating strategies.

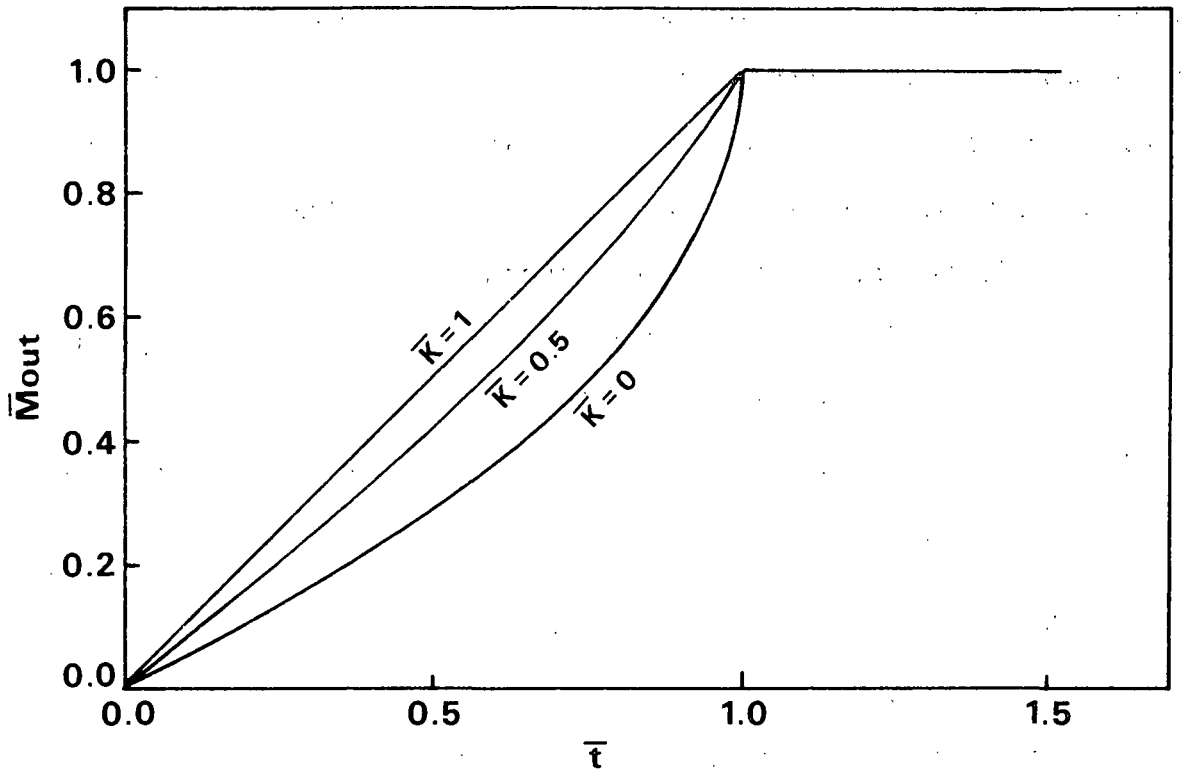


Figure 7. Dimensionless cumulative water removal ($\bar{M}_{out}$) as a function of dimensionless displacement time ($\bar{t}$).

## Experimental Work

### Background

The initial exploration of displacement pressing reported at the March 1984 PAC meeting involved tests performed in a static press device. That is, the sheets were precompressed for several seconds, after which displacement (air) pressure was applied. Although the dryness levels attained (up to about 65%) were very encouraging, these compression times and the displacement times ($\geq$ 0.5 s) used were long in comparison to residence times representative of commercial pressing equipment.

In order to learn whether these high dryness levels can be attained or exceeded within a time period more typical of currently practical pressing operations, the work during the present reporting period has concentrated on

experiments performed in a dynamic pressing configuration. At first, new test heads incorporating a sheet/felt edge seal, a pressure transducer located so as to measure the actual displacement pressure experienced by the sheet, and an improved air supply/distribution arrangement were installed in a drop press simulator. Unfortuantely, satisfactory combinations of mechanical pressure, air pressure, and nip residence time were not readily achieved in this system, and meaningful test results were not obtained. However, shortly after initiation of these drop press trials, the MTS system recently obtained by the Corrosion Group became available for temporary use in this project.

The MTS device can be used as a versatile hydraulic press. For the 2.5-inch diameter handsheets used in the displacement pressing experiments, it can exert mechanical pressures up to about 2000 psi. Furthermore, various pressure-time pulse shapes, such as "square" and haversine, can be selected for application; minimum pulse durations on the order of 10 ms can be achieved. Thus, this system is well-suited for simulation of most pressing conditions of interest. Therefore, the displacement pressing test heads and air supply system were installed in the MTS device. The data presented below were obtained using this arrangement.

Results

Initially, scoping experiments were performed to examine the effects of certain operating variables on displacement pressing performance. For these experiments, 63 $g/m^2$ handsheets formed from 720 CSF bleached softwood kraft (once-dried) pulp were utilized.

In one series, the peak mechanical pressure and nip residence time (displacement time) were varied. The tests were performed using sheets at

43-45% initial dryness. The pressing configuration used comprised a bronze wire/handsheet/felt sandwich pressed between the drilled plates of the two test heads with the wire at the air supply side. A soft rubber gasket surrounded the sandwich to minimize air leakage. A haversine-shaped mechanical pulse was employed with the air supply triggered just prior to initiation of the mechanical pulse. Example mechanical pressure and air pressure responses for this operating mode are given in Fig. 8.

The results of this test series are presented in Fig. 9. It is seen that nearly 50% of the water initially in the sheet (corresponding to final dryness levels of 60% or more) was removed under the maximum time and pressure conditions. For the range of conditions represented in Fig. 9, the peak air pressures ranged from 40 to 80 psi, increasing with mechanical pressure and with displacement time. Some of the factors contributing to the beneficial effect of higher mechanical pressures may be: larger quantities of water squeezed from the fibers and available for displacement, increased air pressure differential across the web due to its increased saturation (air flow resistance), and decreased web thickness. The potentially impeding effect of increased liquid flow resistance at higher compression levels is apparently insufficient to overcome these beneficial effects. The displacement pressing results are particularly encouraging because they indicate that significant dewatering occurs in times compatible with available pressing equipment (e.g., up to 50 ms).

Because the bronze wire/drilled plate combination yielded marked (dimpled) sheets after pressing, other load spreader/air distributor materials were tried. These included plastic wires and porous metal plates. The use of porous plates tended to result in somewhat reduced water removal. The plastic wire was stiffer than the bronze wire and reduced dimpling without significantly

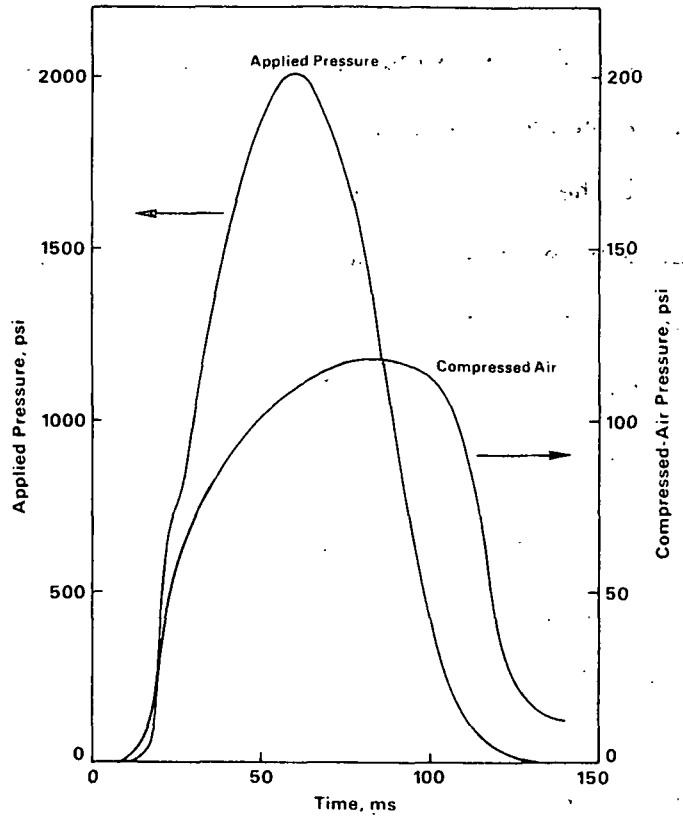


Figure 8. Example applied mechanical pressure and air pressure responses for the haversine mechanical pulse mode.

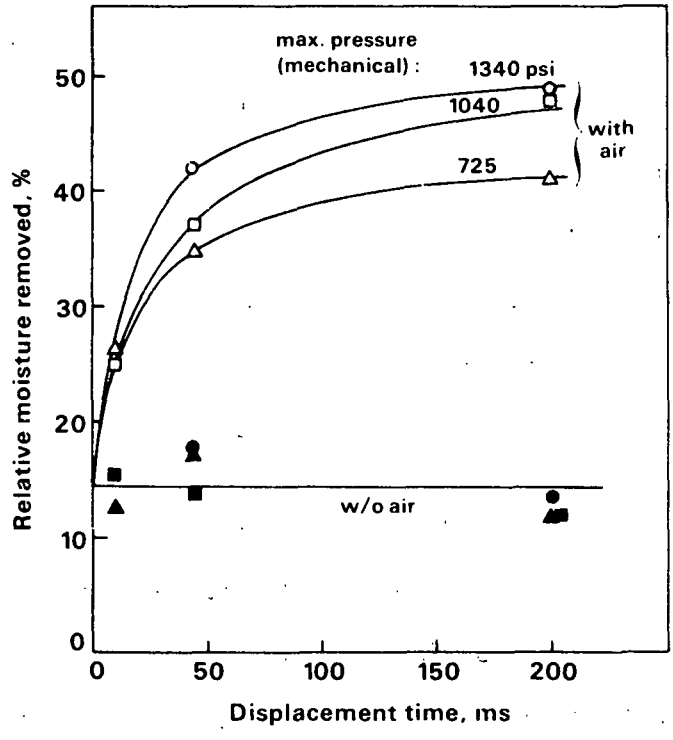


Figure 9. Results of displacement pressing of 63 g/m$^2$ handsheets of once-dried bleached softwood kraft pulp at 720 CSF. Initial dryness = 43-45%.

changing water removal. Therefore, it was adopted for use in subsequent experiments.

Although not studied thoroughly, several tests using "square," rather than haversine, mechanical pulse shapes were performed. In some cases, the displacement air application was delayed by ~50 ms to determine the effect of precompression. No appreciable differences in water removal were observed with these pressing modes, as compared to the haversine pulse results, for similar displacement times.

Increases in peak mechanical pressure (to 2000 psi), air supply pressure (to 200 psi) and sheet initial dryness (to ~49-51%) were also explored. The combined effect of these changes was an increase of several percentage points in final sheet dryness (up to the 64-65% range) within the same time range as shown in Fig. 9. These higher air supply pressure and initial dryness levels were then retained in subsequent tests.

The next phase of experimentation involved comparing the displacement pressing behavior of never-dried pulp (bleached northern softwood kraft), at two freeness levels (690 and 300 CSF), with that of the previously discussed once-dried pulp. One of the operating conditions used involved a "square" mechanical pulse, with ~50 ms precompression time and 130 ms displacement time, at a level of ~1200 psi. For 63 g/m$^2$ handsheets at about 49% initial dryness, the water removal amounts for the 720 CSF once-dried, the 690 CSF never-dried, and the 300 CSF never-dried pulp handsheets were 47%, 33%, and 20%, respectively. Rather similar results were found using other pulse shapes and somewhat shorter displacement times. For all three sheet types, pressing without displacement air yielded about 15% water removal.

The effects of displacement time and pulp freeness have been investigated in one of the most definitive portions of the displacement pressing study so far. Handsheet samples of 63 g/m$^2$ basis weight, formed from never-dried, bleached northern softwood kraft pulp at freeness levels of 300 and 690 CSF and having an initial dryness of about 50%, were employed. Mechanical pressure pulses of "square" shape, at a level of about 1200 psi, were used. The compressed air supply was "triggered" after 50 ms of sheet compression. Typical mechanical and air pressure responses are shown in Fig. 10. The water removal curves resulting from these tests are shown in Fig. 11 and 12. Comparison data for pressing without displacement air are shown in the figures, too. In the case of the 690 CSF pulp, the displacement times needed to achieve significant dryness increases were comparable to the response time of the air supply system (i.e., about 40 ms). Thus, the maximum (and average) air pressures felt by the sheet tend to increase with displacement time (see Fig. 11). If constant air pressures had been applied, the water removal at short displacement times would likely have been somewhat greater, and the curve would be flatter at longer times. In the case of the 300 CSF pulp, the time scale for water removal was well beyond the response time of the air system, so the peak air pressures were found to be about the same for all tests. Interestingly, the peak air pressure was greater for the low freeness pulp sheets than for the high freeness ones (~180 psi vs. 120 psi), probably due to differences in sheet flow resistance.

The data presented in Fig. 11 and 12 indicate that significant increments of water removal via displacement pressing are achievable at high ingoing dryness levels. The amount of water available for displacement appears to be somewhat greater for the high freeness case. Importantly, the majority of the water removal occurred in a time period (~35 ms) comparable to the residence

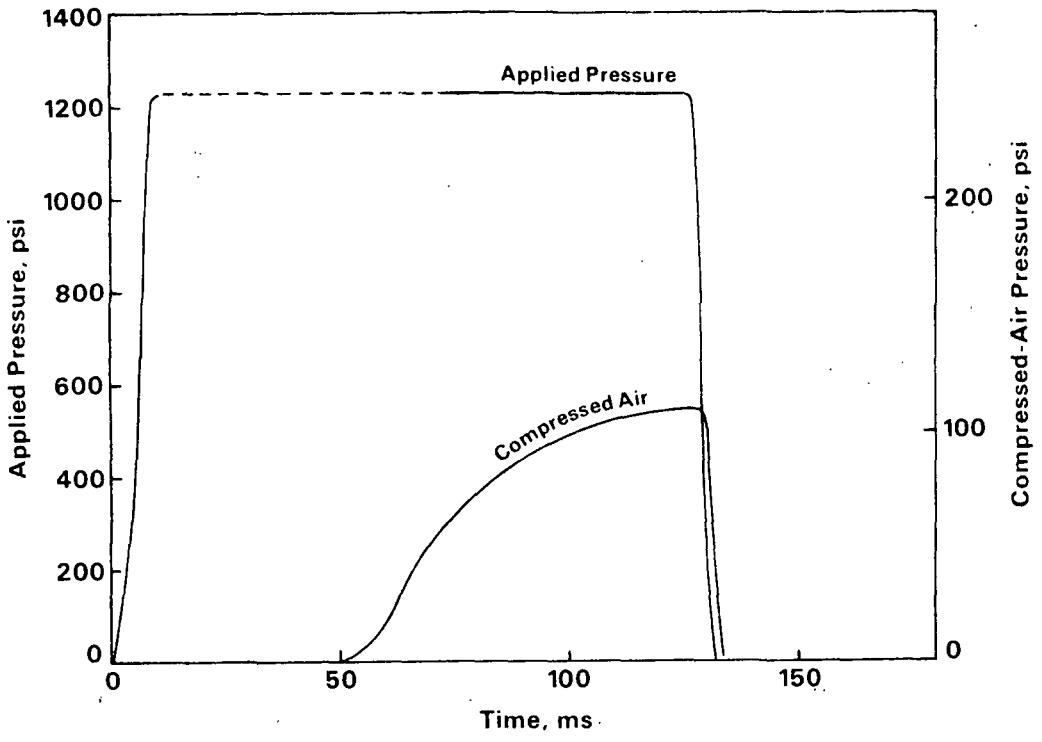


Figure 10. Mechanical and air pressure responses for "square" pulse with air supply "triggered" after 50 ms of sheet compression.

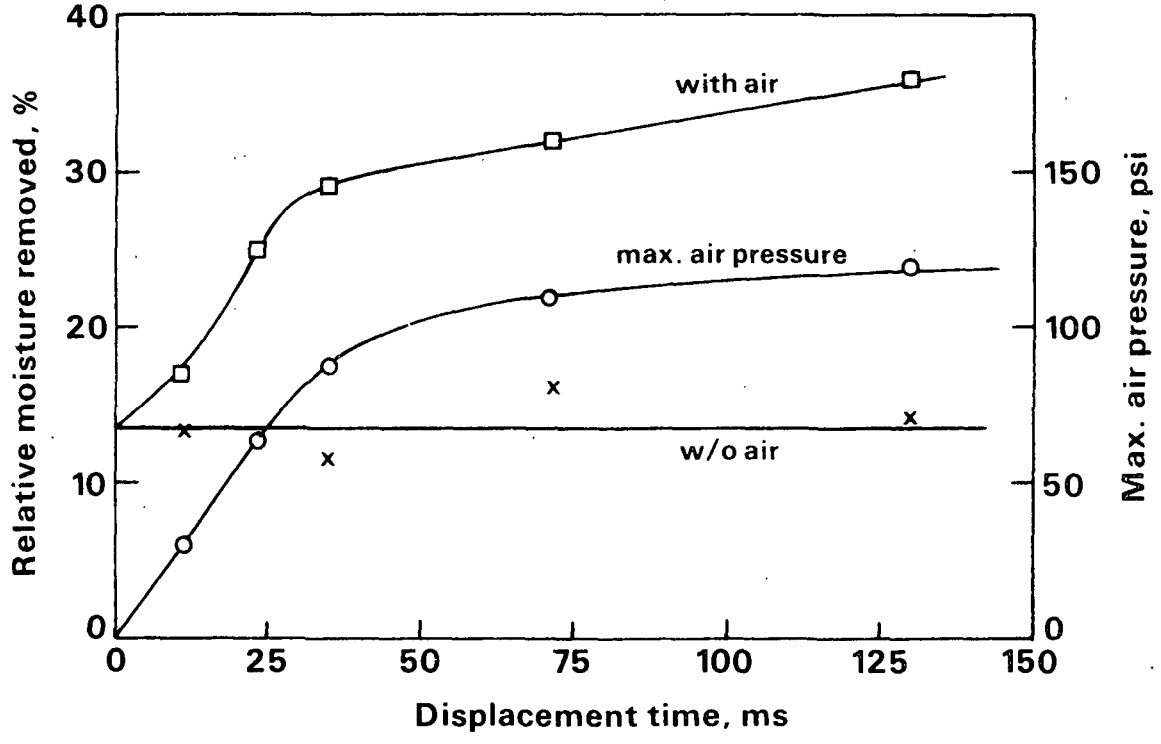


Figure 11. Results of displacement pressing of 63 g/m$^2$ handsheets of never-dried bleached northern softwood kraft pulp at 690 CSF. Initial dryness ≈ 50%.

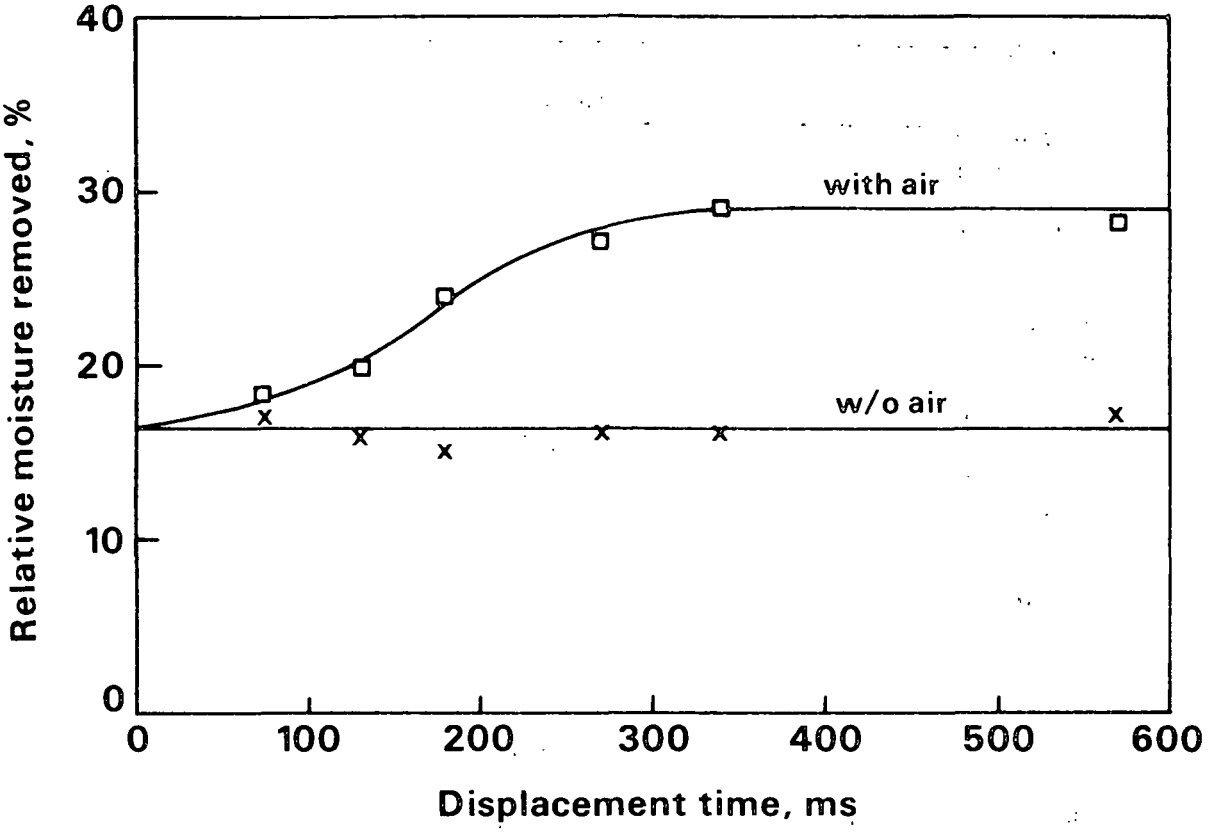


Figure 12. Results of displacement pressing of 63 g/m$^2$ handsheets of never-dried bleached northern softwood kraft pulp at 300 CSF. Initial dryness ≈ 50%.

time in an extended nip press in the 690 CSF case. For the 300 CSF pulp, the dewatering time was nearly an order of magnitude longer (~300 ms).

It is interesting to note that the shapes of the displacement pressing curves in Fig. 11 and 12 are in good agreement with that predicted by the simplified model presented earlier in the report. Furthermore, the experimental dewatering times are in reasonable quantitative agreement with those calculated (using estimated parameter values where necessary) from the "drying time" equation resulting from the simplified analysis.

PLANS FOR THE FUTURE

The results reported above demonstrate that, for lightweight sheets formed from high freeness pulps, displacement pressing can yield attractive

amounts of water removal and high dryness levels under operating conditions that seem reasonable from an engineering (and cost) standpoint. In the near future, experiments to better define the extent of the region of expected practicality for displacement pressing will be undertaken. In addition, ideas for increasing the size of this region and ideas related to the implementation of displacement pressing will be investigated. Two schemes for improving the performance that will be tried are: (1) use of a steam shower to preheat the web in an effort to increase the quantity and rate of water removal, and (2) restriction of the air flow through and from the water receiver, in order to reduce the consumption of compressed air.

As part of the future work, a wider range of ingoing sheet moisture contents (wetter sheets) will be considered and final (dry) sheet density will be measured in addition to water removal. The resulting data will give an indication of the degree of control over density-related properties attainable through substitution of the displacement mechanism for direct mechanical pressing.

When the domain of probable commercial viability of displacement pressing has been more clearly established, a comprehensive technical performance evaluation of displacement pressing within this region will be initiated. A base of water removal and paper properties data will be developed that will allow engineering and economic evaluations to be performed.

REFERENCES

1. Holden, G. R., U. S. pat. 3,284,285(Nov. 8, 1966).
2. Brundrett, E.; Baines, O., Tappi 49(3):97-101(1966).
3. Kawka, W.; Rogut, R., Przeglad Papierniczy 26(2):52-6(1970).

4. Kawka, W.; Ingielewicz, H., Przeglad Papierniczy 28(11):381-7(Nov., 1972).

5. Kawka, W., Przeglad Papierniczy 30(1):10-18(Jan., 1974).

6. Kawka, W.; Ingielewicz, H., Przeglad Papierniczy 34(2):53-8(Feb., 1978).

7. Kawka, W.; Ingielewicz, H.; Marek, I., Przeglad Papierniczy 34(3):82-7 (March, 1978).

8. Kawka, W.; Stepien, K., Przeglad Papierniczy 35(11):402-4(Nov., 1979).

9. Kawka, W.; Szwarcsztajn, E., EUCEPA-79 International Conf., London, May 21-24, 1979, Paper No. 31.

10. Kawka, W.; Przeglad Papierniczy 39(11/12):403-7(Nov.-Dec., 1983).

## HIGH EFFICIENCY PRESSING

### INTRODUCTION

The primary motivation for this part of the project is the finding reported by University of Maine-Orono (UMO) researchers that a given press impulse can give much greater water removal if pressing is done (in a laboratory compression tester) with a smooth porous plate as the water receiver than if it is done (in a pilot press) with a felt as the water receiver. Recent work on this part of the project has been devoted to tests aimed at showing the effect of water receiver type (felt vs. porous plate) on water removal, in general, and to attempts to corroborate the UMO findings, in particular. This work and plans for the future are reviewed here.

### RECENT/CURRENT WORK

#### Background

Because the emphasis of the high-efficiency pressing study is initially on determining whether porous plates promote greater water removal than felts, a variety of porous plates were obtained for use in the experiments. The ones used in the work reported here are identified in Table 1.

Table 1. Porous plate characteristics.

| Designation | Material | Approx. pore size, μ | Surface |
|---|---|---|---|
| SB10 | Sintered bronze | 10 | Unground |
| SB30 | Sintered bronze | 30 | Unground |
| SB40 | Sintered bronze | 40 | Unground |
| SS40[a] | Sintered stainless steel | 40 | Ground |
| SS100 | Sintered stainless steel | 100 | Ground |

[a]This is similar to the plate used in UMO study.

A pressing pedestal (see Fig. 13) was fabricated for use in the water removal experiments. It is a vented nip configuration (drilled plate) and has provision for use with any of the porous plates. When a felt is employed, it is placed on top of a very coarse (250 μ pore size) porous plate installed in the pedestal.

Most of the results reported here were obtained from tests using a drop weight press simulator. However, in order to more readily and reproducibly simulate long nip residence time (e.g., 20 ms), high-impulse conditions pertinent to the corroboration of certain UMO results, the (Corrosion Group) MTS system has been employed in some of the most recent experiments. The use of the pressing pedestal in either of these pressing devices makes it possible to obtain direct comparative data on water receiver performance at fixed test conditions.

## Results

Initial, exploratory experiments were performed using 60 g/m$^2$ handsheets formed from (once-dried) bleached softwood kraft pulp at about 700 CSF. The initial moisture ratio of the samples was 3.0 for all the tests.

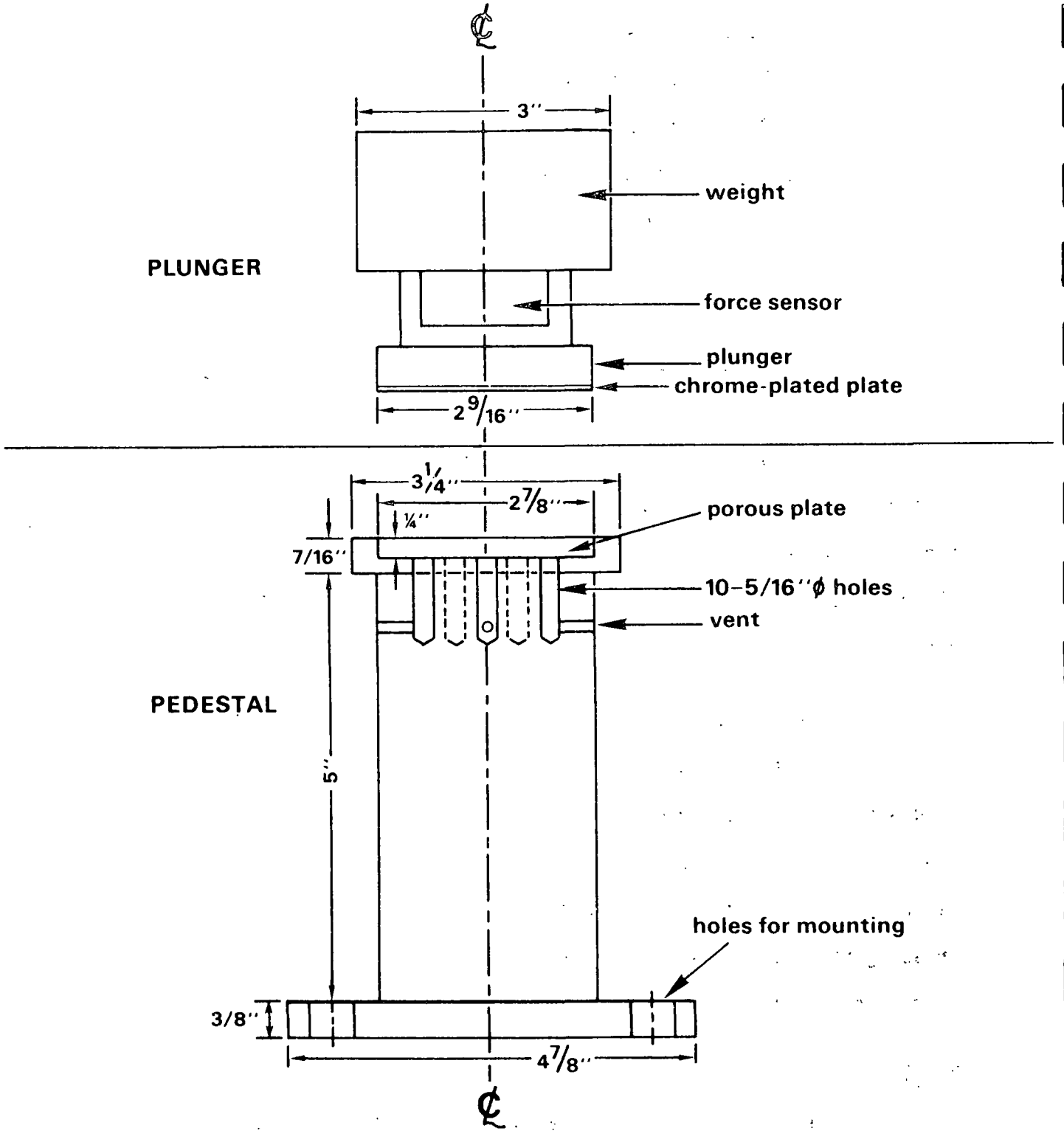


Figure 13. Pressing configuration for high-efficiency pressing study.

For the purpose of comparison of porous plate performance with felt performance, it was considered appropriate to operate each water receiver at that initial moisture ratio for which water removal from the sheet is maximized. Based on tests at an operating condition of 600 psi peak mechanical pressure and 6.0 ms nip residence time, it was found that all the porous plates performed best when initially dry, while the felt performance was 6-7% better at 0.3 moisture ratio (the optimum value) than when dry. These "best" moisture conditions were then used in all subsequent experiments.

The water removal data from the tests just described and from tests at a higher impulse level are presented in Table 2 for the felt and the three best porous plates. For these test conditions, the felt promotes greater water removal than that achieved with any of the porous plates. The ranking of the three porous plates seems to be in agreement with expectations. That is, the rather smooth, small-pored plate is best; the very smooth, but larger-pored, plate is next; and the least-smooth plate is worst. Two other, still coarser, plates yielded even poorer performance.

Table 2. Effect of water receiver on water removal for 60 $g/m^2$ sheets of 700 CSF (once-dried) BSWK at 3.0 initial moisture ratio.

| Water Receiver | Water Removed at 600 psi Peak Load, 6 ms Nip Time, $g/m^2$ | Water Removed at 1900 psi Peak Load, 6 ms Nip Time, $g/m^2$ |
|---|---|---|
| Felt (conditioned) | 119 | 144 |
| SB10 | 96 | 106 |
| SS40 | 82 | 93 |
| SB30 | 73 | 76 |

A few other felts were next tried, at the same two operating conditions, in order to ascertain the importance of felt type. These included: a felt similar to the one used previously but unconditioned, a coarser felt, and a layered felt with one coarse layer. While the original felt remained at the top of the performance ranking, two of the other three had nearly as good performance, giving about 10 g/m$^2$ less water removal. The layered felt performed approximately the same as the best porous plate (SB10). The felt performance ranking was in accordance with expectations, since the coarser felts performed more poorly than the finer ones. The main conclusion from this test series is that, as a group, felts give better water removal than porous plates, at least for the (small) range of operating conditions studied.

In order to take the investigation a step closer to the conditions covered by the UMO study, some sheets were prepared from (never-dried) bleached northern softwood kraft (BNSWK) pulp at 300 CSF. This is similar to the pulp used in many of the tests performed in the original UMO study. For tests at the same basis weight, initial moisture and impulse conditions as used in the work discussed above, the results were as given in Table 3. While the quantities of water removal are about half those in Table 2, reflecting the greater difficulty in removing water from low freeness pulps, the ordering is the same; the felt again has superior performance. In some similar tests at a higher basis weight (75 g/m$^2$), the SS40 plate showed slightly better performance than the SB10 plate, but still the felt was best.

With the availability of the MTS system, it became possible to easily duplicate an operating condition (225 psi <u>average</u> pressure, 20 ms nip residence time) for which UMO water removal data were available over a range of basis weights, for both the felt and the SS40 plate as water receivers. Thus, a

Table 3. Effect of water receiver on water removal for 60 g/m$^2$ sheets of 300 CSF BNSWK at 3.0 initial moisture ratio.

| Water Receiver | Water Removed at 600 psi Peak Load, 6 ms Nip Time, g/m$^2$ | Water Removed at 1900 psi Peak Load, 6 ms Nip Time, g/m$^2$ |
|---|---|---|
| Felt (conditioned) | 60 | 74 |
| SB10 | 45 | 59 |
| SS40 | 37 | 51 |
| SB30 | 34 | 41 |

rather direct attempt at corroboration of the UMO data was possible. The results of recent IPC tests and the UMO data are compared in Fig. 14. With the exception of the data at basis weights of 75 and 100 g/m$^2$, which are seemingly "out of line" for yet undiscovered reasons, the IPC data are seen to follow the UMO (Beloit) pilot press data (based on felt as the water receiver) fairly closely. For the conditions represented in Fig. 14, the IPC measurements indicate that felt performance continues to exceed porous plate performance at low basis weight, while the two water receivers behave rather similarly at high basis weight.

In an attempt to more closely simulate conditions used in many of the UMO laboratory tests, some tests similar to those just described, but with a "square" mechanical pressure pulse rather than a haversine pulse, were performed with the SS40 plate as water receiver. The water removal levels resulting from these tests showed a similar trend with basis weight, but slightly lower magnitudes, as those shown in Fig. 14.

## PLANS FOR THE FUTURE

In the near future, efforts to corroborate available UMO data or to explain the lack of confirmation will continue, using the MTS system. In the

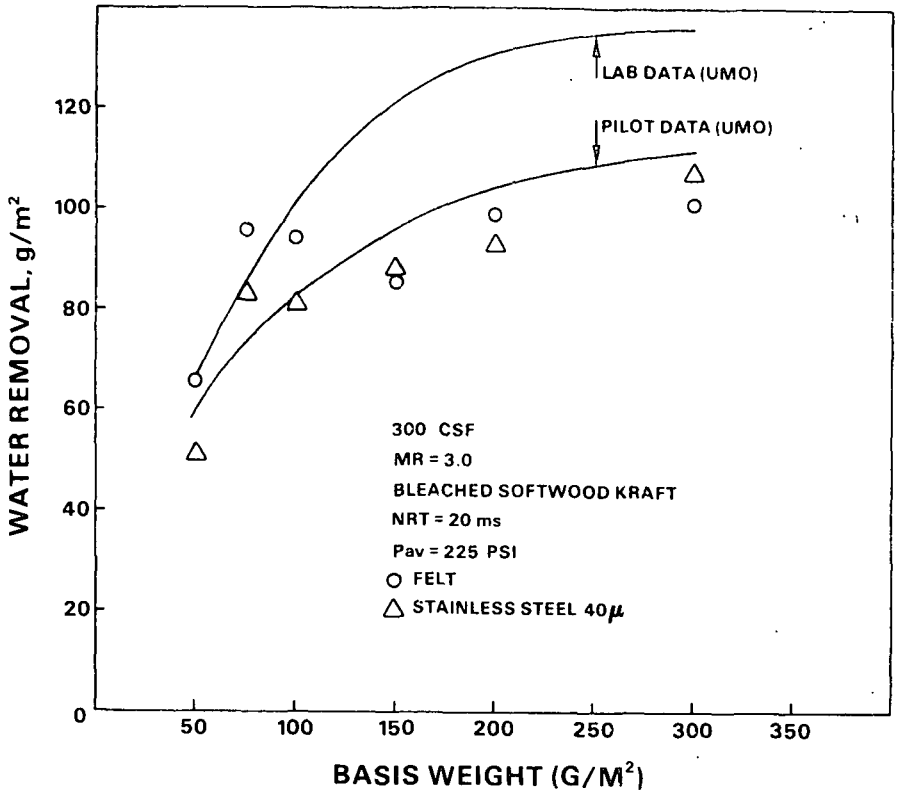


Figure 14. Comparison of data from the MTS system with results of the UMO study.

case of pressing with a felt, experiments will also be conducted in the small pilot press used earlier for impulse drying experiments, in order to determine the degree to which the MTS system simulates press nip conditions. If more promising results are obtained (with respect to potential efficiency gains), work directed toward determining the water receiver characteristics that control pressing efficiency will be initiated.

THE INSTITUTE OF PAPER CHEMISTRY

Appleton, Wisconsin

Status Report

to the

ENGINEERING PROJECT ADVISORY COMMITTEE

Project 3470

# FUNDAMENTALS OF DRYING

October 1, 1984

PROJECT SUMMARY FORM

DATE: September 14, 1984

PROJECT NO. & TITLE: 3470 - Fundamentals of Drying

PROJECT LEADER: F. Ahrens

IPC GOAL:

Reduction of the "necessary minimum" complexity (number and/or sophistication) of process steps.

OBJECTIVE:

To develop an understanding and a data base sufficient for commercialization of advanced water removal systems, based on high-intensity drying principles, that will result in reduced capital cost/increased machine productivity, reduced quantity and/or quality of energy use, and a favorable impact on paper properties.

CURRENT FISCAL BUDGET: $150,000

SUMMARY OF RESULTS SINCE LAST REPORT: (February, 1984 - August, 1984)

Preparations for the technical performance evaluation program, in which drying tests and paper properties evaluations will be performed on handsheet samples representing six important paper and board grades over a broad range of conditions, have nearly been completed. Needed hardware and fiber furnishes have been procured. Test procedures have been established, the test program definition is nearly complete, and a computer data base has been developed. The test program will begin soon.

Water removal and heat transfer experiments at impulse drying conditions have shown that preheating the web results in a significant increase in water removal and a reduction in energy use per unit of water removed. This is due to increased liquid-phase dewatering. An analysis capability for the generation of impulse dryer design information using laboratory results as input is under development.

# FUNDAMENTALS OF DRYING

## INTRODUCTION

The technical feasibility of improving the water removal process by application of high-intensity water removal techniques such as impulse drying and thermal/vacuum drying has been adequately demonstrated during the last few years. In addition, with the assistance of students involved in the academic research program, considerable fundamental understanding of these processes has been and is being achieved.

The primary objective of present and future work in this project is to extend the current understanding of high-intensity water removal principles/performance to include the comprehensive data base required for their effective and efficient commercial application. The long-range plan for meeting this objective was reviewed in the previous status report and at the March, 1984 PAC meeting.

During the present reporting period, project work has mainly centered on preparation for the broad technical performance evaluation program that will provide data needed to more completely characterize the performance of advanced drying systems and for determining the most attractive applications. In addition, modest efforts have been made in the areas of laboratory investigation of impulse drying (primarily dealing with energy use and dewatering mechanisms) and engineering considerations relative to implementation of advanced water removal systems. A review of progress in these three categories and a presentation of plans for the future is given in this report.

# TECHNICAL PERFORMANCE EVALUATION OF HIGH-INTENSITY WATER REMOVAL PROCESSES

## INTRODUCTION

The plan to perform bench-scale drying tests on handsheet samples representing six important paper and board grades over a broad range of operating conditions was discussed in the preceding status report. This work will result in a data base covering water removal rates, energy use and paper properties. In this section, the recent work in preparation for the technical performance evaluation program is reviewed. Areas covered include: hardware design/procurement, furnish selection/procurement, test procedures specification, test program definition, and computer data base preparations. Much of the preparatory work in these areas is completed, and the actual experimental program will be started in the near future.

## HARDWARE DESIGN/PROCUREMENT

One of the important requirements for the technical performance evaluation program is the availability of a versatile drying system capable of operating over a wide range of pressure, temperature, and time conditions. The successful application of the Corrosion Group's MTS system to pressing studies this summer has contributed to a decision to base the required drying system on the use of MTS components. The new system will be installed in the Water Removal Laboratory and will actually enable either pressing or drying tests to be run with a simple interchange of test heads. The major MTS components ordered (due to arrive in early-to-mid October) include a 22,000 lb maximum force hydraulic actuator (incorporating an LVDT displacement transducer), servovalves sized to enable mechanical pulses of 10 ms or longer to be applied to

the test sample, servo control unit, load cell, and hydraulic power supply with accumulators and control unit. A load frame to accommodate the MTS components and necessary test heads has been designed at IPC and is being constructed.

The LVDT and load cell will produce position and load signals that can be used for feedback control of the servovalve. Work is in progress on development of a control system that will use these signals in conjunction with a function generator that produces specified pulse programs (e.g., "square," haversine, ramp, etc.) for closed-loop control of the servovalve. This will allow a variety of pressure-time conditions to be applied to the web. Also incorporated in the control system will be a sequence generator that initializes the system configuration at the start of a test and initiates specified events during the run.

A set of drying test heads, with associated base plates and couplings, has been designed and constructed for use in the versatile test system. They will accommodate 5-inch diameter handsheets which are large enough to produce test specimens needed for paper properties evaluations but small enough to allow mechanical pressures in excess of 1000 psi to be applied to the sheet during a drying experiment. The heated head is instrumented with a 0.25-inch diameter surface thermocouple for use in heat transfer measurement and with a pressure transducer to measure the vapor pressure developed at the hot surface. The opposing head has provision for water receiver and handsheet installation. An optional bellows arrangement is available for installation around the test heads in order to permit establishment of a vacuum environment during thermal/vacuum drying tests. It is intended to install the new test heads in the Corrosion Group MTS system for initial trial in the near future.

An existing APPLE computer-based data acquisition system will be employed in the test program. Minor hardware and software modifications are being made to improve the system capability. A "BURPLE" interface will be used to transfer data from the APPLE to the Burroughs computer for manipulation.

FURNISH SELECTION/PROCUREMENT

The process of selecting and procuring pulp supplies for the technical performance evaluation program is nearly complete. Suitable stocks have already been requested and received for the following grades: (1) newsprint, (2) writing paper, (3) tissue, and (4) linerboard (primary liner). Contacts have been made regarding folding carton and corrugating medium stocks, and these materials are expected soon. Several companies have cooperated in supplying the various stocks needed for this program, and the assistance provided is appreciated.

TEST PROCEDURES SPECIFICATION

The procedures and requirements for handsheet preparation, handling, and post-test properties evaluation needed for a successful technical performance evaluation program have been tentatively defined. A brief review of these procedures is given below.

Preparation

A 5-inch inside diameter thin stainless steel ring will be installed in the standard handsheet mold to facilitate the direct formation of 5-inch handsheets. The sheets will be prepared in quantity and stored at high moisture content in a refrigerated space. Final pressing of test sheets to desired

moisture ratios for experiments will be performed within one or two days of expected use, after which the sheets will be sealed and refrigerated until needed. Pressing will be done at pressures of several hundred psi, with the sheets sandwiched between smooth metal disks and blotters. Experiments to determine pressing pressure and time conditions required to achieve given moisture ratios, for the various sheet types, are in progress. Periodic checks of basis weight variability will be made during the test program.

Since each paper grade represented in the test program will have a unique set of meaningful paper properties tests to be performed, the number of handsheets required per test condition to provide sufficient test samples will vary with grade. A range of 4-9 sheets per test condition has been estimated.

Handling

In pretest handsheet handling, including installation in the drying apparatus, operations (including human contact) that might contaminate the sheets will be avoided. It has been qualitatively observed that contamination by human contact can reduce the liquid dewatering occurring in impulse drying.

Since the majority of planned drying experiments will result in less than fully-dry sheets, the post-test handling procedure is particularly critical. To minimize uncontrolled moisture loss, and concomitant shrinkage, from the partially-dried sheets, they will be sealed in plastic bags until it is convenient to complete their drying. The final drying will be done at temperature and pressure conditions similar to those in a conventional dryer section. The target final moisture content will be about 5%. Sheets will then be sealed in plastic bags again until transfer to the paper testing laboratory, after which they will be handled in a standard manner.

Properties Evaluation

A detailed list of properties to be evaluated for each of the six representative grades was presented in the preceding PAC status report. This list has been considered in more detail recently, in order to define more clearly the appropriate test methods. In some cases, minor modifications to standard procedures will be made to accommodate use of nonstandard specimen sizes, etc. During the evaluation phase, individual test specimens (and results) will be identified with respect to their parent handsheet, which in turn will be identified in terms of drying run sequence, etc.

## TEST PROGRAM DEFINITION

The variables of possible interest in the technical performance evaluation program are numerous. Therefore, a careful selection of primary variables for inclusion in the study, and of test conditions, is important to its timely completion. The following variables are considered to be of prime importance: (1) grade (furnish), (2) basis weight, (3) initial moisture ratio, (4) initial sheet temperature, (5) ambient pressure, (6) peak applied mechanical pressure, (7) initial hot surface temperature, and (8) residence time at drying conditions. Some additional variables may warrant limited investigation, but do not seem appropriate for full-scale inclusion in the test program. These include mechanical pressure pulse shape, water receiver type and moisture content, prepressing conditions, hot surface treatment, etc.

Some comments on the primary variables are appropriate. Several of them are discrete variables or have limited ranges, requiring only two or three levels of testing. These include: grade (six possibilities), basis weight (probably two per grade), initial moisture ratio (three), initial web

temperature (two cases will be considered: room temperature and preheated to ~212°F), and ambient pressure (two cases will be considered: atmospheric and thermal/vacuum with a room temperature heat sink that establishes the vacuum level). The residence time variable is somewhat special in that only times less than or equal to the drying time are meaningful. Unfortunately, the drying time is a function of the other operating variables, such as surface temperature and applied mechanical pressure, and is thus not known a priori. If the drying time relationships were approximately determined via preliminary experiments prior to the main test program, then the selection of residence times for use in the main study would be facilitated. This approach appears to be the proper one.

Because the execution of the full test program suggested by the primary variables given above will likely take a year or more, it has been decided to first perform an "overview" series, having a probable duration of a few months. In this phase of the work, the initial moisture ratio will be deleted from study, the "thermal/vacuum" ambient pressure cases will be minimal, and only two levels of surface temperature and applied mechanical load will be employed for each grade.

In addition to providing test samples for paper properties evaluation, the drying experiments will provide extensive performance data on water removal and energy use. The quantities to be measured in the test program include: instantaneous applied mechanical pressure, instantaneous hot surface temperature, instantaneous vapor pressure at the hot surface, total water (weight) loss, and chemical tracer loss. Certain of these variables are used in subsequent calculations. In particular, the temperature data are used to calculate the heat flux and cumulative thermal energy input to the sheet, the mechanical pressure data are used to calculate impulse, and the chemical tracer data are used to estimate the amount of liquid dewatering.

## COMPUTER DATA BASE PREPARATION

Because the scope of the technical performance evaluation program is wide, it is especially important to have an efficient means for handling, storing, retrieving, manipulating, and presenting the data. A versatile information storage and retrieval system (INSYTE) that runs on IPC's Burroughs computer will be used to provide these capabilities. The data base structure is currently in the final stages of development. A remote terminal, in the Water Removal Laboratory, will be used to enter data with the aid of specially formatted screens. Each experiment (handsheet) will be given a unique identification number to facilitate information storage and retrieval. The data base will provide for storage of five classes of information: (1) identification information (sheet type, nominal test conditions, etc.), (2) experimental data (sheet weights, actual operating conditions, etc.), (3) calculated data (heat flux, impulse, etc.), (4) general paper properties (tensile, ultrasonic, etc.), and (5) grade-specific paper properties. Simple calculations, such as moisture ratios, unit conversions, etc., will be performed within INSYTE at the time of information retrieval and report generation. Some of the benefits of using INSYTE include the capability for data sorting and analysis, ready generation of predefined report types, and, especially, reduced need for specialized software development prior to initiation of the test program.

## LABORATORY STUDIES

Most of the experimental work this reporting period has centered on two aspects of impulse drying. These are: (1) measurement of liquid water removal, with special emphasis on evaluation of the effect of sheet preheating and on evaluating the use of LiCl as a tracer, and (2) measurement of

instantaneous heat flux and total thermal energy transfer under a variety of conditions having different levels of liquid water removal. These topics and other recent work are discussed in this section.

## LIQUID WATER REMOVAL

Several impulse drying experiments have been performed recently, in the heated drop press, in order to quantify the dewatering that occurs when the web is preheated, as compared to that which occurs when it is initially near room temperature. In the experiments, low pressure steam was used to preheat some of the sheets, bringing them quickly to near 212°F, just prior to a "drop," without appreciably changing their weight.

In the initial trials, 50 $g/m^2$ sheets of unbleached softwood kraft at 570 CSF with an initial dryness of about 40% were impulse dried at 1000 psi peak pressure, 600°F initial surface temperature and 7 ms nip residence time. It was found that the water removal, expressed as a fraction of the water initially in the sheet, increased from 37% for the nonpreheated case to 64% for the preheated case. It is surmised that this large effect is mainly due to the earlier occurrence of high vapor pressure at the hot surface in the preheated web case, causing a greater tendency for liquid-phase dewatering of the web while it is compressed.

The effect of preheating on liquid dewatering has been investigated in a series of tests using handsheets to which a water soluble chemical tracer was added during the sheetmaking process. At first, sodium fluorescein was used as the tracer, as had been done in earlier work reported at the last PAC meeting. However, most of the tests involved sheets having LiCl as the tracer. This

chemical is potentially superior because of its lower molecular weight, enabling it to diffuse more readily into the intrafiber water.

The impulse drying experiments were performed on 50 g/m$^2$ sheets of three pulp types: unbleached softwood kraft at 570 CSF and bleached northern softwood kraft at 680 CSF and at 300 CSF. In all cases, the initial sheet dryness was about 40% and the operating conditions involved peak mechanical pressures of 750-800 psi, initial surface temperature of about 600°F, and nip residence times of 9-11 ms. The results of these experiments are given in Fig. 1. It is seen that preheating yields large increases in total water removal, accompanied by large increases in liquid water removal as expected. In fact, examination of the data reveals that, except for the 300 CSF case (which appears to be anomalous), the additional liquid water removal that occurs with preheated webs is equal to or slightly greater than the total additional water removed. This behavior is physically reasonable, because one would expect the heat transfer to the sheet (responsible for the vapor removal that occurs) to be about the same or slightly less when drying the preheated sheets, as compared to the heat transfer to nonpreheated sheets.

## HEAT TRANSFER

The significant liquid-phase dewatering component of water removal that occurs during impulse drying, as reported in the preceding section, suggests that a potential exists for considerably reduced energy consumption in drying. In order to explore this aspect more fully, a number of impulse drying experiments were performed recently in which the instantaneous heat flux and cumulative energy transfer were measured using the "dynamic calorimetry" technique (based on the response of the hot surface temperature) described in

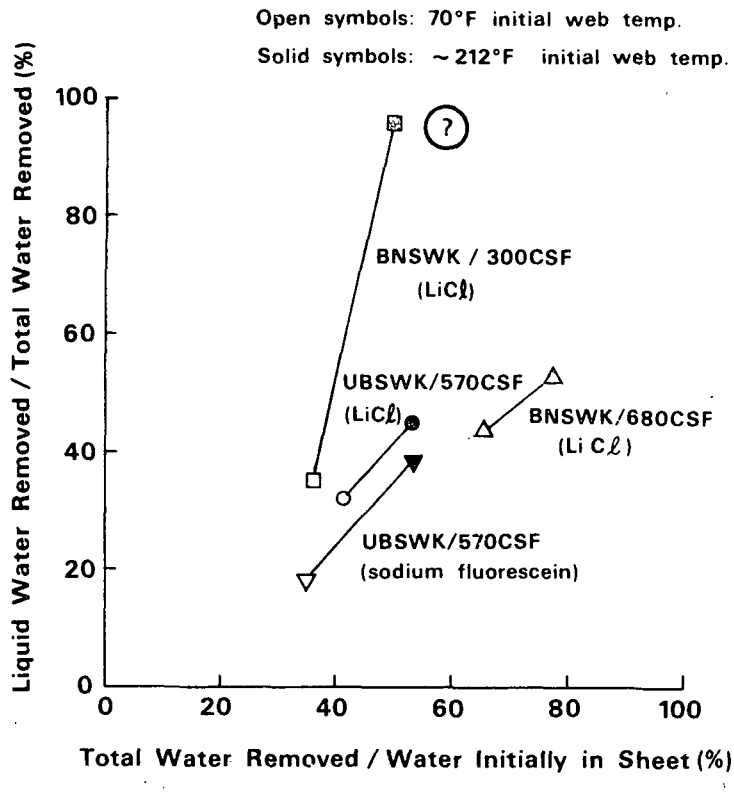


Figure 1. Effect of web preheating on total and liquid water removal in impulse drying. Liquid transfer based on chemical tracer transfer from sheet to felt. Conditions: 50 g/m$^2$ sheets at 40% initial dryness, 750-800 psi mechanical pressure, 600°F surface temperature, 9-11 ms nip residence time.

previous PAC reports. A typical example of the heat transfer results is shown in Fig. 2.

Many of the heat transfer experiments were performed for sheet and operating conditions like those used in the water removal experiments that yielded the data in Fig. 1. The energy transfer results from these tests are presented in Table 1. Three aspects of these results are in good qualitative agreement with physically-reasoned expectations. First, slightly more energy transfer occurred when the sheets were initially unheated. This is explained by the larger average driving force (hot surface-to-sheet temperature difference) for heat transfer in the unheated case. Compatible with this finding, the peak

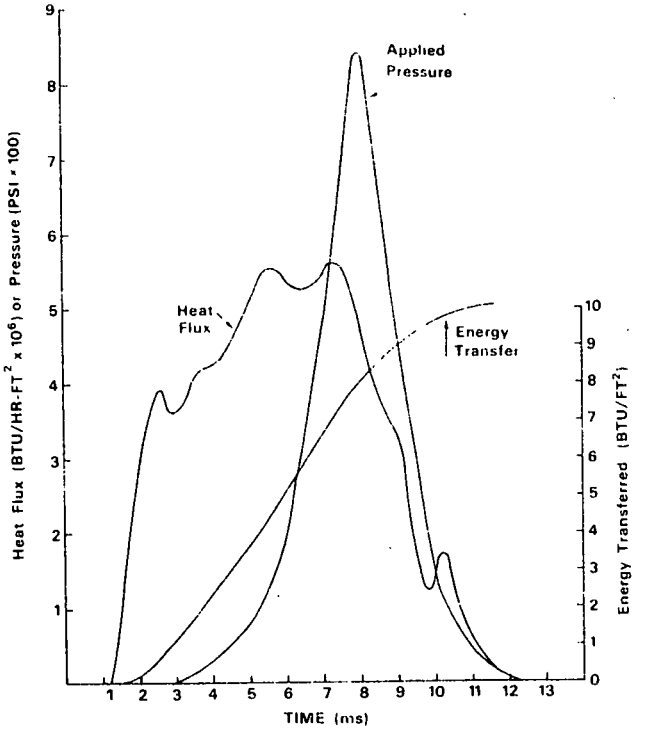


Figure 2. Example of instantaneous heat flux and cumulative energy transfer from hot surface to web under impulse drying conditions: non-preheated 50 g/m$^2$ BNSWK (300 CSF) sheet at 41% initial dryness, 617°F initial surface temperature, 9 ms nip residence time.

Table 1. Energy transfer results for impulse drying of 50 g/m$^2$ sheets (40% dryness) at 750-850 psi peak mechanical pressure, 600°F surface temperature and 10 ms nip residence time.

| Pulp/CSF | Preheat | Thermal Energy Transfer, Btu/ft$^2$ | Specific[a] Energy Transfer, Btu/lb$_m$ | $\left(\frac{\text{Actual}}{\text{Calculated}}\right)^b$ Energy Transfer |
|---|---|---|---|---|
| UBSWK/570 | yes | ~9 | ~1100 | 1.83 |
| UBSWK/570 | no | ~10.5 | ~2100 | 1.71 |
| BNSWK/300 | yes | 8 | ~1125 | ? |
| BNSWK/300 | no | 10 | ~1800 | 1.54 |
| BNSWK/680 | yes | 8.5 | ~700 | 1.37 |
| BNSWK/680 | no | 11 | 1040 | 1.22 |

[a]Per unit of water lost from sheet.
[b]Calculated energy transfer is based on water removal data in Fig. 1.

heat fluxes were found to be somewhat greater in the unheated than in the preheated cases (4 - 6 x $10^6$ Btu/hr-ft$^2$ vs. 5 - 8 x $10^6$ Btu/hr-ft$^2$). Second, and most important, the specific energy transfer (energy per unit mass of water removed from the web) is far less when the web is preheated than when it is nonpreheated. This is a result of the greater proportion of liquid-phase dewatering that occurs when the web is preheated. Third, although the "actual" energy transfer exceeds the amount calculated by an energy balance (using measured liquid and total water removal data and estimated final sheet temperatures), the actual/calculated energy transfer ratios are about the same, for a given pulp/CSF, with and without preheating. This suggests that the reduction in measured specific energy with preheating is consistent with the increase in percent liquid-phase water removal.

The actual/calculated energy transfer ratios given in Table 1 are somewhat disturbing. They indicate that from 22 to 83% more energy was needed for water removal than that amount specified by mass and energy balance considerations. There are at least two possible causes for the higher than expected "actual" energy transfer values. First, there could be appreciable heat loss (not accounted for in the calculated energy transfer values) from the heated web to the moisture in the felt. That is, the high actual energy transfer could be a real effect resulting from the very intensive operating conditions. Second, it could be that the surface thermocouple cools more quickly than the rest of the hot surface, due to its construction and installation details, thus indicating a larger energy transfer than really occurred. Other possibilities are that the quantities of water removal and/or the energy balance model might be somewhat in error. Efforts to resolve this matter will be made as part of future research.

OTHER WORK

In addition to the water removal and heat transfer work just reported, two other areas were briefly investigated recently. First, the water removal occurring in impulse drying in the heated drop press was compared with that occurring, for "identical" sheet and operating conditions, in the heated roll apparatus. For the case of drying 50 g/m$^2$ UBSWK/570 CSF sheets at 800 psi peak pressure, 600°F surface temperature and 10 ms nip residence time, the percent of initial moisture removed was about the same with either dryer (33.9% for drop press, 32.7% for roll press). Thus, it appears to be valid to use data from either dryer interchangeably to characterize impulse drying performance.

The second brief study involved determining the effect of pressing (water receiver) configuration on impulse drying performance. The drop press was used, at similar operating conditions to those described above. The standard configuration uses a sheet/felt/rubber sandwich on the pedestal. It was found that use of a porous plate under the felt, for venting, yielded about 3-4% greater water removal than occurs with the standard configuration. When the felt was removed, however, and the sheet was pressed directly against the porous plate, less than half the original water removal occurred. It appears that the porous plate was incapable of accepting the rapid transfer of the full liquid and vapor load, probably causing a significant back pressure to develop. Since the plate is a fairly good heat conductor, a thermal quenching of the web drying process may also have been a contributing factor.

## ENGINEERING CONSIDERATIONS

The data presented earlier in the report, dealing with the effect of web preheating on water removal and energy consumption for impulse drying, have

some engineering and economic consequences deserving mention. The total water removal increased considerably (e.g., by 25-40%) through the use of preheating. Thus, a considerable dryer size and capital cost reduction should result from this operating strategy. Since the cost per unit size may be large for an impulse dryer, this should be an important factor in the overall system economics. Although an expenditure of energy (probably low pressure steam) would be needed for web preheating upstream of the dryer, the cost of this energy use is expected to be small compared to the value of the energy savings within the dryer due to the increased liquid-phase dewatering. This is particularly true because relatively costly energy will be needed to maintain the high surface temperatures demanded by equipment size considerations.

A quantitative economic evaluation of alternative design and operating strategies of the type just discussed requires as input capital and operating cost-related engineering information for the proposed dryer system and other mill processes (e.g., the steam and power system) that are impacted by the new drying technology. The preliminary development of an analysis capability for use in the generation of needed information pertaining to the impulse drying system is in progress. Graduate student, M. Nightingale, is assisting with this work.

## PLANS FOR THE FUTURE

In the near future, all of the components needed for the versatile new drying system will be available for installation. Soon thereafter, the conduct of the technical performance evaluation program will become the major laboratory activity for several months. Concurrently, the engineering analysis capability currently under development will be completed and extended. Test program data

will be used to develop data on the engineering aspects of implementation. The MAPPS program will be used as needed in the assessment of mill-wide effects of advanced water removal systems.

THE INSTITUTE OF PAPER CHEMISTRY

Appleton, Wisconsin

Status Report

to the

ENGINEERING PROJECT ADVISORY COMMITTEE

Project 3479

# HIGHER CONSISTENCY PROCESSING

October 1, 1984

PROJECT SUMMARY FORM

DATE: Sept. 7, 1984

PROJECT NO. & TITLE: 3479 - Higher Consistency Processing

PROJECT LEADER: J. D. Sinkey

IPC GOAL: Reduction of the complexity of screening, cleaning, and forming systems.

OBJECTIVE: To identify or develop methods and principles by which the relative motions and positions of individual fibrous particles in 2-6% consistency slurries may be controlled, enabling practical separation and forming processes to be carried out at these levels.

CURRENT FISCAL BUDGET: $130,000

SUMMARY OF RESULTS SINCE LAST REPORT: (February, 1984 - August, 1984)

A list of potential approaches to higher consistency forming and separation was assembled, followed by critical assessment with respect to several criteria. That preliminary assessment indicated particular promise for the study of particle separation in zones of high shear and by spraying, and certain elongational flow techniques applied to forming. It was proposed that the separation processes could be studied with a two-roll adjustable nip apparatus. Such an apparatus has been designed and constructed, and installation in the pulp lab is being completed. An experimental plan for exploratory studies of fiber preparation has been devised and is being carried out. Results pertaining to the effects of surface speeds and gaps on particle separation between counter-rotating rolls are expected to be obtained before the October meeting.

# INTRODUCTION

As a result of an assessment of several possible avenues to follow in high consistency processing research, three approaches were deemed to be worthy of further exploratory work. They were: particle separation in a liquid shear field, separation of sprayed particles, and the application of elongational flow to high consistency forming. It was specifically proposed that particle separation be studied in a device consisting of two rolls capable of high surface speeds with adjustable gaps between them.

This report includes brief discussion of forces which would affect particle motion in such a device, as well as a description of the apparatus. In addition to the discharge from the nip into a submerged liquid phase, the case of discharge into vapor phase is also considered. The latter case may permit employing surface tension as an additional separating force.

The study of elongational flow for high consistency forming is the subject of a separate exploratory project. A high consistency flow loop is being designed and installed in the pulp lab for this and other HC work.

# BACKGROUND

## INTERTIAL MIGRATION IN A SHEAR FIELD

Figure 1 illustrates the apparatus, indicating counter-rotating rolls (same surface direction at nip), with discharge into a vapor phase. As discussed later, the experimental plan also includes studies with co-rotating rolls, moving at various relative speeds, and submerged discharge.

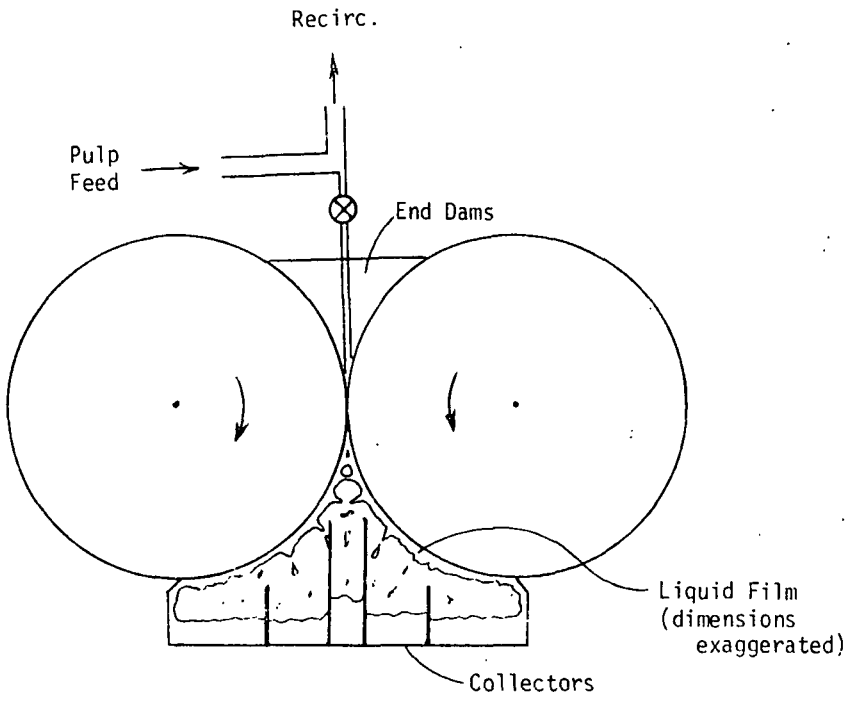


Figure 1. Counter-rotating rolls discharging to vapor phase.

In considering the nature of the velocity gradients which one might expect to encounter in such a situation, one may postulate flow fields of the form indicated in Fig. 2, in the case of a symmetrical feed. It has been well established (1-3) that suspended particles migrate across such shear fields at speeds and directions dependent on the size and nature of the particle, and the bulk flow geometry. Rigid spheres and other bodies in tube (Poiseuille) flow tend to migrate to an equilibrium position between the tube wall and centerline. Flexible rods or fibers tend to migrate to a position of minimum shear (4); longer fibers apparently migrate faster than shorter fibers (5). Hence, one would expect to see a certain separation of large fibers from small particles and water across the nip and post-nip liquid-phase regions, depending on geometry, gap, speeds, and residence time.

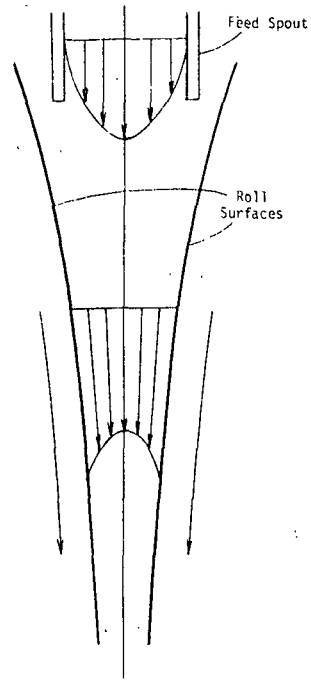


Figure 2. Possible velocity profiles in entrance to a symmetrical nip.

In the high shear gradients, it is likely that the particle would experience considerable intertial force (continued acceleration) even in the outgoing portions of the nip.

CENTRIFUGAL FORCES

As a particle exits the nip, centrifugal force tends to move it away from the center of each roll:

$$F_c = \frac{mv^2}{R} \left(\frac{\rho_p - \rho}{\rho_p}\right)$$

where $m$ = particle mass,

$R$ = distance from roll center,

$v$ = velocity component tangential to roll surface,

$\rho$, $\rho_p$ = densities of bulk fluid and particle, respectively.

Near the nip center, of course, both rolls contribute substantial centrifugal force, whereas a particle which remains in the liquid phase much beyond the nip is influenced centrifugally by only one roll. As a result of the centrifugal forces, one would expect a concentration of more massive and dense particles near the plane between the rolls, while lighter particles would remain more concentrated near the roll surfaces. This would tend to reinforce the shear migration phenomenon effects.

DRAG AND NETWORK FORCES

The motion of a particle suspended in a fluid is inhibited by drag force

$$F_D = \frac{mC_D u^2 \rho \sigma}{2}$$

where, $C_D$ = drag coefficient,

$u$ = particle velocity relative to fluid,

$\sigma$ = particle specific surface.

The drag coefficient, of course, depends on the projected shape of the particle and its surface frictional characteristics. Drag would be particularly important in the high-shear nip region.

As consistency increases, the number of fiber-to-fiber contacts increases. This results in an increase in the amount of interfiber frictional force which must be overcome to move a fibrous particle from its position in a network. Wahren (6) estimated the magnitude of these forces, by considering the force needed to bend a fiber segment to a minimum radius equal to the fiber length l. Hence, the network frictional force on a fiber

$$F_N = \frac{\mu S \bar{n}^2}{\ell 2}$$

where $\mu$ = interfiber friction coefficient

$S$ = fiber bending stiffness (EI)

$\bar{n}$ = ave. number of contact points.

At 3-10% consistency, he estimated the magnitude of the force necessary to pull a fiber loose to be 2-100 mN/m. The surface of tension of water $\gamma$ = 72 m/Nm.

Network forces become more important as the aspect ratio of the particle increases, but, of course, would be less relevant to the separation of dirt or other small particles. In all cases, both drag and network forces act in a direction which inhibits relative particle movement.

SURFACE TENSION FORCES

All the above forces may be active in the apparatus of Fig. 1, whether the nip exit is submerged, or the discharge is open as illustrated. In the latter case, however, surface tension presents an additional force acting on particles attempting to escape from the liquid phase:

$$F_S = \frac{m\gamma\sigma\cos\theta}{\ell}$$

where $\theta$ = the fiber-liquid contact angle.

Hence, particles with high wettability and high specific surface would tend more to be held in the liquid film on the roll surface.

INSTABILITY FACTORS

There are several operative factors in this system which would cause instabilities, tending to confound effective separation. They would be especially important at liquid surfaces, in the open discharge case.

A boundary layer of air tends to follow the roll surface into a nip in such a system (7). It is especially difficult to remove at higher speeds. It may be dealt with by roll flooding and submerged doctors in the inlet zone.

Film splitting is an obvious source of instability in a system, as in Fig. 1. At relatively low speeds, the fluid forms a stable meniscus at the nip exit, which splits into the two films on the outgoing roll surfaces (7). At higher speeds, cavitation occurs in the liquid phase beyond the nip, followed by formation of fingers of liquid which fling off the surface, because of higher centrifugal force at the larger radius. In the present system, it is likely that the larger particles in the center of the nip would be flung off in this mist directly below the nip exit. The influence of this misting on separation is difficult to predict.

In addition to these irregular and sometimes severe disturbances in the film stability with counter-rotating rolls, Babchin and Clish (7) analyzed ring-type disturbances which occur at definite frequencies. These regular disturbances occur as a result of competition between centrifugal force and surface tension in the dynamic meniscus. The rings, which circle the rolls perpendicular to the axes, are produced to varying degrees with practically all types of fluids in a counter-rotating roll device. With co-rotating rolls, ring-type and irregular disturbances were noted at certain roll speed ratios. An important consideration in this system was found to be the velocity gradient across the boundary air layer which follows the metering (reverse) roll into the gap (7).

SHORT-TERM GOALS

The brief discussion above considered forces one would expect to encounter in the apparatus of Fig. 1, and certain fiber parameters which influence them. It seems quite possible that the proper application and balance

of these forces would afford a useful principle for the separation of dirt, and possibly shives or other fibrous material from the main fibrous constituents. In the near term, it is expected that data will be obtained which will indicate the viability of such force balances to effect separations, in the several operating configurations being considered.

The following section provides greater detail of the apparatus which has been constructed for this exploratory work, and the experimental plan to be followed.

## EXPERIMENTAL

### APPARATUS

The two chrome-plated rolls of Fig. 1 are cantilevered, and driven from a common shaft via belts and pulleys, at a speed ratio of 1.5:1. This shaft, in turn, is connected to a 10 HP variable speed drive, again with a pulley ratio of 1.5:1. At a motor speed of 1750 RPM, the rolls can theoretically attain nearly 4000 RPM. Given the roll diameter (both 24.61 cm.), surface speeds of 2500 cm./sec. can be attained at half speed. One of the roll assemblies is laterally movable for gap adjustment. Speed differentials between rolls are attainable by changing pulley sizes. Appropriate modifications to the drive shaft arrangement can be made for the co-rotating roll system.

### EXPERIMENTAL PLAN

For the initial exploratory work, the pulp feed will consist of a mixture of mechanical and chemical pulps, with small amounts of "dirt-type" contamination. Preliminary assessment of separation will be on the basis of freeness, consistency, and visual estimation of dirt content in the fractions collected. Later work may involve more extensive analysis of the fractions (fiber

length, specific surface, etc.), as well as the possible use of model fibers (rayon) in mixtures. In addition, the initial consistencies used will be below 1%, to minimize the deleterious network force effects; higher consistencies will only be studied after conditions are established under which a separation principle is shown to be operative.

For the work with the counter-rotating roll system, some experimentation with inlet geometry may be needed to provide uniform non-plugging flow into the nip at reasonable speeds and gaps. Post-nip separation will be studied as a function of flow rate (up to 40 l/min.), speeds (up to 2500 cm./s), and gap (0.1-3.0 mm), in both the film splitting and submerged discharge configurations. The latter configuration will be achieved by raising the two center-collector partitions and flooding the central chamber.

Subsequent work with the co-rotating roll system is to follow a similar approach. After that, a third option to consider is a configuration similar to a trailing blade coater, with a pulp film being applied to a single moving roll surface through a gap between the roll and a stationary blade.

For the study of the application of forces to sprayed particles, several alternative methods of atomization have been considered. The most uniformly fine sprays can be produced by an air-blast technique, whereby compressed air or other gas is used at high velocity to break up liquid emerging from a nozzle (8). However, good atomization requires an air-to-liquid mass ratio of 0.1-0.2. For the envisioned mill-scale application, this would necessitate prohibitively large air compressor capacity and horsepower requirements. Of course, the use of pressurized steam would be even more energy-intensive. Simple hydraulic atomization by discharge under pressure through nozzles, produces relatively coarse droplets (8). Since it has the advantage of simplicity however, it will be com-

pared with the sprays generated from the roll device. For preliminary experimentation, the forces to be studied with the sprayed particles would be air jets and gravity.

## PRESENT ACTIVITY

At the time of this writing, the rolls are being ground and balanced to minimize run-out and vibration at high speeds. The feed piping and plexiglas discharge collectors have been fabricated, and are being installed. It is expected that data collection will begin presently.

## REFERENCES

1. Goldsmith, N. L.; Mason, S. G. Rheology: Theory and Applications (Ed. F. R. Eirich), Vol. 4, Academic Press (1967).

2. Hallow, J. S.; Wills, G. B. Ind. Eng. Chem. Fund. 9:603(1970).

3. Oroskar, A. R. Spray fractionation. Ph.D. thesis, Univ. of Wisc.,1981.

4. Karnis, A; Goldsmith, H.; Mason, S. G. Can. J. Chem. Eng. 44:181(1966).

5. Olgard, G. Tappi 53(7):1240(1970).

6. Wahren, D. Fiber structures in papermaking operations. Proceedings, Paper Science and Technology - the Cutting Edge. The Institute of Paper Chemistry, Appleton, WI, May 8-10, 1979, pp.112-29.

7. Babchin, A. J.; Clish, R. J. Stability and disturbance of coating films, Progress Report One, Project 2696-67, The Institute of Paper Chemistry, Appleton, WI, March 5, 1980.

8. Green, H. L.; Lane W. R. Particulate clouds: Dusts, smokes, and mists. Van Nostrand, Princeton, 1957, pp34-46.

THE INSTITUTE OF PAPER CHEMISTRY

Appleton, Wisconsin

Status Report

to the

ENGINEERING PROJECT ADVISORY COMMITTEE

Project 3556

# FUNDAMENTALS OF KRAFT LIQUOR CORROSIVITY

October 1, 1984

PROJECT SUMMARY FORM

DATE: Sept. 17, 1984

PROJECT NO. & TITLE: 3556 - Fundamentals of Kraft Liquor Corrosivity

PROJECT LEADER: R. A. Yeske

IPC GOAL: Increase the useful life of equipment by proper selection of materials of construction, and by identifying suitable process conditions.

OBJECTIVE: Use electrochemical methods to understand the corrosion processes occurring in kraft process streams as the basis for timely detection and elimination of corrosion and corrosion-assisted cracking the kraft pulp mill.

CURRENT FISCAL BUDGET: $130,000

SUMMARY OF RESULTS SINCE LAST REPORT: (February, 1984 - August, 1984)

Efforts to qualify on-line corrosion monitoring methods for use in white liquor environments are continuing. The electrical resistance method for corrosion monitoring has been found to be accurate when measuring the corrosion of carbon steel in white liquor. Earlier studies showing the successful use of the linear polarization method have now been supplemented with field studies that continue to show the utility of this corrosion monitoring method. Furthermore, the correction factors necessary for use with linear polarization monitoring in laboratory simulations have been found to be accurate for testing in actual liquors. Both the linear polarization and electrical resistance methods have been found to be accurate and simple enough for use by inexperienced mill personnel.

A field testing program to characterize white liquor corrosivity in actual white liquor clarifiers has been initiated. In the first mill visit, episodes of high corrosivity have been encountered, and liquor samples were automatically taken during these episodes for chemical analysis to search for corrosion accelerants. Additional mill visits are underway.

Corrosion weight loss testing continues in an effort to identify potential corrosion accelerants in white liquors. Tests have shown that polysulfides at intermediate concentration can induce corrosion rates as high as 60 mils/year, but the high corrosion rate is transient. In contrast to published reports, long term exposure in polysulfide-doped white liquors results in passivation with low long-term corrosion rate.

Preliminary tests have shown that increased white liquor velocity can result in a dramatic increase in the rate of corrosion of carbon steel by white liquor. In fact, liquor velocities of 1 m/s are sufficient to increase the corrosion rate by a factor of 30 relative to corrosion rates in stagnant liquors. This effect is larger than any other liquor variable considered to date.

## INTRODUCTION

Corrosion and corrosion-assisted cracking are severe problems for materials exposed to kraft liquors. Corrosion damages pumps, valves, storage tanks, clarifiers, piping, digester vessels and other components exposed to white, green and black liquors. The high cost of corrosion damage by kraft liquors has long been recognized, but little has been done to control this form of damage, aside from replacement with expensive stainless steels.

The overall objective of this project is to reduce the costs of corrosion by kraft liquors, by 1) developing methods to detect the onset of severe corrosion damage, and 2) identifying remedies for corrosion that are less expensive than replacement in kind or retrofitting existing equipment with stainless steel.

Although many different corrosion problems occur in various kraft liquors, the most severe problem currently experienced is corrosion of plain carbon steel by kraft white liquor. This form of damage seriously reduces the useful lifetime of tanks, clarifiers, piping, and ancillary equipment used in the preparation, storage and transport of white liquor. Lifetimes as short as five years have been reported in some liquor storage tanks and clarifiers, whose replacement costs may be as high as $200,000.

The study of corrosion of carbon steel in white liquor is currently focused on two areas:

- Detection of excessive corrosion rates, and
- Understanding of the effects of liquor variables on corrosion rates.

The first topic is being addressed because the corrosion rate caused by white liquor varies appreciably with time in a typical pulp mill. Apparently,

variations in the composition of the liquor are responsible for fluctuations in the rate of corrosion ranging from acceptable to excessive. Detection of excessive corrosion rates is the first step in the process of identifying the origins of excessive corrosion and eventual control by manipulation of liquor composition. The second topic listed above is being addressed to provide guidance regarding the type of liquor changes that can influence corrosion rates in white liquor. A clear understanding of the effects of temperature, liquor velocity, liquor composition, etc., is necessary as a guide for controlling corrosion damage, once excessive corrosion rates are detected.

In earlier status reports on this project, progress was reported on detection of excessive corrosion rates by on-line monitoring methods. The linear polarization method was found to give a continuous indication of the corrosion rate of carbon steel in simulated white liquors, provided care was taken in calculation of the corrosion rate from the guiding electrochemical equations. Errors were detected in corrosion monitoring by the linear polarization method when the simulated white liquors contained a high concentration of the oxidant, $Na_2S_x$ (polysulfide). However, this situation could be detected and accommodated by measurement of the electrochemical potential developed at the carbon steel/liquor interface; a high potential always accompanies errors in the corrosion monitoring results. In previous reports, the effect of concentration of various liquor species on the corrosivity of white liquor toward carbon steel was also discussed. Polysulfides (at low to moderate concentrations) and thiosulfates — both minor constituents of typical white liquors — were found to raise the corrosion rate dramatically.

In the present period, the research effort has been focused on the following areas:

i) Examination of the use of electrical resistance methods to monitor corrosion rates in kraft white liquor.

ii) Extension of the evaluation of the linear polarization method for corrosion monitoring to determine corrosion rate in actual liquors during mill site trials.

iii) Continued examination of the effect of liquor composition on corrosivity toward carbon steel.

iv) Preliminary examination of the effect of liquor velocity on the corrosivity of white liquor toward carbon steel.

Although these studies are not yet complete, the results provide considerable insight into the corrosion processes occurring in white liquors.

## RESULTS

### ELECTRICAL RESISTANCE METHOD FOR ON-LINE CORROSION MONITORING

The electrical resistance (ER) method is being evaluated as a method for on-line corrosion monitoring in white liquor, with potential for considerable simplification in interpretation compared to the linear polarization tests. The ER method is essentially an electronically determined weight loss test, wherein a suitable element is exposed to the liquor and allowed to corrode; the extent of corrosion is monitored by changes in electrical resistivity of the element as its current-carrying cross-section is diminished by corrosion. In the current tests, the sensing element is a wire made from a carbon steel typically used in vessel construction in the recausticizing plant. The progress of corrosion attack is monitored during exposure to simulated white liquor by making the sensing element an active element in an auto-balancing AC bridge circuit. Changes in resistance of the element are calibrated in terms of changes in wire diameter that occur as a result of corrosion.

Although the wire-element, ER method is the essence of simplicity — and that is the appeal of the method — there are some potential pitfalls in

the use of this method to monitor corrosion rates in white liquor. First, the measured resistance depends not only on the cross-section of the wire, but also on the temperature of the wire. Temperature-compensation is provided through use of a dummy element in the probe exposed to the same temperature as the active sensing element, but isolated from corrosion. Nonetheless, fluctuations in temperature may cause fluctuations in corrosion rates, even to the extent of a decrease in the apparent resistivity. Second, the corrosion products from corrosion of carbon steels by white liquor are metal sulfides, which may or may not have electrical conductivity, depending on composition and structure. If these compounds precipitate on the sensing wire element during corrosion, anomalous changes in resistance — and apparent corrosivity — may be encountered. Finally, the probe may fail by degradation of the materials of construction of the probe itself — seals, body, etc., — during exposure to white liquor.

To evaluate the ER method for corrosion monitoring in white liquor, the corrosion rates determined by exposure of the probe to simulated liquors were compared with average corrosion rates of weight loss coupons exposed simultaneously. Agreement between the integrated ER corrosion rate and the average corrosion rate of the weight loss coupons was taken as verification of the accuracy of the ER method. A Rohrback Model 4100 Corrosometer is being used to follow corrosion rates in these tests, with a Rohrback Type W-40 probe used as the sensing element. The wire in the sensing element is a 1010 steel wire whose diameter was chosen to optimize probe sensitivity while retaining a reasonable probe lifetime. The weight loss coupons were cylindrical specimens of 1018 carbon steel exposed at the same time as the probe elements. Both weight loss and ER probes were exposed to five different liquors for two week periods.

The results of ER tests shown in Table 1 indicate excellent agreement between the ER results and the weight loss results in each of the five environ-

ments. Furthermore, the ER tests (and the companion weight loss tests) corroborate the effect of thiosulfate and high polysulfides reported in preceding progress reports. The raw data showing changes with time in ER units (roughly, a measure of the percent change in useful corrosion lifetime of the probe) are shown in Fig. 1. In each case, some anomalies in the corrosion rate data are evident in the first 24 hours of the test, apparently as the corrosion films form and temperature compensation is established. Thereafter, the corrosion rate observed in the reference environment (Environment A) remains more or less constant, corresponding to a uniform daily increase in the resistance of the element. Additions of 5 g/L thiosulfate to the reference environment increased the corrosion rate significantly, while 25 g/L of $Na_2S_2O_3$ raised the corrosion rate by nearly a factor of three. The overall corrosion rate is also approximately constant over the period of exposure in the thiosulfate-doped liquors. Finally, additions of 5 and 10 g/L of sulfur to form passivating polysulfides in the liquor produced no significant corrosion of either the ER probe element or the weight loss coupons. In this respect, the ER probe provides an immediate, direct assessment of the corrosion rate in high polysulfide solutions, whereas the linear polarization (LD) method resulted in anomalies in these liquors.

Table 1. Electrical resistance method results.

| | Environment | | | | | |
|---|---|---|---|---|---|---|
| Envt. | NaOH, g/L | $Na_2S$, g/L | $Na_2S_x$ (as S°), g/L | $Na_2S_2O_3$, g/L | ER, mpy | Avg. Wt. Loss, mpy |
| A | 100 | 33 | -- | -- | 13 | 13 |
| B | 100 | 33 | -- | 25 | 44 | 42 |
| C | 100 | 33 | 10 | -- | 3 | 5 |
| D | 100 | 33 | -- | 5 | 20 | 23 |
| E | 100 | 33 | -- | 5 | 23 | 12 |
| G | 100 | 33 | 5 | -- | 1 | 3 |

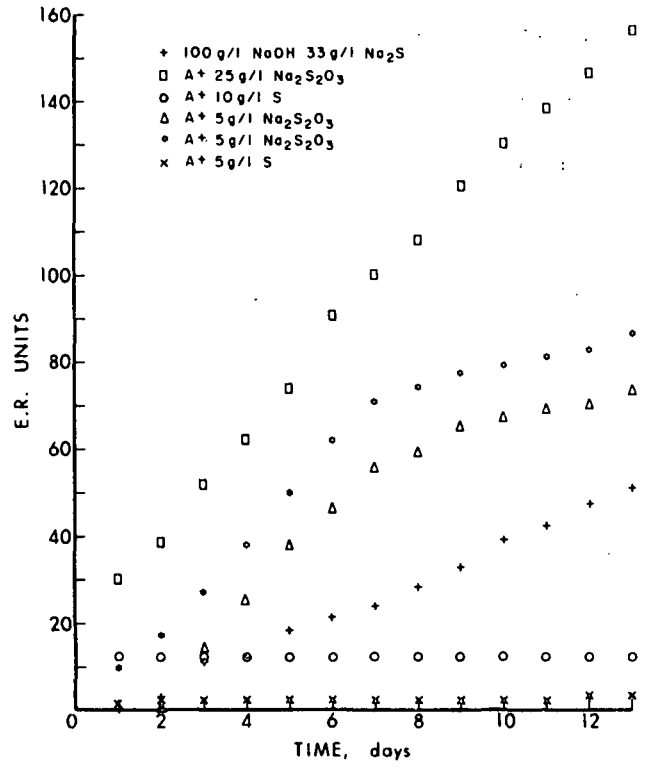


Figure 1. Raw ER probe results.

Thus, tests on ER probes exposed to white liquor for two-week periods indicate that the ER method provides an accurate measurement of corrosion rate, once the initial "settling-in" period is over. Apparently, conductive deposits do not compromise the corrosion measurement using this method. The elevated temperatures of test solutions also did not compromise the corrosion rate measurement, although no attempt was made to follow the accommodation of rapid fluctuations in temperature in this study. Finally the ER method apparently retains its accuracy in high-polysulfide environments, whereas complications arise with the LP method in these liquors. The ER method apparently offers simplicity of operation compared to the linear polarization method.

Some drawbacks are evident with the ER method, however. The inexpensive laboratory probes used in this study developed a seal failure after expo-

sure to white liquor for one month. Glass seals are used to isolate the wire element, and this glass was not resistant to the hot caustic used in the exposure tests. There was also evidence of blistering of the fiber-reinforced polymeric body of the probe after one month exposure. More resistant probes of teflon and stainless steel construction are available commercially for hot caustic applications, but these probes are fairly expensive. A second drawback of the ER method is that the raw data is not presented as an instantaneous corrosion rate, but is instead presented as a number reflecting total corrosion penetration of the probe. Therefore, the method provides no indication of the instantaneous corrosion rate, but only an average of the corrosion rate over a short time period. For the probe used, and the corresponding corrosion rates, an hour of exposure was required to detect significant changes in the corrosion rate. Thus, the ER method is not as instantaneous as the linear polarization method.

In spite of these minor shortcomings, the ER method appears to be a simple but powerful diagnostic tool for monitoring the corrosivity of white liquor. The simplicity of the method makes it particularly attractive for use in mills by engineers and technicians without formal training in corrosion engineering.

## CORROSION RATE MONITORING IN THE PULP MILL — LINEAR POLARIZATION TESTING

With encouragement from successful use of the linear polarization (LP) method in laboratory simulations, attention has been turned toward demonstration of the accuracy of the method in actual liquors during on-site testing. The objective of this task is to verify the laboratory results and to determine if LP tests retain their accuracy under actual mill conditions. A second objective of the in-mill testing is to characterize changes in liquor corrosivity and to determine if these changes can be related to changes in liquor composition.

Several member company mills were contacted to arrange for on-site testing in white liquor. These mills were selected to examine corrosivity of liquors involved in production of a variety of kraft pulp products. At the time of this report, one mill visit of one month duration was completed and a second visit was underway. Visits to four additional mills are scheduled in the next reporting period.

During the mill visits, a probe assembly containing several LP electrodes is lowered into the white liquor through the manhole in the roof of the white liquor clarifier. Eight LP tests on different carbon steel electrodes are conducted simultaneously using the Petrolite Model 1010 corrosion monitor. In addition to the eight carbon steel electrodes, the probe assembly contains two reference electrodes, two counter electrodes and two additional weight loss coupons. With the help of the mill personnel, corrosion rate and rest potential data are obtained from each of the eight electrodes for a one-month period. At the completion of the exposure, the weight losses of all electrodes are determined and compared with the time-integrated corrosion rates determined by the LP tests. The correction factor determined in the laboratory study ($CR_{actual} = CR_{meas.}/2.8$) was used to adjust the as-measured LP data for the Tafel slope and oxidation numbers reported as ($\beta/Z$) in previous reports.

In the first mill visit (mill A), duplicate electrodes of 1018 and A285C carbon steels used in the earlier laboratory studies were exposed, together with two special carbon steels based on the A285C composition. The first of these special steels — labelled A285C-SPEC — was taken from a specially prepared heat of A285 with high levels of copper and nickel and low levels of silicon. Wensley (1) has shown that this modification of A285C was somewhat more resistant to corrosion by white liquor. The second special steel was ASTM A283 — another plain carbon steel with composition close to that of A285C.

A sampling apparatus was also placed in operation at the mill, with liquor sampling automatically triggered by an upward excursion in corrosion rate detected at one of the electrodes (a 1018 electrode). A different liquor sample was taken every time the instantaneous corrosion rate at the selected electrode exceeded 75 mpy. The sample bottles containing the liquors were sent to the Institute for acidimetric analysis of NaOH, $Na_2S$, and $Na_2CO_3$; for potentiometric titration of $Na_2S_x$; and ion chromatographic analysis of $Na_2SO_3$, $Na_2S_2O_3$, and $Na_2SO_4$.

The rate of corrosion of a typical carbon steel electrode (1018), as determined by LP methods, is shown in Fig. 2. After an initial burst of corrosion activity on the bare electrodes immediately after immersion, the corrosion rates detected on the eight electrodes ranged from less than one to more than 75 mils per year (mpy). The rest potentials developed at the steel/liquor interface during the exposure ranged from -200 to -110 mV versus silver/silver-sulfide, corresponding to an active corrosion condition.

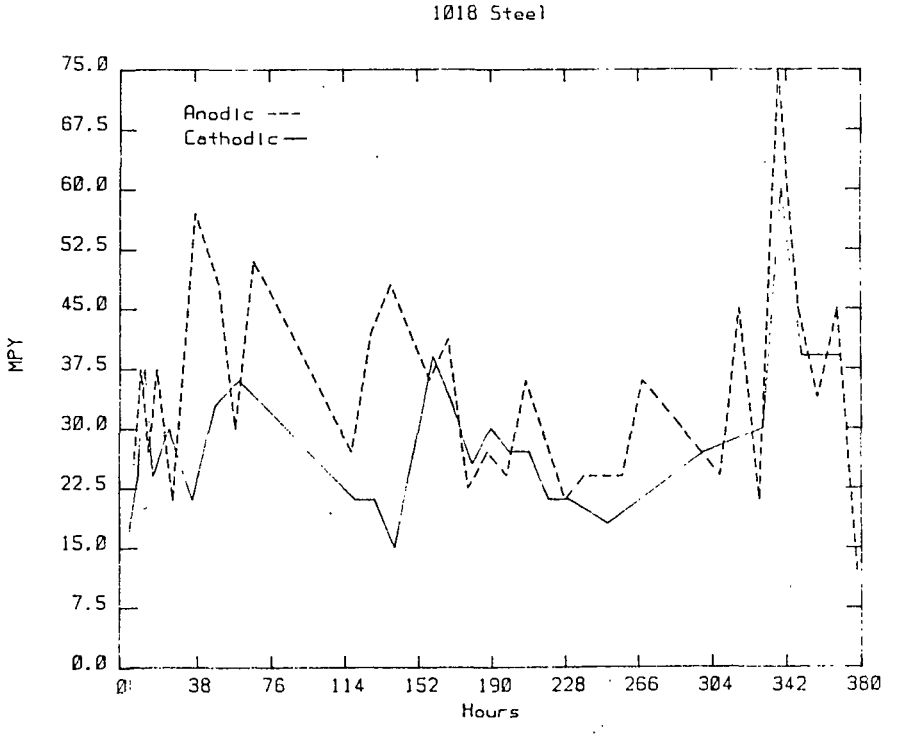


Figure 2. In mill corrosion of 1018 carbon steel exposed to white liquor (corrected for 2.8 factor).

For some of the steel electrodes — particularly A283 specimens — the corrosion rate soared to more than 75 mpy for several hours. Similar excursions in corrosion rate were observed on the 1018 carbon steel specimens, but no such excursions were detected on the A285C or A285C-SPEC steels. In some cases, several coupons would participate jointly in these excursions, while other excursions involved only one specimen at a time.

Liquors sampled during the 75 mpy excursions failed to reveal differences in the concentration of major constituents — NaOH, $Na_2S$, and $Na_2CO_3$. Test results on the minor constituents were not available at the time of this report.

As shown in Table 2, there is very good agreement between the averaged LP corrosion rates — corrected for appropriate values of the proportionality constant ($\beta/Z$) — and the average corrosion rates determined by the weight loss on the individual electrodes. The agreement is good for 1018, A285C, and A285C-SPEC steels, but the $(\beta/Z)^*$ correction required to bring one set of A285C-SPEC steel data steel data into agreement is not the 2.8 value consistently found in earlier tests. The reason for this discrepancy is not yet apparent, although the A285C-SPEC steel was clearly the least labile material in terms of corrosion rate and rest potential.

It is also interesting to note that the corrosion rates of the special A285-SPEC steel were similar to those reported for a generic A285C steel, in contrast to the results of Wensley and Charlton (1). In fact, the corrosion rate of all the A280 series steels was similar, and the 1018 carbon steel only corroded at a slightly higher rate.

Thus, while the origin of episodes of high corrosivity remains an engima, it does appear that the LP method for corrosion rate monitoring has the same good accuracy in the field as it had in the laboratory studies reported

earlier. Apparently, the LP method for on-line monitoring of corrosivity of white liquors will prove to be a powerful tool for investigating the causes of episodic high corrosivity in actual white liquors.

Table 2. Linear polarization results in mill liquor.

| Material | LP Corrosion Rate[a] | Weight Loss Rate, mpy | $(\beta/Z)^b$ |
|---|---|---|---|
| 1018 #1 | 29.9 | 29.7 | 2.83 |
| A285C #1 | 23.3 | 23.2 | 2.80 |
| A283 #1 | 31.0 | 25.8 | 3.37 |
| A285SPEC #1 | 14.1 | 22.9 | 1.73 |
| 1018 #2 | 33.3 | 39.9 | 2.70 |
| A285C #2 | 23.6 | 27.1 | 2.44 |
| A283 #2 | 30.6 | 29.0 | 2.96 |
| A285SPEC #2 | 20.0 | 23.9 | 2.34 |

[a]LP corrosion rate taken as the averaged cathodic and anodic rates, corrected by a $(\beta/Z)$ factor of 2.8.
[b]$(\beta/Z)$ correction required to bring LP and weight data into agreement.

## LIQUOR VELOCITY EFFECTS ON WHITE LIQUOR CORROSIVITY

Tests are underway to characterize the effects of liquor velocity on the rate of corrosion of carbon steel exposed to simulated white liquor. Preliminary results indicate that the velocity effect may be greater than any other liquor variable investigated to date, although some inconsistencies must be expunged from the data.

A flow channel system has been constructed to expose multiple weight loss coupons to white liquor flowing at controlled velocities up to 3 meters/sec. Cylindrical coupons are exposed along the axis of pipe sections of various internal diameters, through which white liquor flows at a controlled velocity.

The average velocity of liquor flow in the annular region between the coupons and the pipe wall is determined by a paddle wheel flow sensor. A liquor temperature of 90°C is maintained by immersion of the entire flow channel in a heated water bath. In the present study, 1018 carbon steel specimens are exposed, five at a time, to each of four velocities. The reference liquor used in previous studies, containing 100 g/L NaOH and 33 g/L $Na_2S$, was also used in these initial test runs.

The results of three initial test runs at twelve different liquor velocities are summarized in Table 3. The most striking result in Table 3 is the extraordinary corrosion rates achieved in the high flow velocity situations.

Table 3. Effects of flow velocity on corrosion rate in a simulated white liquor[a].

| Velocity, m/s | Annular Cross-sectional Area, $cm^2$ | Run No. | Corrosion Rate |
|---|---|---|---|
| 0.07 | 4.8 | 5 | 23.6 |
| 0.12 | 2.7 | 5 | 25.6 |
| 0.14 | 4.8 | 4 | 65.0 |
| 0.21 | 1.5 | 5 | 36.5 ? |
| 0.25 | 2.7 | 4 | 80.0 |
| 0.30 | 4.8 | 3 | 99.0 |
| 0.43 | 1.5 | 4 | 120.0 |
| 0.50 | 2.7 | 3 | 143.0 |
| 0.66 | 0.5 | 5 | 46.0 ? |
| 0.86 | 1.5 | 3 | 138.0 |
| 1.32 | 0.5 | 4 | 150.0 |
| 2.62 | 0.5 | 3 | 148.0 |

[a]100 g/L NaOH, 33 g/L $Na_2S$, 90°C.

Corrosion rates of 150 mils/year are in evidence, whereas corrosion tests in static environments of similar composition usually result in corrosion rates of 10 mils/year or less. It is clear that increased flow velocity has a remarkable, deleterious effect on the corrosion resistance of carbon steel exposed to white liquor. This result substantiates field observations of very rapid corrosion of carbon steel piping carrying white liquors; it may also explain the higher corrosion rates detected at the liquid level line as being caused by wave action, since even low velocity liquor is twice as corrosive as stagnant white liquor.

A troublesome aspect of the velocity effects study is the apparent lack of agreement between tests at similar velocities in different test runs and in pipe sections of different diameters. A careful assessment of the hydrodynamics conditions in the flow system is planned to address this point.

EFFECTS OF LIQUOR COMPOSITION ON CORROSION RATES

Weight loss tests over two month exposures, complemented by diagnostic polarization curve generation, are being conducted to characterize the effects of different solute species on the corrosivity of white liquor toward carbon steel. To date, tests in binary $NaOH/Na_2S$ solutions have found little effect of composition on corrosion rate for simulated liquors approximating actual liquor compositions. A corrosion rate of 5 to 10 mils/year is typically encountered in these tests, which reflects the low concentration of oxidizing species present in these binary liquors.

In the current test program, corrosion rates are being measured in ternary $NaOH/Na_2S/Na_2S_x$ solutions, to determine the effect of polysulfide on the corrosion rate. Results described in the literature and short-term linear polarization studies have shown that low to moderate levels of polysulfide in white liquors accelerate the corrosion rate of carbon steel. The current test

series examines the long-term effects of polysulfides on corrosion rates.

In this effort, weight loss coupons are exposed to simulated white liquors containing various amounts of NaOH, $Na_2S$, and elemental sulfur (which forms polysulfides by reacting with the sulfide). Four coupons are exposed to each of the selected environments, with one coupon removed after two, four, six, and eight weeks of exposure. To insure against the effects of consumption of polysulfide by the corrosion processes via

$$Fe + S_x^{=} \longrightarrow FeS + S_{x-1}^{=} ,$$

the contents of each test chamber were replaced every three days throughout each exposure. All handling of the solutions, including liquor replacement and coupon removal, was done in a nitrogen-filled glove bag to prevent oxidation of the sulfide species in the liquor. Mead Amalgam and acidimetric titration tests on several of the liquors indicated that no significant change in liquor compositions occurred as a result of the exposures.

The results of the tests available to date for the ternary $NaOH/Na_2S/Na_2S_x$ exposures are summarized in Table 4.

Table 4. White liquor studies.

Weight Loss Results - 2 Weeks

mpy

| NaOH, g/L | $Na_2S$, g/L | S° as elemental sulfur, g/L | | | | | | |
|---|---|---|---|---|---|---|---|---|
| | | 0 | 0.5 | 1.0 | 1.5 | 2.0 | 5.0 | 1.0 |
| 60 | 10 | 2.3 | 5.0 | 3.6 | 0.6 | 0.9 | 0.5 | 0.8 |
| | 20 | 2.1 | 6.1 | 9.5 | 0.8 | 18.2 | 3.3 | 3.8 |
| | 30 | 4.3 | 17.7 | 15.4 | 13.3 | 18.9 | 3.8 | 3.3 |
| | 40 | 5.2 | 21.8 | 19.7 | 14.4 | 15.4 | 6.4 | 1.1 |
| 80 | 10 | 2.2 | 5.3 | 0.5 | 0.7 | 1.1 | 0.4 | 0.6 |
| | 20 | 2.9 | 7.6 | 8.8 | 12.4 | 20.4 | 1.7 | 2.2 |
| | 30 | 3.4 | 21.7 | 13.9 | 19.1 | 18.6 | 2.0 | 2.4 |
| | 40 | 4.5 | 15.7 | 14.2 | 17.1 | 22.0 | 4.8 | 2.4 |
| 100 | 10 | 3.4 | 7.7 | 10.8 | 1.7 | 7.7 | 1.2 | 1.2 |
| | 20 | 2.7 | 10.2 | 15.9 | 22.5 | 17.9 | 1.1 | 1.2 |
| | 30 | 4.3 | 9.0 | 24.7 | 19.0 | 20.3 | 11.8 | 2.6 |
| | 40 | 4.1 | 20.9 | 35.0 | 51.3 | 62.4 | 9.4 | 2.1 |

Weight Loss Results - 4 Weeks

mpy

| NaOH, g/L | $Na_2S$, g/L | S° as elemental sulfur, g/L | | | | | | |
|---|---|---|---|---|---|---|---|---|
| | | 0 | 0.5 | 1.0 | 1.5 | 2.0 | 5.0 | 1.0 |
| 60 | 10 | 0.6 | 2.6 | 0.8 | 1.0 | 0.5 | 0.6 | 0.5 |
| | 20 | -- | 4.9 | 4.3 | 12.6 | 1.3 | 2.0 | 2.1 |
| | 30 | 3.6 | 8.7 | 6.0 | 6.0 | 1.6 | 1.8 | 1.9 |
| | 40 | 4.1 | 12.4 | 19.9 | 14.8 | 9.7 | 0.8 | 0.7 |
| 80 | 10 | 2.1 | 3.0 | 9.6 | 0.7 | 0.8 | 1.0 | 0.8 |
| | 20 | 2.6 | 4.0 | 4.5 | 6.7 | 8.5 | 2.1 | 1.5 |
| | 30 | 3.3 | 16.1 | 7.3 | 9.7 | 14.7 | 1.4 | 1.8 |
| | 40 | 5.4 | 18.0 | 7.1 | 10.2 | 11.9 | 6.7 | 2.1 |
| 100 | 10 | 4.4 | 4.9 | 6.3 | 1.9 | 1.4 | 1.2 | 1.2 |
| | 20 | 3.6 | 10.3 | 11.6 | 14.0 | 21.5 | 2.0 | 1.7 |
| | 30 | 3.6 | 8.2 | 14.0 | 10.2 | 11.0 | 3.4 | 1.7 |
| | 40 | 4.8 | 21.7 | 35.1 | 26.5 | 37.6 | 4.9 | 1.9 |

Table 4. White liquor studies (continued).

Weight Loss Results - 6 Weeks

mpy

| NaOH, g/L | $Na_2S$, g/L | S° as elemental sulfur, g/L | | | | | | |
|---|---|---|---|---|---|---|---|---|
| | | 0 | 0.5 | 1.0 | 1.5 | 2.0 | 5.0 | 1.0 |
| 60 | 10 | 0.6 | 1.6 | 0.7 | 0.6 | 0.5 | 0.6 | 3.4 |
| | 20 | 2.1 | 2.5 | 2.8 | 0.6 | 1.2 | 0.9 | 0.9 |
| | 30 | 2.7 | 5.0 | 3.6 | 3.6 | 6.5 | 0.6 | 0.4 |
| | 40 | 3.1 | 15.7 | 6.4 | 10.8 | 5.3 | 0.7 | 0.6 |
| 80 | 10 | 2.0 | 2.1 | 6.6 | 0.8 | 0.9 | 0.6 | 0.9 |
| | 20 | 2.4 | 3.0 | 3.6 | 4.3 | 7.0 | 2.0 | 1.3 |
| | 30 | 4.0 | 17.8 | 5.7 | 7.4 | 3.6 | 0.9 | 1.0 |
| | 40 | 4.1 | 13.6 | 4.4 | 6.8 | 8.7 | 4.6 | 1.1 |
| 100 | 10 | 2.8 | 2.6 | 4.1 | 4.9 | 3.0 | 0.6 | 0.8 |
| | 20 | 2.8 | 11.1 | 10.9 | 11.6 | 9.5 | 1.5 | 1.5 |
| | 30 | 3.5 | 5.5 | | | | | |
| | 40 | | | | | | | |

Weight Loss Results - 8 Weeks

mpy

| NaOH, g/L | $Na_2S$, g/L | S° as elemental sulfur, g/L | | | | | | |
|---|---|---|---|---|---|---|---|---|
| | | 0 | 0.5 | 1.0 | 1.5 | 2.0 | 5.0 | 1.0 |
| 60 | 10 | 0.9 | 1.5 | 0.6 | 0.7 | 0.7 | 0.8 | 0.6 |
| | 20 | 2.0 | -- | 2.4 | 5.5 | 1.0 | 0.9 | 0.8 |
| | 30 | 2.7 | 3.4 | 2.5 | 3.1 | 5.3 | 1.7 | 0.5 |
| | 40 | 3.7 | 4.2 | 2.5 | 4.8 | 4.7 | 0.7 | 0.6 |
| 80 | 10 | 1.6 | 1.9 | 0.8 | 0.7 | 0.6 | 0.5 | 0.7 |
| | 20 | 3.1 | 2.2 | 2.6 | 3.9 | 4.6 | 1.4 | 1.3 |
| | 30 | 4.1 | 15.3 | 4.6 | 5.5 | 6.6 | 2.5 | 0.7 |
| | 40 | 4.8 | 10.6 | 3.7 | 6.2 | 6.3 | 3.2 | 0.8 |
| 100 | 10 | 1.9 | 2.0 | 3.0 | 0.9 | 1.0 | 0.8 | 1.1 |
| | 20 | 2.8 | 8.6 | 8.1 | 9.0 | 9.1 | 1.5 | 1.3 |
| | 30 | 4.7 | 4.0 | | | | | |
| | 40 | | | | | | | |

Several points are noteworthy. First, the effect of polysulfide on the corrosion reaction appears to be a transient one, increasing the initial corrosion rate during the first few weeks of exposure, but having lesser effect as the exposure time increases. For tests in the 100 NaOH/40 $Na_2S$/2 S° liquor, for example, the corrosion rate rose to a very high level during the first two week exposure — 62 mils per year — but doubling the exposure to four weeks reduced the average corrosion rate by one-half, and tripling the exposure reduced the average corrosion rate by more than one-third. This behavior suggests that the polysulfide addition increases the corrosion rate to very high levels during some fraction of the initial two-week exposure, but passivation occurs soon after that initial burst of corrosion activity so that corrosion rates are very low in the subsequent weeks of exposure. This passivating ability of low levels of polysulfide in long-term exposures has not previously been reported.

A second noteworthy aspect of the data shown in Table 4 is the dependence of the initial polysulfide effect on the NaOH and $Na_2S$ in the white liquor. In every case, the corrosivity of liquors with 0.5 tgo 2.0 g/L S° was higher than the corrosivity of low and high polysulfide solutions. However, the acceleration of corrosion by polysulfide was not striking until the concentration of $Na_2S$ exceeded 20 g/L. Severe initial attack in white liquor — on the order to 50 mpy — also required a high concentration of NaOH, on the order of 100 g/L or more. At the conclusion of the eight week exposure, however, the dependence of the corrosion rate on the synergistic interaction of $Na_2S_x$, NaOH and $Na_2S$ is diminished considerably by pasivation effects discussed above.

The matrix shown in Table 4 will be completed during the next reporting period, and a similar matrix testing program involving thiosulfate-doped white liquors will be started.

## SIGNIFICANCE TO THE INDUSTRY

Laboratory tests, and now field testing, have shown that commercially available methods for corrosion rate monitoring are accurate in predicting the corrosion rate of carbon steel exposed to white liquor. Some precautions are required for successful use of the linear polarization method, but both the linear polarization and electrical resistance methods are simple enough for use by relatively inexperienced mill personnel. It appears that individual mills can now utilize these two methods to monitor the corrosivity of white liquor in their recausticizing plants.

With the ability to monitor corrosivity thus assured, field tests are now underway to characterize corrosion in actual white liquors in field settings, and to sample liquors during periods of especially high corrosivity. This work may lead to guidelines for controlling corrosion in white liquor by manipulating the recovery and recausticizing conditions. The current test program to isolate white liquor species that control corrosion rates will guide the search for operating conditions that reduce liquor corrosivity.

The tests to characterize the effects of liquor velocity provide graphic evidence of the importance of controlling velocity in the white liquors. Minimizing liquor velocity by system design to avoid high velocity areas can lead to significant increases in the lifetime of carbon steel.

THE INSTITUTE OF PAPER CHEMISTRY

Appleton, Wisconsin

Status Report

to the

ENGINEERING PROJECT ADVISORY COMMITTEE

Project 3309

# FUNDAMENTALS OF CORROSION CONTROL IN PAPER MILLS

October 1, 1984

## FUTURE DIRECTIONS

For the past 18 months, this project has focused on characterization of the metallurgical structure and overall corrosion resistance of suction roll alloys. With the departure of Dr. Bowers, the direction of the project will be changed to bear more closely on the central issue of suction roll performance — namely, corrosion-assisted cracking. Much remains to be done in this critical area.

The immediate objectives of the suction roll study will be to:

i) identify a corrosion fatigue test whose results will correlate with the performance of suction roll alloys in the field,

ii) compare the results of different suction roll corrosion fatigue test methods, so mills will be able to evaluate different vendors claims regarding suction roll performance evaluated by various methods,

iii) characterize the effect on roll performance of various whitewater species with potential for degrading resistance to cracking,

iv) evaluate the role of mean stress on corrosion fatigue performance, as an indication of the effect of residual stresses arising from roll fabrication, and

v) rank all existing and candidate suction roll alloys for cracking resistance according to the same uniform procedure as developed in i), above.

Although these are ambitious objectives and a prolonged effort will be required to achieve them, the issues addressed are of extraordinary interest to an industry currently beset by expensive and unpredictable suction roll failures.

Facilities necessary for the proposed mechanical testing were installed in 1984, with some additional equipment scheduled for installation in 1985. Efforts are underway to obtain sufficient stock material to meet the foreseeable needs of the program, and to prepare the necessary test specimens. Initially, corrosion fatigue and stress corrosion tests will be started to identify a test

that will correlate with the relatively poor performance of Alloy 63 versus the superior performance of Alloy 75. These are similar materials whose cracking resistances differ markedly in service. Tests will also be initiated to compare rotating bending, reversed bending and push-pull fatigue testing of suction roll alloys under otherwise identical conditions, to normalize test results currently available from different suppliers of suction rolls.

THE INSTITUTE OF PAPER CHEMISTRY, APPLETON, WISCONSIN

# SLIDE MATERIAL

for the

# ENGINEERING PROJECT ADVISORY COMMITTEE

October 24-25, 1984

The Institute of Paper Chemistry
Appleton, Wisconsin

TABLE OF CONTENTS


| | | Page |
|---|---|---|
| Project 3384: | Refining of Chemical Pulps for Improved Properties . . | 1 |
| Project 3480: | Wet Pressing Fundamentals . . . . . | 17 |
| Project 3470: | Fundamentals of Drying . . . . . | 34 |
| Project 3479: | Higher Consistency Processing . . . . . | 49 |
| Project 3556: | Fundamentals of Kraft Liquor Corrosivity . . . . . | 57 |
| Project 3309: | Fundamentals of Corrosion Control in Paper Mills . . . | 71 |

Project 3384

# REFINING OF CHEMICAL PULPS FOR IMPROVED PROPERTIES

John D. Sinkey

# REFINING OF CHEMICAL PULPS FOR IMPROVED PROPERTIES

PROGRAM GOAL:

Develop ways to measure and control manufacturing processes

## CONTROL OF AMOUNT OF REFINING

SPECIFIC ENERGY $E_{NET} = \frac{P}{qC}$

## CONTROL OF REFINING SEVERITY

SPECIFIC EDGE LOAD $SEL = \frac{P}{\Omega Z^2 L}$

PROBLEM STATEMENT:

WE HAVE NO GOOD MEASURE OF, OR CONTROL OVER, THE TYPE OR INTENSITY OF REFINING

$$\text{Normal stress } \bar{P}_N = \frac{T}{Z^2 L \bar{\ell}} = \frac{P}{\pi \mu \Omega Z^2 L \bar{\ell}(D - \frac{1}{2}L\cos\theta)}$$

$$\text{Shear stress } \bar{\tau}_f = \mu_f \bar{P}_N = \frac{\mu_f T}{Z^2 L \bar{\ell}} = \frac{(\mu_f/\mu)P}{\pi \Omega Z^2 L \bar{\ell}(D - \frac{1}{2}L\cos\theta)}$$

$$\text{Tensile stress } \bar{\sigma}_f = \frac{\mu_f \bar{P}_N \ell_f}{t_f} = \frac{\mu_f T \ell_f}{Z^2 L \bar{\ell} t_f} = \frac{(\mu_f/\mu)P\ell_f}{\pi \Omega Z^2 L \bar{\ell}(D - \frac{1}{2}L\cos\theta)t_f}$$

EXPERIMENTAL APPROACHES

- IN-REFINER MEASUREMENT OF $P_N$
- VERIFICATION OF $\bar{\tau}_f$ AND $\bar{\sigma}_f$ EXPRESSIONS

TOP VIEW, THROUGH ROTOR BAR

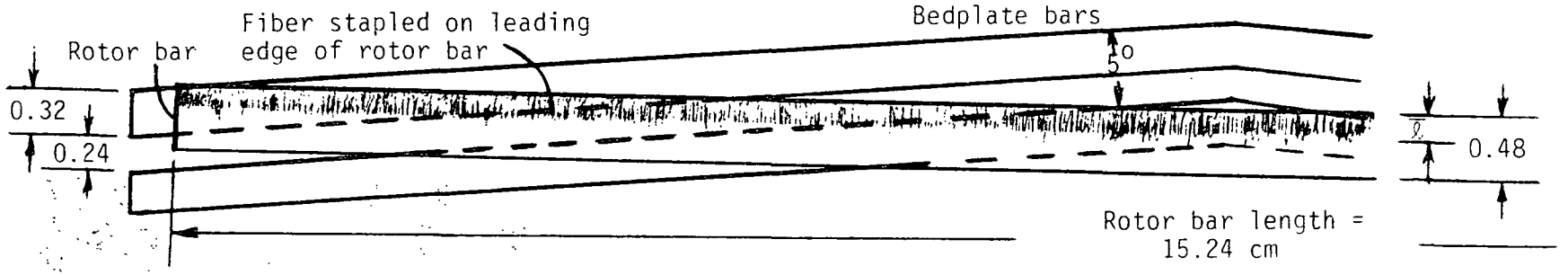


SIDE VIEW

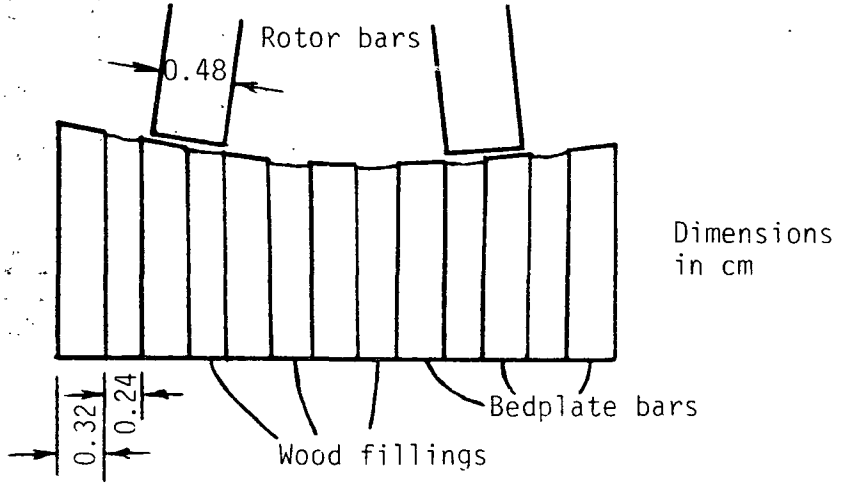


VALLEY BEATER BAR GEOMETRY

## MODEL EQUATIONS FOR VALLEY BEATER

$$\bar{P}_N = \frac{\Lambda}{189\mu\bar{\ell}}$$

$$\bar{\tau}_f = \frac{(\mu_f/\mu)\Lambda}{189\bar{\ell}}$$

$$\bar{\sigma}_f = \frac{(\mu_f/\mu)\Lambda\ell_f}{189\bar{\ell}t_f}$$

## EXPERIMENTAL TASKS

- Set up beater
- Torque sensor
- "High-intensity" conditions
- $P_N$ measurement

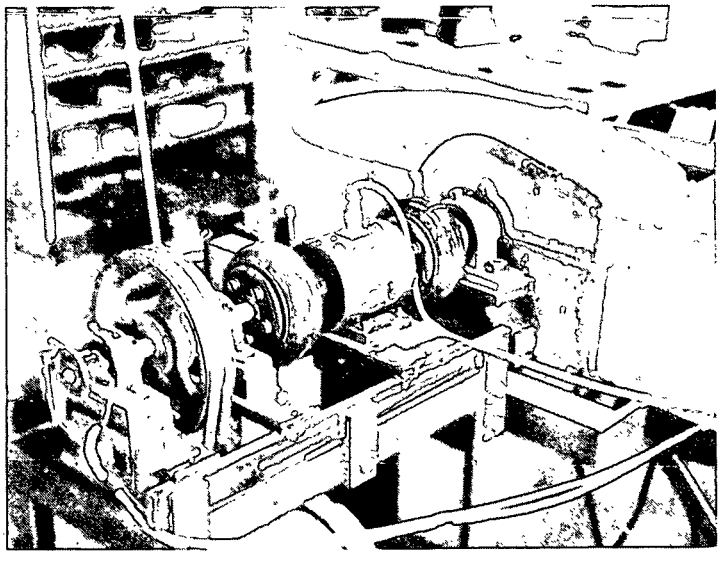

Valley beater with rotor shaft modification to accommodate torque sensor.

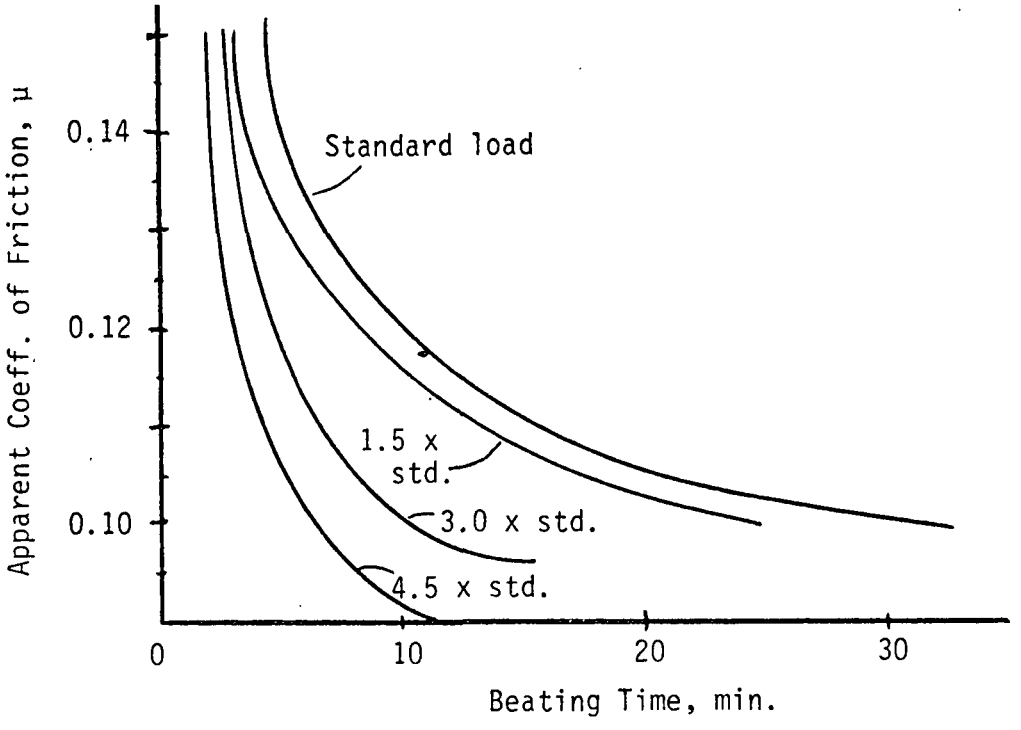
Apparent Coeff. of Friction, μ
0.14
0.12
0.10
Standard load
1.5 x std.
3.0 x std.
4.5 x std.
0
10
20
30
Beating Time, min.

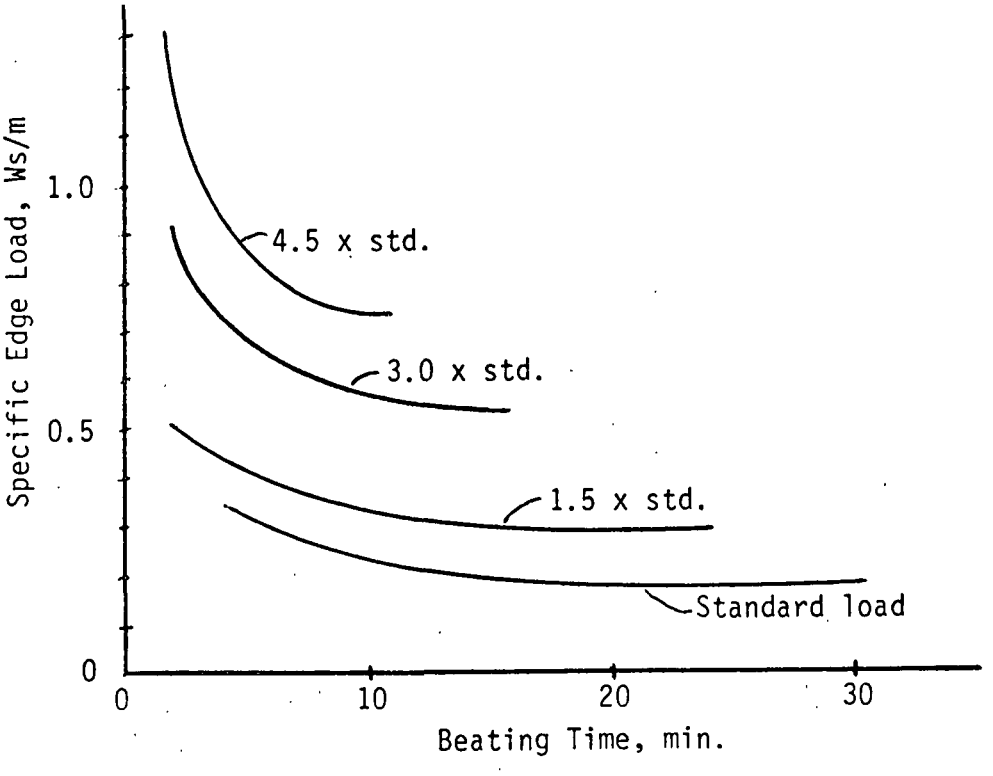
Specific Edge Load, Ws/m
1.0
0.5
0
4.5 x std.
3.0 x std.
1.5 x std.
Standard load
0
10
20
30
Beating Time, min.

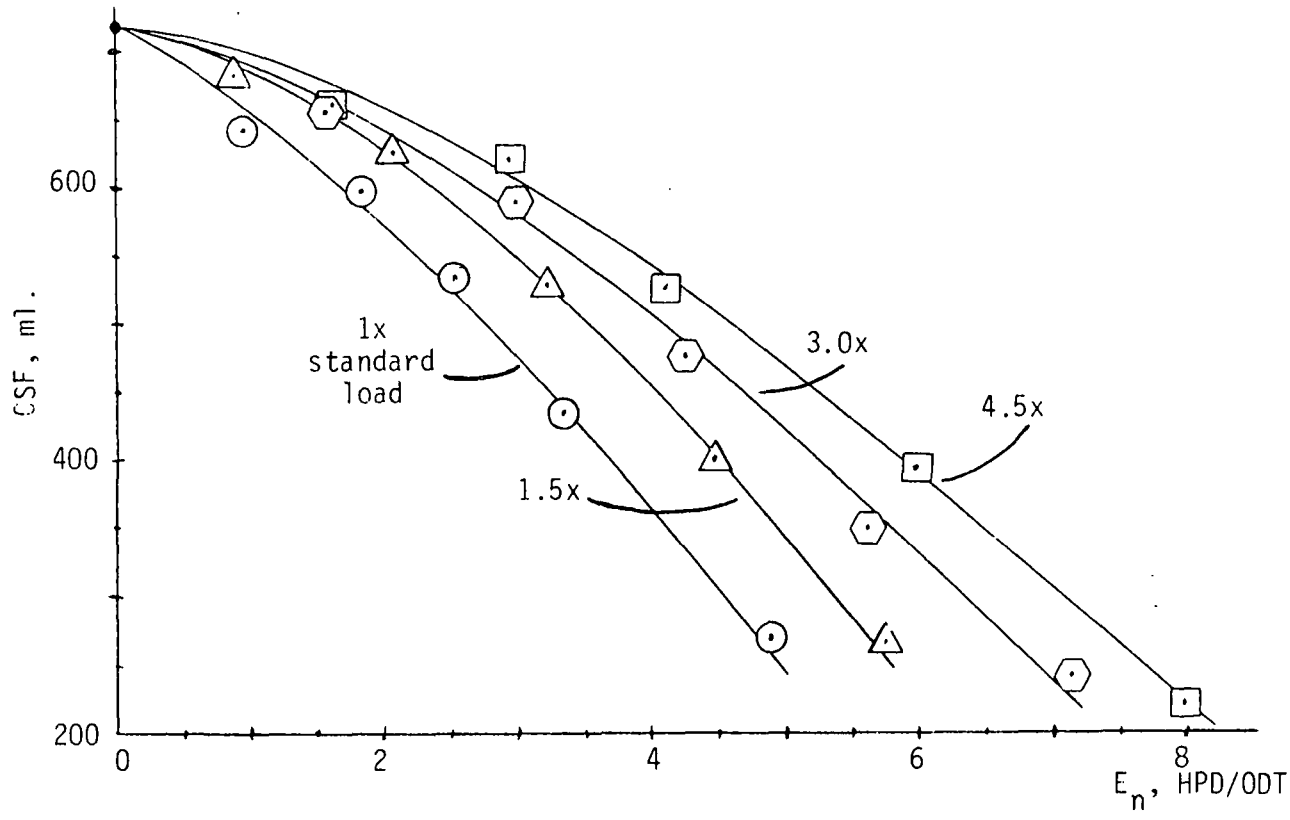


Freeness vs. net specific energy.

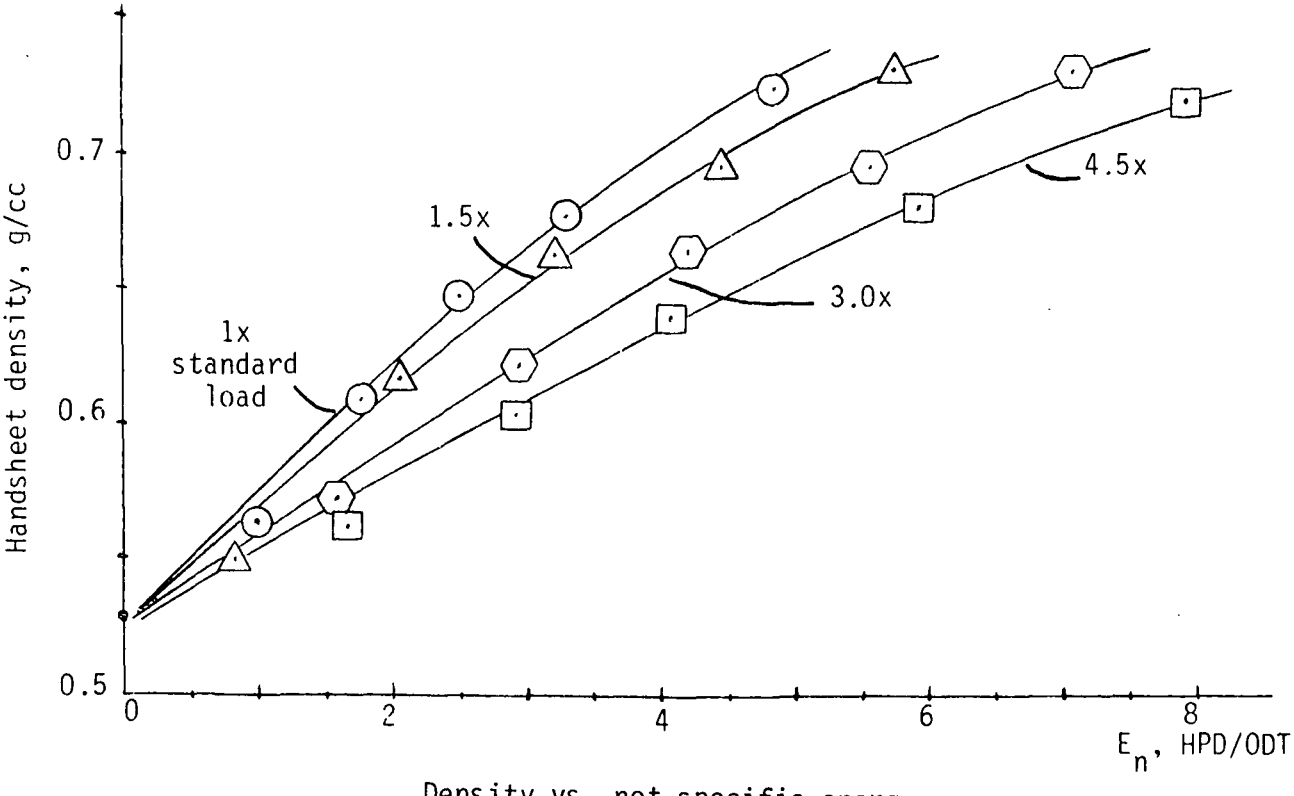


Density vs. net specific energy.

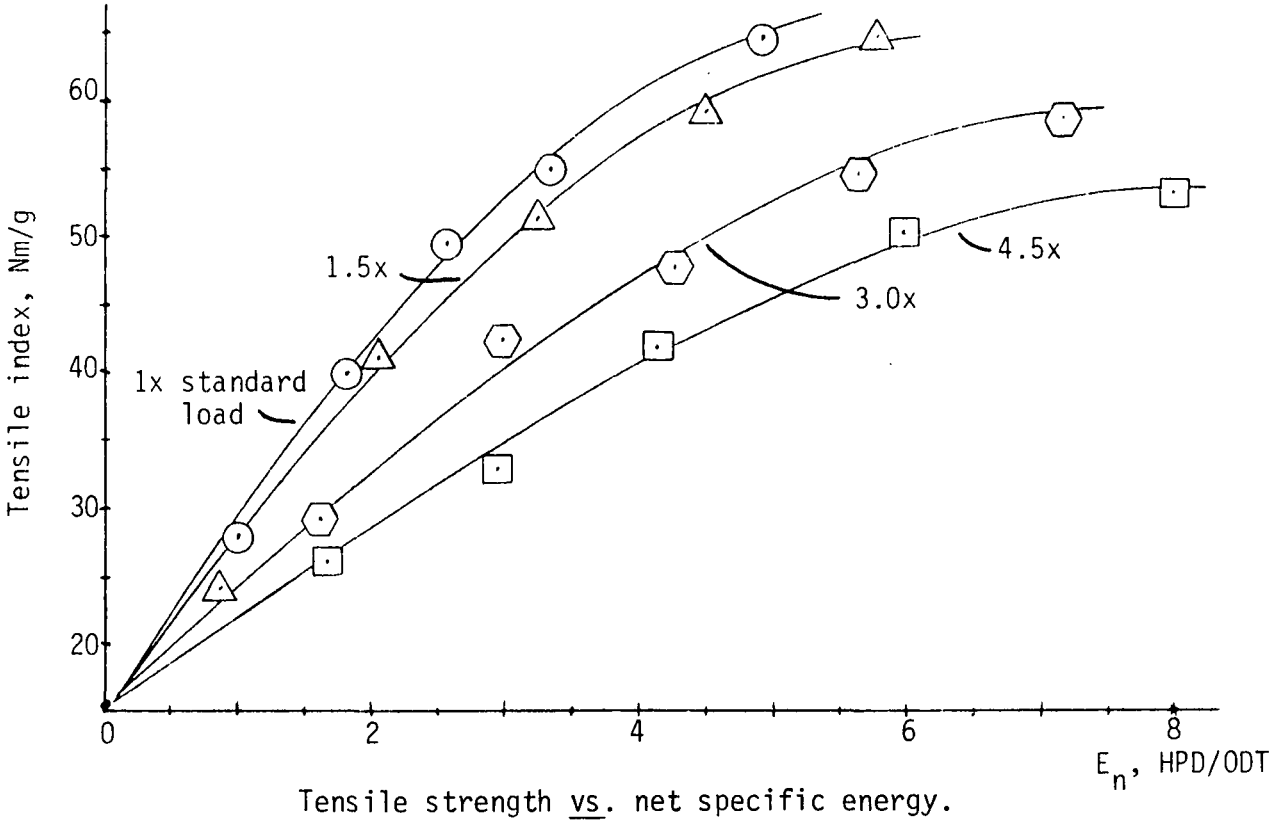


Tensile strength vs. net specific energy.

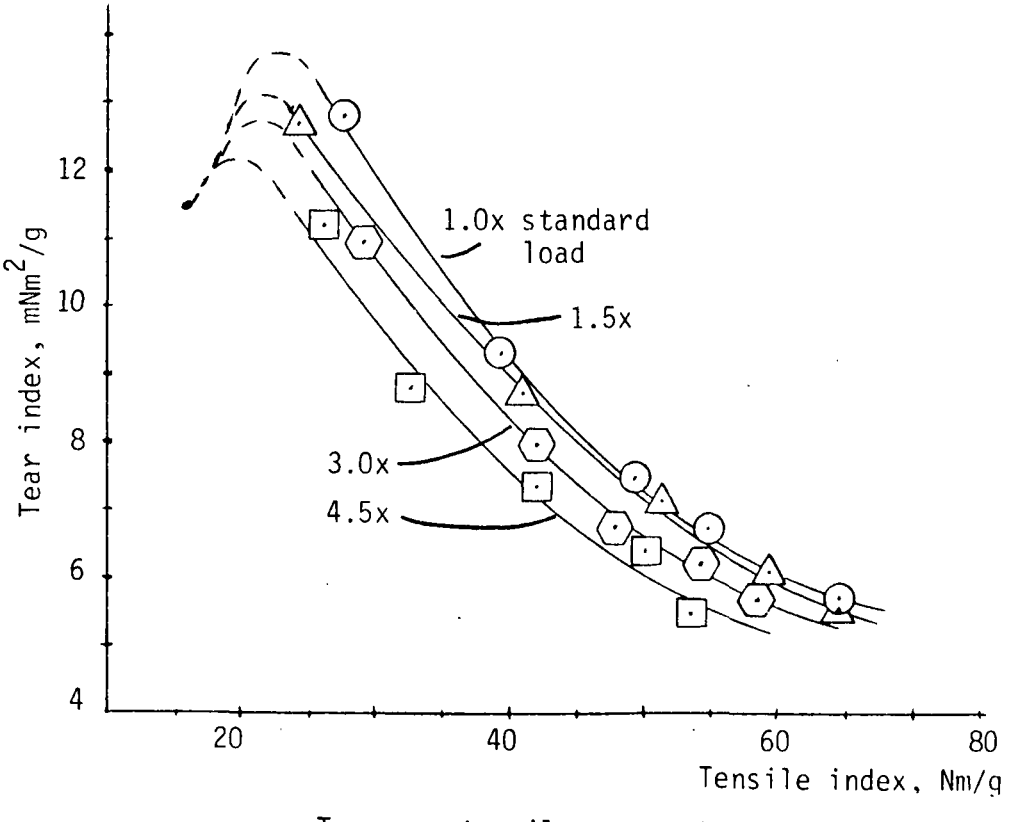


Tear vs. tensile strength.

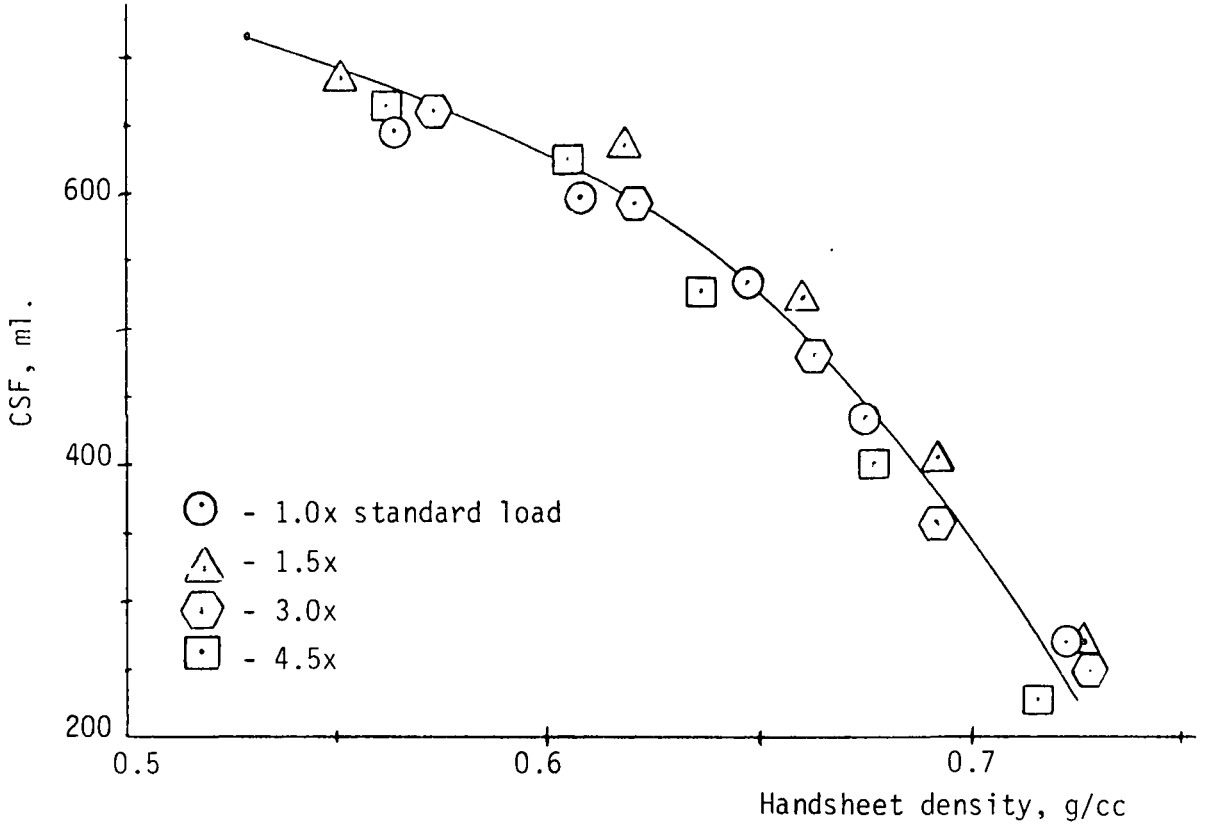


Freeness vs. density.

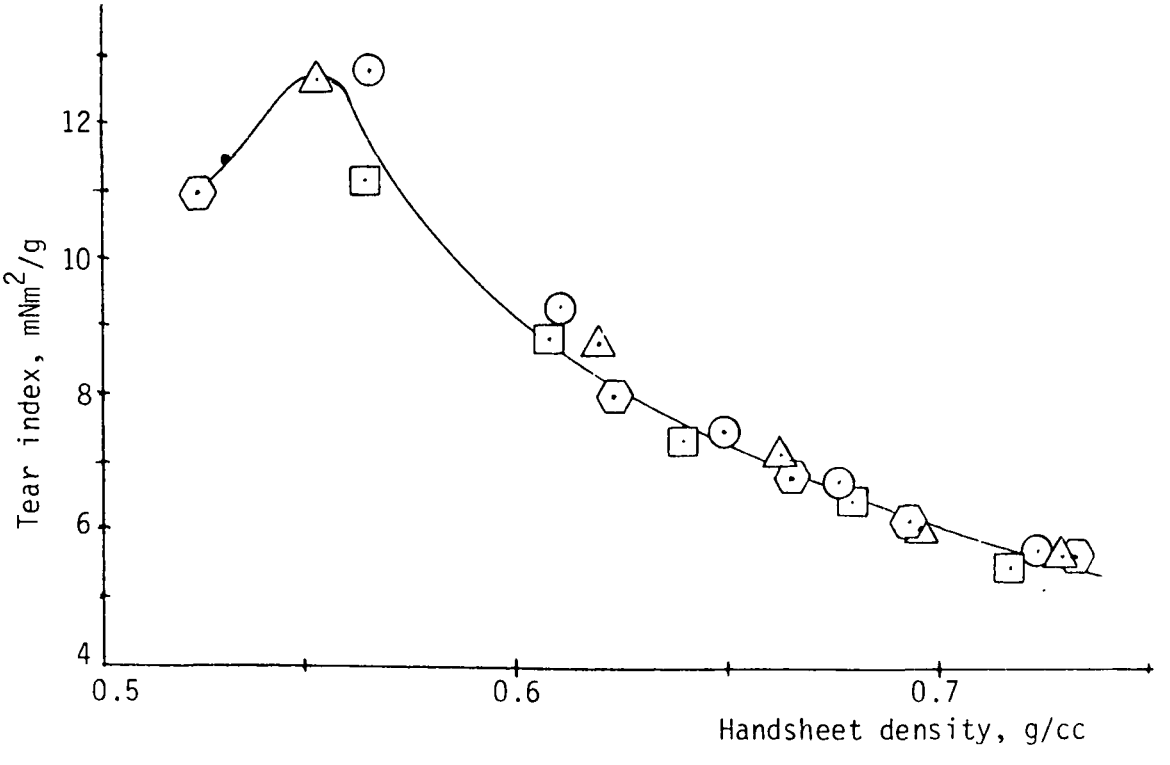


Tear strength vs. density.

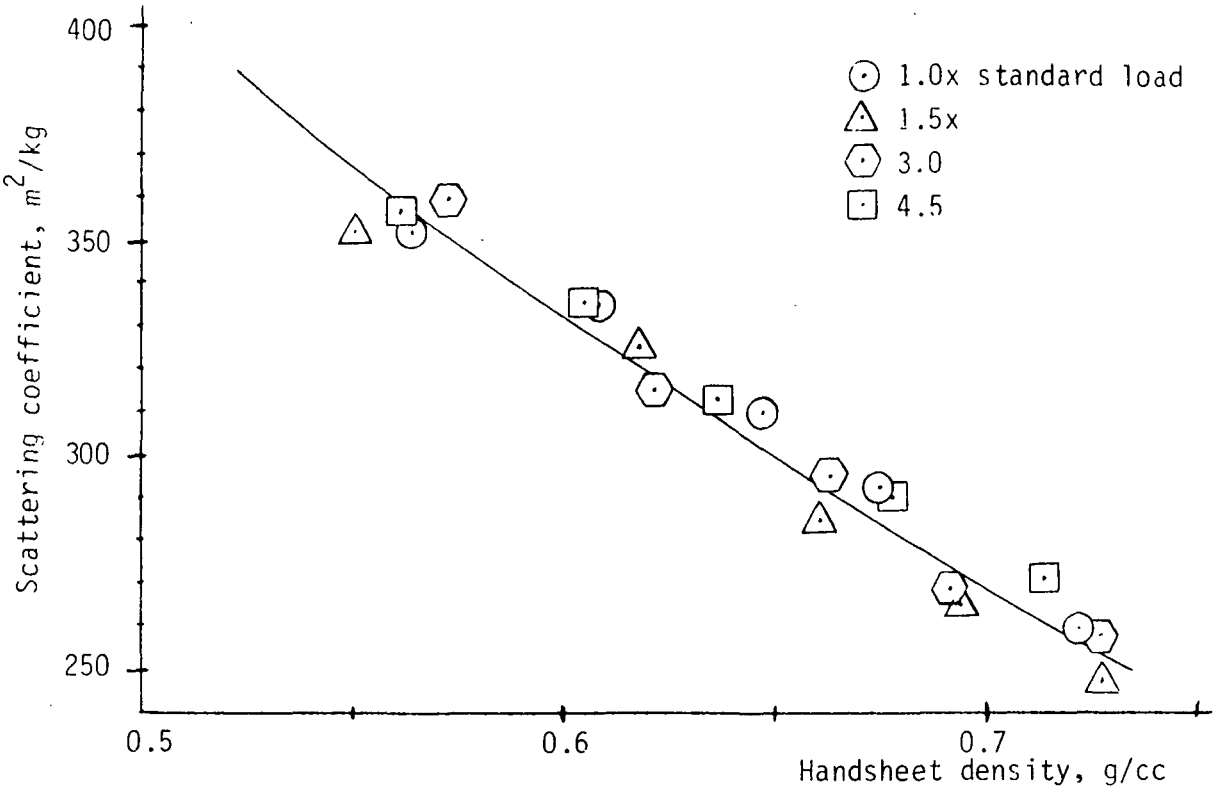


Scattering coefficient vs. density.

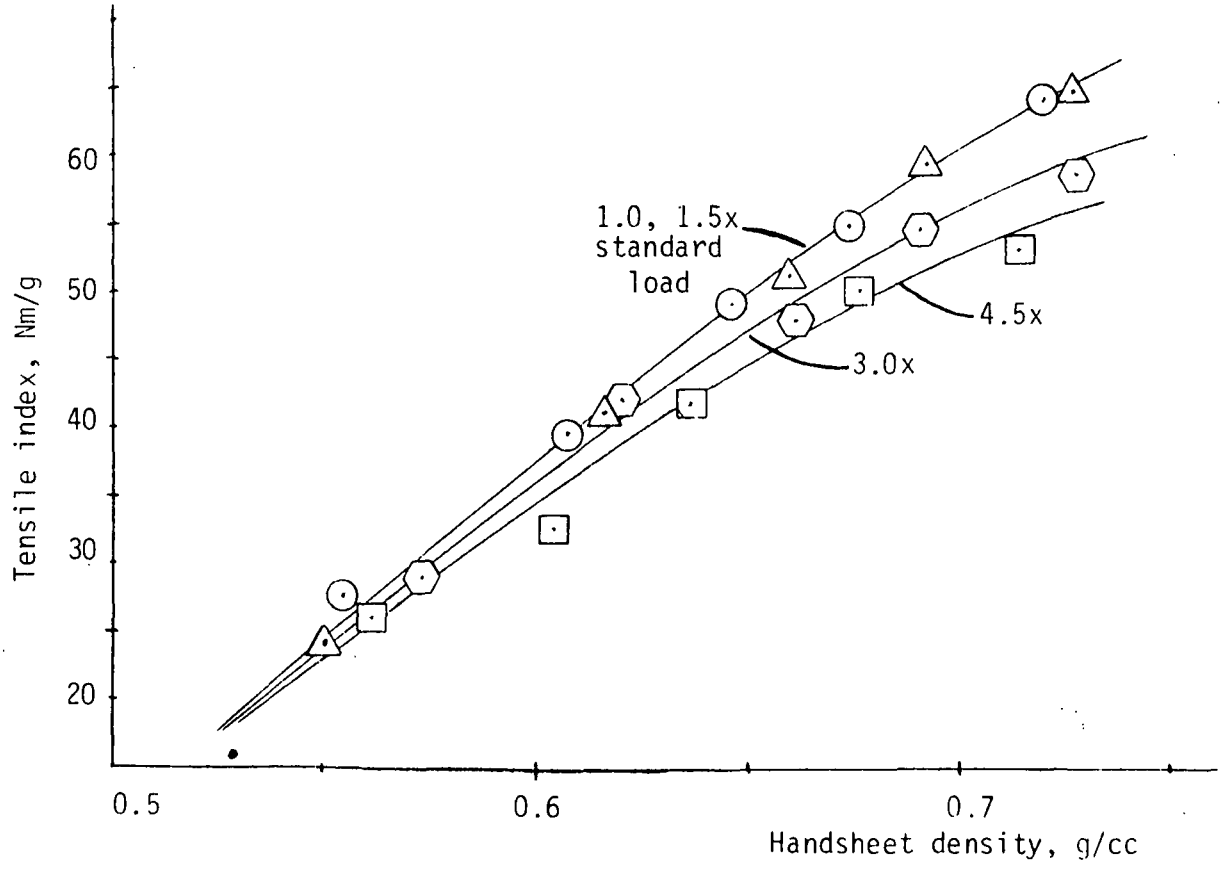


Tensile strength vs. density.

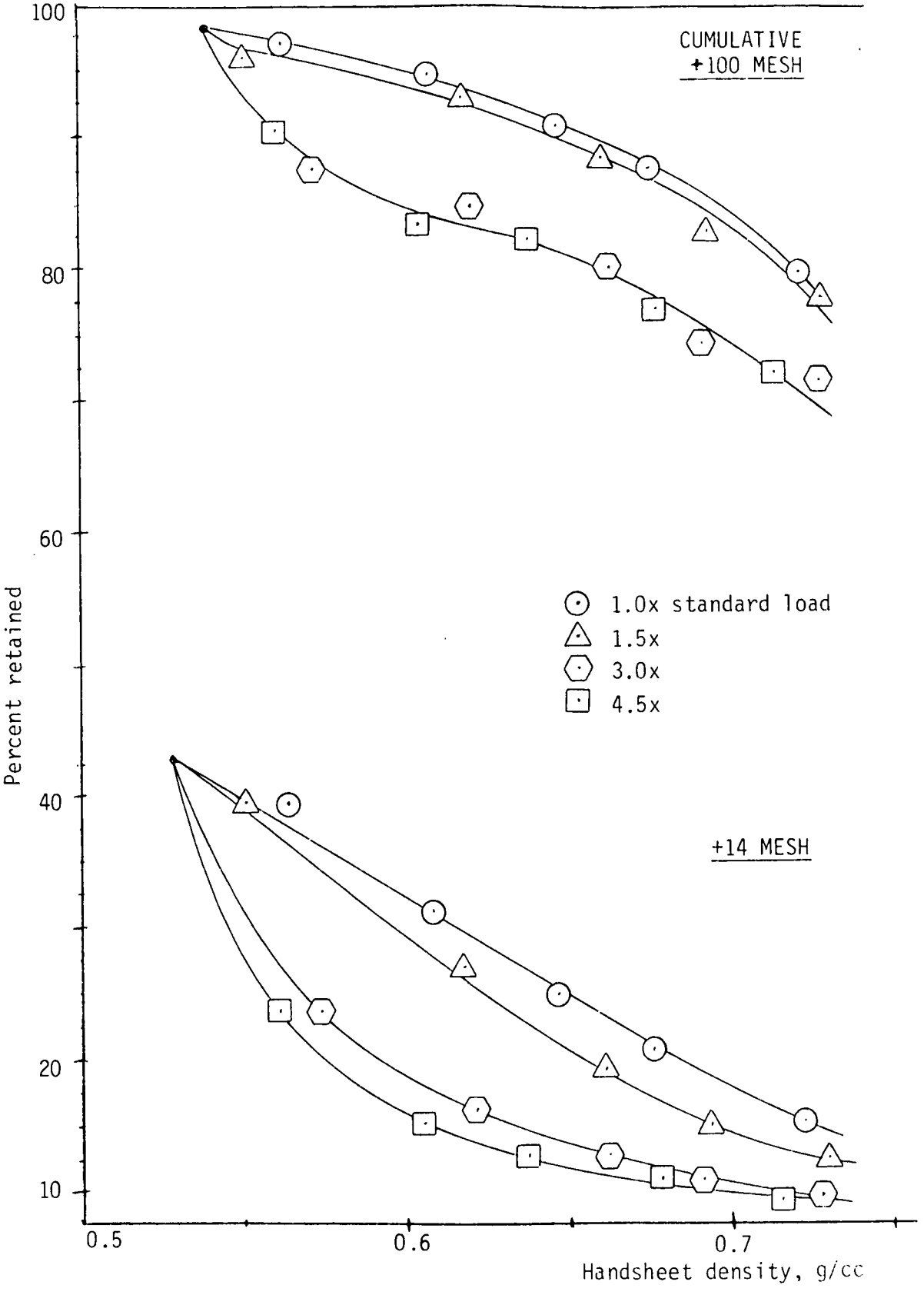


Fiber classification vs. density.

"HIGH-INTENSITY" BEATING

- Measured , E, SEL
- 3.0 x std. load sufficient
- Pulp property effects
- Energy efficiency

MEASUREMENT OF NORMAL AND TANGENTIAL

FORCES ON BEATER BAR SEGMENT

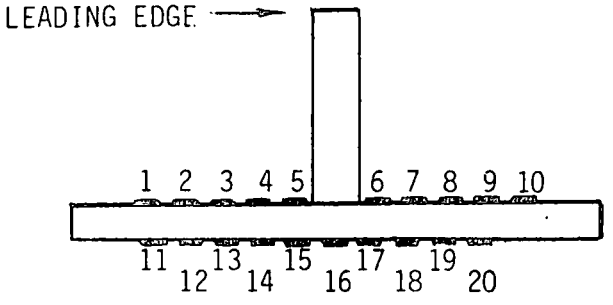


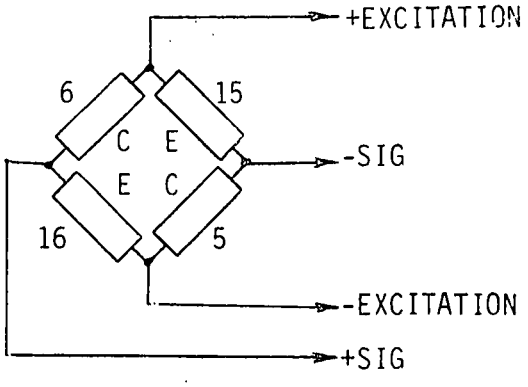


NORMAL CELL

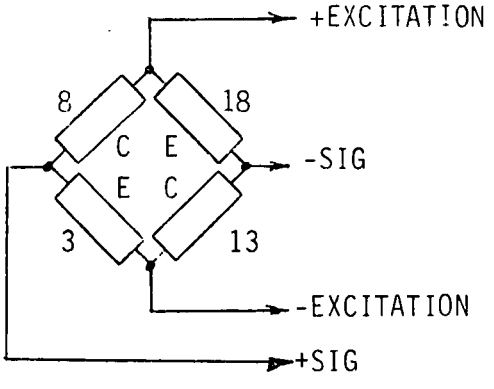


TANGENTIAL CELL

C - Strain gage under compression
E - Strain gage under extension
Excitation: +5V dc
Amplifier Gain: 5625

Strain gage placements on beam and in Wheatstone bridge circuits - initial experiment.

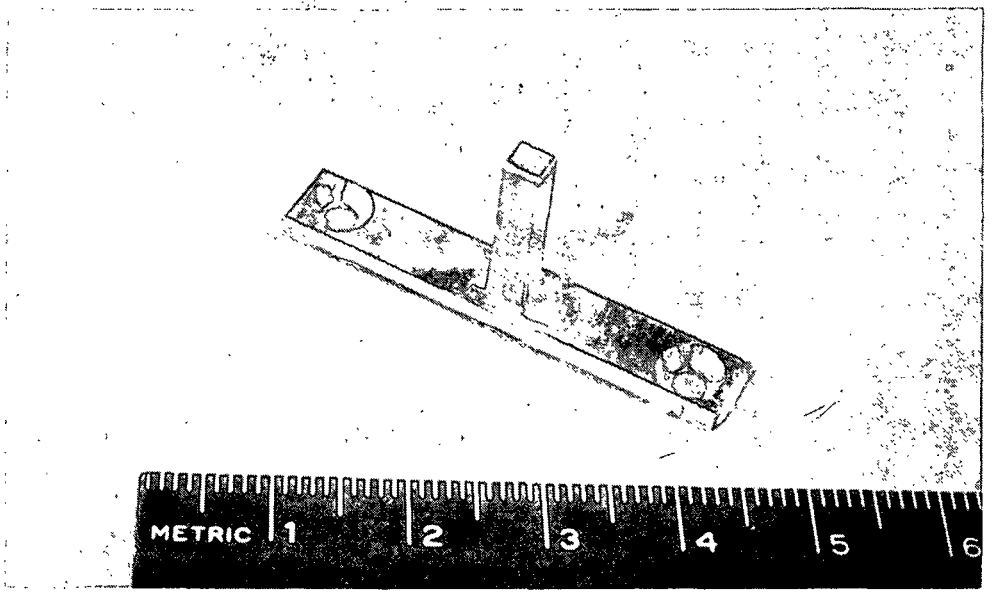


Bar segment and beam prior to strain gage attachment.

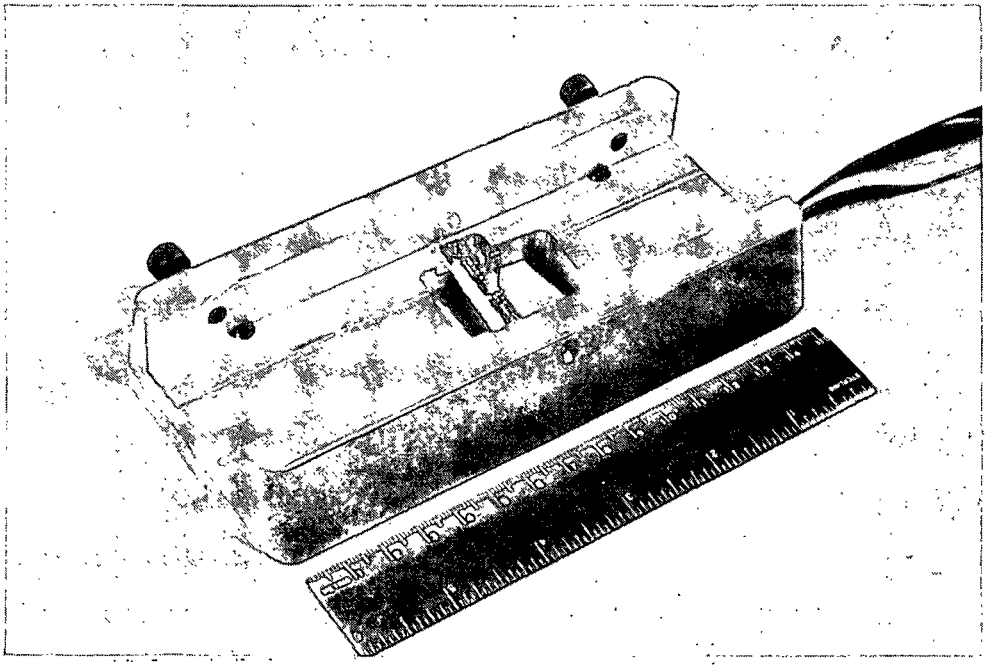

Strain gages attached to beam, bar segment installed in bedplate holder.

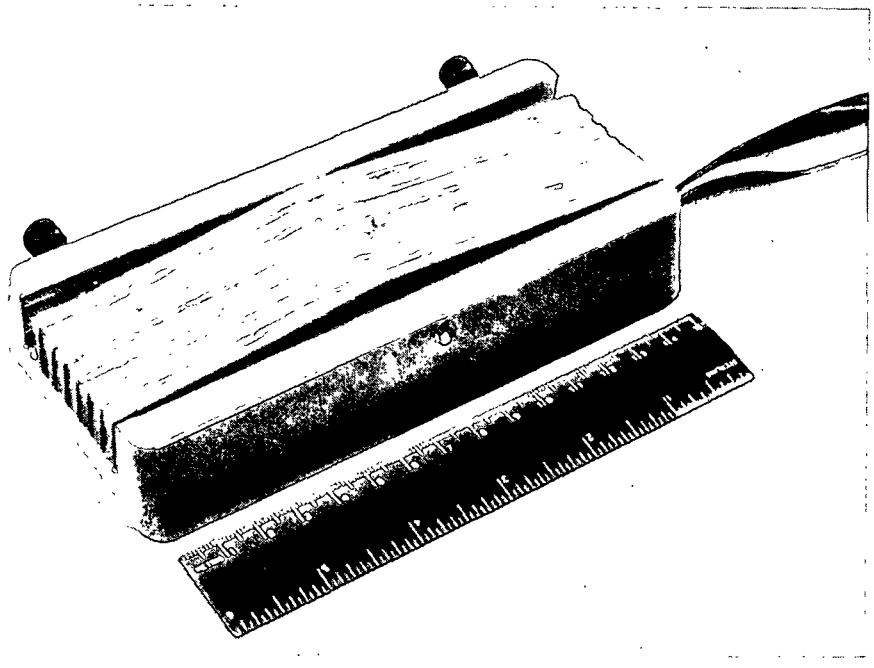

Beater bar assembly in place around instrumented bar segment, prior to potting.

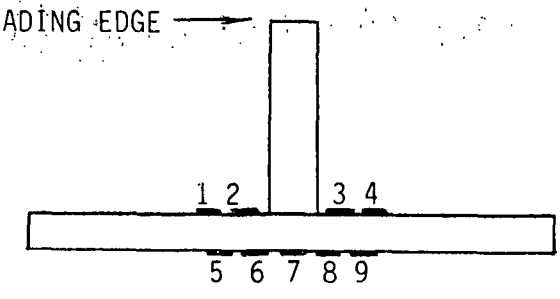


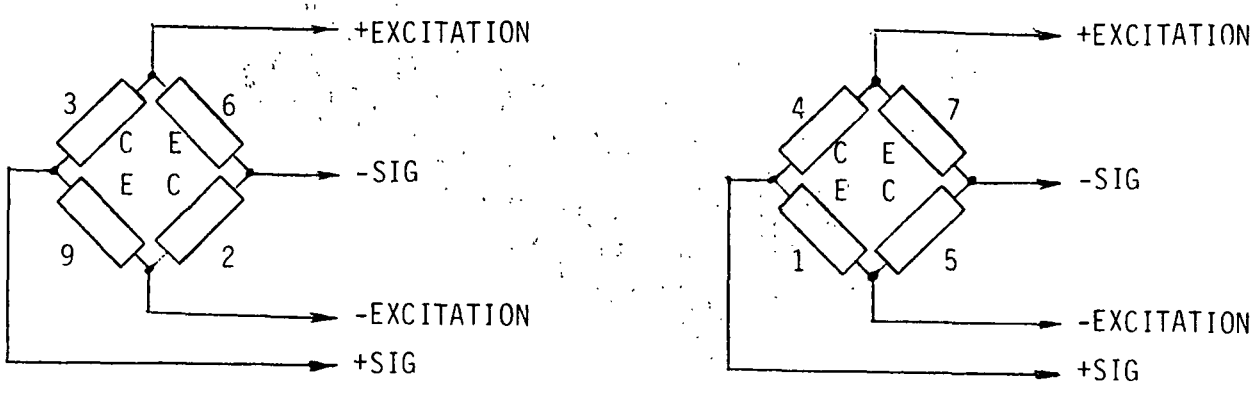


Strain gage placement - second beam.

## FUTURE WORK

- Study of $P_N$
- Dyed fibers
  - Sulfite pulp fractions
  - Rayon
- Hardwoods
- Refiner

Project 3480

# WET PRESSING FUNDAMENTALS

Fred W. Ahrens

# PROJECT 3480

## WET PRESSING FUNDAMENTALS

### OBJECTIVES

1. To increase press effectiveness through improving the water receiving system.

2. To determine the feasibility and performance of displacement pressing in achieving high dryness, press effectiveness, and property control.

# DISPLACEMENT PRESSING

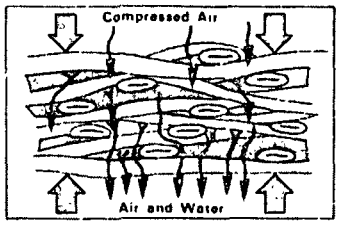


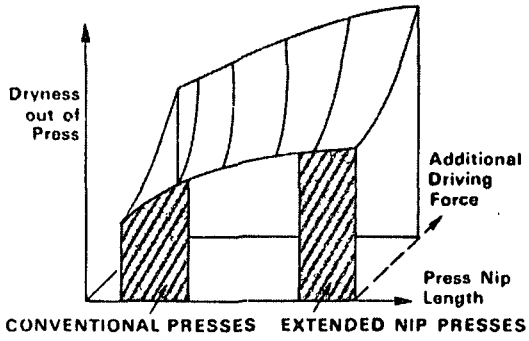


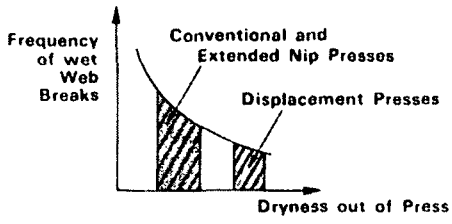

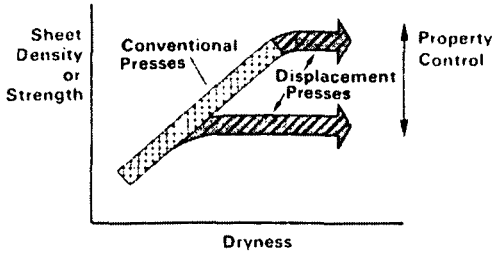


## DISPLACEMENT PRESSING

- PREVIOUS WORK - AIR BLOWTHROUGH
- SIMPLIFIED MODEL
- RECENT EXPERIMENTAL RESULTS
- FUTURE PLANS

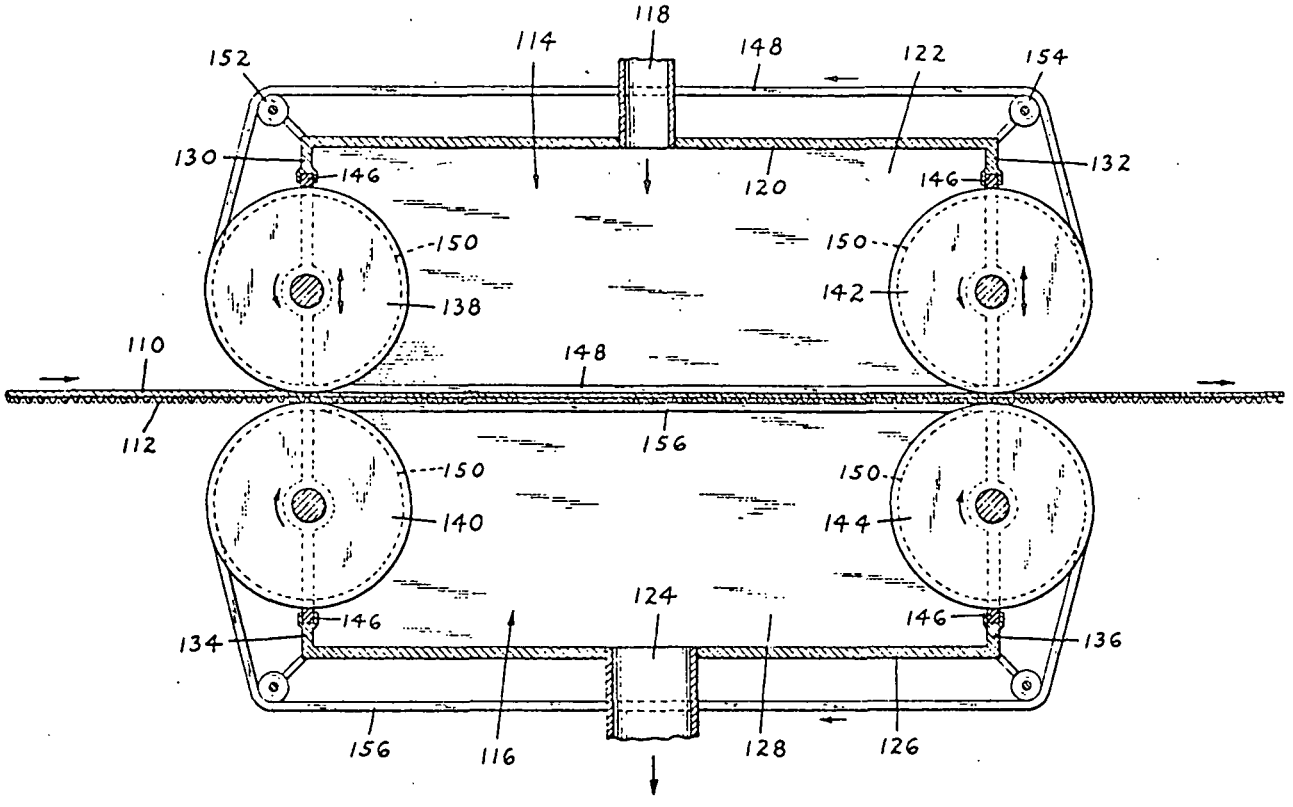


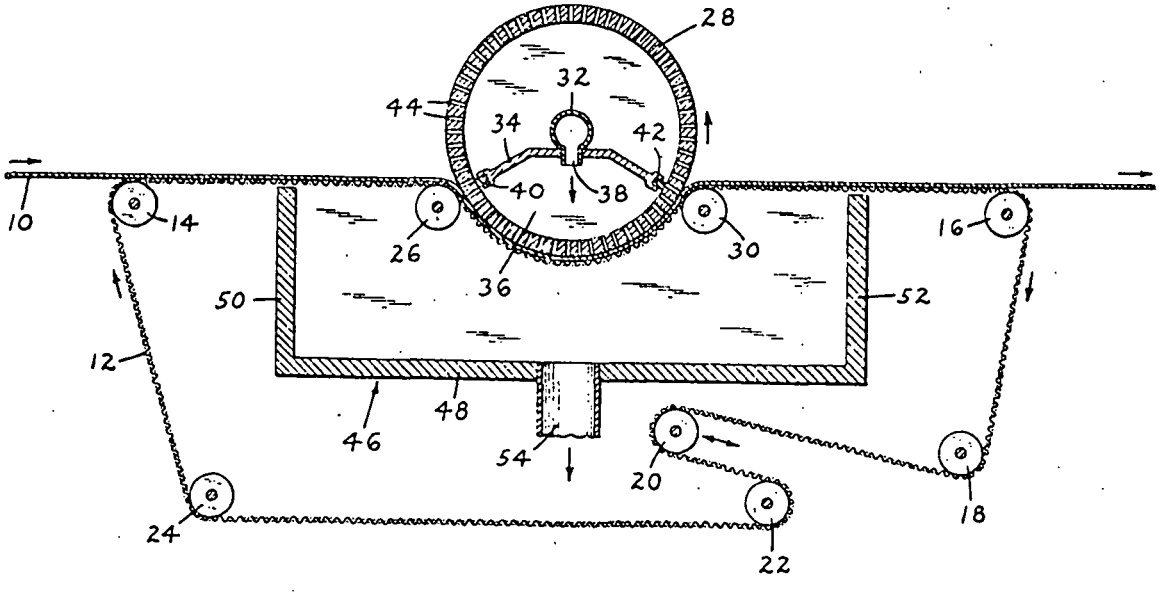


Two blowthrough configurations due to Holden (1).

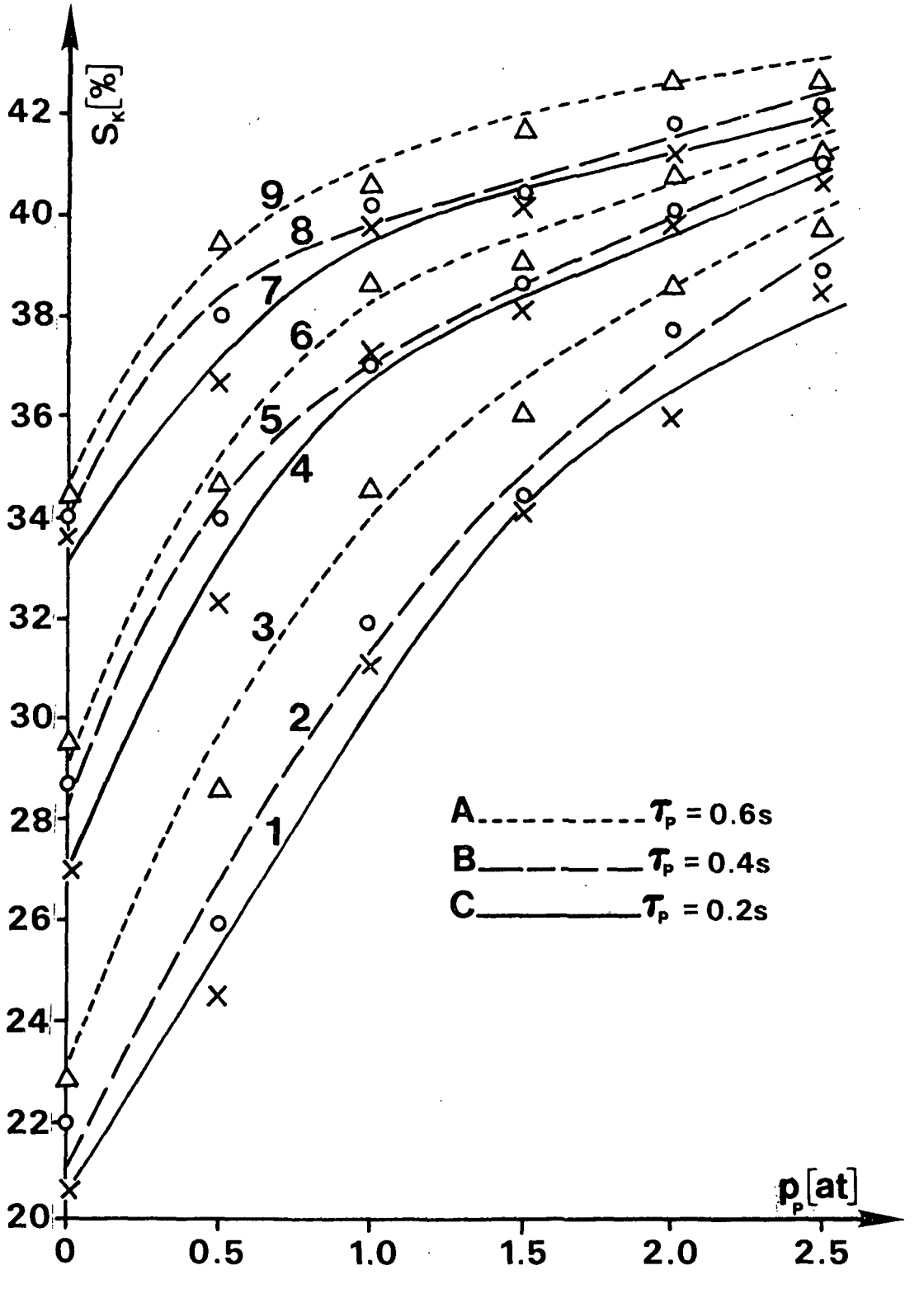


Final dryness ($S_k$) as a function of blowthrough air pressure difference ($p_p$) and blowthrough time ($\tau_p$), initial dryness as a parameter. Initial dryness: 18.8% for 1-3, 25.3% for 4-6, 31.4% for 7-9.

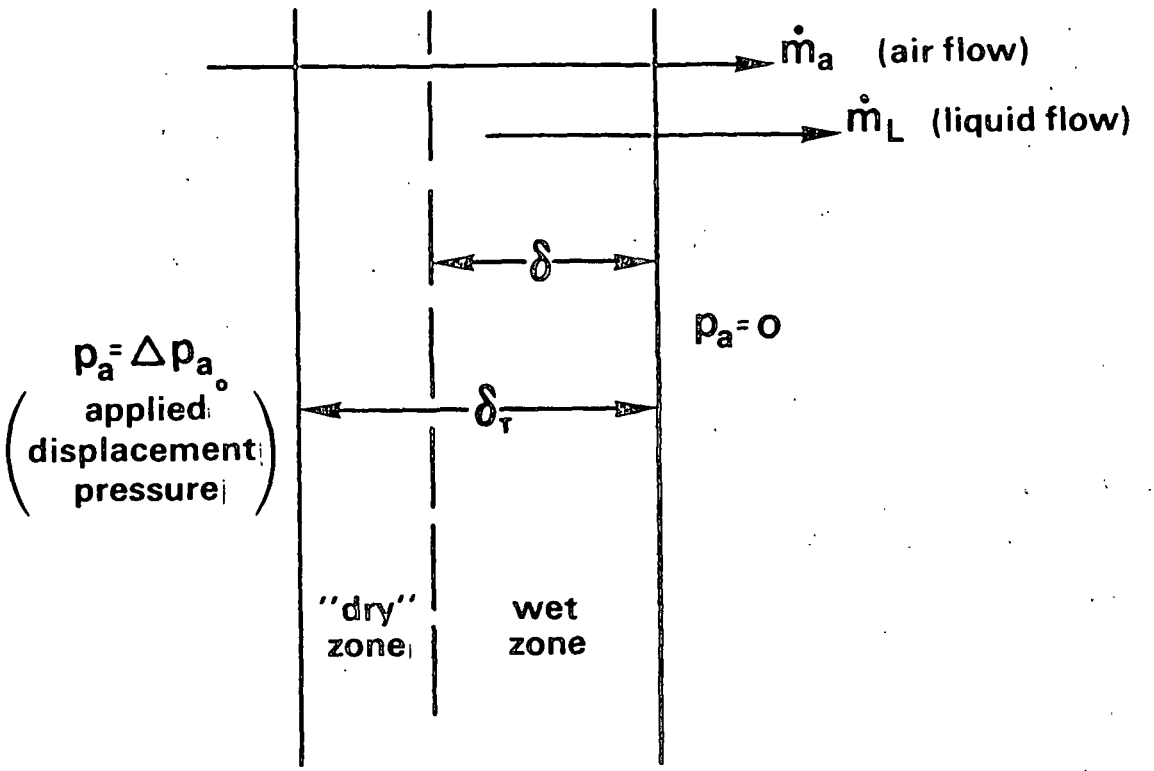


Two-zone model of displacement pressing.

"DRYING TIME"

$$t_D = \frac{(1 + \overline{k})\mu_L \overline{\rho}_L \delta_T^2}{2 \rho_L k_L \Delta p_{a_o}}$$

$$\overline{k} = k_{a_w}/k_{a_d}$$

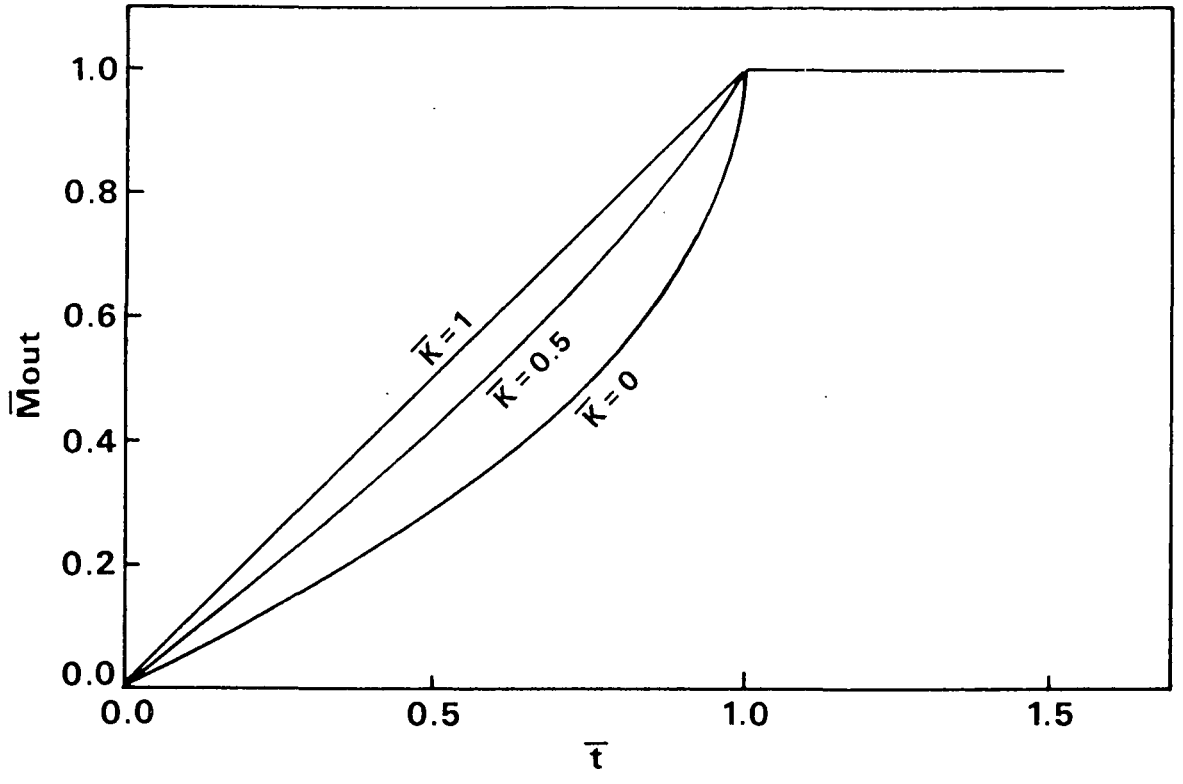


Dimensionless cumulative water removal ($\overline{M}_{out}$) as a function of dimensionless displacement time ($\overline{t}$).

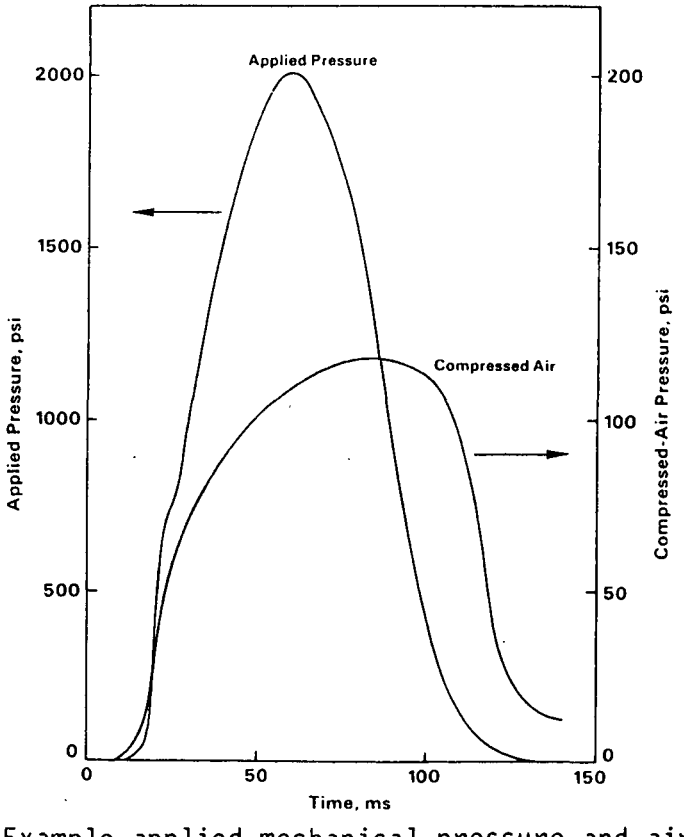


Example applied mechanical pressure and air pressure responses for the haversine mechanical pulse mode.

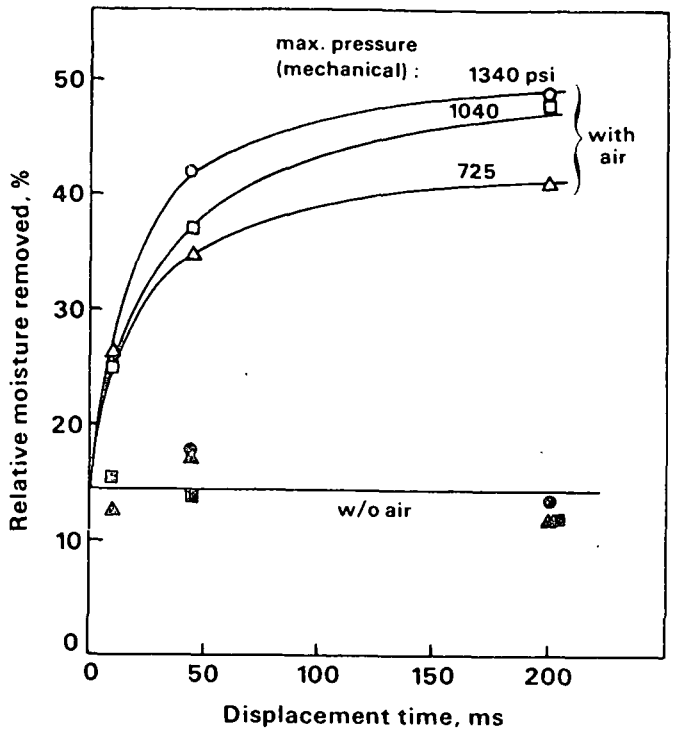


Results of displacement pressing of 63 g/m$^2$ handsheets of once-dried bleached softwood kraft pulp at 720 CSF. Initial dryness = 43-45%.

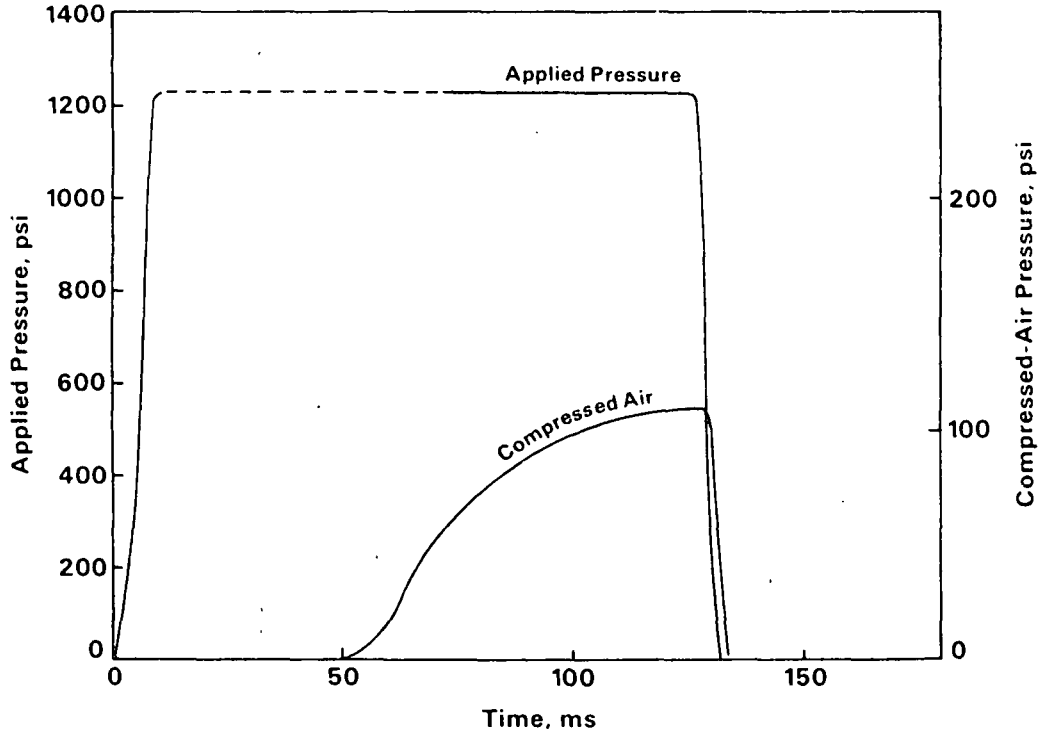


Mechanical and air pressure responses for "square" pulse with air supply "triggered" after 50 ms of sheet compression.

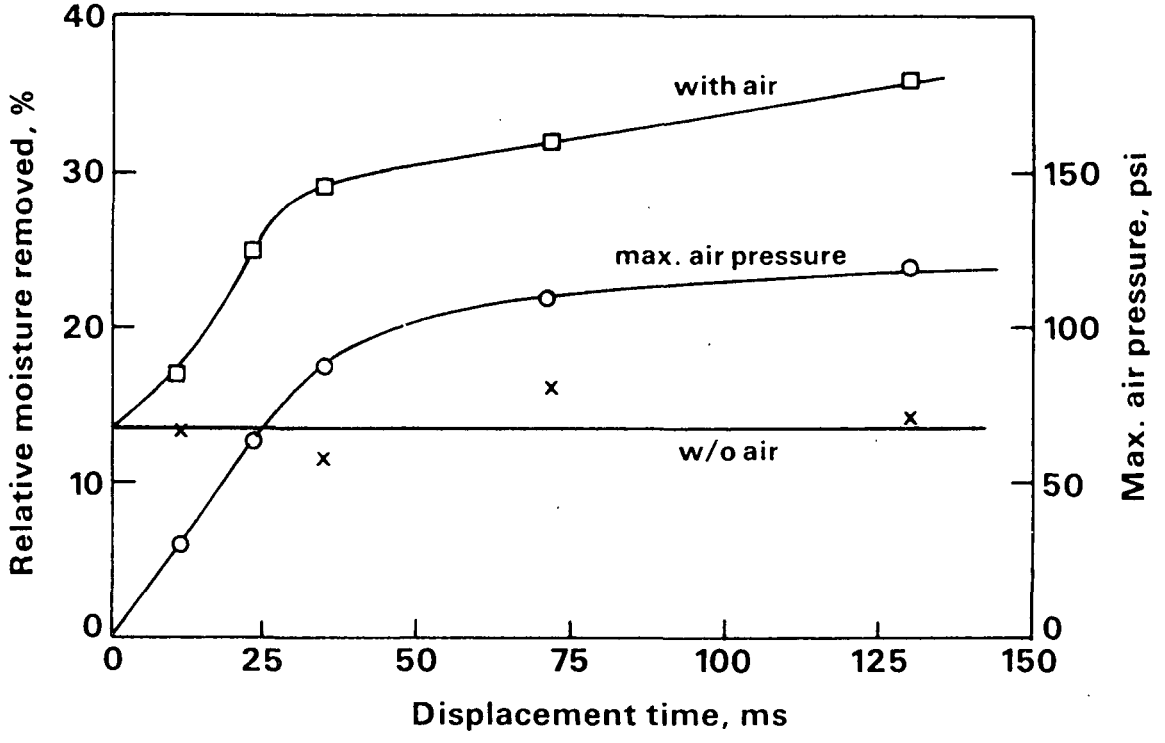


Results of displacement pressing of 63 g/m$^2$ handsheets of never-dried bleached northern softwood kraft pulp at 690 CSF. Initial dryness ≈ 50%.

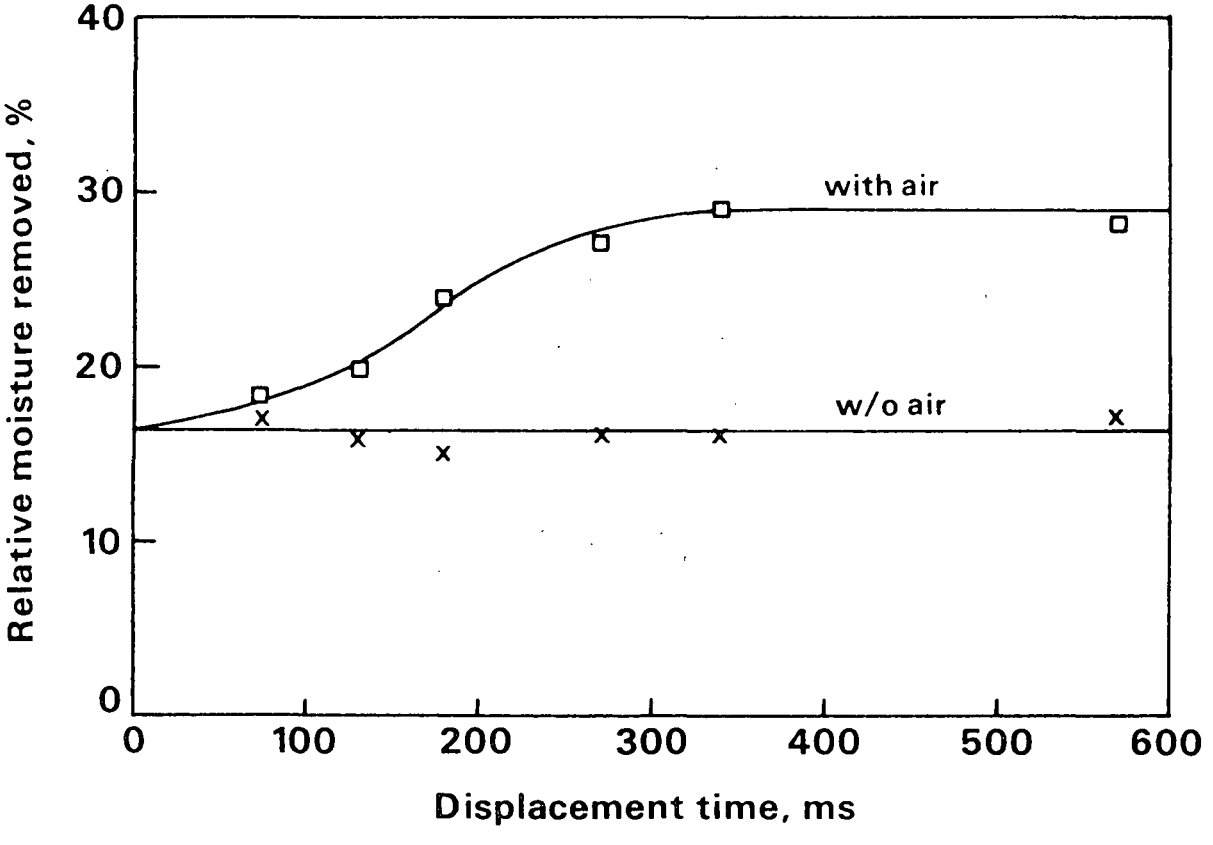


Results of displacement pressing of 63 g/m$^2$ handsheets of never-dried bleached northern softwood kraft pulp at 300 CSF. Initial dryness ≈ 50%.

## "BLIND NIP" RESULTS*

| Blind | $d_{in}$, % | $\Delta d$, % | $p_{air_{max}}$, psi |
|---|---|---|---|
| No | 48.8 | 7.5 | ~78 |
| Yes | 48.5 | 7.2 | ~85 |

*63 g/m$^2$, 690 CSF
$p_M$ = 1500 psi, 60 ms precompression
+ 60 ms displacement time

## EFFECT OF PREHEATING*

| Preheat | $d_{in}$, % | $\Delta d$, % | $p_{air_{max}}$, psi |
|---|---|---|---|
| No | 48.8 | 7.5 | ~78 |
| Yes | 48.3 | ~11 | ~83 |

*63 g/m$^2$, 690 CSF
$p_M$ = 1500 psi, 60 ms precompression
+ 60 ms displacement time

## FUTURE PLANS

1. ASSESS DEGREE OF DENSITY/PROPERTY CONTROL ATTAINABLE WITH DISPLACEMENT PRESSING.
2. DEFINE REGION OF PRACTICAL APPLICABILITY FOR DISPLACEMENT PRESSING.
3. EVALUATE IMPLEMENTATION IDEAS.
4. TECHNICAL PERFORMANCE EVALUATION.

## HIGH EFFICIENCY PRESSING

- RECENT EXPERIMENTAL RESULTS
- FUTURE PLANS

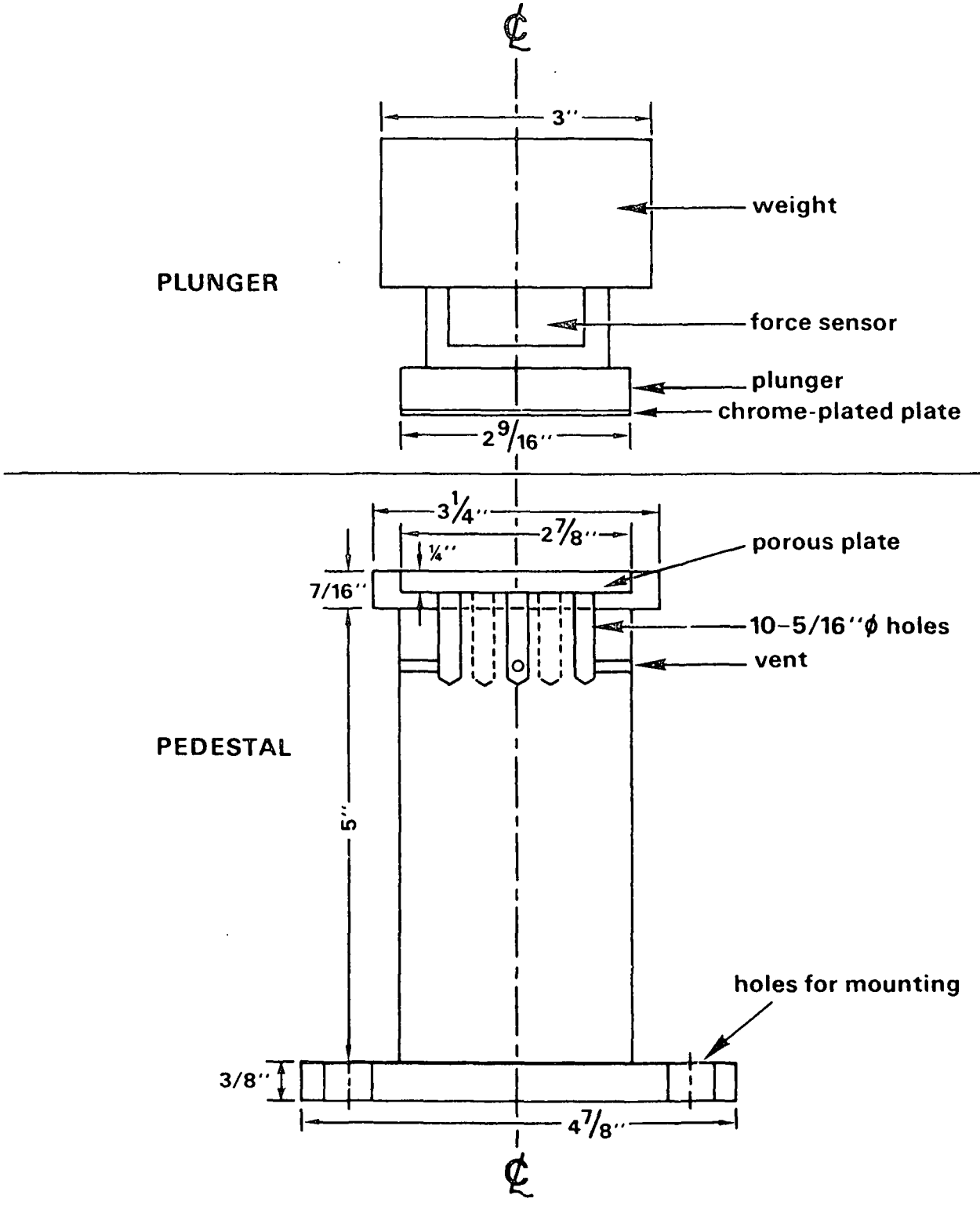


Pressing configuration for high-efficiency pressing study.

Table 1. Porous plate characteristics.

| Designation | Material | Approx. pore size, μ | Surface |
|---|---|---|---|
| SB10 | Sintered bronze | 10 | Unground |
| SB30 | Sintered bronze | 30 | Unground |
| SB40 | Sintered bronze | 40 | Unground |
| SS40[a] | Sintered stainless steel | 40 | Ground |
| SS100 | Sintered stainless steel | 100 | Ground |

[a]This is similar to the plate used in UMO study.

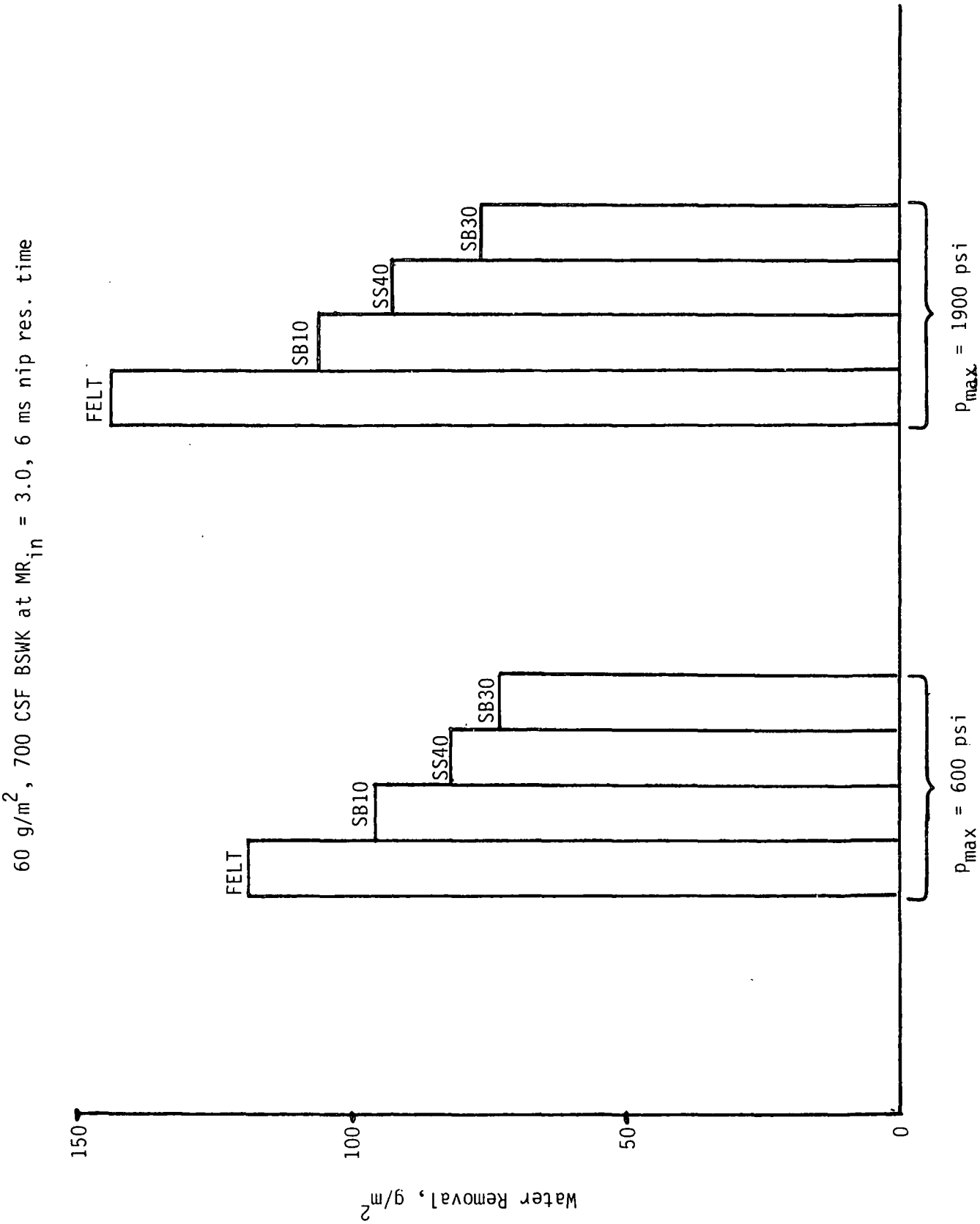
60 g/m², 700 CSF BSWK at MR_in = 3.0, 6 ms nip res. time
Water Removal, g/m²
150
100
50
0
FELT
SB10
SS40
SB30
p_max = 600 psi
FELT
SB10
SS40
SB30
p_max = 1900 psi

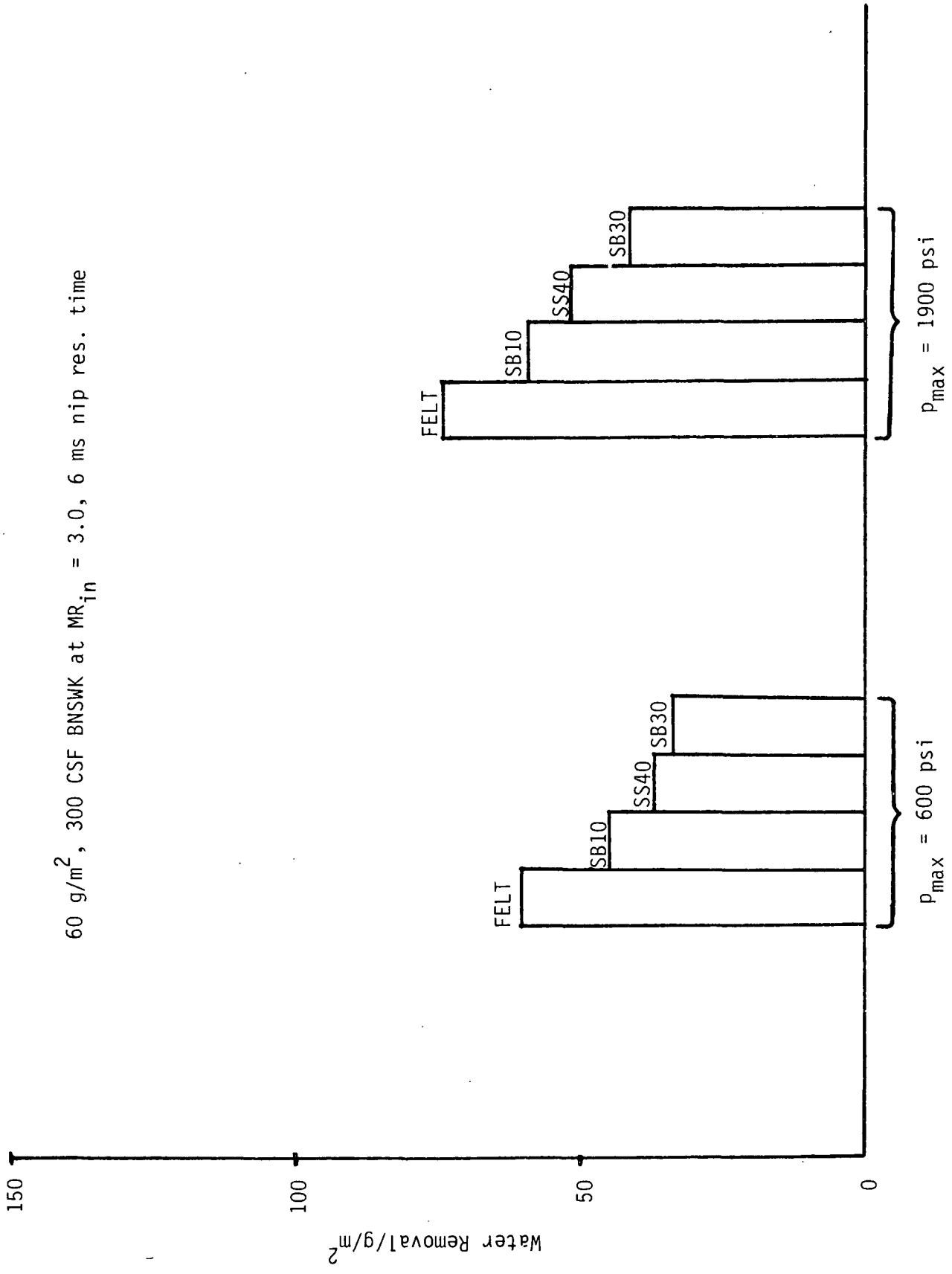
60 g/m², 300 CSF BNSWK at MR_in = 3.0, 6 ms nip res. time
Water Removal/g/m²
150
100
50
0
FELT
SB10
SS40
SB30
p_max = 600 psi
FELT
SB10
SS40
SB30
p_max = 1900 psi

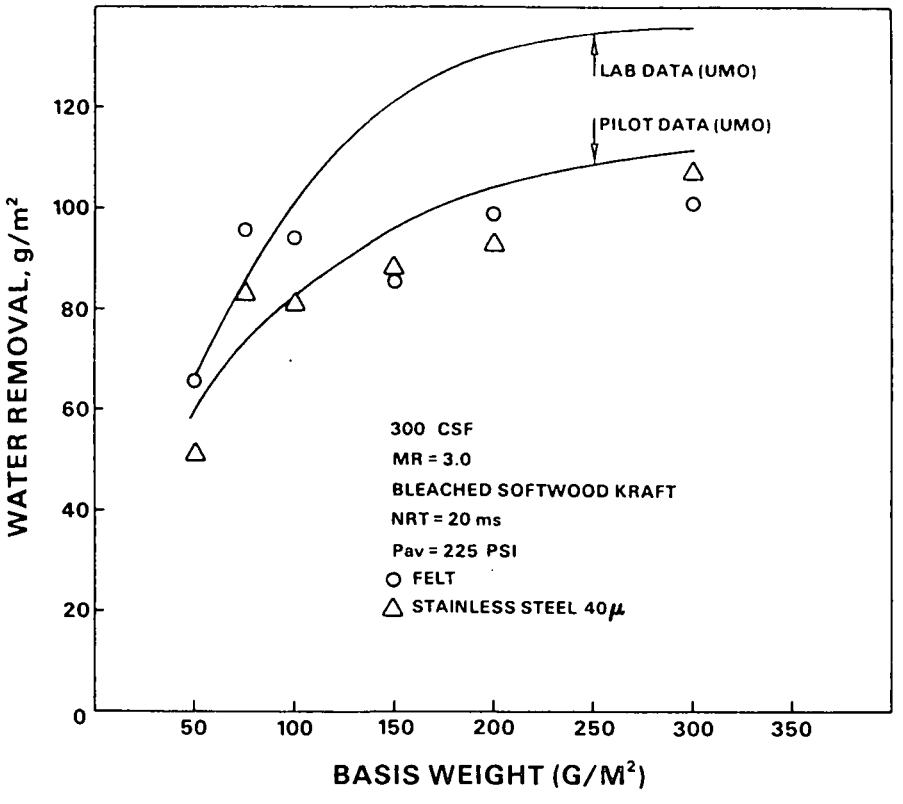


Comparison of data from the MTS system with results of the UMO study.

## FUTURE PLANS

1. EXTEND RANGE OF COMPARISON OF FELTS AND POROUS PLATES.

2. COMPARE WATER REMOVAL IN MTS PRESS SIMULATOR WITH WATER REMOVAL IN PILOT ROLL PRESS.

3. DETERMINE WATER RECEIVER CHARACTERISTICS THAT CONTROL PRESSING EFFICIENCY, IF SIGNIFICANT POTENTIAL FOR IMPROVEMENT IS FOUND.

Project 3470

# FUNDAMENTALS OF DRYING

Fred W. Ahrens

PROJECT 3470

FUNDAMENTALS OF DRYING

OBJECTIVE

To develop an understanding and a data base sufficient for commercialization of advanced water removal systems, based on high-intensity drying principles, that will result in reduced capital cost/increased machine productivity, reduced quantity and/or quality of energy use, and a favorable impact on paper properties.

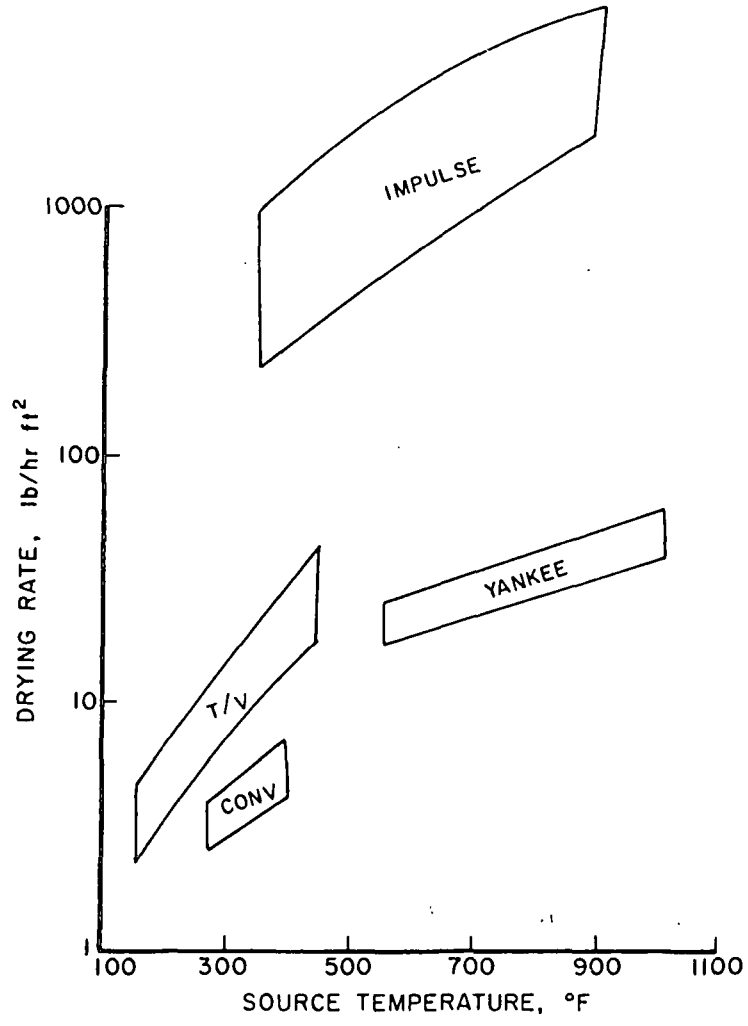
IMPULSE
YANKEE
T/V
CONV
1000
100
10
1
DRYING RATE, lb/hr ft²
100
300
500
700
900
1100
SOURCE TEMPERATURE, °F

## THERMAL/VACUUM DRYING

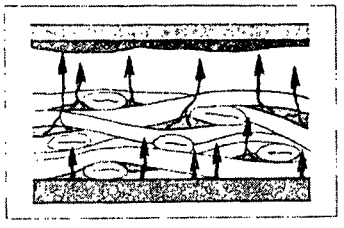

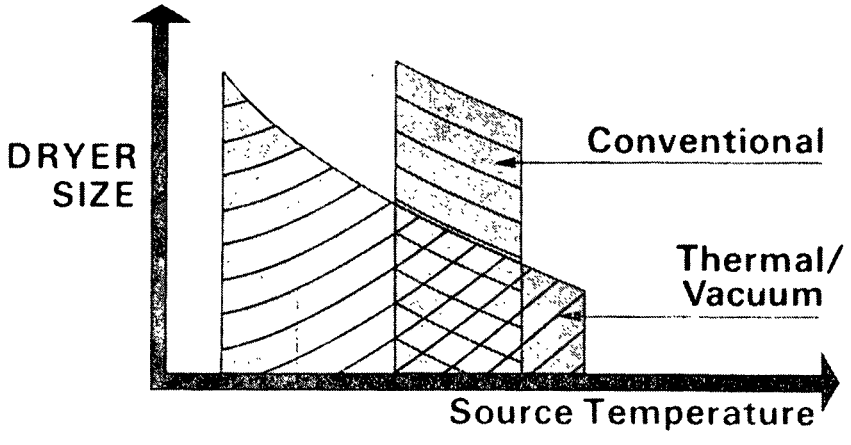


## IMPULSE DRYING

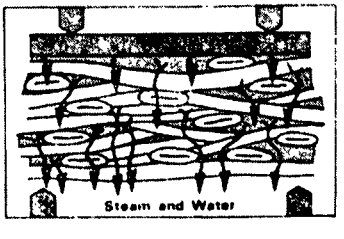

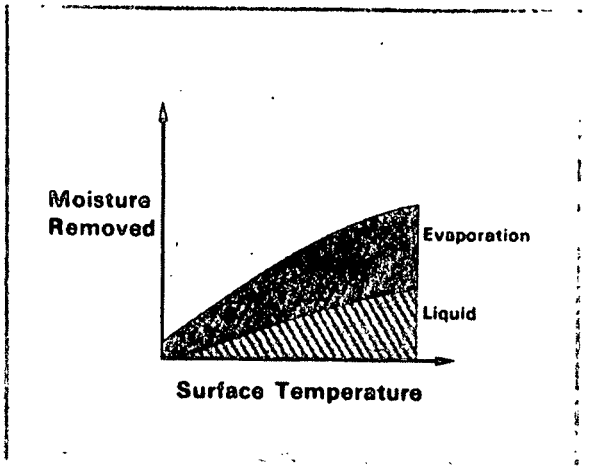
Moisture Removed
Evaporation
Liquid
Surface Temperature

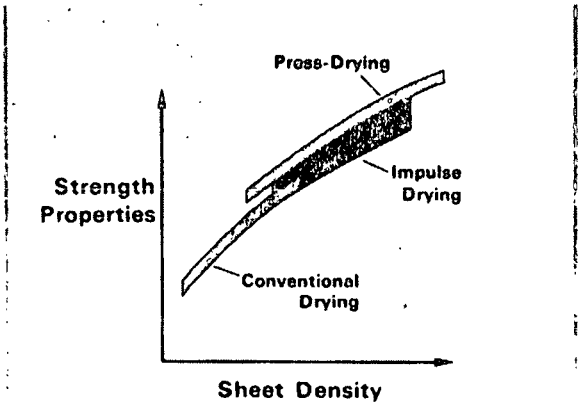
Press-Drying
Impulse Drying
Strength Properties
Conventional Drying
Sheet Density

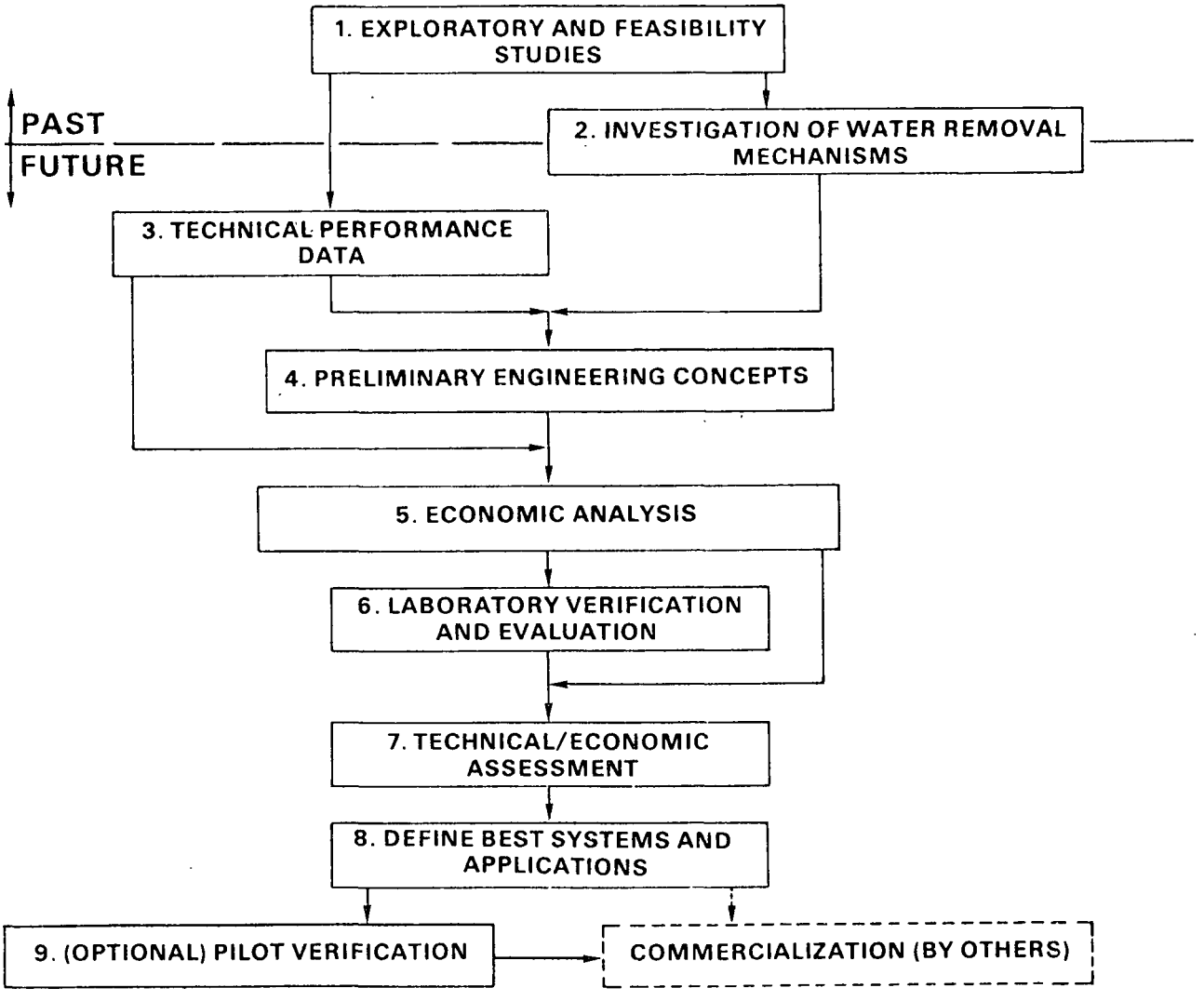


Long-range project elements.

## FUNDAMENTALS OF DRYING

- TECHNICAL PERFORMANCE EVALUATION
- LABORATORY WORK
- ENGINEERING ASPECTS
- FUTURE PLANS

## TECHNICAL PERFORMANCE EVALUATION

- HARDWARE
- FURNISHES
- TEST PROCEDURES
- TEST PROGRAM
- DATABASE

## FURNISHES FOR TECHNICAL PERFORMANCE EVALUATION

- Newsprint
  - (a) TMP
  - (b) $\frac{2}{3}$ GW/$\frac{1}{3}$ kraft
- Writing paper
- Tissue
- Linerboard (primary)
- Corrugating medium
- Carton stock (recycled)

## TEST PROCEDURES

- 5-inch handsheets
- Initial moisture ratio achieved by pressing (except for tissue)
- 4-9 sheets per test condition
- Minimize uncontrolled moisture loss after test
- Complete drying at "conventional" conditions
- Properties tests have been defined

## TEST PROGRAM VARIABLES

- Grade (furnish)
- Basis weight
- Initial moisture ratio
- Initial sheet temperature
- Ambient pressure (atmospheric or vacuum)
- Peak applied pressure
- Initial hot surface temperature
- Residence time*

## MEASUREMENTS

- Instantaneous applied pressure
- Instantaneous surface temperature
- Instantaneous vapor pressure at hot surface
- Total weight loss
- Chemical tracer loss

## CALCULATED INFORMATION

- Impulse
- Instantaneous heat flux to web
- Cumulative thermal energy transfer
- Liquid dewatering

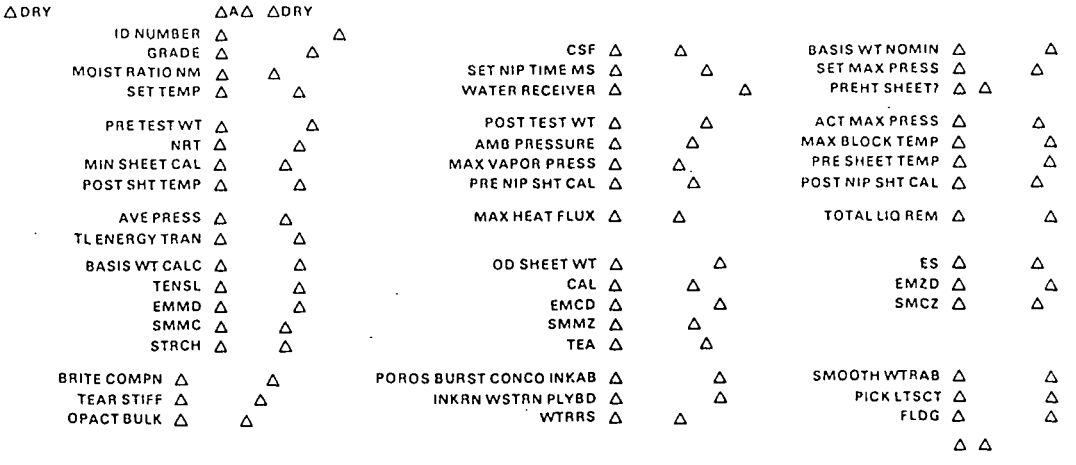

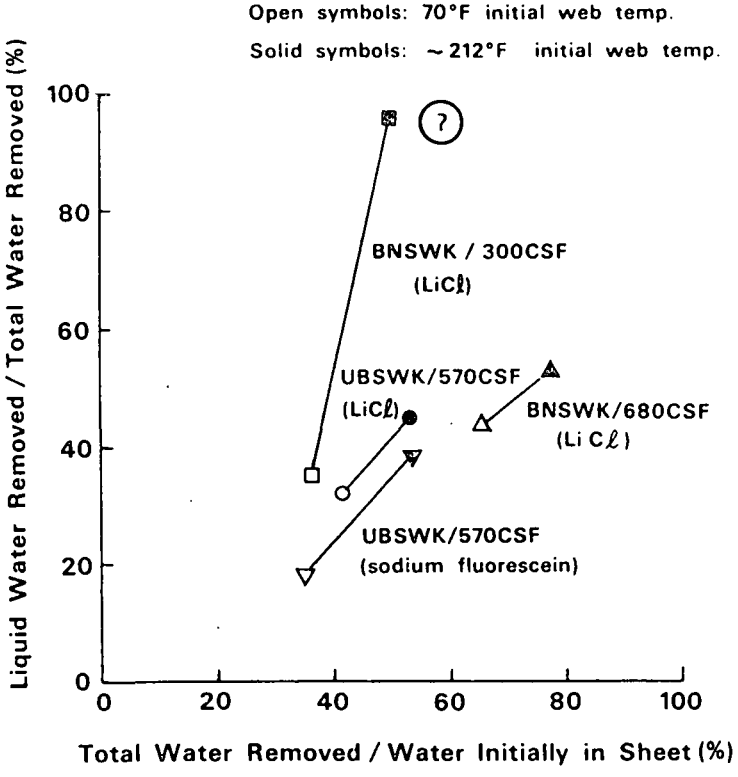


Effect of web preheating on total and liquid water removal in impulse drying. Liquid transfer based on chemical tracer transfer from sheet to felt. Conditions: 50 g/m$^2$ sheets at 40% initial dryness, 750-800 psi mechanical pressure, 600°F surface temperature, 9-11 ms nip residence time.

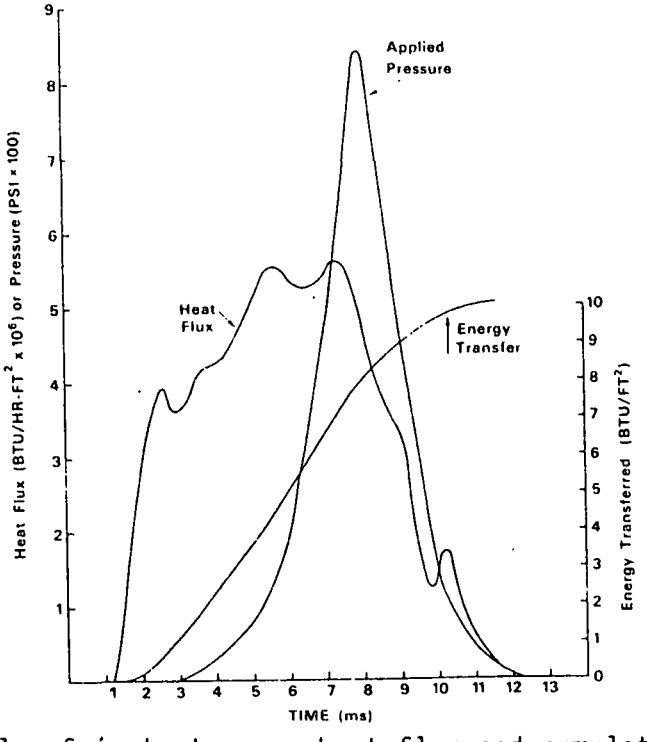


Example of instantaneous heat flux and cumulative energy transfer from hot surface to web under impulse drying conditions: non-preheated 50 g/m$^2$ BNSWK (300 CSF) sheet at 41% initial dryness, 617°F initial surface temperature, 9 ms nip residence time.

SPECIFIC ENERGY TRANSFER ESTIMATE

$$e_{min} = \frac{E_{min}}{(RMR)m_{w_o}} = \underbrace{\left(\frac{C_f}{m_{r_o}} + C_w\right)\frac{(T_B - T_o)}{RMR}}_{\text{Initial sensible heating of wet web}} + \underbrace{(1 - \alpha_L)\Delta h_B}_{\text{Latent heat}} + \underbrace{\frac{C_f(T_H - T_B)}{2\, m_{r_o}}}_{\text{Final sensible heating of "dry zone"}}$$

Table 1. Energy transfer results for impulse drying of 50 g/m$^2$ sheets (40% dryness) at 750-850 psi peak mechanical pressure, 600°F surface temperature and 10 ms nip residence time.

| Pulp/CSF | Preheat | Thermal Energy Transfer, Btu/ft$^2$ | Specific[a] Energy Transfer, Btu/lb$_m$ | $\left(\frac{\text{Actual}}{\text{Calculated}}\right)$[b] Energy Transfer |
|---|---|---|---|---|
| UBSWK/570 | yes | ~9 | ~1100 | 1.83 |
| UBSWK/570 | no | ~10.5 | ~2100 | 1.71 |
| BNSWK/300 | yes | 8 | ~1125 | ? |
| BNSWK/300 | no | 10 | ~1800 | 1.54 |
| BNSWK/680 | yes | 8.5 | ~700 | 1.37 |
| BNSWK/680 | no | 11 | 1040 | 1.22 |

[a]Per unit of water lost from sheet.
[b]Calculated energy transfer is based on water removal data in Fig. 1.

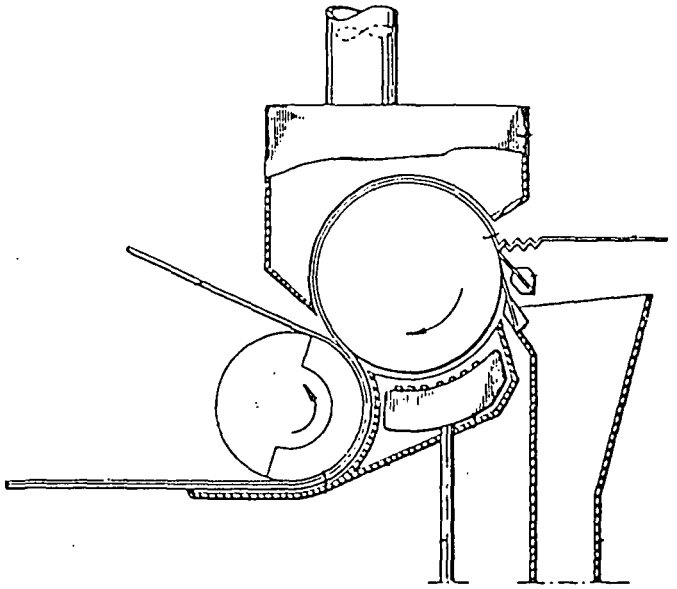

## ENGINEERING/ECONOMIC ISSUES IN WATER REMOVAL

MATT NIGHTINGALE - GRADUATE STUDENT

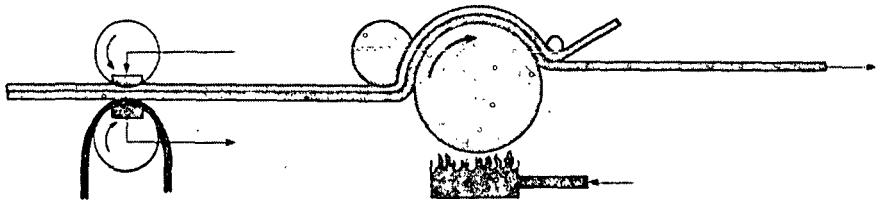

| PRESS | DRYNESS | DRYER | ENERGY | PRODUCT PROPERTIES |
|---|---|---|---|---|
| PRESSING COST? | HIGHER | SMALLER | LESS PER TON<br>HIGHER VALUE | HIGHER DENSITY<br>BETTER BONDING |
| LOWER WATER REMOVAL COST | | LOWER CAPITAL COST | LOWER ENERGY COST | PROPERTY CONTROL<br>LOWER FURNISH COSTS |

OPTIMUM?

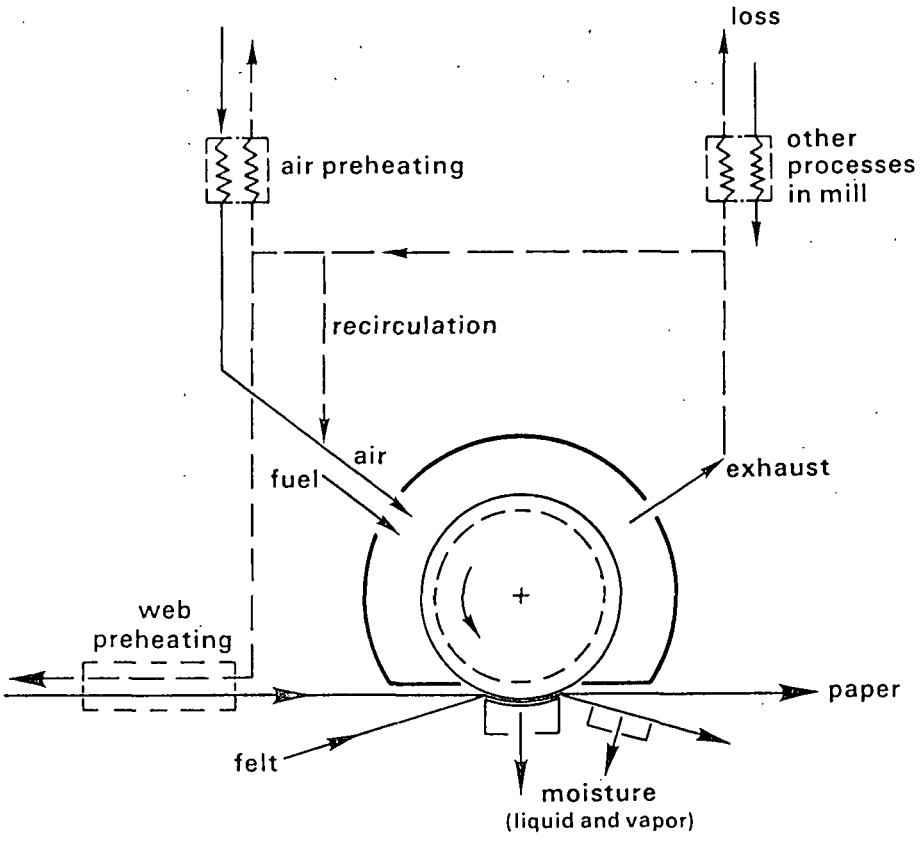


DRYING SECTION (NIP)

| | Specify | Measure | Calculate |
|---|---|---|---|
| Nip width | X | | |
| Shell material | X | | |
| Machine speed | X | | |
| Mechanical pressure | X | | |
| Surface temperature | X | | |
| Grade/furnish | X | | |
| Inlet moisture ratio | X | | |
| Inlet web temperature | X | | |
| Total moisture loss | | X | |
| Liquid loss | | X | |
| Energy transfer | | X | (X) |
| Nip heat flux | | (X) | X |
| Surface temperature drop | | | X |
| Shell thickness (thermal) | | | X |

HEAT INPUT SECTION
(Direct heating with combustion gases)

| | Specify | Calculate |
|---|---|---|
| "Flame" temperature | X | |
| Fuel type | X | |
| Air/fuel ratio | X | |
| Heat recovery parameters | X | |
| Air temperature | (X) | X |
| Fuel flow rate | | X |
| Shroud geometry | X | |
| Heat flux to cylinder | | X |
| Cylinder diameter | | X |

FUTURE PLANS

1. INSTALL NEW MTS-BASED DRYING SYSTEM.

2. CONDUCT THE TECHNICAL PERFORMANCE EVALUATION.

3. EXTEND ENGINEERING ANALYSIS CAPABILITY FOR ADVANCED DRYING SYSTEMS.

4. USE DATA FROM TECHNICAL PERFORMANCE STUDY TO DEVELOP ENGINEERING DATA.

Project 3479

# HIGHER CONSISTENCY PROCESSING

John D. Sinkey

## HIGHER CONSISTENCY PROCESSING

PROGRAM GOAL:

Reduction of the complexity of screening, cleaning, and forming systems.

## PROJECT OBJECTIVE

To identify or develop methods and principles for controlling fiber motion in HC slurries, as applied to practical forming and separation processes.

## SEPARATION AT MOVING ROLL SURFACES

- SHEAR MIGRATION
- SPRAY

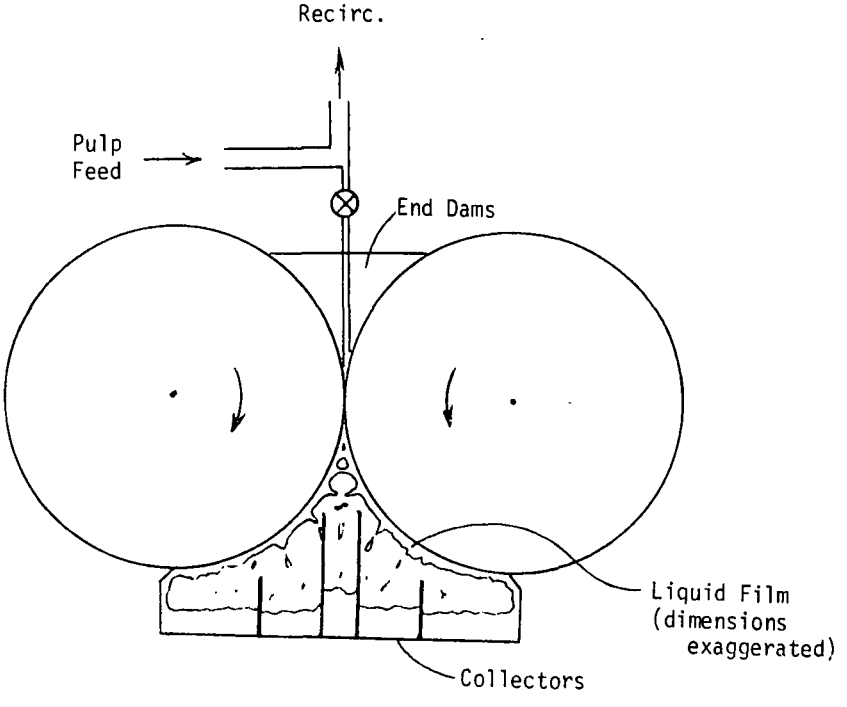
Recirc.
Pulp
Feed
End Dams
Liquid Film
(dimensions
exaggerated)
Collectors

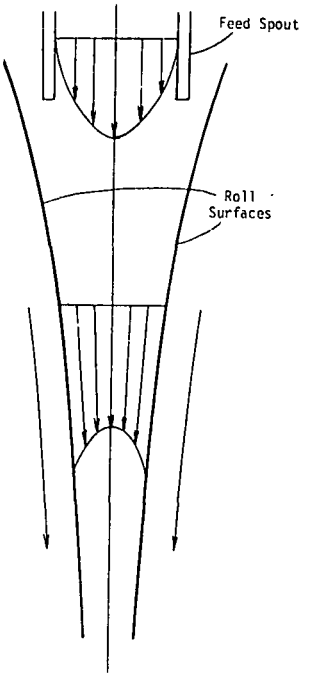
Feed Spout
Roll
Surfaces

## FORCES INVOLVED

- Shear-induced migration
- Centrifugal
- Drag
- Network
- Surface tension

## INSTABILITIES

- Film splitting
- Air boundary layers
- Ring-type disturbances
- Mechanical imprecision

## PRELIMINARY RESULTS

### Symmetrical Feed

| | | Chamber No. | | | | | | |
|---|---|---|---|---|---|---|---|---|
| | Feed | 1 | 2 | 3 | 4 | 5 | 6 | 7 |
| Consistency, % | 0.96 | 0.25 | 0.19 | 0.29 | 1.45 | 0.27 | 0.28 | 0.29 |
| CSF | 578 | 115 | -- | 73 | 668 | 56 | -- | 118 |

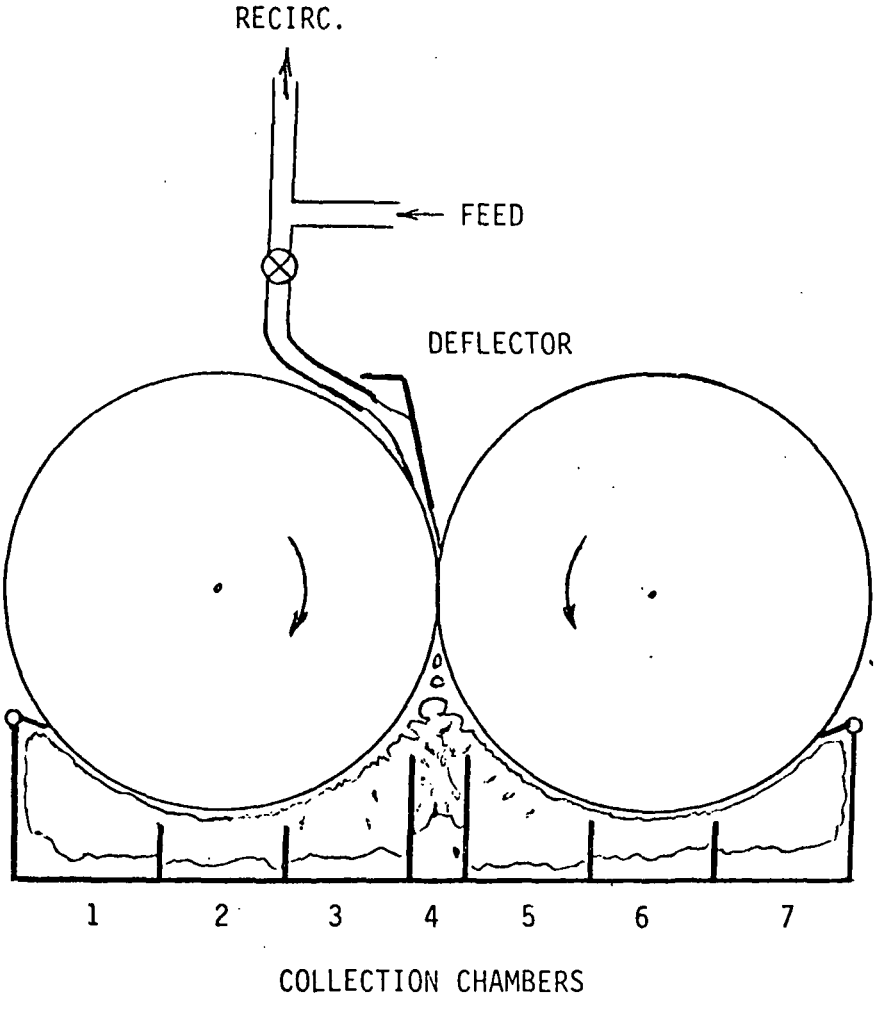


Twin-roll device with nonsymmetrical feed.

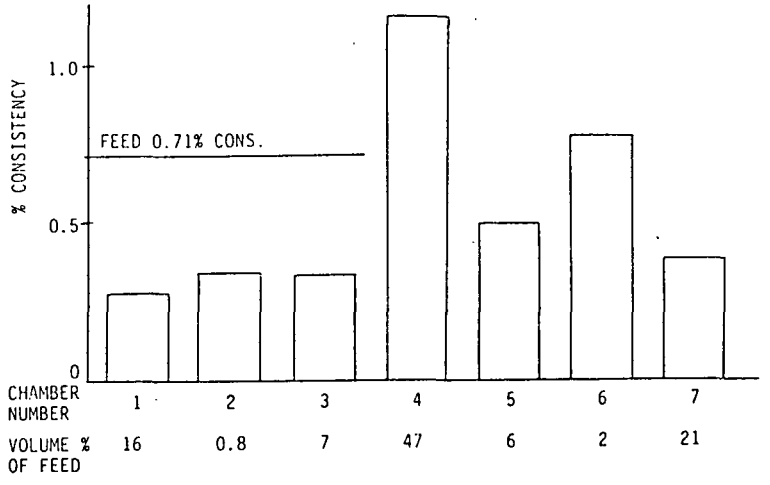
% CONSISTENCY
1.0
0.5
0
FEED 0.71% CONS.
CHAMBER NUMBER
1 2 3 4 5 6 7
VOLUME % OF FEED
16 0.8 7 47 6 2 21

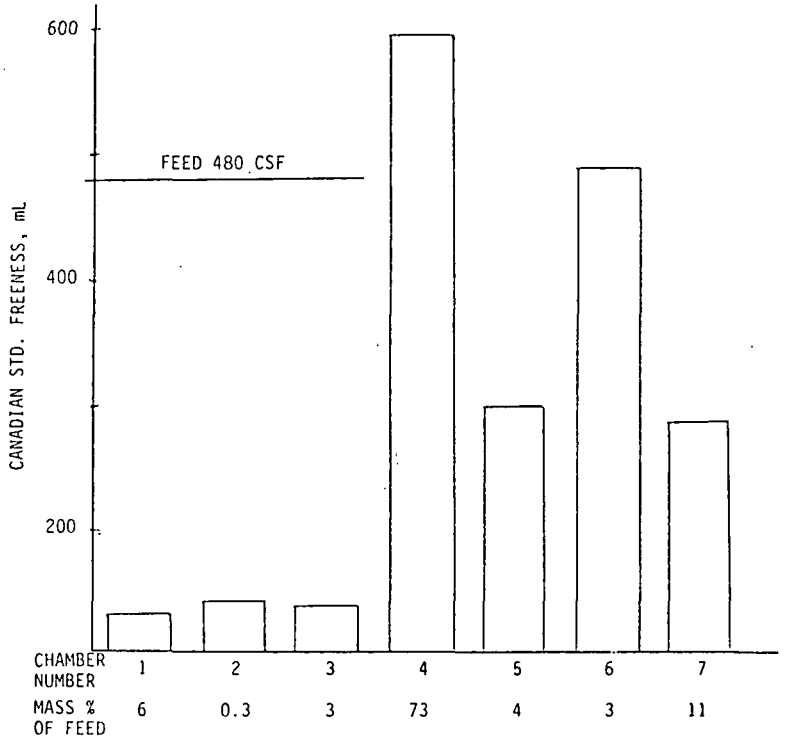
CANADIAN STD. FREENESS, mL
600
400
200
FEED 480 CSF
CHAMBER NUMBER
1 2 3 4 5 6 7
MASS % OF FEED
6 0.3 3 73 4 3 11

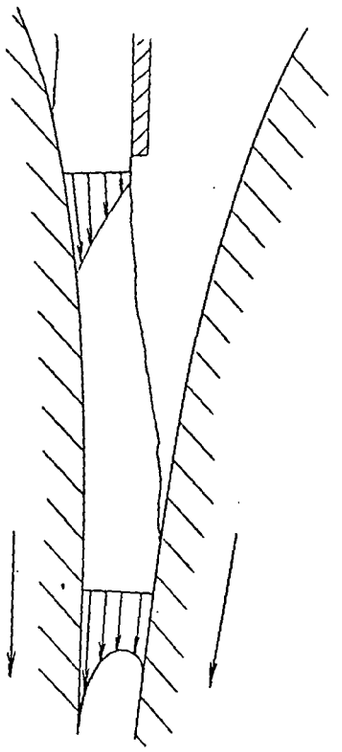

PRESUMED VELOCITY PROFILE-
NONSYMMETRICAL FEED

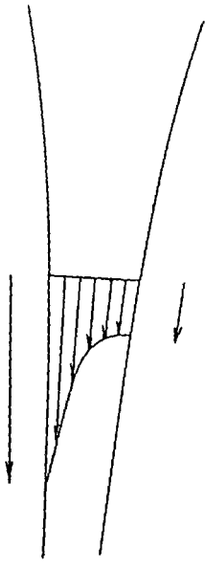

POSSIBLE OPTIMUM
VELOCITY PROFILE
?

## TENTATIVE CONCLUSIONS

- Shear in nip
- $F_C$ *vs.* $F_S$ separation

## FUTURE WORK

- Twin-roll
  - Co-rotating
  - Counter-rotating
- Single roll with blade
- Spray

## POTENTIAL APPLICATIONS

- Screening/cleaning
- Pulp fractionation
- Lightweight contaminants
- Sludge thickening
- Other dewatering

Project 3556

# FUNDAMENTALS OF KRAFT LIQUOR CORROSIVITY

Ronald A. Yeske

# FUNDAMENTALS OF KRAFT LIQUOR CORROSIVITY

OVERALL OBJECTIVES

1. EARLY DETECTION OF CORROSION
2. IDENTIFY COST-EFFECTIVE REMEDIES

## FUNDAMENTALS OF KRAFT LIQUOR CORROSIVITY

PROJECT 3556

WHITE LIQUOR CORROSIVITY

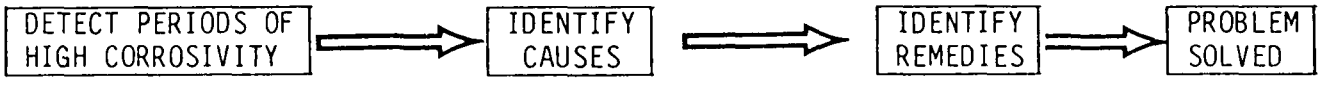


| DETECT PERIODS OF HIGH CORROSIVITY | IDENTIFY CAUSES | IDENTIFY REMEDIES |
|---|---|---|
| * REFERENCE ELECTRODE DEVELOPMENT | * LIQUOR COMPOSITION EFFECTS | ANODIC PROTECTION (FKBG) |
| * LINEAR POLARIZATION METHOD SIMULATION | —> LIQUOR VELOCITY EFFECTS | PROCESS CHEMISTRY CONTROL |
| —> ELECTRICAL RESISTANCE METHOD SIMULATION | —> LIQUOR LEVEL EFFECTS | |
| —> LINEAR POLARIZATION FIELD TESTING | | |
| —> ELECTRICAL RESISTANCE FIELD TESTING | | |

* DONE
—> 1984-85

PREVIOUSLY,

- LINEAR POLARIZATION FOUND TO BE EFFECTIVE IN LAB SIMULATIONS
- SILVER/SILVER-SULFIDE REFERENCE
- ROLE OF NaOH, $Na_2S$ ON WHITE LIQUOR CORROSIVITY
- ROLE OF POLYSULFIDE, THIOSULFATE IN SHORT TERM TESTS

CURRENT EMPHASIS

- ELECTRICAL RESISTANCE METHOD FOR CORROSION MONITORING
- IN-MILL CORROSION TESTING
- LIQUOR COMPOSITION EFFECTS ON CORROSIVITY
- LIQUOR VELOCITY EFFECTS
- REPORTS ISSUED

ELECTRICAL RESISTANCE METHOD

"A REMOTE, ELECTRONIC, MEASUREMENT OF LOSS OF METAL THICKNESS"

ELECTRICAL RESISTANCE METHOD

APPROACH -- "Electrical Weight Loss"

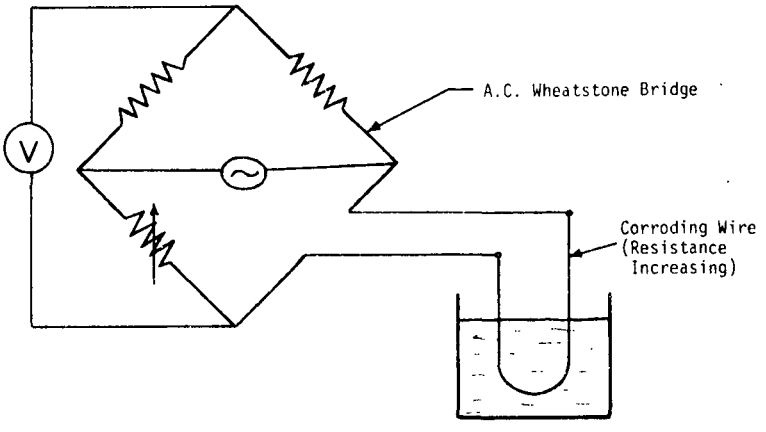


$$R = \frac{\rho(\text{Temp.}) \cdot \text{length}}{\text{Area}}$$

SCHEMATIC OF ELECTRICAL RESISTANCE METHOD FOR CORROSION RATE MONITORING.

ELECTRICAL RESISTANCE METHOD RESULTS

| | Environment | | | | | |
|---|---|---|---|---|---|---|
| Envt. | NaOH, g/L | $Na_2S$, g/L | $Na_2S_x$ (as S°), g/L | $Na_2S_2O_3$, g/L | ER, mpy | Avg. Wt. Loss, mpy |
| A | 100 | 33 | -- | -- | 13 | 13 |
| B | 100 | 33 | -- | 25 | 44 | 42 |
| C | 100 | 33 | 10 | -- | 3 | 5 |
| D | 100 | 33 | -- | 5 | 20 | 23 |
| E | 100 | 33 | -- | 5 | 23 | 12 |
| G | 100 | 33 | 5 | -- | 1 | 3 |

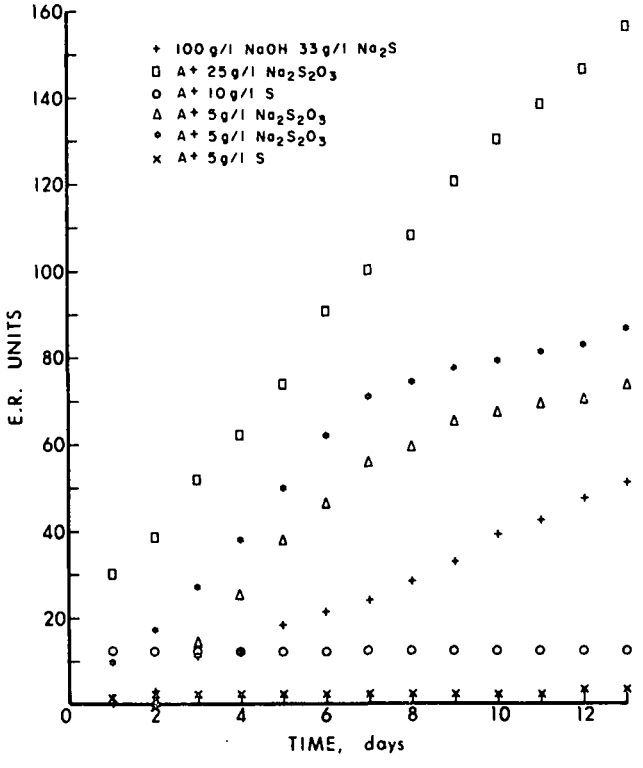


Raw ER probe results.

CONCLUSIONS

- ER METHOD IS SENSITIVE TO CHANGING CORROSION RATES IN LABORATORY STUDIES
- NO EVIDENCE OF CONDUCTIVE FILM EFFECTS
- SEAL FAILURE IN LABORATORY PROBES
- INDUSTRIAL PROBES ARE EXPENSIVE

FUTURE PLANS (ER)

- IN-MILL ER TESTING

CORROSION RATE MONITORING IN THE PULP MILL

APPROACH

- IN-SITU COMPARISON OF CORROSION RATES DETERMINED BY WEIGHT LOSS AND TIME-INTEGRATED LINEAR POLARIZATION
- TESTING IN WHITE LIQUOR CLARIFIERS
- AUTOMATED SAMPLING OF LIQUORS DURING CORROSIVITY EXCURSIONS
- ANALYSIS TO EXAMINE ORIGINS OF CORROSIVITY CHANGES (LINK TO MILL OPERATIONS?)

MATERIALS EXPOSED

- 1018 CARBON STEEL
- A285-C CARBON STEEL
- A285-C SPEC (A LOW-SILICON, HIGH Cr+Ni+Cu STEEL)

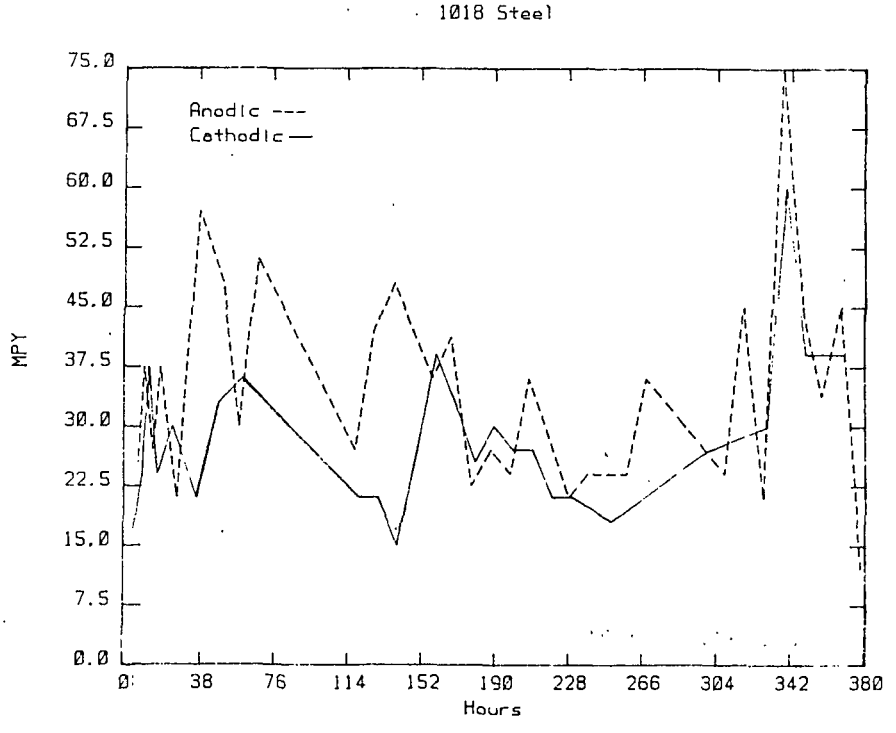


In mill corrosion of 1018 carbon steel exposed to white liquor (corrected for 2.8 factor)

LINEAR POLARIZATION RESULTS IN MILL LIQUOR

| Material | LP Corrosion Rate[a] | Weight Loss Rate, mpy | $(\beta/Z)^b$ |
|---|---|---|---|
| 1018 #1 | 29.9 | 29.7 | 2.83 |
| A285C #1 | 23.3 | 23.2 | 2.80 |
| A283 #1 | 31.0 | 25.8 | 3.37 |
| A285SPEC #1 | 14.1 | 22.9 | 1.73 |
| 1018 #2 | 33.3 | 39.9 | 2.70 |
| A285C #2 | 23.6 | 27.1 | 2.44 |
| A283 #2 | 30.6 | 29.0 | 2.96 |
| A285SPEC #2 | 20.0 | 23.9 | 2.34 |

[a] LP corrosion rate taken as the averaged cathodic and anodic rates, corrected by a $(\beta/Z)$ factor of 2.8.
[b] $(\beta/z)$ correction required to bring LP and weight data into agreement.

LIQUOR ANALYSIS

(g/L as chemical)

| Sample | NaOH | $Na_2S$ | $Na_2CO_3$ | $Na_2S_2O_3$ | $Na_2S_x$* | $Na_2SO_3$ | $Na_2SO_4$ |
|---|---|---|---|---|---|---|---|
| Reference | 92.0 | 39.2 | 32.5 | 6.9 | <0.5 | 11.1 | 5.9 |
| 8/8 | 93.9 | 38.8 | 32.0 | 7.6 | <0.5 | 5.9 | 4.9 |
| 8/10 | 92.9 | 39.6 | 32.5 | 7.5 | <0.5 | 6.9 | 7.6 |
| 8/22 | 98.7 | 35.7 | 30.0 | 4.1 | <0.5 | 4.5 | 4.7 |
| 8/24 | 93.4 | 37.8 | 27.2 | 6.3 | <0.5 | 7.6 | 6.4 |
| 8/29 | -- | -- | -- | 7.1 | <0.5 | 9.7 | 6.5 |

* g/L as elemental sulfur equivalent.

CONCLUSIONS - FIELD STUDIES

- ($\beta$/Z) PARAMETER ALSO VALID IN FIELD TESTS
- FEW SIGNIFICANT FLUCTUATIONS IN CORROSION RATES
- NO MATERIALS EFFECT
- NO CORRELATION WITH CHANGES IN LIQUOR COMPOSITION
- ADDITIONAL FIELD TRIALS REQUIRED

LIQUOR SPECIES EFFECTS

- BINARY NaOH/$Na_2S$ LIQUORS PRODUCED CORROSION RATES OF 5-10 mpy
- LINEAR POLARIZATION TESTS REVEALED SHORT-TERM EFFECTS OF THIOSULFATE, POLYSULFIDE
- THEREFORE, EVALUATE LONG TERM POLYSULFIDE EFFECTS

## WEIGHT LOSS RESULTS - 2 WEEKS

| NaOH, g/L | $Na_2S$, g/L | mpy S° as elemental sulfur, g/L 0 | 0.5 | 1.0 | 1.5 | 2.0 | 5.0 | 1.0 |
|---|---|---|---|---|---|---|---|---|
| 60 | 10 | 2.3 | 5.0 | 3.6 | 0.6 | 0.9 | 0.5 | 0.8 |
| | 20 | 2.1 | 6.1 | 9.5 | 0.8 | 18.2 | 3.3 | 3.8 |
| | 30 | 4.3 | 17.7 | 15.4 | 13.3 | 18.9 | 3.8 | 3.3 |
| | 40 | 5.2 | 21.8 | 19.7 | 14.4 | 15.4 | 6.4 | 1.1 |
| 80 | 10 | 2.2 | 5.3 | 0.5 | 0.7 | 1.1 | 0.4 | 0.6 |
| | 20 | 2.9 | 7.6 | 8.8 | 12.4 | 20.4 | 1.7 | 2.2 |
| | 30 | 3.4 | 21.7 | 13.9 | 19.1 | 18.6 | 2.0 | 2.4 |
| | 40 | 4.5 | 15.7 | 14.2 | 17.1 | 22.0 | 4.8 | 2.4 |
| 100 | 10 | 3.4 | 7.7 | 10.8 | 1.7 | 7.7 | 1.2 | 1.2 |
| | 20 | 2.7 | 10.2 | 15.9 | 22.5 | 17.9 | 1.1 | 1.2 |
| | 30 | 4.3 | 9.0 | 24.7 | 19.0 | 20.3 | 11.8 | 2.6 |
| | 40 | 4.1 | 20.9 | 35.0 | 51.3 | 62.4 | 9.4 | 2.1 |

## WEIGHT LOSS RESULTS - 4 WEEKS

| NaOH, g/L | $Na_2S$, g/L | mpy S° as elemental sulfur, g/L 0 | 0.5 | 1.0 | 1.5 | 2.0 | 5.0 | 1.0 |
|---|---|---|---|---|---|---|---|---|
| 60 | 10 | 0.6 | 2.6 | 0.8 | 1.0 | 0.5 | 0.6 | 0.5 |
| | 20 | -- | 4.9 | 4.3 | 12.6 | 1.3 | 2.0 | 2.1 |
| | 30 | 3.6 | 8.7 | 6.0 | 6.0 | 1.6 | 1.8 | 1.9 |
| | 40 | 4.1 | 12.4 | 19.9 | 14.8 | 9.7 | 0.8 | 0.7 |
| 80 | 10 | 2.1 | 3.0 | 9.6 | 0.7 | 0.8 | 1.0 | 0.8 |
| | 20 | 2.6 | 4.0 | 4.5 | 6.7 | 8.5 | 2.1 | 1.5 |
| | 30 | 3.3 | 16.1 | 7.3 | 9.7 | 14.7 | 1.4 | 1.8 |
| | 40 | 5.4 | 18.0 | 7.1 | 10.2 | 11.9 | 6.7 | 2.1 |
| 100 | 10 | 4.4 | 4.9 | 6.3 | 1.9 | 1.4 | 1.2 | 1.2 |
| | 20 | 3.6 | 10.3 | 11.6 | 14.0 | 21.5 | 2.0 | 1.7 |
| | 30 | 3.6 | 8.2 | 14.0 | 10.2 | 11.0 | 3.4 | 1.7 |
| | 40 | 4.8 | 21.7 | 35.1 | 26.5 | 37.6 | 4.9 | 1.9 |

## WEIGHT LOSS RESULTS - 6 WEEKS

mpy

| NaOH, g/L | $Na_2S$, g/L | S° as elemental sulfur, g/L | | | | | | |
|---|---|---|---|---|---|---|---|---|
| | | 0 | 0.5 | 1.0 | 1.5 | 2.0 | 5.0 | 1.0 |
| 60 | 10 | 0.6 | 1.6 | 0.7 | 0.6 | 0.5 | 0.6 | 3.4 |
| | 20 | 2.1 | 2.5 | 2.8 | 0.6 | 1.2 | 0.9 | 0.9 |
| | 30 | 2.7 | 5.0 | 3.6 | 3.6 | 6.5 | 0.6 | 0.4 |
| | 40 | 3.1 | 15.7 | 6.4 | 10.8 | 5.3 | 0.7 | 0.6 |
| 80 | 10 | 2.0 | 2.1 | 6.6 | 0.8 | 0.9 | 0.6 | 0.9 |
| | 20 | 2.4 | 3.0 | 3.6 | 4.3 | 7.0 | 2.0 | 1.3 |
| | 30 | 4.0 | 17.8 | 5.7 | 7.4 | 3.6 | 0.9 | 1.0 |
| | 40 | 4.1 | 13.6 | 4.4 | 6.8 | 8.7 | 4.6 | 1.1 |
| 100 | 10 | 2.8 | 2.6 | 4.1 | 4.9 | 3.0 | 0.6 | 0.8 |
| | 20 | 2.8 | 11.1 | 10.9 | 11.6 | 9.5 | 1.5 | 1.5 |
| | 30 | 3.5 | 5.5 | | | | | |
| | 40 | | | | | | | |

## WEIGHT LOSS RESULTS - 8 WEEKS

mpy

| NaOH, g/L | $Na_2S$, g/L | S° as elemental sulfur, g/L | | | | | | |
|---|---|---|---|---|---|---|---|---|
| | | 0 | 0.5 | 1.0 | 1.5 | 2.0 | 5.0 | 1.0 |
| 60 | 10 | 0.9 | 1.5 | 0.6 | 0.7 | 0.7 | 0.8 | 0.6 |
| | 20 | 2.0 | -- | 2.4 | 5.5 | 1.0 | 0.9 | 0.8 |
| | 30 | 2.7 | 3.4 | 2.5 | 3.1 | 5.3 | 1.7 | 0.5 |
| | 40 | 3.7 | 4.2 | 2.5 | 4.8 | 4.7 | 0.7 | 0.6 |
| 80 | 10 | 1.6 | 1.9 | 0.8 | 0.7 | 0.6 | 0.5 | 0.7 |
| | 20 | 3.1 | 2.2 | 2.6 | 3.9 | 4.6 | 1.4 | 1.3 |
| | 30 | 4.1 | 15.3 | 4.6 | 5.5 | 6.6 | 2.5 | 0.7 |
| | 40 | 4.8 | 10.6 | 3.7 | 6.2 | 6.3 | 3.2 | 0.8 |
| 100 | 10 | 1.9 | 2.0 | 3.0 | 0.9 | 1.0 | 0.8 | 1.1 |
| | 20 | 2.8 | 8.6 | 8.1 | 9.0 | 9.1 | 1.5 | 1.3 |
| | 30 | 4.7 | 4.0 | | | | | |
| | 40 | | | | | | | |

CONCLUSIONS

- POLYSULFIDE EFFECT ON WHITE LIQUOR CORROSIVITY IS TRANSIENT IN STAGNANT LIQUORS
- PASSIVATION IS PROMOTED BY AS LITTLE AS 0.5 g/L $S^0$
- ACCELERATION OF CORROSION INCREASES AS NaOH, $Na_2S$ INCREASES
- HIGH POLYSULFIDE CONCENTRATIONS PROMOTE IMMEDIATE PASSIVATION, LOW CORROSION RATES

VELOCITY EFFECTS ON LIQUOR CORROSIVITY

- VELOCITIES FROM 0 TO 3 mls.
- 100 g/L NaOH, 33 g/L $Na_2S$
- TEMP. = 90°C

EFFECTS OF FLOW VELOCITY ON CORROSION RATE IN A SIMULATED WHITE LIQUOR[a]

| Velocity, m/s | Annular Cross-sectional Area, $cm^2$ | Run No. | Corrosion Rate |
|---|---|---|---|
| 0.07 | 4.8 | 5 | 23.6 |
| 0.12 | 2.7 | 5 | 25.6 |
| 0.14 | 4.8 | 4 | 65.0 |
| 0.21 | 1.5 | 5 | 36.5 ? |
| 0.25 | 2.7 | 4 | 80.0 |
| 0.30 | 4.8 | 3 | 99.0 |
| 0.43 | 1.5 | 4 | 120.0 |
| 0.50 | 2.7 | 3 | 143.0 |
| 0.66 | 0.5 | 5 | 46.0 ? |
| 0.86 | 1.5 | 3 | 138.0 |
| 1.32 | 0.5 | 4 | 150.0 |
| 2.62 | 0.5 | 3 | 148.0 |

[a]100 g/L NaOH, 33 g/L $Na_2S$, 90°C.

CONCLUSIONS

- PRELIMINARY RESULTS INDICATE LARGE EFFECTS OF VELOCITY ON LIQUOR CORROSIVITY
- ADDITIONAL STUDIES WITH ATTENTION TO HYDRODYNAMICS ARE WARRANTED

FUTURE WORK — WHITE LIQUOR CORROSIVITY

- IN-MILL STUDIES
  - VALIDATION OF LINEAR POLARIZATION
  - VALIDATION OF ELECTRICAL RESISTANCE
  - SAMPLING TO EVALUATE LIQUOR COMPOSITION EFFECTS
  - INSTALL COMPUTER-BASED MONITORING
- SPECIES EFFECTS
  - COMPLETE POLYSULFIDE STUDIES
  - INITIATE THIOSULFATE STUDIES
- LIQUOR VELOCITY
  - IMPROVE HYDRODYNAMIC ASSESSMENT OF FLOW SYSTEM
  - CHARACTERIZE VELOCITY EFFECTS

CONTINUOUS DIGESTER CRACKING — W. ROGERS A291

- SERT TEST IN ACTUAL LIQUOR INDUCES CRACKING — NO POTENTIOSTAT NECESSARY
- TESTS PLANNED ON LIQUORS FROM IMMUNE MILLS

FUTURE WORK — CONTINUOUS DIGESTER CRACKING

- IN-VESSEL POTENTIAL MEASUREMENTS
- IN-SITU SERT TESTING
- ORGANICS CHARACTERIZATION

SIGNIFICANCE TO THE INDUSTRY

i) LINEAR POLARIZATION CORRECTIONS ARE VALID IN MILL TESTING

ii) BOTH LP AND ER TESTS APPEAR SUITABLE FOR CORROSION MONITORING BY MILL PERSONNEL

iii) POLYSULFIDE EFFECTS APPEAR TRANSIENT — SMALL CONCENTRATIONS MAY NOT BE HARMFUL

iv) VELOCITY EFFECTS ON LIQUOR CORROSIVITY ARE LARGE, BUT MORE TESTING IS NEEDED

Project 3309

# FUNDAMENTALS OF CORROSION CONTROL IN PAPER MILLS

Ronald A. Yeske

FUNDAMENTALS OF CORROSION CONTROL IN PAPER MILLS

PROJECT 3309

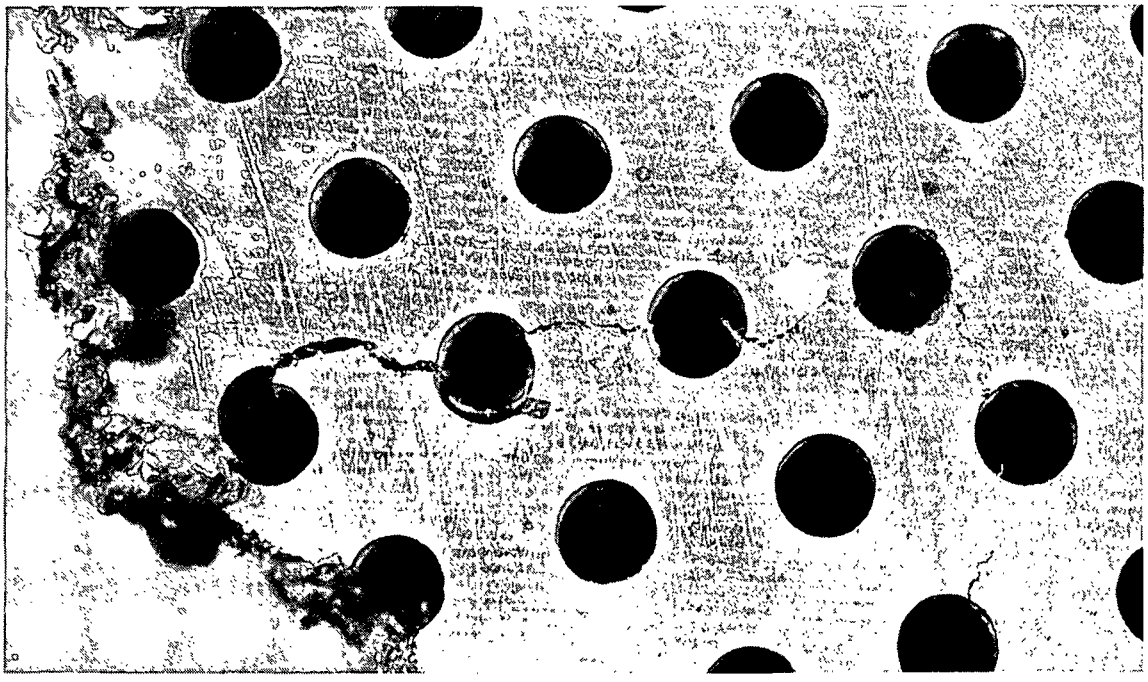

CRACKING IN AN AUSTENETIC STAINLESS STEEL SUCTION ROLL
THAT FAILED IN SERVICE

LONG RANGE OBJECTIVE:

IDENTIFY COST-EFFECTIVE REMEDIES FOR
CORROSION-ASSISTED CRACKING OF SUCTION ROLLS

HIGHLIGHTS OF PROJECT 3309

- CORROSION BEHAVIOR
- METALLURGICAL STRUCTURE
- THIOSULFATE/CHLORIDE SYNERGISM
- SHOT PEENING

CORROSION BEHAVIOR

- NO CORRELATION WITH CRACKING IN SERVICE
- SURFACE FINISH AFFECTS CORROSION
- MARTENSITIC STAINLESS PITS IN A CHLORIDE-CONTAINING WHITEWATER; OTHER ALLOYS ARE IMMUNE
- ONLY MO-BEARING STAINLESS STEELS ARE RESISTANT IN THIOSULFATE/CHLORIDE ENVIRONMENT
- CORROSION RESISTANCE AS FOLLOWS

  VKA 378
  PM-3-1811 MN
  CF3M
  VK171
  A75
  PM-2-2505
  CA15
  PM-4-1300

- NO FLOW EFFECTS

TEST SOLUTIONS

| | pH | $SO_4^=$ | $Cl^-$ | $S_2O_3^=$ | Comments |
|---|---|---|---|---|---|
| TAPPI I | 3.5 | 1000 | 100 | -- | $Al_2(SO_4)_3$, |
| TAPPI II | 3.5 | 1000 | 1000 | -- | NaCl |
| WW1 | 4.1 | 500 | 200 | 50 | $Na_2SO_4$, NaCl, $Na_2S_2O_3$ |
| WW2 | 4.1 | 500 | 200 | -- | |
| WW3 | 4.1 | 500 | -- | 50 | |

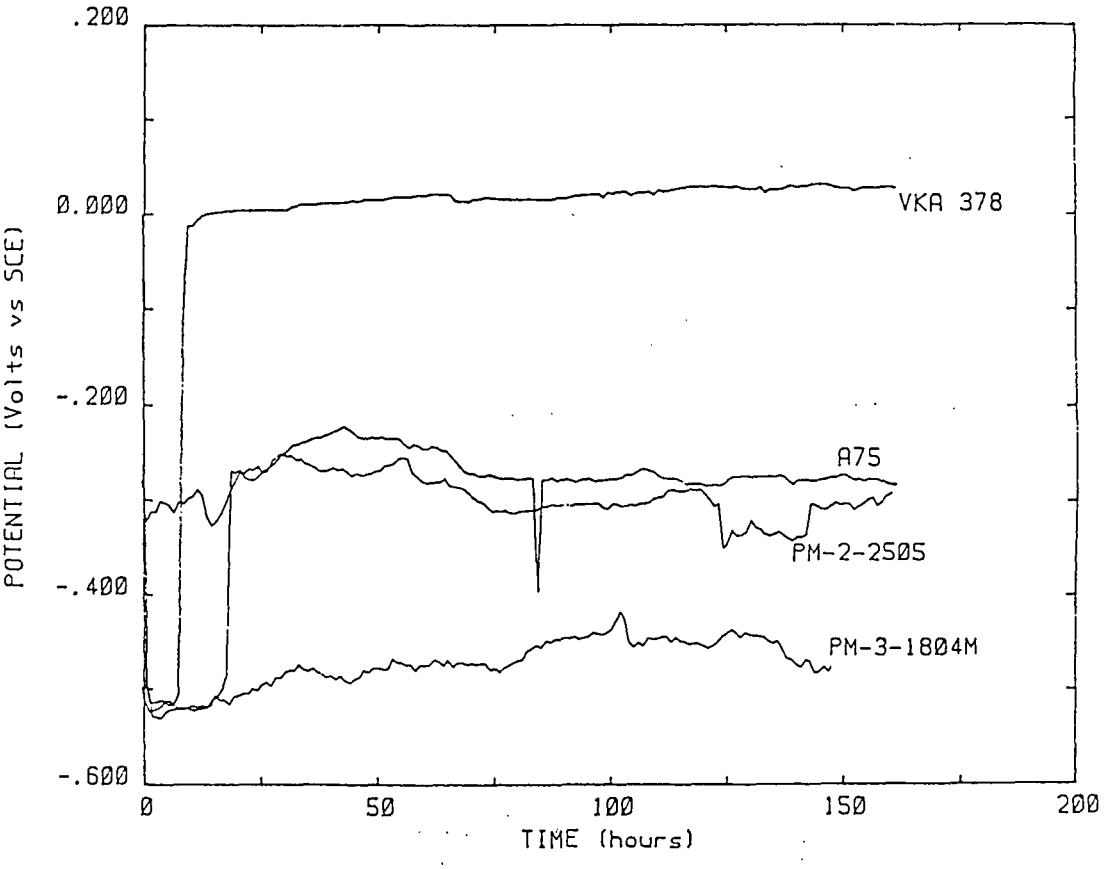


POTENTIAL DECAY OF DUPLEX STAINLESS STEELS EXPOSED TO A CHLORIDE + THIOSULFATE SOLUTION (WW1)

MICROSTRUCTURE

- CAST ALLOYS HAVE MORE DEFECTS THAN FORGED
- ALL ALLOYS EXHIBITED SOME PRESENCE OF DEFECTS — ALLOY 378 WAS LEAST AFFECTED
- CA-15 AND ALLOY 75 COULD NOT BE POLISHED TO EXCLUDE INCLUSIONS
- CENTRIFUGALLY CAST IN BRONZE HAD LARGER INCLUSIONS THAN CONCAST BRONZE

THIOSULFATE/CHLORIDE SYNERGISM

- DUPLEX STAINLESS STEELS WERE RESISTANT TO WHITEWATERS WITH CHLORIDE OR THIOSULFATE
- RESISTANCE WAS DEGRADED SIGNIFICANTLY WHEN BOTH THIOSULFATE AND CHLORIDES WERE PRESENT
- DITTO, CF3M AUSTENITIC ALLOY

SHOT-PEENING

- CORROSION RESISTANCE OF SHOT-PEENED SURFACES WAS GENERALLY BETTER THAN POLISHED OR AS-MACHINED SURFACES

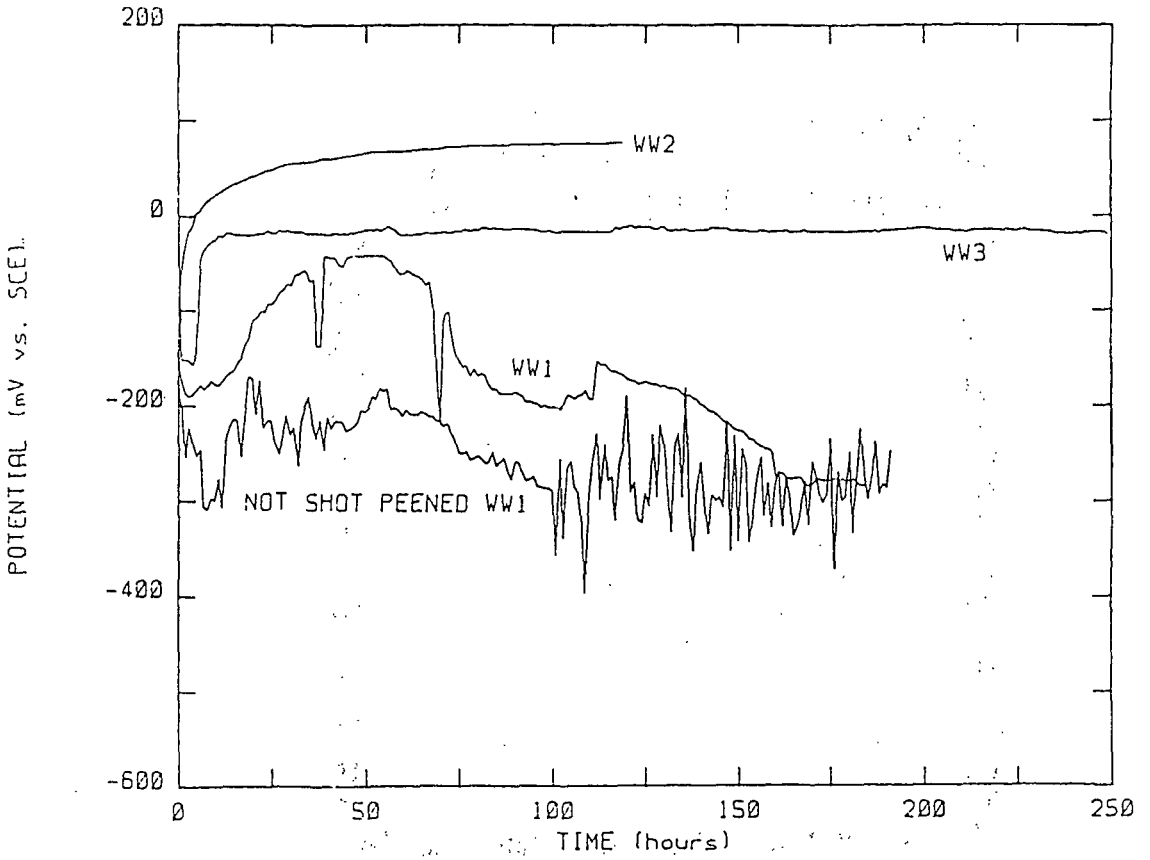


POTENTIAL DECAY RESULTS FOR ALLOY 171 IN CHLORIDE (WW2), THIOSULFATE (WW3), AND THIOSULFATE + CHLORIDE (WW1) SOLUTIONS

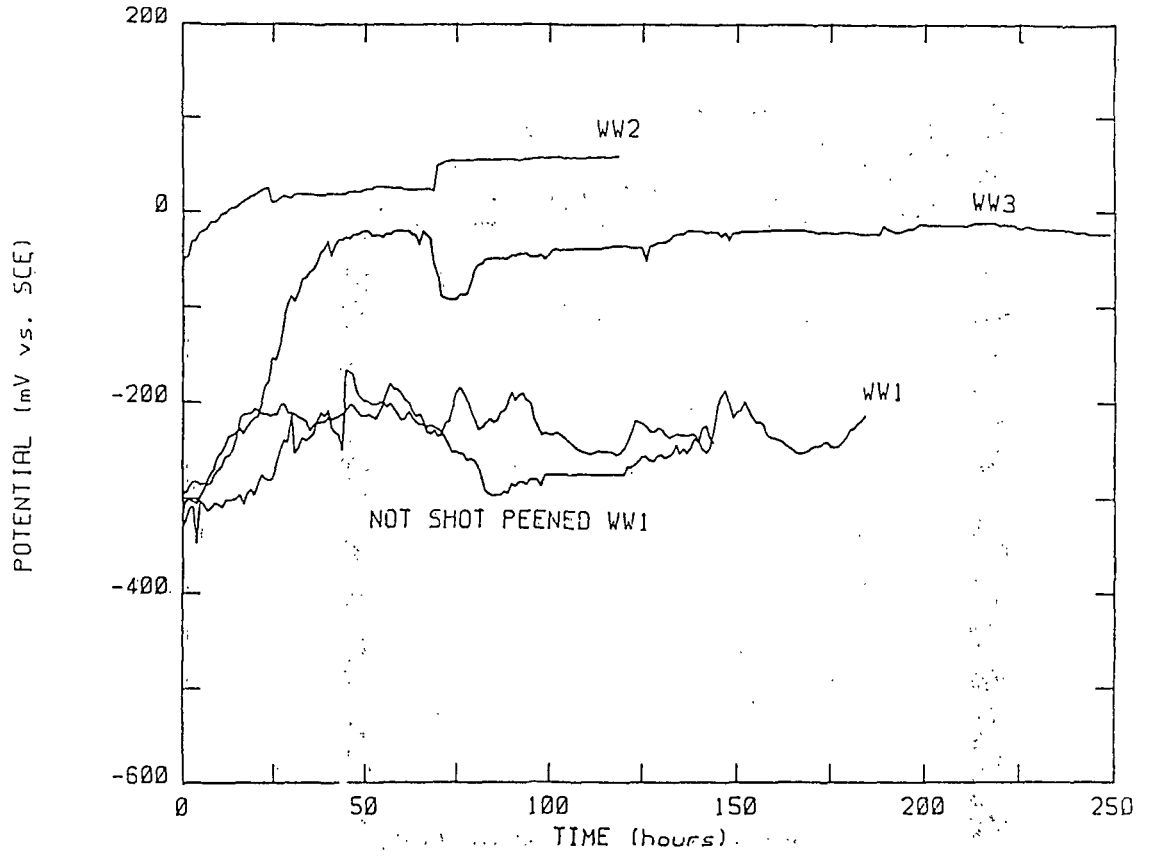


POTENTIAL DECAY OF ALLOY 75 EXPOSED TO CHLORIDE (WW2), THIOSULFATE (WW3), AND CHLORIDE + THIOSULFATE (WW1) SOLUTIONS

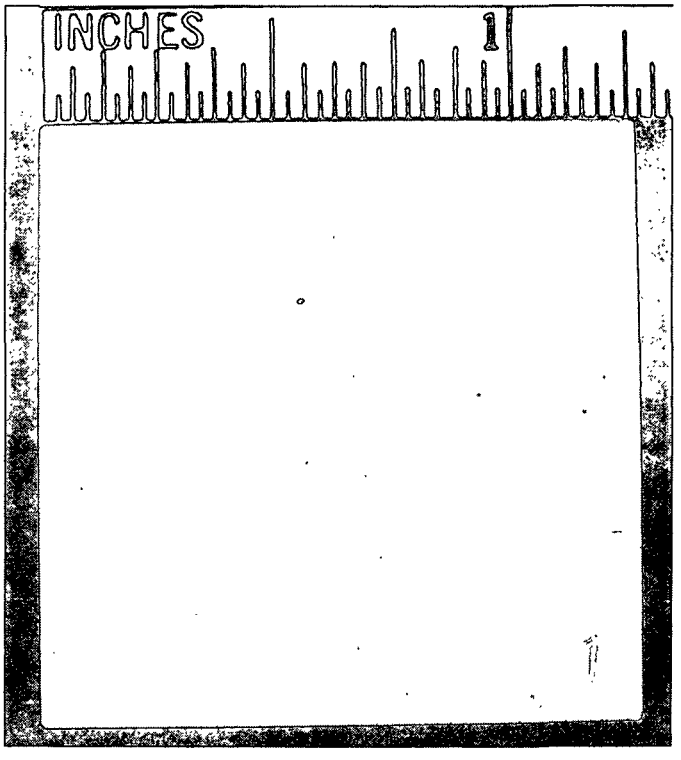


ALLOY 75 EXPOSED TO WW3 (THIOSULFATE) SOLUTION

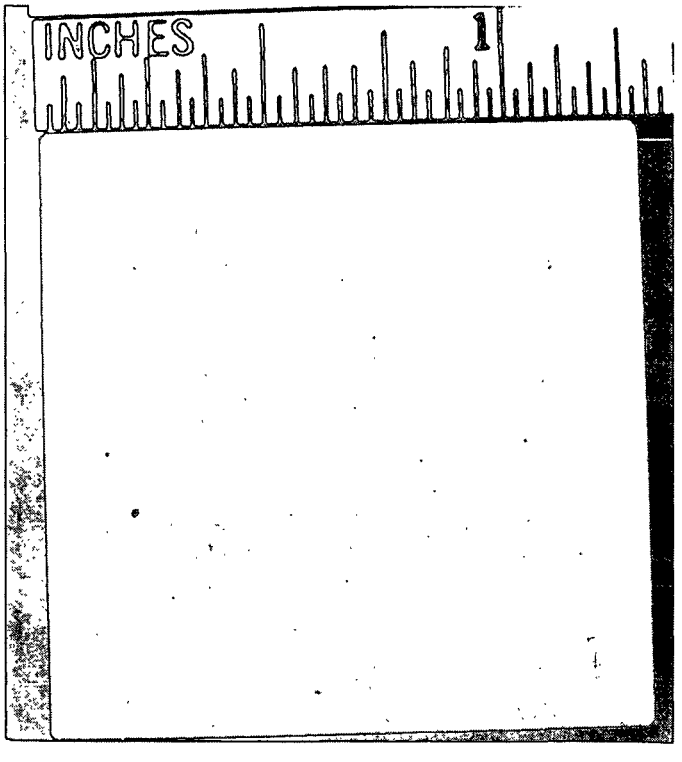


ALLOY 75 EXPOSED TO WW2 (CHLORIDE)

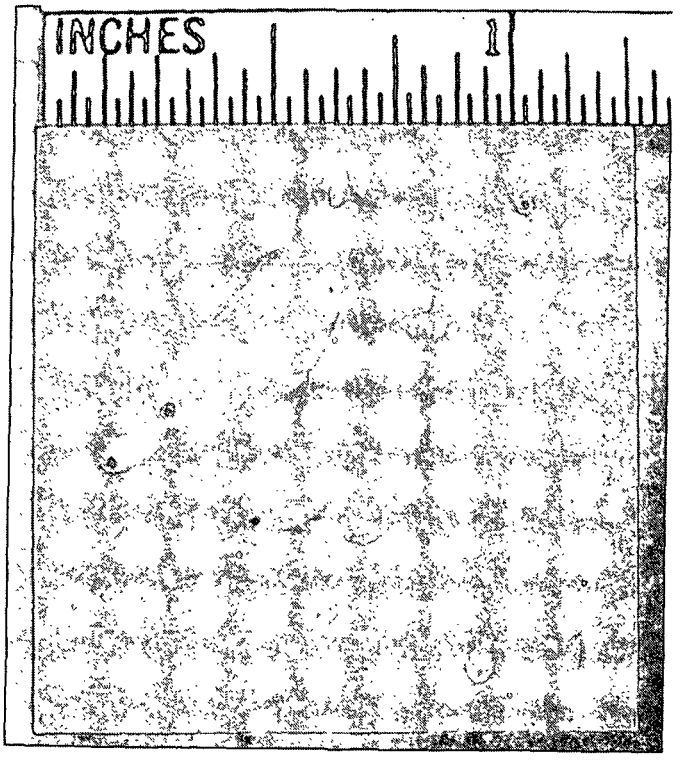


ALLOY 75 EXPOSED TO WW1 (CHLORIDE + THIOSULFATE)

FUTURE DIRECTIONS

SUCTION ROLL CRACKING STUDIES

THE ROLE OF THE INSTITUTE

° UNBIASED ADVOCATE FOR MEMBER COMPANIES

° LIMITED MANPOWER, FACILITIES

° UNIQUE EXPERTISE

THEREFORE . . .

• ADDRESS ISOLATED ISSUES OF CRITICAL IMPORTANCE

• AVOID "MATRIX TESTING" PITFALLS

SOME CRITICAL ISSUES

i) HOW TO EVALUATE VENDORS CLAIMS?

- ° DIFFERENT TEST METHODS
- ° DIFFERENT ENVIRONMENTS
- ° DIFFERENT EMPHASIS

ii) WHAT ACCELERATED TEST CAN BE USED TO PREDICT ROLL PERFORMANCE?

- • NOT FATIGUE LIFETIME (S-N DATA)
- ° NOT CRACK GROWTH RATE DATA
- ° NOT CORROSION RESISTANCE

iii) WHAT WHITEWATER SPECIES ARE DELETERIOUS?

- ° CHLORIDES
- ° THIOSULFATES
- ° SYNERGISM

iv) WHAT CHARACTERISTICS ARE DESIRABLE IN A ROLL ALLOY?

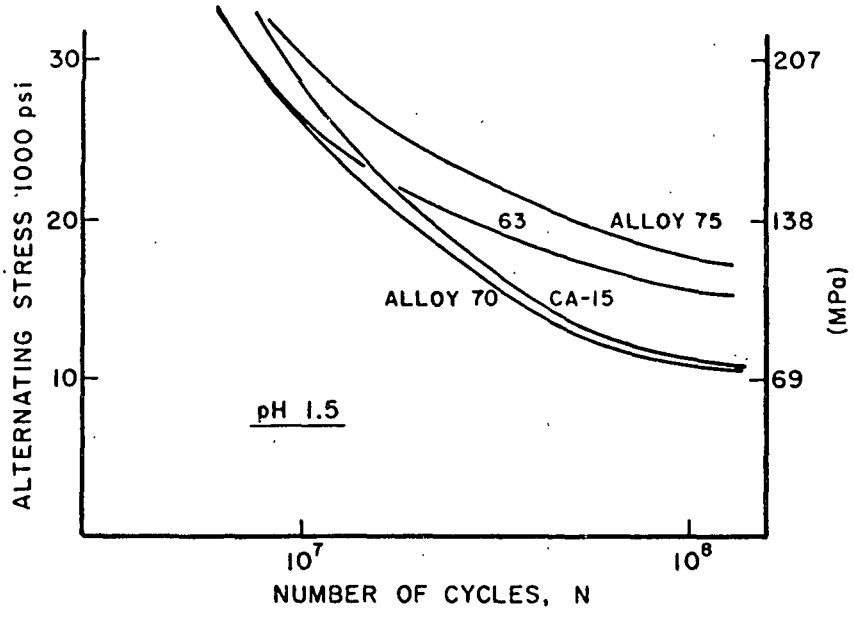


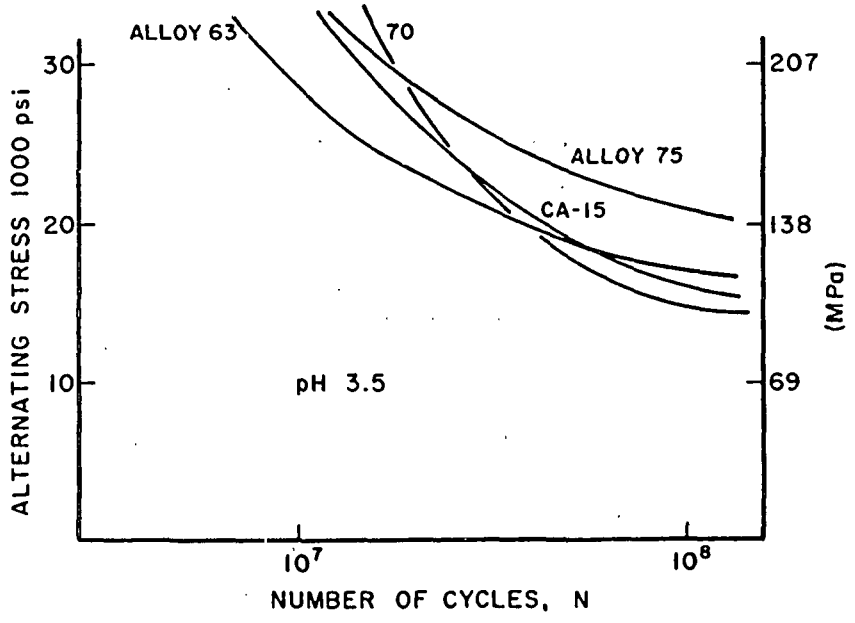


VESTOLA
1984 TAPPI ENGINEERING CONFERENCE

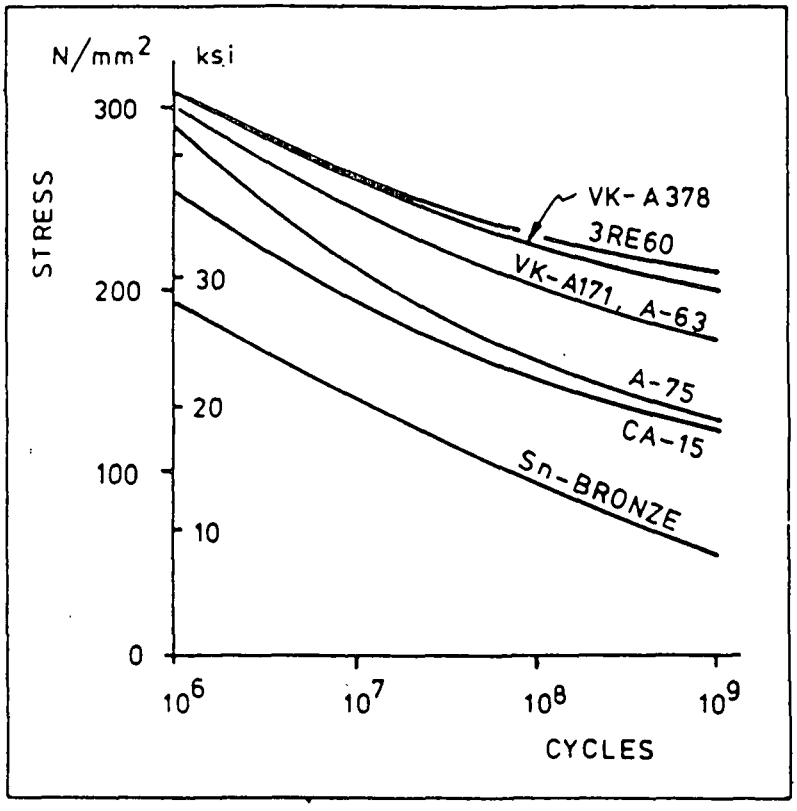


VESTOLA
1984 TAPPI ENGINEERING CONFERENCE

NEAR-TERM OBJECTIVES

i) IDENTIFY AN ACCELERATED TEST THAT CORRELATES WITH FIELD PERFORMANCE (e.g., ALLOY 75 vs. ALLOY 63)

ii) NORMALIZE FATIGUE TEST METHODS OF DIFFERENT VENDORS. (TO FACILITATE EVALUATION OF CURRENT ROLL ALLOYS)

INTERMEDIATE TERM OBJECTIVES

iii) ESTABLISH EFFECTS OF WHITEWATER SPECIES, USING i) ABOVE

iv) EVALUATE MEAN STRESS EFFECTS

v) RANK ALLOYS USING PROCEDURE i)

COMPARISON OF FATIGUE TEST METHODS

- ROTATING BENDING vs. REVERSED BENDING
- SMOOTH vs. NOTCHED
- 1750 cpm vs. 3000+ cpm
- 20, 100, 600 ppm $Cl^-$
- APPLES AND ORANGES

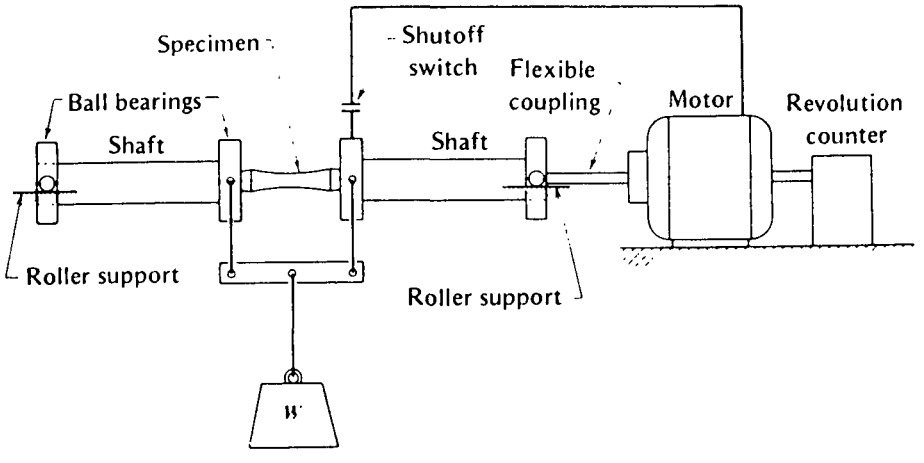


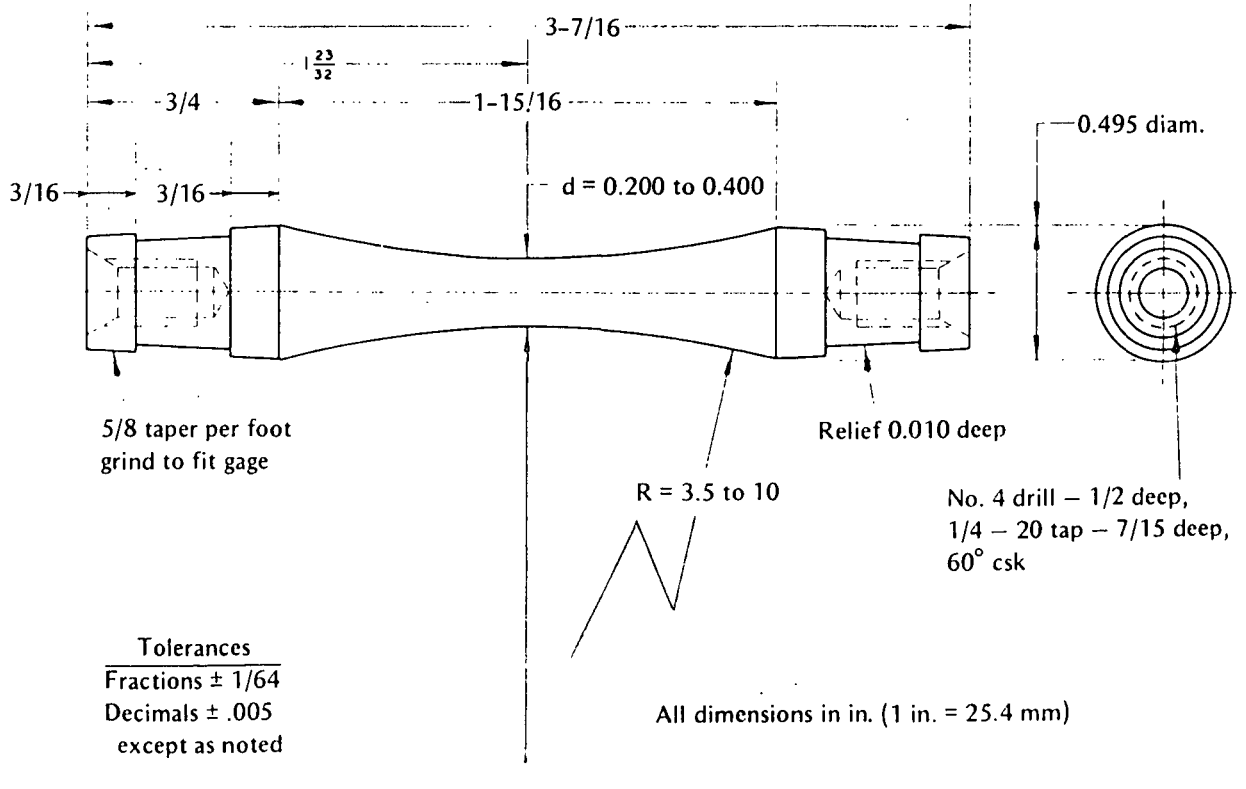


R. R. MOORE ROTATING BENDING FATIGUE TEST

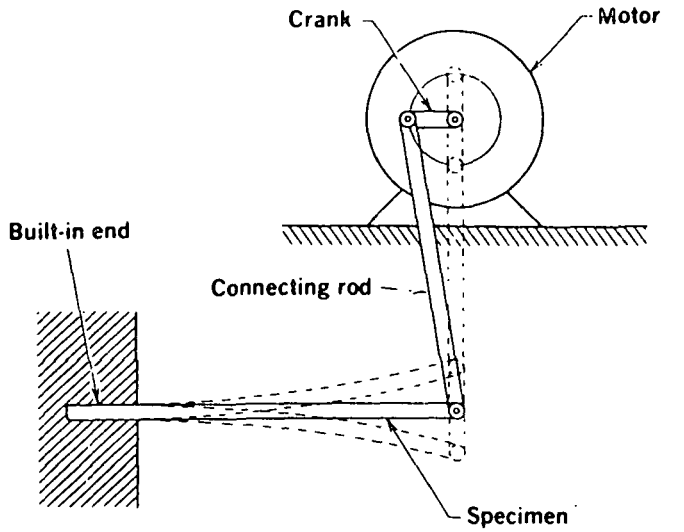


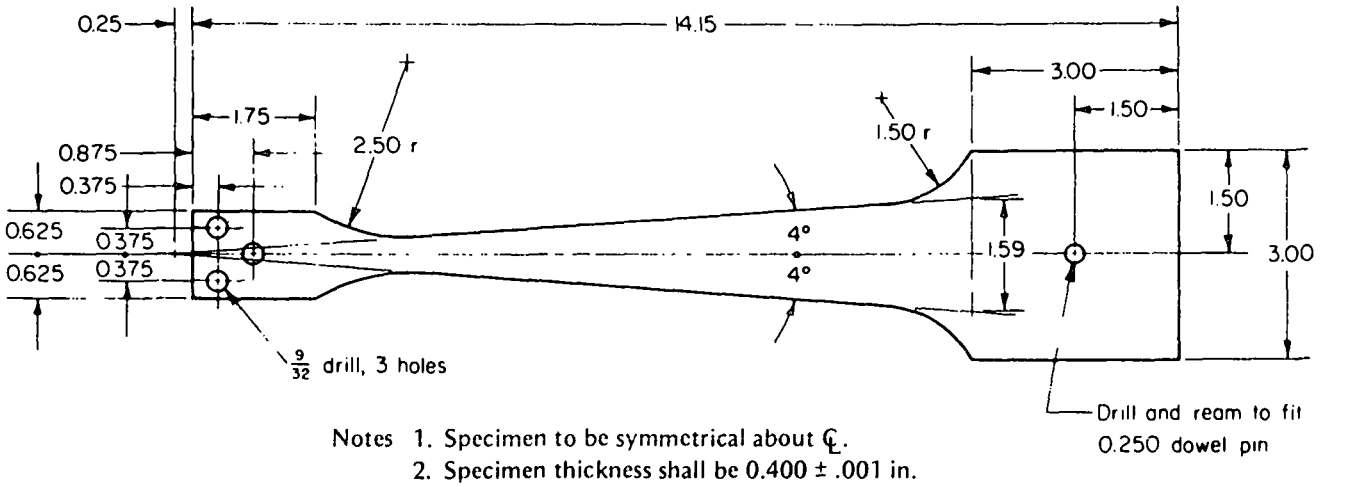


Notes 1. Specimen to be symmetrical about ℄.
2. Specimen thickness shall be 0.400 ± .001 in.
3. All dimensions in inches.

REVERSED BENDING FATIGUE TEST

SOME CANDIDATE TESTS . . .

- NEAR-THRESHOLD FATIGUE CRACK GROWTH
- MEAN STRESS SENSITIVITY CRACK INVITATION AND GROWTH
- SENSITIVITY TO PRE-EXISITING, CORROSION-INDUCED SURFACE DAMAGE

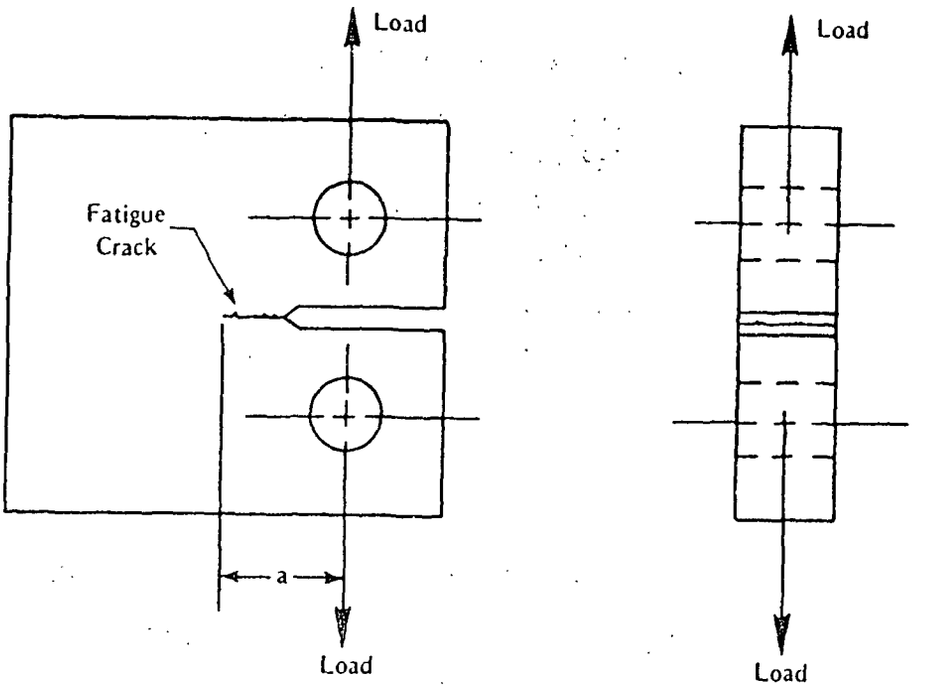
Load
Fatigue Crack
a
Load
Load
Load

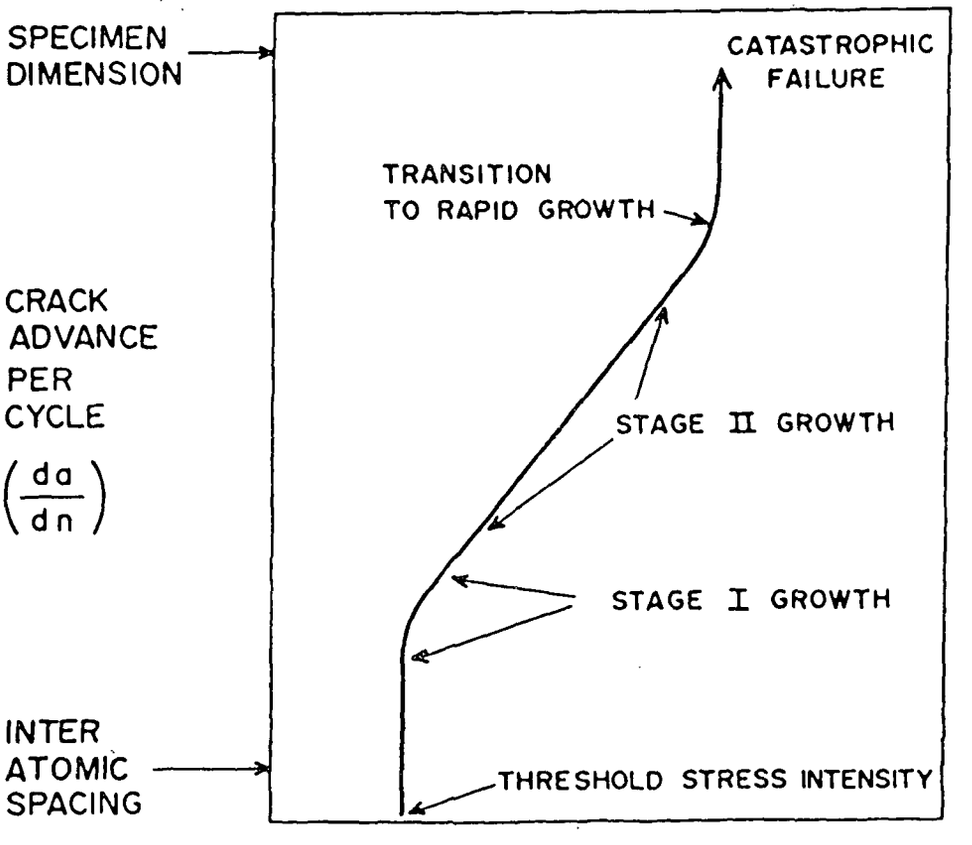
SPECIMEN DIMENSION
CATASTROPHIC FAILURE
TRANSITION TO RAPID GROWTH
CRACK ADVANCE PER CYCLE
$\left(\frac{da}{dn}\right)$
STAGE II GROWTH
STAGE I GROWTH
INTER ATOMIC SPACING
THRESHOLD STRESS INTENSITY
STRESS INTENSITY RANGE, ΔK

HOW TO EVALUATE CANDIDATE TEST METHODS?

- COMPARE TEST RESULTS ON ALLOYS WITH DIFFERENT PERFORMANCE RECORDS
  - ALLOY 75 (NO FAILURES)
  - ALLOY 63 (70% FAILURE RATE)
  - 3RD60 (A FEW FAILURES)
  - ALLOY VKA 378 (NO FAILURES)

AVENUES FOR IMPROVED PERFORMANCE (LONG-TERM)

- IDENTIFY AGGRESSIVE CHEMICAL SPECIES IN WHITEWATER AND EXPUNGE
- IDENTIFY ALLOY CHARACTERISTICS WITH DESIRABLE CRACKING RESISTANCE
- IDENTIFY SURFACE TREATMENTS TO PROLONG LIFE
- IDENTIFY CHEMICAL ADDITIVES THAT PROLONG LIFE